

JAERI-Data/Code

98-024



**COMPILATION OF BENCHMARK RESULTS  
FOR FUSION RELATED NUCLEAR DATA**

November 1998

Fujio MAEKAWA, Masayuki WADA, Chihiro ICHIHARA\*,  
Yo MAKITA\*\*, Akito TAKAHASHI\*\* and Yukio OYAMA

日本原子力研究所  
Japan Atomic Energy Research Institute

本レポートは、日本原子力研究所が不定期に公刊している研究報告書です。  
入手の問合わせは、日本原子力研究所研究情報部研究情報課（〒319-1195 茨城県那珂郡東海村）あて、お申し越しください。なお、このほかに財団法人原子力弘済会資料センター（〒319-1195 茨城県那珂郡東海村日本原子力研究所内）で複写による実費領布をおこなっております。

This report is issued irregularly.

Inquiries about availability of the reports should be addressed to Research Information Division, Department of Intellectual Resources, Japan Atomic Energy Research Institute, Tokai-mura, Naka-gun, Ibaraki-ken, 319-1195, Japan.

© Japan Atomic Energy Research Institute, 1998

編集兼発行 日本原子力研究所

Compilation of Benchmark Results for Fusion Related Nuclear Data

Fujio MAEKAWA, Masayuki WADA, Chihiro ICHIHARA\*,  
Yo MAKITA\*\*, Akito TAKAHASHI\*\* and Yukio OYAMA†

Department of Materials Science  
Tokai Research Establishment  
Japan Atomic Energy Research Institute  
Tokai-mura, Naka-gun, Ibaraki-ken

(Received September 7, 1998)

This report compiles results of benchmark tests for validation of evaluated nuclear data to be used in nuclear designs of fusion reactors. Parts of results were obtained under activities of the Fusion Neutronics Integral Test Working Group organized by the members of both Japan Nuclear Data Committee and the Reactor Physics Committee. The following three benchmark experiments were employed used for the tests: (i) the leakage neutron spectrum measurement experiments from slab assemblies at the D-T neutron source at FNS/JAERI, (ii) in-situ neutron and gamma-ray measurement experiments (so-called clean benchmark experiments) also at FNS, and (iii) the pulsed sphere experiments for leakage neutron and gamma-ray spectra at the D-T neutron source facility of Osaka University, OKTAVIAN. Evaluated nuclear data tested were JENDL-3.2, JENDL Fusion File, FENDL/E-1.0 and newly selected data for FENDL/E-2.0. Comparisons of benchmark calculations with the experiments for twenty-one elements, i.e., Li, Be, C, N, O, F, Al, Si, Ti, V, Cr, Mn, Fe, Co, Ni, Cu, Zr, Nb, Mo, W and Pb, are summarized.

Keywords : Fusion, Benchmark Test, FNS, OKTAVIAN, Nuclear Data, Neutron, Secondary Gamma-Ray, JENDL-3.2, JENDL Fusion File, FENDL/E-1.0, FENDL/E-2.0

---

\* Center for Neutron Science

\*\* Kyoto University

\*\*\* Osaka University

核融合関連核データのベンチマーク結果集

日本原子力研究所東海研究所物質科学部研究部

前川 藤夫・和田 政行・市原 千博\*・牧田 陽\*\*・高橋 亮人\*\*・大山 幸夫<sup>+</sup>

(1998年9月7日受理)

本レポートは、核融合炉の核設計で使われる評価済み核データの精度検証を目的として行ったベンチマークテストの結果をまとめたものである。一部の成果はシグマ委員会と炉物理委員会の合同で組織された核融合炉ニュートロニクス積分テストワーキンググループの活動として得られたものである。以下の3種のベンチマーク実験をテストに使用した：  
(i) 原研FNSのD-T中性子源を用いて行われた飛行時間法による平板体系からの漏洩中性子スペクトル測定実験、(ii) 同じくFNSで行われた体系内における中性子及び $\gamma$ 線測定実験(クリーンベンチマーク実験)、及び(iii) 大阪大学のD-T中性子源施設OKTAVIANにおいて漏洩中性子及び $\gamma$ 線スペクトルを測定したパルス球実験。JENDL-3.2、JENDL Fusion File、FENDL/E-1.0 及び新たに FENDL/E-2.0 に選択された評価済み核データをテストの対象とした。Li, Be, C, N, O, F, Al, Si, Ti, V, Cr, Mn, Fe, Co, Ni, Cu, Zr, Nb, Mo, W, Pb の総計21元素に関するベンチマーク計算結果と実験値との比較が収録されている。

---

東海研究所：〒319-1195 茨城県那珂郡東海村白方白根 2-4

<sup>+</sup> 中性子科学研究センター

<sup>\*</sup> 京都大学

<sup>\*\*</sup> 大阪大学

## Contents

1. Introduction -----	1
2. Nuclear Data and Transport Calculation Code -----	2
3. FNS Time-of-Flight Experiment -----	3
3.1 Brief Description of the Experiment -----	3
3.2 Benchmark Calculation -----	3
3.3 Results for JENDL-3.2, JENDL Fusion File & FENDL/E-1.0 -----	4
3.4 Results for FENDL/E-2.0 -----	5
4. FNS Clean Benchmark Experiment -----	6
4.1 Brief Description of the Experiment -----	6
4.2 Benchmark Calculation -----	7
4.3 Results for JENDL-3.2, JENDL Fusion File & FENDL/E-1.0 -----	7
4.4 Results for FENDL/E-2.0 -----	10
5. OKTAVIAN Pulsed Sphere Experiment -----	11
5.1 Brief Description of the Experiment -----	11
5.2 Benchmark Calculation -----	11
5.3 Results for Neutron Spectrum -----	12
5.4 Results for Secondary Gamma-Ray Spectrum -----	13
6. Overview of Results for Each Element -----	14
7. Summary -----	22
Acknowledgment -----	22
References -----	23
Appendix Input Data of MCNP -----	130

## 目 次

1. はじめに .....	1
2. 核データと輸送計算コード .....	2
3. FNS 飛行時間法実験 .....	3
3.1 実験の概要 .....	3
3.2 ベンチマーク計算 .....	3
3.3 JENDL-3.2, JENDL Fusion File 及び FENDL/E-1.0 に関する結果 .....	4
3.4 FENDL/E-2.0 に関する結果 .....	5
4. FNS クリーンベンチマーク実験 .....	6
4.1 実験の概要 .....	6
4.2 ベンチマーク計算 .....	7
4.3 JENDL-3.2, JENDL Fusion File 及び FENDL/E-1.0 に関する結果 .....	7
4.4 FENDL/E-2.0 に関する結果 .....	10
5. OKTAVIAN パルス球実験 .....	11
5.1 実験の概要 .....	11
5.2 ベンチマーク計算 .....	11
5.3 中性子スペクトルの結果 .....	12
5.4 2次 $\gamma$ 線スペクトルの結果 .....	13
6. 各元素の結果の概要 .....	14
7. まとめ .....	22
謝 辞 .....	22
参考文献 .....	23
付 錄 MCNP の入力データ .....	130

## 1. Introduction

A number of fusion neutronics benchmark experiments has been conducted at the two major D-T neutron source facilities in Japan, Fusion Neutronics Source<sup>1)</sup> (FNS) at Japan Atomic Energy Research Institute and OKTAVIAN<sup>2)</sup> at Osaka University, for more than fifteen years. A large amount of benchmark experimental data have been accumulated for fusion reactor relevant materials, such as tritium breeding materials, neutron multiplication materials, structural materials, plasma facing materials, shielding materials, and so on.

On the other hand, after the release of Japanese Evaluated Nuclear Data Library version 3.1<sup>3)</sup> (JENDL-3.1) at the end of 1990, cross section data in JENDL-3.1 were revised to produce a new version of JENDL, JENDL-3.2<sup>4)</sup>, and it was released in June 1994. As one of the JENDL special purpose files, JENDL Fusion File<sup>5)</sup> (hereafter, JENDL-FF) has been also evaluated for fusion applications in which accurate treatment of energy-angle-dependent double-differential cross sections for high energy neutrons was implemented.

In the mean time, an international standard nuclear data file for fusion, Fusion Evaluated Nuclear Data Library version 1<sup>6)</sup>, FENDL/E-1.0 (hereafter, FENDL-1), was released from International Atomic Energy Agency (IAEA) in May, 1994. The FENDL-1 library was a collection of best cross section data from national nuclear data libraries of Japan, USA and Russia, i.e., JENDL-3.1, ENDF/B-VI<sup>7)</sup> and BROND-2<sup>8)</sup>, respectively. It was adopted officially as a reference nuclear data library for Engineering Design Activities of International Thermonuclear Experimental Reactor (ITER).

Cross section data for many isotopes in FENDL-1 have been updated to FENDL/E-2.0 (hereafter, FENDL-2) by newly evaluated cross section data of new national libraries, i.e., JENDL-FF, ENDF/B-VI, BROND-2 and European Fusion File version-3<sup>9)</sup> (EFF-3), and so on. In June, 1996, the IAEA Consultants' Meeting on Selection of Basic Evaluations for the FENDL-2 Library was held at Karlsruhe, Germany.<sup>10)</sup> Results for the benchmark test by the Japanese group and other international participants as well as microscopic cross section data provided were reviewed at the meeting, and consultants selected the best evaluation to be adopted in FENDL-2 for each isotope. These selected evaluations were approved finally at the IAEA Advisory Group Meeting on Extension and Improvement of the FENDL Library for Fusion Applications held at Vienna, Austria, March 1997.<sup>11)</sup> Further modifications were, however, requested for some of the selected evaluations at the meeting.

To examine validity of comprehensive cross section data in JENDL-3.2, JENDL-FF and FENDL-1, and also candidates evaluations for FENDL/E-2.0, we conducted benchmark tests of cross section data in these libraries. Fusion neutronics benchmark experiments performed at the two major D-T neutron source facilities in Japan, FNS and OKTAVIAN, were employed for the tests. Most parts of the benchmark tests were obtained under the

Fusion Neutronics Integral Test Working Group\* organized by the members of both Japan Nuclear Data Committee and the Reactor Physics Committee.

This report summarizes results for the benchmark tests for JENDL-3.2, JENDL-FF and FENDL-1 as well as the candidate evaluations for FENDL-2. Details of the experiments, transport calculations and comparisons of the experiments and calculations are given in references to be specified later. Chapter 2 deals with the nuclear data bases and the transport calculation code used for the benchmark calculations. Results for FNS TOF experiments, FNS clean benchmark experiments and OKTAVIAN pulsed sphere experiments are described in Chapters 3, 4 and 5, respectively. Results for the benchmark tests for each element are discussed in Chapter 6. A summary is given in Chapter 7.

## 2. Nuclear Data and Transport Calculation Code

As the first step of the benchmark test, cross section data in JENDL-3.2, JENDL-FF and FENDL-1 were examined. Table 2.1 summarizes cross section data selected for FENDL-1. Cross sections for some of light elements, i.e., Li, C, N and O, are not given in JENDL-FF.

As the second step, new candidate evaluations for FENDL-2 except for JENDL-FF were examined. Table 2.1 also shows the selected cross sections for FENDL-2. Some of the candidates were newly evaluated data: silicon isotopes from ENDF/B-VI and iron-56 from EFF-3. Some others were combinations of two evaluations: a combination of JENDL-FF and ENDF/B-VI for carbon-12 and that of JENDL-FF and BROND-2 for nitrogen-14. The rest were modified data: niobium-93 and molybdenum in JENDL-FF with revisions of some cross section data. A newly evaluated cross section data of aluminum in EFF-3 were not included although they are one of the candidate evaluations, because its transport cross section was not available.

The continuous energy Monte Carlo transport calculation code MCNP-4A<sup>12)</sup> was used commonly. The MCNP-4A code has a great advantage for the benchmark test because cross section data are accurately treated in the continuous energy representation as they are in the original nuclear data file. The code can also treat the double-differential type cross sections adopted in JENDL-FF, ENDF/B-VI, and so on.

\* Fusion Neutronics Integral Test Working Group: Y. Oyama (Group Leader, JAERI), C. Ichihara (Kyoto Univ.), K. Ueki (Ship Research Institute), K. Kosako (Sumitomo Atomic Industries, Ltd.), A. Takahashi (Osaka Univ.), K. Hayashi (Hitachi Engineering Co. Ltd.), H. Maekawa (JAERI), F. Maekawa (JAERI), K. Maki (Hitachi Co. Ltd.) and T. Mori (JAERI)

Transport cross section libraries for MCNP processed from JENDL-3.2, JENDL-FF and FENDL/E-1.0 are FSXLIB-J3R2<sup>13)</sup>, FSXLIB-JFF<sup>14)</sup> and FENDL/MC-1.0<sup>15)</sup>, respectively. Transport cross sections for other evaluations were fetched from IAEA via internet. Photon and electron transport cross sections used are MCPLIB and EL, respectively, included in the MCNP-4A code package. To calculate dosimetry reaction rates, the FSXDOS-J3 library<sup>14)</sup> processed from JENDL Dosimetry File<sup>16)</sup> was used commonly. To calculate gamma-ray heating rate, gamma-ray KERMA factors derived from the DLC-99/HUGO library<sup>17)</sup> was used.

### 3. FNS Time-of-Flight Experiment

#### 3.1 Brief Description of the Experiment

Angular neutron spectra leaking from various materials with a cylindrical slab geometry placed in front of the D-T neutron source were measured by the Time-Of-Flight (TOF) method with an NE213 liquid organic scintillation detector. Seven materials, lithium oxide, beryllium, graphite, liquid-nitrogen, liquid-oxygen, iron and lead, were assembled in the slab geometry. The slab diameters were in a range from 600 mm to 1000 mm while thicknesses ranged from 48 mm to 600 mm. Leakage neutron spectra were measured at several angles from 0 to 66.8 degrees with respect to the deuteron beam direction. In most cases, spectra were measured in an energy range from 50 keV up to 14-MeV. Details of the experiments are described in Refs. 18) ~ 24). Numerical data of the measured spectra are given in Refs. 25) and 26).

#### 3.2 Benchmark Calculation

Benchmark calculations with MCNP-4A were performed in the same manner described in Refs. 19) ~ 25). Examples of input data of MCNP for each material are given in the Appendix.

The three nuclear data libraries, JENDL-3.2, JENDL-FF and FENDL-1, are used for all the calculations. Some calculations were supplemented for new candidates of FENDL-2. The candidates were modified versions of JENDL-FF for graphite and liquid-nitrogen, and a combination of EFF-3 (Fe-56) and FENDL-1 (Fe-54, -57 & -58) for iron.

The experimental data were compared with calculations in Refs. 18) ~ 24) although nuclear data used in the calculations were somewhat outdated. Calculated results with the recent nuclear data libraries such as JENDL-3.2, JENDL-FF and FENDL-1 are briefly reported in Refs. 27) ~ 31).

### 3.3 Results for JENDL-3.2, JENDL Fusion File & FENDL/E-1.0

The calculated neutron spectra with JENDL-3.2, JENDL-FF and FENDL-1 are compared with the experimental data in the following figures. Results for JENDL-3.1 are also included in some figures.

Lithium Oxide	48.0 mm thickness	Fig. 3.3.1
	200.0 mm thickness	Fig. 3.3.2
	400.0 mm thickness	Fig. 3.3.3
Beryllium	50.8 mm thickness	Fig. 3.3.4
	152.4 mm thickness	Fig. 3.3.5
Graphite	50.6 mm thickness	Fig. 3.3.6
	202.4 mm thickness	Fig. 3.3.7
	404.8 mm thickness	Fig. 3.3.8
Nitrogen	200.0 mm thickness	Fig. 3.3.9
Oxygen	200.0 mm thickness	Fig. 3.3.10
Iron	50.0 mm thickness	Fig. 3.3.11
	200.0 mm thickness	Fig. 3.3.12
	400.0 mm thickness	Fig. 3.3.13
	600.0 mm thickness	Fig. 3.3.14
Lead	50.8 mm thickness	Fig. 3.3.15
	203.2 mm thickness	Fig. 3.3.16
	406.4 mm thickness	Fig. 3.3.17

The measured and calculated neutron fluxes are integrated in several energy intervals, and calculated to experimental (C/E) ratios are derived. The C/E ratios are compared in the following figures.

Lithium Oxide	48.0 mm thickness	Fig. 3.3.18
	200.0 mm thickness	Fig. 3.3.19
	400.0 mm thickness	Fig. 3.3.20
Beryllium	50.8 mm thickness	Fig. 3.3.21
	152.4 mm thickness	Fig. 3.3.22
Graphite	50.6 mm thickness	Fig. 3.3.23
	202.4 mm thickness	Fig. 3.3.24
	404.8 mm thickness	Fig. 3.3.25
Nitrogen	200.0 mm thickness	Fig. 3.3.26
Oxygen	200.0 mm thickness	Fig. 3.3.27
Iron	50.0 mm thickness	Fig. 3.3.28
	200.0 mm thickness	Fig. 3.3.29

	400.0 mm thickness	Fig. 3.3.30
	600.0 mm thickness	Fig. 3.3.31
Lead	50.8 mm thickness	Fig. 3.3.32
	203.2 mm thickness	Fig. 3.3.33
	406.4 mm thickness	Fig. 3.3.34

### 3.4 Results for FENDL/E-2.0

Results for benchmark calculations with the modified JENDL-FF data for graphite and nitrogen, and the combined iron data of EFF-3 (Fe-56) and ENDF/B-VI (Fe-54, -57, -58) are shown in the following figures. Typical thicknesses of slabs are chosen for the comparisons.

Graphite	202.4 mm thickness	Fig. 3.4.1
Nitrogen	200.0 mm thickness	Fig. 3.4.2
Iron	200.0 mm thickness	Fig. 3.4.3

The C/E ratios for these results are shown in the following figures.

Graphite	202.4 mm thickness	Fig. 3.4.4
Nitrogen	200.0 mm thickness	Fig. 3.4.5
Iron	200.0 mm thickness	Fig. 3.4.6

## 4. FNS Clean Benchmark Experiment

### 4.1 Brief Description of the Experiment

The in-situ measurement experiments conducted at FNS are called as “clean benchmark experiments” on seven materials; lithium oxide, beryllium, graphite, iron, copper, tungsten and type-316 stainless steel (SS316). A cylindrical experimental assembly made of each material was placed in front of the D-T neutron source of FNS. Detectors were inserted in the assembly at several positions along the central axis of the cylinder. Many nuclear responses related to both neutrons and gamma-rays were measured with various experimental techniques. The measured quantities and the techniques were;

- (i) a small sphere (14 mm  $\phi$ ) NE213 organic scintillation counter with the unfolding technique for neutron spectra above 1 MeV,
- (ii) a set of proton recoil gas proportional counters for neutron spectra between 3 keV and 1 MeV,
- (iii) the slowing down time method for neutron spectra below 10 keV,
- (iv) the foil activation method with HP-Ge detectors for dosimetry reaction rates,
- (v) fission chambers of U-235, U-238 and so on for fission rates,
- (vi) lithium-containing pellet irradiation with the liquid scintillation counting method for tritium production rates,
- (vii) a pair of lithium glass scintillation counters for tritium production rates by lithium-6,
- (viii) a deuterated liquid organic scintillation counter with the unfolding technique for gamma-ray spectra, and
- (ix) thermoluminescence dosimeters (TLDs) for gamma-ray heating rates.

Details of the experiments for each materials are described in the following references:

Lithium oxide	Refs. 25), 32)
Beryllium	Refs. 25), 33)
Graphite	Refs. 25), 34)
Iron	Refs. 35) ~ 39)
Copper	Refs. 35), 40) ~ 42)
Tungsten	Refs. 35), 43)
SS316	Refs. 39), 44) ~ 47).

## 4.2 Benchmark Calculation

Benchmark calculations with MCNP-4A were performed for the clean benchmark experiments. Details of the calculations are described in Refs. 25), 35), 42) and 47). Examples of input data of MCNP for each materials are given in Appendix.

The three nuclear data libraries, JENDL-3.2, JENDL-FF and FENDL-1, are used for all the calculations. Some calculations were supplemented for new candidates of FENDL-2. The candidates were modified versions of JENDL-FF for graphite and a combination of EFF-3 (Fe-56) and FENDL-1 (Fe-54, -57 & -58) for iron.

In most of the references given in the previous section 4.1, results for benchmark calculations are compared with the experimental data. As for JENDL-3.2, JENDL-FF and FENDL-1, results for benchmark test are discussed in the following references.

Iron	Refs. 38), 39)
Tungsten	Refs. 43)
SS316	Refs. 39), 48)

In addition, Refs. 27) ~ 31) deal with comprehensive results for benchmark test for the recent three nuclear data libraries by analyzing the clean benchmark experiments. References 49) ~ 51) also deal with results for benchmark test for the recent three nuclear data libraries especially focussing on the secondary gamma-ray data.

## 4.3 Results for JENDL-3.2, JENDL Fusion File & FENDL/E-1.0

### Lithium Oxide

Results for calculations with JENDL-3.2 and FENDL-1 are compared with the experimental data in the following figures.

Neutron spectrum at 216 mm depth	Fig. 4.3.1
Neutron spectrum at 418 mm depth	Fig. 4.3.2
C/E ratios of dosimetry reaction rates	Fig. 4.3.3 (a) ~ (k)

### Beryllium

Results for calculations with JENDL-3.2, JENDL-FF and FENDL-1 are compared with the experimental data in the following figures.

Neutron spectrum at 127 mm depth	Fig. 4.3.4
Neutron spectrum at 279 mm depth	Fig. 4.3.5
C/E ratios of dosimetry reaction rates	Fig. 4.3.6 (a) ~ (l)

Graphite

Results for calculations with JENDL-3.2 and FENDL-1 are compared with the experimental data in the following figures.

Neutron spectrum at 117 mm depth	Fig. 4.3.7
Neutron spectrum at 218 mm depth	Fig. 4.3.8
Neutron spectrum at 320 mm depth	Fig. 4.3.9
Neutron spectrum at 421 mm depth	Fig. 4.3.10
C/E ratios of dosimetry reaction rates	Fig. 4.3.11 (a) ~ (h)

Iron

Results for calculations with JENDL-3.2, JENDL-FF and FENDL-1 are compared with the experimental data in the following figures.

Neutron spectrum at 110 mm depth	Fig. 4.3.12
Neutron spectrum at 210 mm depth	Fig. 4.3.13
Neutron spectrum at 310 mm depth	Fig. 4.3.14
Neutron spectrum at 410 mm depth	Fig. 4.3.15
Neutron spectrum at 610 mm depth	Fig. 4.3.16
Neutron spectrum at 810 mm depth	Fig. 4.3.17
C/E ratios of integral neutron fluxes	Fig. 4.3.18 (a) ~ (f)
C/E ratios of dosimetry reaction rates	Fig. 4.3.19 (a) ~ (j)
Gamma-ray spectrum at 300 mm depth	Fig. 4.3.20
Gamma-ray spectrum at 500 mm depth	Fig. 4.3.21
Gamma-ray spectrum at 700 mm depth	Fig. 4.3.22
C/E ratios of gamma-ray heating rate of iron	Fig. 4.3.23

Type 316 Stainless Steel (SS316)

Results for calculations with JENDL-3.2, JENDL-FF and FENDL-1 are compared with the experimental data in the following figures.

Neutron spectrum at -10 mm depth	Fig. 4.3.24
Neutron spectrum at 102 mm depth	Fig. 4.3.25
Neutron spectrum at 229 mm depth	Fig. 4.3.26
Neutron spectrum at 356 mm depth	Fig. 4.3.27
Neutron spectrum at 533 mm depth	Fig. 4.3.28
Neutron spectrum at 711 mm depth	Fig. 4.3.29
Neutron spectrum at 914 mm depth	Fig. 4.3.30
C/E ratios of integral neutron fluxes	Fig. 4.3.31 (a) ~ (h)
C/E ratios of dosimetry reaction rates	Fig. 4.3.32 (a) ~ (o)
Gamma-ray spectrum at 102 mm depth	Fig. 4.3.33

Gamma-ray spectrum at 356 mm depth	Fig. 4.3.34
Gamma-ray spectrum at 711 mm depth	Fig. 4.3.35
Gamma-ray spectrum at 914 mm depth	Fig. 4.3.36
C/E ratios of gamma-ray heating rate of SS316	Fig. 4.3.37

**Copper**

Results for calculations with JENDL-3.2, JENDL-FF and FENDL-1 are compared with the experimental data in the following figures.

Neutron spectrum at 76 mm depth	Fig. 4.3.38
Neutron spectrum at 228 mm depth	Fig. 4.3.39
Neutron spectrum at 380 mm depth	Fig. 4.3.40
Neutron spectrum at 532 mm depth	Fig. 4.3.41
C/E ratios of integral neutron fluxes	Fig. 4.3.42 (a) ~ (h)
C/E ratios of dosimetry reaction rates	Fig. 4.3.43 (a) ~ (k)
Gamma-ray spectrum at 76 mm depth	Fig. 4.3.44
Gamma-ray spectrum at 228 mm depth	Fig. 4.3.45
Gamma-ray spectrum at 380 mm depth	Fig. 4.3.46
Gamma-ray spectrum at 532 mm depth	Fig. 4.3.47
C/E ratios of gamma-ray heating rate of copper	Fig. 4.3.48

**Tungsten**

Results for calculations with JENDL-3.2, JENDL-FF and FENDL-1 are compared with the experimental data in the following figures.

Neutron spectrum at 76 mm depth	Fig. 4.3.49
Neutron spectrum at 228 mm depth	Fig. 4.3.50
Neutron spectrum at 380 mm depth	Fig. 4.3.51
C/E ratios of dosimetry reaction rates	Fig. 4.3.52 (a) ~ (d)
Gamma-ray spectrum at 76 mm depth	Fig. 4.3.53
Gamma-ray spectrum at 228 mm depth	Fig. 4.3.54
Gamma-ray spectrum at 380 mm depth	Fig. 4.3.55
C/E ratios of gamma-ray heating rate of tungsten	Fig. 4.3.56

#### 4.4 Results for FENDL/E-2.0

##### Graphite

Results for calculations with JENDL-3.2, which is same as JENDL-FF, and the modified JENDL-FF data are compared with the experimental data in the following figures.

Neutron spectrum at 320 mm depth	Fig. 4.4.1
Neutron spectrum at 572 mm depth	Fig. 4.4.2
C/E ratios of dosimetry reaction rates	Fig. 4.4.3 (a) ~ (d)

##### Iron

Results for calculations with FENDL-1 and the combination of FENDL-2, i.e., EFF-3 for Fe-56 and FENDL-1 for other three iron isotopes, are compared with the experimental data in the following figures.

Neutron spectrum at 410 mm depth	Fig. 4.4.4
Neutron spectrum at 810 mm depth	Fig. 4.4.5
C/E ratios of integral neutron fluxes	Fig. 4.4.6 (a) ~ (f)
C/E ratios of dosimetry reaction rates	Fig. 4.4.7 (a) ~ (d)
C/E ratios of gamma-ray heating rate of iron	Fig. 4.4.8

A serious error was found in the gamma-ray production cross section of Fe-56 data in EFF-3. As shown in Fig. 4.4.8, gamma-ray heating rates of iron were calculated considerably larger than the experimental data with EFF-3. It was turn out from an analysis of another benchmark experiment on iron<sup>52)</sup> that the error has been corrected in the final FENDL/E-2.0 library available since April, 1998.

## 5. OKTAVIAN Pulsed Sphere Experiment

### 5.1 Brief Description of the Experiment

A series of pulsed sphere experiments for 14-MeV neutron transmission has been performed at OKTAVIAN using spherical piles made of a variety of materials.<sup>53-56)</sup> Sample materials were Be, Li, LiF, CF<sub>2</sub>, Al, Si, Ti, Cr, Mn, Co, Cu, Zr, Nb, Mo and W. All the materials except for Be were packed in spherical shells by stainless steel or mild iron containers. For the Be measurement, a set of beryllium spherical shells of solid metal were used to make spheres with four different thicknesses by combining these shells. Overall thicknesses of the beryllium shells ranged from 45.5 mm to 11.65 mm. A D-T neutron target of the OKTAVIAN pulse beam line was centered at a spherical pile, and pulsed neutrons of ~ 2 ns in width were generated at the target. A neutron spectrum leaking from the spherical pile in an energy range from 14 MeV to 0.1 MeV was measured by the Time-Of-Flight method with an NE-218 scintillation detector located at ~ 11 m from the target.

Another series of pulsed sphere experiment for secondary gamma-ray spectrum was also performed at OKTAVIAN.<sup>57) ~ 59)</sup> Gamma-ray spectra leaking from sample materials, i.e., LiF, CF<sub>2</sub>, Al, Si, Ti, Cr, Mn, Co, Cu, Nb, Mo, W and Pb, were measured. Gamma-rays were detected with an NaI(Tl) scintillator located at 5.8 m from the target. Neutron events were discriminated by the flight time difference of neutrons and gamma-rays with adopting a time gate of 60 ~ 80 ns from the time of D-T neutron generation. Only gamma-rays were detected in the time gate. Due to this time gate, the measured spectra were dominated by gamma-rays from threshold reactions such as the (n,n') and (n,2n) reactions rather than gamma-rays from the (n, $\gamma$ ) reaction.

Numerical data of the measured neutron and gamma-ray spectra are compiled in Ref. 25).

### 5.2 Benchmark Calculation

Benchmark calculations were performed by MCNP-4A with JENDL-3.2, JENDL-FF and FENDL-1. Some other cross section libraries were also used for neutron calculations. The measured source neutron spectrum was used as a neutron source in the calculations. For leakage neutron spectrum calculations, an outer surface of the spherical pile was used for a surface crossing estimator. To take the time gate effect into account for secondary gamma-ray calculations, a surface crossing estimator was placed at the same distance from the D-T neutron source as the experiment, and the time cut-off was employed in the calculations. As gamma-rays were produced by interactions of source neutrons with the structural materials of the target, another series of calculations was performed starting with the target gamma-rays. Calculated gamma-ray spectra including the target gamma-rays were compared with the experimental spectrum. Details of the

analysis are given in Refs. 49), 60) ~ 63). Examples of input data for MCNP are given in Appendix. Calculations were also performed with the newly evaluated silicon data in ENDF/B-VI that was selected for FENDL-2.

Detailed discussions on the calculated results for JENDL-3.2, JENDL-FF and FENDL-1 are given in Refs. 28) ~ 31), 49) ~ 51) and 61) ~ 65).

### 5.3 Results for Neutron Spectrum

Neutron spectra calculated with JENDL-3.2, JENDL-FF and FENDL-1, and some other cross section libraries are compared with the experimental data in the following figures. The cross section library of "EFF" included in these figures stands for EFF version 2.4.

Lithium	Fig. 5.3.1
Lithium fluoride (LiF)	Fig. 5.3.2
Teflon (CF <sub>2</sub> )	Fig. 5.3.3
Aluminum	Fig. 5.3.4
Silicon (40 cm diam.)	Fig. 5.3.5
Silicon (40 cm diam.) (including the new ENDF/B-VI evaluation)	Fig. 5.3.6
Silicon (60 cm diam.)	Fig. 5.3.7
Titanium	Fig. 5.3.8
Chromium	Fig. 5.3.9
Manganese	Fig. 5.3.10
Cobalt	Fig. 5.3.11
Copper	Fig. 5.3.12
Zirconium	Fig. 5.3.13
Niobium	Fig. 5.3.14
Molybdenum	Fig. 5.3.15
Tungsten	Fig. 5.3.16
Beryllium (45.5 mm thickness)	Fig. 5.3.17
Beryllium (76.5 mm thickness)	Fig. 5.3.18
Beryllium (104.5 mm thickness)	Fig. 5.3.19
Beryllium (116.5 mm thickness)	Fig. 5.3.20

The measured and calculated neutron fluxes integrated in several energy bins are compared as C/E ratios. Tables 5.1 ~ 5.4 summarizes these C/E ratios.

## 5.4 Results for Secondary Gamma-Ray Spectrum

Gamma-ray spectra calculated with JENDL-3.2, JENDL-FF and FENDL-1 are compared with the experimental data in the following figures.

Lithium fluoride (LiF)	Fig. 5.4.1
Teflon (CF <sub>2</sub> )	Fig. 5.4.2
Aluminum	Fig. 5.4.3
Silicon	Fig. 5.4.4
Titanium	Fig. 5.4.5
Chromium	Fig. 5.4.6
Manganese	Fig. 5.4.7
Cobalt	Fig. 5.4.8
Copper	Fig. 5.4.9
Niobium	Fig. 5.4.10
Molybdenum	Fig. 5.4.11
Tungsten	Fig. 5.4.12
Lead	Fig. 5.4.13

Also, gamma-ray spectra from the silicon sphere calculated with ENDF/B-VI and JENDL-FF are compared with the experimental data in Fig. 5.4.14.

The measured and calculated gamma-ray spectra are integrated in the two ways to compare numerically each other.

$$I_E = \int E \cdot \phi_\gamma(E) \cdot dE \quad (5-1)$$

$$I_N = \int \phi_\gamma(E) \cdot dE \quad (5-2)$$

The  $I_E$  corresponds to the total gamma-ray energy observed while  $I_N$  means just the total number of gamma-ray fluxes. C/E ratios for the two integral quantities,  $I_N$  and  $I_E$  are compared in Figs. 5.4.15 and 5.4.16, respectively.

## 6. Overview of Results for Each Element

Results of benchmark test for each element are briefly summarized in this chapter.

### Lithium

Neutron: FNS TOF and Clean Benchmark Experiments on Li<sub>2</sub>O  
OKTAVIAN Experiment on Lithium, LiF and CF<sub>2</sub>

In the comparisons of neutron spectra for the FNS-TOF experiment as shown in Figs. 3.3.1 ~ 3.3.3 and also OKTAVIAN experiment on lithium as shown in Fig. 5.3.1, both JENDL-3.2 (= JENDL-FF) and FENDL-1 (= ENDF/B-VI, FENDL-2) calculations follow very nicely the experimental spectra. In the FNS clean benchmark experiment, most of the reaction rates for either threshold reactions for high energy neutrons and exothermic reactions for low energy neutrons, including the most important tritium production reactions of <sup>6</sup>Li(n, $\alpha$ )T and <sup>7</sup>Li(n,n' $\alpha$ )T, are predicted adequately by all the calculations. Consequently, JENDL-3.2, JENDL-FF and FENDL-1 cross sections are very accurate.

### Beryllium

Neutron: FNS TOF and Clean Benchmark Experiments on Beryllium  
OKTAVIAN Experiment on Beryllium

In the FNS-TOF experiment shown in Figs. 3.3.4 and 3.3.5, results by JENDL-FF (= FENDL-2) and FENDL-1 (= ENDF/B-VI) agree very well with the experimental data while those by JENDL-3.2 are slightly larger than the experimental data at  $\sim$  1 MeV. On the other hand, in the OKTAVIAN experiment, neutron fluxes calculated by JENDL-3.2 are closer to the experimental data compared with those calculated by JENDL-FF and FENDL-1. Since both results seem to be inconsistent, further investigation is needed.

### Carbon

Neutron: FNS TOF and Clean Benchmark Experiments on Graphite

Judging from the results of the FNS-TOF experiment as shown in Figs. 3.3.6 ~ 3.3.8, neutron spectra calculated by JENDL-3.2 (= JENDL-FF) are better than those by FENDL-1 (= ENDF/B-VI). A part of JENDL-3.2 cross section data of carbon was replaced with ENDF/B-VI cross section data for FENDL-2. Figure 3.4.1 compares neutron spectra

before and after the replacement. Both calculations agree very well with the experimental data for elastic and discrete inelastic scattering peaks and broad spectra below 3 MeV mostly produced by neutrons from the  $^{12}\text{C}(\text{n},\text{n}')3\alpha$  reaction. Both JENDL-3.2 and modified JENDL-FF also predict various reaction rates as shown in Fig. 4.4.3. This good prediction suggests accurate cross section data for either high- and low-energy neutrons.

#### Gamma-ray: OKTAVIAN Experiment on CF<sub>2</sub>

Gamma-rays emitted from  $^{12}\text{C}$  induced by threshold reactions have a unique energy of 4.44 MeV. The gamma-ray peak is clearly observed in Fig. 5.4.2. Since the measured and calculated gamma-ray peak areas agree within 10 %, gamma-ray production data of carbon in JENDL-FF (= FENDL-2) and FENDL-1 are valid.

#### Nitrogen

##### Neutron: FNS TOF Experiment on Liquid-Nitrogen

In the comparisons of neutron spectra from liquid nitrogen, JENDL-3.2 (= JENDL-FF for  $^{14}\text{N}$ ) gives better spectra compared with FENDL-1 (= BROND-2). Slightly modified cross section of JENDL-3.2 is adopted for FENDL-2. Since the modification is minor, neutron spectra calculated with cross sections before and after the modification are almost the same as shown in Fig. 3.4.2. The experimental spectra are predicted adequately by both cross sections.

#### Oxygen

##### Neutron: FNS TOF Experiment on Liquid-Oxygen and Li<sub>2</sub>O FNS Clean Benchmark Experiments on Li<sub>2</sub>O

As previously described in the section of lithium, very good results are obtained for the FNS experiments on lithium oxide. This fact implies adequate cross section of oxygen for both JENDL-FF (= JENDL-3.2, FENDL-2) and FENDL-1 (= ENDF/B-VI). The results of FNS-TOF experiment on pure liquid oxygen support the fact. Neutron spectra calculated by both JENDL-FF and FENDL-1 agree very well with the experimental data.

## **Fluorine**

Neutron: OKTAVIAN Experiment on LiF and CF<sub>2</sub>

Experimental data are available only for chemical compounds with fluorine, i.e., LiF and CF<sub>2</sub>. Although accurate cross sections are given for lithium and carbon as mentioned previously, calculated spectra with JENDL-FF and FENDL-1 (= ENDF/B-VI, FENDL-2) are considerably smaller than the experimental data as found in Figs. 5.3.2 and 5.3.3, and Table 5.1. According to this result, cross section data of fluorine in both JENDL-FF and FENDL-1 should be re-evaluated.

Gamma-ray: OKTAVIAN Experiment on LiF and CF<sub>2</sub>

Gamma-ray spectra are measured for chemical compounds of fluorine, i.e., LiF and CF<sub>2</sub>, however, all the gamma-rays except for the 4.44 MeV line from <sup>12</sup>C are produced from fluorine. As shown in Figs. 5.4.1, 5.4.2, 5.4.15 and 5.4.16, secondary gamma-ray data of fluorine in both JENDL-FF and FENDL-1 are adequate.

## **Aluminum**

Neutron: OKTAVIAN Experiment on Aluminum

Neutron spectra calculated by JENDL-FF and FENDL-1 (= JENDL-3.1, FENDL-2) almost agree well with the experimental data except for slight overestimation of neutron fluxes at  $\sim 0.5$  MeV by both, as shown in Fig. 5.3.4.

Gamma-ray: OKTAVIAN Experiment on Aluminum

Both JENDL-FF and FENDL-1 predict very nicely the experimental data as shown in Fig. 5.4.3, 5.4.15 and 5.4.16.

## **Silicon**

Neutron: OKTAVIAN Experiment on Silicon

As shown in Figs. 5.3.5 ~ 5.3.7, neutron spectra calculated by FENDL-1 (= BROND-2) are larger than the experimental data. Calculated spectrum with the new silicon evaluation of ENDF/B-VI shows very good agreement with the experimental data. The selection of the new ENDF/B-VI evaluation for FENDL-2 is reasonable.

**Gamma-ray: OKTAVIAN Experiment on Silicon**

As shown in Figs. 5.4.4 and 5.4.14, gamma-ray spectrum calculated by FENDL-1 gives smaller than the measured spectrum, while both JENDL-FF and ENDF/B-VI predict adequately the measured spectrum.

**Titanium****Neutron: OKTAVIAN Experiment on Titanium**

Cross section data of titanium in JENDL-3.1 are taken as the data of FENDL-1, FENDL-2 and EFF-2.4, and cross section data in JENDL-3.1, JENDL-3.2 and JENDL-FF are very similar. Therefore, as shown in Fig. 5.3.8, all the calculated spectra except for that by BMCCS are very similar. Cross section of JENDL-3.1 is adopted for FENDL-2. Neutron fluxes calculated by all the JENDL based cross sections are larger than the experimental data below 5 MeV.

**Gamma-ray: OKTAVIAN Experiment on Titanium**

Although slight discrepancies between the measured and calculated gamma-ray spectra are found, agreements between both spectra are good as shown in Fig. 5.4.6.

**Chromium****Neutron: OKTAVIAN Experiment on Chromium**

Both the ENDF/B-VI (= FENDL-1 and FENDL-2) and JENDL-FF calculations agree well with the experimental data, as shown in Fig. 5.3.9.

**Gamma-ray: OKTAVIAN Experiment on Chromium**

As shown in Fig. 5.4.6, Gamma-ray spectrum calculated by ENDF/B-VI follows the measured spectrum. On the other hand, spectrum by JENDL-FF are larger and smaller than the measured spectrum in the energy ranges of 1.5 ~ 5 MeV and > 5 MeV, respectively.

## Manganese

**Neutron:** OKTAVIAN Experiment on Manganese

Both the ENDF/B-VI (= FENDL-1 and FENDL-2) and JENDL-FF calculations agree well with the experimental data, as shown in Fig. 5.3.10.

**Gamma-ray:** OKTAVIAN Experiment on Manganese

Both gamma-ray spectra calculated by JENDL-FF and FENDL-1 agree well with the experimental data, as shown in Fig. 5.4.7.

## Iron

**Neutron:** FNS TOF and Clean Benchmark Experiments on Iron

For both FNS experiments, calculations with JENDL-FF, FENDL-1 (= ENDF/B-VI) and FENDL-2 (EFF-3 for  $^{56}\text{Fe}$ , ENDF/B-VI for  $^{54}, 57, 58\text{Fe}$ ) predict within 10 % the measured neutron fluxes for the entire energy range from 14 MeV down to 1 eV. These cross section data of iron are fairly reliable.

**Gamma-ray:** FNS Clean Benchmark Experiment on Iron

As shown in Figs. 4.3.23 and 4.4.8, C/E ratios of gamma-ray heating calculated by FENDL-1 and JENDL-FF are very close to unity for iron thicknesses up to 800 mm while those by FENDL-2 and JENDL-3.2 are rather large at the positions near the D-T neutron source. The overestimation of gamma-ray heating rates by FENDL-2 and JENDL-3.2 indicates too large gamma-ray production cross sections for high energy neutrons. Note that the FENDL-2 cross section data including too large gamma-ray production cross sections used for the benchmark test have been already revised in the final FENDL-2 library available since 1998. The new iron data in FENDL-2 provide almost the same results for gamma-rays with those calculated by FENDL-1 and JENDL-FF.<sup>52)</sup>

## Cobalt

**Neutron:** OKTAVIAN Experiment on Cobalt

All the calculations in Fig. 5.3.11 predict adequately the 14-MeV neutron fluxes,

however, neutron fluxes below 10 MeV are calculated smaller than the experimental data by all the cross section data. Both FENDL-1 and FENDL-2 adopt ENDF/B-VI.2 cross section data.

#### Gamma-ray: OKTAVIAN Experiment on Cobalt

Gamma-ray spectra calculated by JENDL-FF and JENDL-3.2 agree well with the experimental data while spectrum by FENDL-1 is smaller than the experimental data above 3 MeV, as shown in Fig. 5.4.8.

### **SS-316**

#### Neutron: FNS Clean Benchmark Experiments on SS-316

As a general trend, agreements of the calculated results by FENDL-1 and JENDL-FF with the experimental data are nearly the same as those for iron because iron is the main constituent of SS-316. Both calculations predict adequately the experimental data. The agreements for SS-316 are, however, slightly worse than those for iron. This fact suggests that some cross sections for constituents of SS-316 other than iron, i.e., chromium, nickel, manganese, molybdenum, and so on, may contain some inaccurate data.

#### Gamma-ray: FNS Clean Benchmark Experiment on SS-316

Gamma-ray heating rates and spectra are calculated with good accuracy by both FENDL-1 and JENDL-FF.

### **Copper**

#### Neutron: FNS Clean Benchmark Experiment on Copper OKTAVIAN Experiment on Copper

For both FNS and OKTAVIAN experiments, neutron spectrum fluxes for a high energy region above 1 keV are adequately calculated by FENDL-1 (= ENDF/B-VI, FENDL-2) and JENDL-FF. In a low energy region below 1 keV, however, neutron fluxes by both calculations are considerably smaller than the experimental data as shown in Figs. 4.3.38 ~ 4.3.41.

**Gamma-ray: FNS Clean Benchmark Experiment on Copper  
OKTAVIAN Experiment on Copper**

Gamma-ray spectra for the OKTAVIAN experiment (Fig. 5.4.9) and for the FNS experiment near the D-T neutron source (Figs. 4.3.44 and 45) calculated by FENDL-1 and JENDL-FF agree well with the experimental data. This result suggests valid gamma-ray production cross sections for threshold reactions in both libraries. On the other hand, gamma-ray spectra measured at deep inside of the FNS copper assembly (Figs. 4.3.46 and 4.3.47) are not reproduced accurately. Gamma-ray peaks observed at 8 MeV are represented too strong by both calculations. Gamma-ray spectra associated with the  $(n,\gamma)$  reaction induced mainly by low energy neutrons should be modified.

**Zirconium**

Neutron: OKTAVIAN Experiment on Zirconium

As a whole, agreements of calculated spectra by JENDL-FF (= FENDL-2) and FENDL-1 (BROND-2) are good as shown in Fig. 5.3.13.

**Niobium**

Neutron: OKTAVIAN Experiment on Niobium

As shown in Fig. 5.3.14, FENDL-1 (= BROND-2) and JENDL-FF (= FENDL-2) calculations almost agree with the experimental data in a high energy range above 5 MeV while both calculations give larger neutron fluxes below 1 MeV.

Gamma-ray: OKTAVIAN Experiment on Niobium

All the three calculated spectra in Fig. 5.4.10 almost follow the experimental gamma-ray spectrum.

**Molybdenum**

Neutron: OKTAVIAN Experiment on Molybdenum

Neutron fluxes between 5 and 10 MeV calculated by FENDL-1 (JENDL-3.1) are 30 % smaller than the experimental data. This underestimation is modified in JENDL-FF

(FENDL-2). Neutron fluxes calculated by JENDL-FF agree well with the experimental fluxes.

#### Gamma-ray: OKTAVIAN Experiment on Molybdenum

All the three calculated spectra in Fig. 5.4.11 agree very well with the experimental gamma-ray spectrum.

### Tungsten

Neutron: FNS Clean Benchmark Experiment on Tungsten  
OKTAVIAN Experiment on Tungsten

As clearly represented in Fig. 4.3.51, a broad peak of low energy neutron flux between 1 keV to 10 MeV calculated by JENDL-3.2 shifts toward lower energy compared with the experimental data. The low energy peak by FENDL-1 (= ENDF/B-VI) is smaller than the experimental data. The low energy peak is best predicted by JENDL-FF (FENDL-2) among the three calculations in Fig. 4.3.51.

Gamma-ray: FNS Clean Benchmark Experiment on Tungsten  
OKTAVIAN Experiment on Tungsten

All the three calculated spectra in Figs. 4.3.53 ~ 4.3.55 and 5.4.12 almost agree with the experimental gamma-ray spectrum.

### Lead

Neutron: FNS TOF Experiment on Lead

As shown in Figs. 3.3.15 ~ 3.3.17, low energy parts of neutron spectra calculated by JENDL-3.2 are softer than the experimental data while both FENDL-1 (= ENDF/B-VI, FENDL-2) and JENDL-3.2 gives adequate neutron spectra.

Gamma-ray: OKTAVIAN Experiment on Lead

As shown in Fig. 5.4.13, gamma-ray spectra calculated by both FENDL-1 and JENDL-FF almost agree well with the experimental data.

## 7. Summary

Results for benchmark calculations for the three series of fusion neutronics experiments, i.e., FNS-TOF experiment, FNS clean benchmark experiment and the OKTAVIAN pulsed sphere experiment, were compiled. Three evaluated nuclear data libraries, JENDL-3.2, JENDL Fusion File and FENDL/E-1.0, as well as some candidate cross sections for FENDL/E-2.0 were used for the benchmark test. Comparisons of benchmark calculation results with the experimental data for as many as twenty-one elements, i.e., Li, Be, C, N, O, F, Al, Si, Ti, V, Cr, Mn, Fe, Co, Ni, Cu, Zr, Nb, Mo, W and Pb, are included. The results have contributed to improvement of quality of the data in JENDL-3.2 and JENDL Fusion File. The results have also contributed to give a guide line for the selection of cross sections to be adopted for FENDL/E-2.0. We hope these benchmark results will be used for further improvement of JENDL and other evaluated nuclear data libraries, and also, for validating nuclear designs of fusion reactors.

## Acknowledgment

The authors gratefully acknowledge Dr. Y. Ikeda and Dr. H. Maekawa for their help to conduct the benchmark calculations. They also wish to express all the members of the Fusion Neutronics Integral Test Working Group and the Shielding Integral Test Working Group of the Japanese Nuclear Data Committee for useful discussions for this work.

## References

- 1) Nakamura T., Maekawa H., Ikeda Y. and Oyama Y.: "A DT Neutron Source for Fusion Neutronics Experiments at the JAERI", Proc. International Ion Eng. Congress - ISIAT '83 & IAPT '83, Kyoto, Japan, Vol. 1, pp. 567-570 (1983).
- 2) Sumita K., Takahashi A., Iida T., Yamamoto J., Imoto S. and Matsuda K.: "Osaka University 14-MeV Intense Neutron Source and Its Utilizations for Fusion Studies (OKTAVIAN Program)", Proc. 12th Symposium on Fusion Technology, KFA, Jülich, Germany, Sep. 13-17, 1982, pp. 975-680 (1983).
- 3) Shibata K., et al.: "Japanese Evaluated Nuclear Data Library, Version-3 -- JENDL-3 --", JAERI 1319 (1990).
- 4) Nakagawa T., Shibata K., Chiba S., Fukahori T., Nakajima Y., Kikuchi Y., Kawano T., Kanda Y., Osawa T., Matsunobu H., Kawai M., Zukeiran A., Watanabe T., Igarashi S., Kosako K. and Asami T.: "Japanese Evaluated Nuclear Data Library Version 3 Revision-2: JENDL-3.2", J. Nucl. Sci. Technol., 32, pp. 1259-1271 (1995).
- 5) Chiba S., Yu B. and Fukahori T.: "Evaluation of JENDL Fusion File", JAERI-M 92-027, pp. 35-44, Japan Atomic Energy Research Institute (1992); Chiba S., Fukahori T., Yu B. and Kosako K.: "Evaluation of the Double-Differential Cross Sections of Medium-Heavy Nuclei for JENDL Fusion File", Proc. 3rd Specialists' Meeting on Nuclear Data for Fusion Reactors, November 29 - 30, 1995, Tokai, Japan, JAERI-Conf 96-005, pp. 45-54 (1996).
- 6) Ganesan S. and McLaughlin P. K., "FENDL/E Evaluated Nuclear Data Library of Neutron Nuclear Interaction Cross-Sections and Photon Production Cross-Sections and Photon-Atom Interaction Cross Sections for Fusion Applications Version 1.0 of May 1994", IAEA-NDS-128, International Atomic Energy Agency (1995).
- 7) Rose P. F. (Ed.): "ENDF-201 ENDF/B-VI Summary Documentation", BNL-NCS-17541, Brookhaven National Laboratory (1991).
- 8) Blokhin A. I., Ignatyuk A. V., Kuzminov B. D., Koshcheev V. N., Manokhin V. N., Manturov G. N. and Nikolaev M. N.: "Library of Evaluated Neutron data Files", Proc. International Conference on Nucl. Data for Science and Technology, Jülich, Germany, May 13-17, 1991, pp. 800-803 (1992).
- 9) Gruppelaar H. and Kopecky J.: "Status Report EFF/EAF Projects May 1994 - European Fusion and Activation File Project", Proc. International Conference on Nucl. Data for Science and Technology, Gatlinburg, Tennessee, USA, May 9-13, 1994, pp. 699-701 (1994).

- 10) Pashchenko A. B.: "Summary Report of IAEA Consultants' Meeting on Selection of Basic Evaluations for the FENDL-2 Library", Proc. of IAEA Consultants' Meeting, Karlsruhe, Germany, June 24-28, 1996, INDC(NDS)-356 (1996).
- 11) Herman M. and Pashchenko A. B.: "Extension and Improvement of the FENDL Library for Fusion Applications (FENDL-2)", Report on IAEA Advisory Group Meeting, IAEA Headquarters, Vienna, Austria, March 3-7, 1997, INDC(NDS)-373 (1997).
- 12) Briesmeister J. F. (Ed.): "MCNP - A General Monte Carlo N-Particle Transport Code, Version 4A", LA-12625-M, Los Alamos National Laboratory (1993).
- 13) Kosako K., Maekawa F., Oyama Y., Uno Y. and Maekawa H.: "FSXLIB-J3R2: A Continuous Energy Cross Section Library for MCNP Based on JENDL-3.2", JAERI-Data/Code 94-20 (1994); Kosako K., Yamano N., Maekawa F. and Oyama Y.: "Production and Verification of the MCNP Cross Section Library FSXLIB-J3R2 Based on JENDL-3.2", Proc. ANS 1996 Radiation Protection and Shielding Division Topical Meeting, Cape Cod, Massachusetts, U.S.A., Apr. 21-25, 1996, pp. 1088-1095 (1996).
- 14) Kosako K.: "Present Status of Cross Section Libraries", Proc. 3rd Specialists' Meeting on Nuclear Data for Fusion Reactors, Tokai, Japan, Nov. 29 - 30, 1995, JAERI-Conf 96-005, pp. 55-62 (1996).
- 15) Ganesan S. and Wienke H.: "FENDL/MC-1.0 Library of Continuous Energy Cross Sections in ACE Format for Neutron-Photon Transport Calculations with the Monte Carlo N-Particle Transport Code System MCNP 4A", IAEA-NDS-169 (1995).
- 16) Nakazawa M., Kobayashi K., Iwasaki S., Iguchi T., Sakurai K., Ikeda Y. and Nakagawa T.: "JENDL Dosimetry File", JAERI 1325 (1991).
- 17) Roussin R. W., Knight J. R., Hubbell J. H. and Howerton R. J.: "Description of the DLC-99/HUGO Package of Photon Interaction Data in ENDF/B-V Format", ORNL/RSIC-46 (ENDF-335), Oak Ridge National Laboratory (1983).
- 18) Oyama Y. and Maekawa H.: "Spectral Measurement of Angular Neutron Flux on the Restricted Surface of Slab Assemblies by the Time-Of-Flight Method", Nucl. Instrum. Meth, A245, pp. 173-181 (1986).
- 19) Oyama Y. and Maekawa H.: "Measurement and Analysis of an Angular Neutron Flux on a Beryllium Slab Irradiated with Deuterium-Tritium Neutrons", Nucl. Sci. Eng., 97, pp. 220-234 (1987).
- 20) Oyama Y., Yamaguchi S. and Maekawa H.: "Measurement and Analyses of Angular Neutron Flux Spectra on a Graphite and Lithium-Oxide Slabs Irradiated with 14.8 MeV Neutrons", J. Nucl. Sci. Technol., 25, pp. 419-428 (1988).

- 21) Oyama Y.: "Experimental Study of Angular Neutron Flux Spectra on a Slab Surface to Assess Nuclear Data and Calculational Methods for a Fusion Reactor Design", JAERI-M 88-101 (1988).
- 22) Maekawa H. and Oyama Y.: "Experiment on Angular Neutron Flux Spectra from Lead Slabs Bombarded by D-T Neutrons", Fusion Eng. Des., 18, pp. 287-291 (1991).
- 23) Oyama Y., Maekawa H. and Kosako K.: "Measurement and Analyses of Angular Neutron Flux Spectra Leaking from Liquid Nitrogen, Liquid Oxygen and Iron Slabs", Proc. International Conference on Nucl. Data for Science and Technology, May 13-17, 1991, Jülich, Germany, pp. 337-340 (1991).
- 24) Oyama Y., Kosako K. and Maekawa H.: "Measurement and Calculations of Angular Neutron Flux Spectra from Iron Slabs Bombarded with 14.8-MeV Neutrons", Nucl. Sci. Eng., 115, pp. 24-37 (1993).
- 25) Sub Working Group of Fusion Reactor Physics Subcommittee (Ed.): "Collection of Experimental Data for Fusion Neutronics Benchmark", JAERI-M 94-014 (1994).
- 26) Oyama Y., Yamaguchi S. and Maekawa H.: "Experimental Results of Angular Neutron Flux Spectra Leaking from Slabs of Fusion Reactor Candidate Materials (I)", JAERI-M 90-092 (1990).
- 27) Oyama Y., Maekawa F. and Wada M.: "Integral Data Test of JENDL-3.2 and Fusion File Using FNS Benchmark Experiments", Proc. 3rd Specialists' Meeting on Nuclear Data for Fusion Reactors, Nov. 29-30, 1995, Tokai, JAERI, JAERI-Conf 96-005, pp. 70-79 (1996).
- 28) Fischer U. and the International Working Group on Experimental and Calculational Benchmarks on Fusion Neutronics for FENDL Validation: "Benchmark Validation of the FENDL-1 Nuclear Data Library -A Co-ordinated International Effort -", Fusion Technol., 30, pp. 1093-1100 (1996).
- 29) Maekawa F.: "Integral Test of JENDL Fusion File", Proc. '96 Symposium on Nuclear Data, Tokai, JAERI, Nov. 21-22, 1996, JAERI-Conf 97-005, pp. 21-26 (1997).
- 30) Oyama Y., Maekawa F. and Wada M.: "Integral Data Test of FENDL-1 Library and Japanese Candidates of FENDL-2 Using FNS Experiments", Proc. International Conference on Nucl. Data for Science and Technology, May 19-24, 1997, Trieste, Italy, pp. 1206-1208 (1998).
- 31) Wu Y. and Fischer U.: "Integral Data Tests of the FENDL-1, EFF-2, EFF-3 and JENDL-FF Fusion Nuclear Data Libraries", Proc. International Conference on Nucl. Data for Science and Technology, May 19-24, 1997, Trieste, Italy, pp. 1155-1157 (1998).

- 32) Maekawa H., Ikeda Y., Oyama Y., Yamaguchi S., Tsuda K., Fukumoto T., Kosako K., Yoshizawa M. and Nakamura T.: "Fusion Blanket Benchmark Experiments on a 60 cm-thick Lithium-Oxide Cylindrical Assembly", JAERI-M 86-182 (1986).
- 33) Maekawa H., Yamaguchi S., Konno C., Oyama Y., Ikeda Y., Sekiyama K. and Kosako K.: "Benchmark Experiment and Analysis of a Beryllium Cylindrical Assembly", Fusion Technol., 19, pp. 1949-1954 (1991).
- 34) Maekawa H., Ikeda Y., Oyama Y., Yamaguchi S., Tsuda K., Fukumoto T., Kosako K., Yoshizawa M. and Nakamura T.: "Benchmark Experiments on a 60 cm-thick Graphite Cylindrical Assembly", JAERI-M 88-034 (1988).
- 35) Maekawa F., Konno C., Kasugai Y., Oyama Y. and Ikeda Y.: "Data Collection of Fusion Neutronics Benchmark Experiment Conducted at FNS/JAERI", JAERI-Data/Code 98-021 (1998).
- 36) Oishi K., Ikeda Y., Konno C. and Nakamura T.: "Measurement and Analysis of Neutron Spectra in a Large Cylindrical Iron Assembly Irradiated by 14 MeV Neutrons", Proc. 7th International Conference Radiation Shielding, Bournemouth, United Kingdom, Sept. 12-16, 1988, pp. 331-340, United Kingdom Atomic Energy Authority, Winfrith and the Organization for Economic Cooperation and Development, Nuclear Energy Agency (1988).
- 37) Konno C., Ikeda Y., Kosako K., Oyama Y., Maekawa H., Nakamura T. and Bennet E. F.: "Measurement and Analysis of Low Energy Neutron Spectrum in a Large Cylindrical Iron Assembly Bombarded by D-T Neutrons", Fusion Eng. Des., 18, 297 (1991).
- 38) Maekawa F. and Oyama Y.: "Measurement of Neutron Energy Spectra below 10 keV in an Iron Shield Bombarded by D-T neutrons and Benchmark Test of Recent Evaluated Nuclear Data Libraries from 14 MeV Down to 1 eV", Nucl. Sci. Eng., 125, 205 (1997).
- 39) Maekawa F., Oyama Y., Konno C., Wada M. and Ikeda Y.: "Measurement of Gamma-Ray Spectra and Heating Rates in Iron and Stainless Steel Shields Bombarded by Deuterium-Tritium Neutrons and Validation of Secondary Gamma-Ray Data in Evaluated Nuclear Data Libraries", Nucl. Sci. Eng., 126, 187 (1997).
- 40) Konno C., Maekawa F., Oyama Y., Ikeda Y. and Maekawa H.: "Benchmark Experiment on Copper with D-T Neutrons for verification of Neutron Transport and Related nuclear Data of JENDL-3.1", ISFNT-3, Fusion Eng. Des., 28, 745 (1995).
- 41) Maekawa F., Oyama Y., Konno C., Ikeda Y. and Maekawa H.: "Benchmark Experiment on Copper with D-T Neutrons for Verification of Secondary Gamma-ray Data in JENDL-3.1", ISFNT-3, Fusion Eng. Des., 28, 753 (1995).

- 42) Maekawa F., Oyama Y., Konno C., Ikeda Y., Kosako K. and Maekawa H.: "Benchmark Experiment on a copper Slab Assembly Bombarded by D-T Neutrons", JAERI-M 94-038 (1994).
- 43) Maekawa F., Konno C., Oyama Y., Wada M., Uno Y. and Ikeda Y.: "Benchmark Experiment on Tungsten Assembly Bombarded with D-T Neutrons", Proc. International Conference on Nucl. Data for Science and Technology, Trieste, Italy, May 19-24, 1997, pp. 1218-1220 (1998).
- 44) Konno C., Maekawa F., Ikeda Y., Oyama Y., Kosako K. and Maekawa H.: "Bulk Shielding Experiments on Large SS316 Assemblies", Fusion Technol., 21, 2169 (1992).
- 45) Maekawa F., Konno C., Kosako K., Oyama Y., Ikeda Y. and Maekawa H.: "Analysis of Bulk Shielding Experiments on Large SS316 Assemblies", Fusion Technol., 21, 2107 (1992).
- 46) Konno C., Maekawa F., Oyama Y., Ikeda Y., Kosako K. and Maekawa H.: "Bulk Shielding Experiments on Large SS316 Assemblies Bombarded by D-T Neutrons Volume I: Experiment", JAERI-Research 94-043 (1994).
- 47) Maekawa F., Konno C., Kosako K., Oyama Y., Ikeda Y. and Maekawa H.: "Bulk Shielding Experiments on Large SS316 Assemblies Bombarded by D-T Neutrons, Volume II: Analysis", JAERI-Research 94-044 (1994).
- 48) Konno C., Maekawa F., Oyama Y., Ikeda Y., Wada M. and Maekawa H.: "Validation of Nuclear Calculations with FENDL/E-1.1 and JENDL Fusion File Based on Fusion Bulk Shielding Experiments on Large SS316 Assemblies", to be published in Fusion Technol. (1998).
- 49) Maekawa F. and Oyama Y.: "Benchmark Test of Gamma-Ray Production Data in JENDL-3.2 and FENDL-1", Proc. of 1st Research Co-ordination Meeting on Measurement, Calculation and Evaluation of Photon Production Data, Bologna, Italy, Nov. 14-17, 1994, INDC(NDS)-334, pp. 139-145 (1995).
- 50) Shibata K. and Maekawa F.: "Gamma-Ray Production Data in JENDL-3.2", Proc. of Specialists' Meeting on Measurement, Calculation and Evaluation of Photon Production Data, Bologna, Italy, Nov. 9-11, 1994, NEA/NSC/DOC(95)1, pp. 317-327 (1995).
- 51) Maekawa F.: "Nuclear Data Test with Gamma-Ray Integral Experiments", Proc. 3rd Specialists' Meeting on Nuclear Data for Fusion Reactors, Tokai, JAERI, Nov. 29-30, 1995, JAERI-Conf 96-005, pp. 92-101 (1996).
- 52) Maekawa F., Konno C., Wada M., Uno Y., Kasugai Y. and Ikeda Y.: "Duct Streaming Experiment for ITER Volume II: Analysis", ITER/EDA Task T-362 Report, to be published as a JAERI-Research Report (1998).

- 53) Ichihara C., Hayashi S. A., Kobayashi K. and Kimura I.: "The Measurement of Leakage Neutron Spectra from Various Sphere Piles with 14 MeV Neutrons", Proc. International Conference on Nucl. Data for Science and Technology, Mito, Japan, May 30-June 3, 1988, pp. 319-322 (1988).
- 54) Ichihara C., Hayashi S. A., Kobayashi K., Kimura I., Yamamoto J. and Takahashi A.: "Measurement of Leakage Neutron Spectra from Various Sphere Piles for Fusion Reactor Related Materials with 14 MeV Neutrons", Proc. 2nd Specialists' Meeting on Nuclear Data for Fusion Reactors", Tokai, JAERI, Dec. 21-21, 1990, JAERI-M 91-062, pp. 255-267 (1991).
- 55) Ichihara C., Kobayashi K., Hayashi S. A., Kimura I., Yamamoto J. and Takahashi A.: "Leakage Neutron Spectra from Various Sphere Piles with 14 MeV Neutrons", JAERI-M 94-014, pp. 63-125, (1994).
- 56) Murakami Y., Yoshioka K., Yamanaka K., Takahashi A., Sumita K.: "Leakage Spectra from Beryllium Sphere and Beryllium-Lithium Sphere", JAERI-M 94-014, pp.18-31 (1994)
- 57) Yamamoto J., Kanaoka T., Murata I., Takahashi A. and Sumita K.: "Gamma-Ray Emission Spectra from Spheres with 14-MeV Neutron Source", JAERI-M 89-026, pp. 232-242, (1989).
- 58) Yamamoto J.: "Integral Experiment on Gamma-Ray Production at OKTAVIAN", Proc. 2nd Specialists' Meeting on Nuclear Data for Fusion Reactors", Tokai, JAERI, Dec. 21-21, 1990, JAERI-M 91-062, pp. 118-125, (1991).
- 59) Yamamoto J., Kanaoka T., Murata I., Takahashi A. and Sumita K.: "Gamma-Ray Energy Spectra Emitted from Spheres with 14-MeV Neutron Source", JAERI-M 94-014, pp. 32-62, (1994).
- 60) Maekawa F., Kosako K. and Oyama Y.: "Verification of Gamma-Ray Data in JENDL-3.1 through Analysis of OKTAVIAN Experiment", Proc. International Conference on Nucl. Data for Science and Technology, Gatlinburg, Tennessee, USA, May 9-13, 1994, pp. 792-794 (1994).
- 61) Maekawa F. and Oyama Y.: "Benchmark Test of 14-MeV Neutron-Induced Gamma-Ray Production Data in JENDL-3.2 and FENDL/E-1.0 through Analysis of the OKTAVIAN Experiments", Nucl. Sci. Eng., 123, 272 (1996).
- 62) Ichihara C., Hayashi S. A., Yamamoto J., Kimura I. and Takahashi A.: "Benchmark Test of JENDL-3.2 with Pulsed Sphere Experiment Using OKTAVIAN", Proc. '94 Symposium on Nuclear Data, Tokai, JAERI, Nov. 17-18, 1994, JAERI-Conf 95-008, pp. 173-176 (1995).

- 63) Ichihara C., Hayashi S. A., Kimura I., Yamamoto J., Makita Y., Takahashi A., Ueki K. and Hayashi K.: "Benchmark Study on Neutron Cross Sections Based on Pulsed Sphere Experiment", Proc. 3rd Specialists' Meeting on Nuclear Data for Fusion Reactors, Tokai, JAERI, Nov. 29-30, 1995, JAERI-Conf 96-005, pp. 80-91 (1996).
- 64) Ichihara C., Hayashi S. A., Kimura I., Yamamoto J. and Takahashi A.: "Nuclear Data Benchmark with Pulsed Sphere Experiment at OKTAVIAN", Proc. International Conference on Nucl. Data for Science and Technology, Trieste, Italy, May 19-24, 1997, pp. 1209-1211 (1998).
- 65) Ichihara C., Hayashi S. A., Kimura I., Yamamoto J. and Takahashi A.: "Benchmark Validation by Means of Pulsed Sphere Experiment at OKTAVIAN", Proc. '97 Symposium on Nuclear Data, Tokai, JAERI, Nov. 27-28, 1997, JAERI-Conf 98-003, pp. 174-179 (1998).

Table 2.1 List of selected cross section data for FENDL/E-1.0 and FENDL/E-2.0.  
Nuclides treated in this report are indicated in bold letters.

Nuclide	FENDL/E-1.0	FENDL/E-2.0
1-H -1	ENDF-VI	ENDF-VI
1-H -2	ENDF-VI	BROND-2 + JENDL-FF
1-H -3	ENDF-VI	ENDF-VI
2-He-3	ENDF-VI.1	ENDF-VI.1
2-He-4	ENDF-VI	ENDF-VI
<b>3-Li-6</b>	<b>ENDF-VI.1</b>	<b>ENDF-VI.1</b>
3-Li-7	ENDF-VI	ENDF-VI
<b>4-Be-9</b>	<b>ENDF-VI</b>	<b>JENDL-FF</b>
5-B -10	ENDF-VI.1	ENDF-VI.1
5-B -11	ENDF-VI.1	ENDF-VI.1
6-C -12	ENDF-VI.1	JENDL-FF + ENDF-VI.1
7-N -14	BROND-2	JENDL-FF + BROND-2
7-N -15	BROND-2	BROND-2
8-O -16	ENDF-VI	JENDL-FF
9-F -19	ENDF-VI	ENDF-VI
11-Na-23	JENDL-3.1	JENDL-3.1
12-Mg-nat	JENDL-3.1	JENDL-3.1
<b>13-Al-27</b>	<b>JENDL-3.1</b>	<b>EFP-3</b>
<b>14-Si-nat</b>	<b>BROND-2</b>	<b>ENDF-VI (isotopes)</b>
15-P -31	ENDF-VI	ENDF-VI
16-S -nat	ENDF-VI	ENDF-VI
17-Cl-nat	ENDF-VI	ENDF-VI
19-K -nat	ENDF-VI	ENDF-VI
20-Ca-nat	JENDL-3.1	JENDL-3.1
<b>22-Ti-nat</b>	<b>JENDL-3.1</b>	<b>JENDL-3.1</b>
23-V -51	ENDF-VI	JENDL-FF
<b>24-Cr-50</b>	<b>ENDF-VI</b>	<b>ENDF-VI</b>
<b>24-Cr-52</b>	<b>ENDF-VI</b>	<b>ENDF-VI</b>
<b>24-Cr-53</b>	<b>ENDF-VI</b>	<b>ENDF-VI</b>
<b>24-Cr-54</b>	<b>ENDF-VI</b>	<b>ENDF-VI</b>
25-Mn-55	ENDF-VI	ENDF-VI
26-Fe-54	ENDF-VI.1	ENDF-VI.1
26-Fe-56	ENDF-VI.1	EFP-3
26-Fe-57	ENDF-VI.1	ENDF-VI.1
26-Fe-58	ENDF-VI.1	ENDF-VI.1
27-Co-59	ENDF-VI.2	ENDF-VI.2
28-Ni-58	ENDF-VI.1	ENDF-VI.1
28-Ni-60	ENDF-VI.1	ENDF-VI.1
28-Ni-61	ENDF-VI.1	ENDF-VI.1
28-Ni-62	ENDF-VI.1	ENDF-VI.1
28-Ni-64	ENDF-VI.1	ENDF-VI.1
29-Cu-63	ENDF-VI.2	ENDF-VI.2
29-Cu-65	ENDF-VI.2	ENDF-VI.2
31-Ga-nat	---	JENDL-3.2
<b>40-Zr-90</b>	<b>BROND-2</b>	<b>JENDL-FF</b>
<b>40-Zr-91</b>	<b>BROND-2</b>	<b>JENDL-FF</b>
<b>40-Zr-92</b>	<b>BROND-2</b>	<b>JENDL-FF</b>
<b>40-Zr-94</b>	<b>BROND-2</b>	<b>JENDL-FF</b>
<b>40-Zr-95</b>	<b>BROND-2</b>	<b>JENDL-FF</b>
<b>40-Zr-96</b>	<b>BROND-2</b>	<b>JENDL-FF</b>
<b>41-Nb-93</b>	<b>BROND-2</b>	<b>JENDL-FF</b>
<b>42-Mo-nat</b>	<b>JENDL-3.1</b>	<b>JENDL-FF</b>
50-Sn-nat	BROND-2	BROND-2
56-Ba-138	ENDF-VI	ENDF-VI
73-Ta-181	JENDL-3.1	JENDL-3.1
<b>74-W -182</b>	<b>ENDF-VI</b>	<b>JENDL-FF</b>
<b>74-W -183</b>	<b>ENDF-VI</b>	<b>JENDL-FF</b>
74-W -184	ENDF-VI	JENDL-FF
74-W -186	ENDF-VI	JENDL-FF
82-Pb-204	ENDF-VI.1	ENDF-VI.1
82-Pb-206	ENDF-VI	ENDF-VI
82-Pb-207	ENDF-VI.1	ENDF-VI.1
82-Pb-208	ENDF-VI	ENDF-VI
83-Bi-209	JENDL-3.1	JENDL-3.1

**Table 5.1 Summary of C/E ratios for leakage neutron fluxes from the lithium, lithium fluoride, Teflon ( $\text{CF}_2$ ), aluminum and silicon (40 cm diam.) spheres for the OKTAVIAN pulsed sphere experiment.**

Material	Energy Range [MeV]	Experiment Flux	JENDL-3.2 Flux	C/E	JENDL-FF Flux	C/E	JENDL-3.1 Flux	C/E	FENDL/MC-1 Flux	C/E	EFF-2 Flux	C/E	BMCCS Flux	C/E
Li 40cm $\rho = 0.534$ $1.3 \text{ MFP}$	$10 < \text{En} < 20$	7.73E-01	7.43E-01	0.961	7.43E-01	0.961	7.42E-01	0.960	7.48E-01	0.968	7.38E-01	0.955		
	$5 < \text{En} < 10$	9.40E-02	7.06E-02	0.751	7.06E-02	0.752	6.99E-02	0.744	6.35E-02	0.675	7.12E-02	0.758		
	$1 < \text{En} < 5$	1.31E-01	1.28E-01	0.975	1.28E-01	0.973	1.29E-01	0.982	1.29E-01	0.981	1.26E-01	0.958		
	$0.1 < \text{En} < 1$	7.83E-02	7.93E-02	1.012	7.94E-02	1.013	7.97E-02	1.017	7.61E-02	0.972	8.25E-02	1.053		
	total	1.08E+00	1.02E+00	0.948	1.02E+00	0.948	1.02E+00	0.948	1.02E+00	0.944	1.02E+00	0.945		
LiF 60cm $\rho = 1.79$ $3.5 \text{ MFP}$	$10 < \text{En} < 20$	1.81E-01	2.06E-01	1.137	2.07E-01	1.141	1.63E-01	0.900	1.95E-01	1.076	1.62E-01	0.891		
	$5 < \text{En} < 10$	6.67E-02	6.22E-02	0.932	6.47E-02	0.970	4.22E-02	0.692	5.57E-02	0.834	5.13E-02	0.769		
	$1 < \text{En} < 5$	1.73E-01	1.48E-01	0.856	1.48E-01	0.858	1.49E-01	0.862	1.48E-01	0.856	1.52E-01	0.881		
	$0.1 < \text{En} < 1$	2.05E-01	1.23E-01	0.597	1.21E-01	0.590	1.35E-01	0.658	1.39E-01	0.680	1.47E-01	0.719		
	total	6.26E-01	5.39E-01	0.861	5.41E-01	0.864	4.89E-01	0.781	5.38E-01	0.860	5.13E-01	0.819		
CF2 40cm $\rho = 1.30$ $0.7 \text{ MFP}$	$10 < \text{En} < 20$	9.01E-01	6.91E-01	0.767	6.91E-01	0.768	6.39E-01	0.709	6.86E-01	0.761			6.53E-01	0.724
	$5 < \text{En} < 10$	1.08E-01	5.89E-02	0.545	6.00E-02	0.555	5.64E-02	0.521	6.56E-02	0.606			6.25E-02	0.578
	$1 < \text{En} < 5$	2.27E-01	1.42E-01	0.625	1.41E-01	0.624	1.38E-01	0.804	1.40E-01	0.617			1.74E-01	0.770
	$0.1 < \text{En} < 1$	1.03E-01	6.29E-02	0.611	6.23E-02	0.605	7.47E-02	0.726	6.64E-02	0.645			7.25E-02	0.704
	total	1.34E+00	9.54E-01	0.713	9.55E-01	0.714	9.52E-01	0.711	9.57E-01	0.715			9.62E-01	0.719
Al 40cm $\rho = 1.22$ $0.5 \text{ MFP}$	$10 < \text{En} < 20$	6.74E-01	7.15E-01	1.060	7.16E-01	1.062	7.09E-01	1.051	7.09E-01	1.051	7.09E-01	1.052		
	$5 < \text{En} < 10$	4.96E-02	3.93E-02	0.792	4.06E-02	0.819	3.20E-02	0.644	3.20E-02	0.644	4.04E-02	0.814		
	$1 < \text{En} < 5$	1.47E-01	1.32E-01	0.893	1.31E-01	0.889	1.49E-01	1.010	1.49E-01	1.010	1.46E-01	0.992		
	$0.1 < \text{En} < 1$	6.93E-02	8.73E-02	1.260	8.62E-02	1.244	8.43E-02	1.217	8.43E-02	1.217	7.95E-02	1.147		
	total	9.40E-01	9.73E-01	1.034	9.74E-01	1.035	9.74E-01	1.036	9.74E-01	1.036	9.75E-01	1.037		
Si 40cm $\rho = 1.30$ $0.55 \text{ MFP}$	$10 < \text{En} < 20$	7.57E-01	7.38E-01	0.974	7.09E-01	0.936	7.38E-01	0.974	6.52E-01	0.861	7.38E-01	0.974		
	$5 < \text{En} < 10$	4.51E-02	3.09E-02	0.685	2.93E-02	0.648	3.11E-02	0.689	2.96E-02	0.655	3.19E-02	0.707		
	$1 < \text{En} < 5$	1.34E-01	1.04E-01	0.776	1.15E-01	0.857	1.04E-01	0.774	9.93E-02	0.741	9.85E-02	0.735		
	$0.1 < \text{En} < 1$	5.89E-02	4.98E-02	0.847	6.48E-02	1.101	5.02E-02	0.853	1.06E-01	1.797	4.29E-02	0.728		
	total	9.95E-01	9.22E-01	0.927	9.18E-01	0.922	9.23E-01	0.927	8.87E-01	0.891	9.11E-01	0.915		

Table 5.2 Summary of C/E ratios for leakage neutron fluxes from the silicon (60 cm diam.), titanium, chromium, manganese and cobalt spheres for the OKTAVIAN pulsed sphere experiment.

Material	Energy Range [MeV]	Experiment Flux	JENDL-3.2 Flux	C/E	JENDL-FF Flux	C/E	JENDL-3.1 Flux	C/E	FENDL/MC-1 Flux	C/E	EFF-2 Flux	C/E	BMCCS Flux	C/E
Si 60cm $\rho = 1.30$ 0.1 MFP	10<En<20	4.80E-01	5.26E-01	1.096	5.30E-01	1.104	5.26E-01	1.095	4.42E-01	0.920	4.27E-01	0.888	5.15E-01	1.073
	5<En<10	4.69E-02	3.59E-02	0.764	3.71E-02	0.789	3.56E-02	0.755	3.34E-02	0.712	4.16E-02	0.887	2.85E-02	0.607
	1<En<5	1.71E-01	1.67E-01	0.976	1.70E-01	0.995	1.67E-01	0.975	1.35E-01	0.791	1.83E-01	1.069	1.28E-01	0.755
	0.1<En<1	9.32E-02	1.08E-01	1.163	9.74E-02	1.045	1.09E-01	1.171	1.80E-01	1.931	1.09E-01	1.170	1.29E-01	1.387
	total	7.91E-01	8.37E-01	1.058	8.35E-01	1.055	8.37E-01	1.058	7.90E-01	0.999	7.60E-01	0.961	8.02E-01	1.013
Ti 40 cm $\rho = 1.54$ 0.5 MFP	10<En<20	5.94E-01	7.09E-01	1.193	7.10E-01	1.195	6.85E-01	1.154	7.05E-01	1.186	6.86E-01	1.155	7.17E-01	1.207
	5<En<10	3.84E-02	3.86E-02	1.006	3.93E-02	1.023	3.81E-02	0.993	3.73E-02	0.970	3.87E-02	1.008	3.28E-02	0.856
	1<En<5	1.52E-01	1.76E-01	1.160	1.75E-01	1.154	2.14E-01	1.414	2.09E-01	1.377	2.15E-01	1.418	2.08E-01	1.342
	0.1<En<1	8.61E-02	1.34E-01	1.560	1.35E-01	1.562	1.30E-01	1.508	1.21E-01	1.408	1.27E-01	1.469	1.10E-01	1.279
	total	8.70E-01	1.06E+00	1.216	1.06E+00	1.216	1.07E+00	1.227	1.07E+00	1.232	1.07E+00	1.225	1.06E+00	1.222
Cr 40cm $\rho = 3.72$ 0.7 MFP	10<En<20	5.49E-01	5.45E-01	0.993	5.63E-01	1.025	5.62E-01	1.024	5.41E-01	0.987	5.33E-01	0.972	5.71E-01	1.040
	5<En<10	4.10E-02	4.09E-02	0.998	4.16E-02	1.014	4.09E-02	0.998	4.62E-02	1.127	3.96E-02	0.965	8.90E-02	2.171
	1<En<5	2.21E-01	2.39E-01	1.080	2.39E-01	1.056	2.33E-01	1.053	2.47E-01	1.118	2.73E-01	1.236	2.14E-01	0.969
	0.1<En<1	2.11E-01	2.38E-01	1.131	2.24E-01	1.062	2.26E-01	1.072	2.25E-01	1.068	2.25E-01	1.069	1.89E-01	0.897
	total	1.022E+00	1.06E+00	1.041	1.06E+00	1.039	1.06E+00	1.039	1.06E+00	1.037	1.07E+00	1.049	1.06E+00	1.041
Mn 60cm $\rho = 4.37$ 3.4 MFP	10<En<20	1.54E-01	1.51E-01	0.982	1.52E-01	0.985	1.44E-01	0.936	1.45E-01	0.937	1.45E-01	0.940	1.47E-01	0.955
	5<En<10	2.79E-02	3.08E-02	1.104	3.03E-02	1.085	2.46E-02	0.880	2.68E-02	0.961	2.70E-02	0.968	1.40E-02	0.501
	1<En<5	2.71E-01	2.98E-01	1.097	3.01E-01	1.111	3.03E-01	1.116	3.01E-01	1.110	3.04E-01	1.121	1.86E-01	0.685
	0.1<En<1	6.61E-01	7.13E-01	1.080	7.11E-01	1.077	7.18E-01	1.098	7.14E-01	1.080	7.13E-01	1.079	7.50E-01	1.135
	total	1.11E+00	1.19E+00	1.071	1.19E+00	1.073	1.19E+00	1.068	1.19E+00	1.065	1.19E+00	1.067	1.10E+00	0.985
Co 40cm $\rho = 1.94$ 0.5 MFP	10<En<20	7.26E-01	7.13E-01	0.982	7.04E-01	0.969	6.96E-01	0.959	7.15E-01	0.986	7.24E-01	0.998	7.24E-01	0.997
	5<En<10	5.56E-02	3.85E-02	0.694	3.70E-02	0.667	4.17E-02	0.751	2.94E-02	0.529	2.86E-02	0.516	2.54E-02	0.458
	1<En<5	2.96E-01	1.92E-01	0.650	2.00E-01	0.677	1.98E-01	0.670	1.92E-01	0.650	1.88E-01	0.637	1.95E-01	0.658
	0.1<En<1	2.42E-01	1.57E-01	0.650	1.64E-01	0.678	1.71E-01	0.707	1.65E-01	0.681	1.56E-01	0.643	1.47E-01	0.606
	total	1.32E+00	1.10E+00	0.834	1.10E+00	0.838	1.11E+00	0.839	1.10E+00	0.835	1.10E+00	0.831	1.09E+00	0.827

**Table 5.3**  
**Summary of C/E ratios for leakage neutron fluxes from the copper, zirconium,  
niobium, molybdenum and tungsten spheres for the OKTAVIAN pulsed  
sphere experiment.**

Material	Energy Range [MeV]	Experiment Flux	JENDL-3.2 Flux	JENDL-FF Flux	C/E	JENDL-3.1 Flux	C/E	FENDL/MC-1 Flux	C/E	EFF-2 Flux	C/E	BMCCS Flux	C/E		
Cu 60cm $\rho=6.01$ 4.7 MFP	10<En<20	7.94E-02	8.53E-02	1.074	9.26E-02	1.165	8.45E-02	1.064	8.18E-02	1.030	8.21E-02	1.033	7.45E-02	0.938	
	5<En<10	1.33E-02	1.32E-02	0.993	1.44E-02	1.082	1.22E-02	0.915	1.67E-02	1.251	1.68E-02	1.261	7.11E-03	0.533	
	1<En<5	1.45E-01	1.41E-01	0.974	1.52E-01	1.050	1.40E-01	0.964	1.53E-01	1.059	1.55E-01	1.070	1.26E-01	0.870	
	0.1<En<1	6.60E-01	7.18E-01	1.088	7.00E-01	1.060	7.09E-01	1.074	7.16E-01	1.084	7.17E-01	1.086	7.10E-01	1.076	
	total	8.98E-01	9.58E-01	1.067	9.59E-01	1.068	9.45E-01	1.053	9.67E-01	1.078	9.71E-01	1.081	9.18E-01	1.023	
Zr 60cm $\rho=2.84$ 2.0 MFP	10<En<20	3.12E-01	3.59E-01	1.149	3.60E-01	1.153	3.00E-01	0.961	3.75E-01	1.200	3.53E-01	1.129	3.54E-01	1.132	
	5<En<10	3.33E-02	3.22E-02	0.965	3.28E-02	0.986	4.57E-02	1.374	3.98E-02	1.196	5.45E-02	1.636	5.47E-02	1.644	
	1<En<5	3.08E-01	3.34E-01	1.087	3.30E-01	1.071	3.81E-01	1.238	3.74E-01	1.217	4.75E-01	1.545	4.74E-01	1.541	
	0.1<En<1	4.41E-01	5.50E-01	1.245	5.44E-01	1.233	5.40E-01	1.223	4.89E-01	1.107	4.41E-01	0.993	4.38E-01	0.992	
	total	1.03E+00	1.165	1.27E+00	1.157	1.27E+00	1.157	1.27E+00	1.157	1.28E+00	1.167	1.32E+00	1.209	1.32E+00	1.206
Nb 28cm $\rho=4.39$ 1.1 MFP	10<En<20	5.10E-01	5.30E-01	1.040	5.30E-01	1.039	5.36E-01	1.051	5.29E-01	1.038	5.30E-01	1.040	5.38E-01	1.056	
	5<En<10	3.55E-02	3.30E-02	0.930	3.39E-02	0.954	4.21E-02	1.187	3.94E-02	1.110	4.13E-02	1.163	3.21E-02	0.904	
	1<En<5	2.19E-01	2.27E-01	1.035	2.28E-01	1.041	2.27E-01	1.035	2.73E-01	1.244	3.18E-01	1.450	2.18E-01	0.996	
	0.1<En<1	3.35E-01	4.49E-01	1.340	4.52E-01	1.350	4.21E-01	1.256	4.17E-01	1.244	3.72E-01	1.110	4.37E-01	1.304	
	total	1.10E-00	1.24E+00	1.127	1.24E+00	1.132	1.23E+00	1.115	1.26E+00	1.144	1.26E+00	1.147	1.23E+00	1.114	
Mo 60cm $\rho=2.15$ 1.5 MFP	10<En<20	5.24E-01	4.49E-01	0.857	4.50E-01	0.859	4.66E-01	0.890	4.68E-01	0.894	4.66E-01	0.889	4.32E-01	0.824	
	5<En<10	4.26E-02	3.56E-02	0.835	3.64E-02	0.854	2.83E-02	0.664	3.02E-02	0.709	3.45E-02	0.809	2.94E-02	0.888	
	1<En<5	2.87E-01	2.64E-01	0.918	2.65E-01	0.921	2.85E-01	0.991	2.85E-01	0.993	2.92E-01	1.015	3.72E-01	1.296	
	0.1<En<1	5.16E-01	4.83E-01	0.937	4.81E-01	0.933	4.85E-01	0.940	4.79E-01	0.928	4.47E-01	0.866	4.88E-01	0.945	
	total	1.37E-00	1.23E+00	0.899	1.23E+00	0.900	1.26E-00	0.923	1.26E+00	0.922	1.24E+00	0.904	1.32E+00	0.965	
W 40cm $\rho=4.43$ 0.8 MFP	10<En<20	7.07E-01	6.40E-01	0.906	6.42E-01	0.908	6.50E-01	0.920	6.50E-01	0.920	6.50E-01	0.920	6.38E-01	0.902	
	5<En<10	4.09E-02	2.47E-02	0.604	2.51E-02	0.614	2.63E-02	0.643	2.94E-02	0.720	2.68E-02	0.656	3.03E-02	0.740	
	1<En<5	2.41E-01	1.90E-01	0.788	1.90E-01	0.786	2.11E-01	0.876	2.12E-01	0.879	2.13E-01	0.882	2.67E-01	1.106	
	0.1<En<1	3.59E-01	3.60E-01	1.003	3.56E-01	0.992	3.15E-01	0.878	3.03E-01	0.843	3.12E-01	0.869	2.58E-01	0.717	
	total	1.35E-00	1.22E+00	0.901	1.21E+00	0.900	1.20E-00	0.892	1.19E+00	0.886	1.20E+00	0.891	1.19E+00	0.884	

Table 5.4 Summary of C/E ratios for leakage neutron fluxes from the beryllium spheres with four thicknesses for the OKTAVIAN pulsed sphere experiment.

	Energy Range	FENDL/E-1.0	JENDL-3.2	JENDL-Fusion File
Beryllium Sphere Inner Radius: 128.0 mm Outer Radius: 173.5 mm Thickness: 45.5 mm	> 10 MeV 5-10 MeV 1-5 MeV 0.1-1 MeV Total	1.08 ± 0.01 0.95 ± 0.01 0.94 ± 0.01 0.95 ± 0.01 1.02 ± 0.01	1.08 ± 0.01 1.00 ± 0.01 1.08 ± 0.01 0.99 ± 0.01 1.06 ± 0.01	1.09 ± 0.01 0.99 ± 0.01 0.97 ± 0.01 0.91 ± 0.01 1.03 ± 0.01
Beryllium Sphere Inner Radius: 97.0 mm Outer Radius: 173.5 mm Thickness: 76.5 mm	> 10 MeV 5-10 MeV 1-5 MeV 0.1-1 MeV Total	1.77 ± 0.12 0.69 ± 0.01 0.68 ± 0.01 0.78 ± 0.01 1.01 ± 0.02	1.78 ± 0.12 0.73 ± 0.01 0.79 ± 0.01 0.85 ± 0.01 1.07 ± 0.02	1.80 ± 0.12 0.73 ± 0.01 0.70 ± 0.01 0.76 ± 0.01 1.02 ± 0.02
Beryllium Sphere Inner Radius: 69.0 mm Outer Radius: 173.5 mm Thickness: 104.5 mm	> 10 MeV 5-10 MeV 1-5 MeV 0.1-1 MeV Total	1.43 ± 0.01 0.82 ± 0.01 0.80 ± 0.01 0.89 ± 0.01 1.01 ± 0.01	1.43 ± 0.01 0.87 ± 0.01 0.93 ± 0.01 1.00 ± 0.01 1.09 ± 0.01	1.45 ± 0.01 0.86 ± 0.01 0.83 ± 0.01 0.89 ± 0.01 1.03 ± 0.01
Beryllium Sphere Inner Radius: 57.0 mm Outer Radius: 173.5 mm Thickness: 116.5 mm	> 10 MeV 5-10 MeV 1-5 MeV 0.1-1 MeV Total	1.35 ± 0.01 0.89 ± 0.01 0.85 ± 0.01 0.92 ± 0.01 1.02 ± 0.01	1.35 ± 0.01 0.95 ± 0.02 0.99 ± 0.01 1.04 ± 0.01 1.11 ± 0.01	1.38 ± 0.01 0.93 ± 0.01 0.88 ± 0.01 0.92 ± 0.01 1.04 ± 0.01

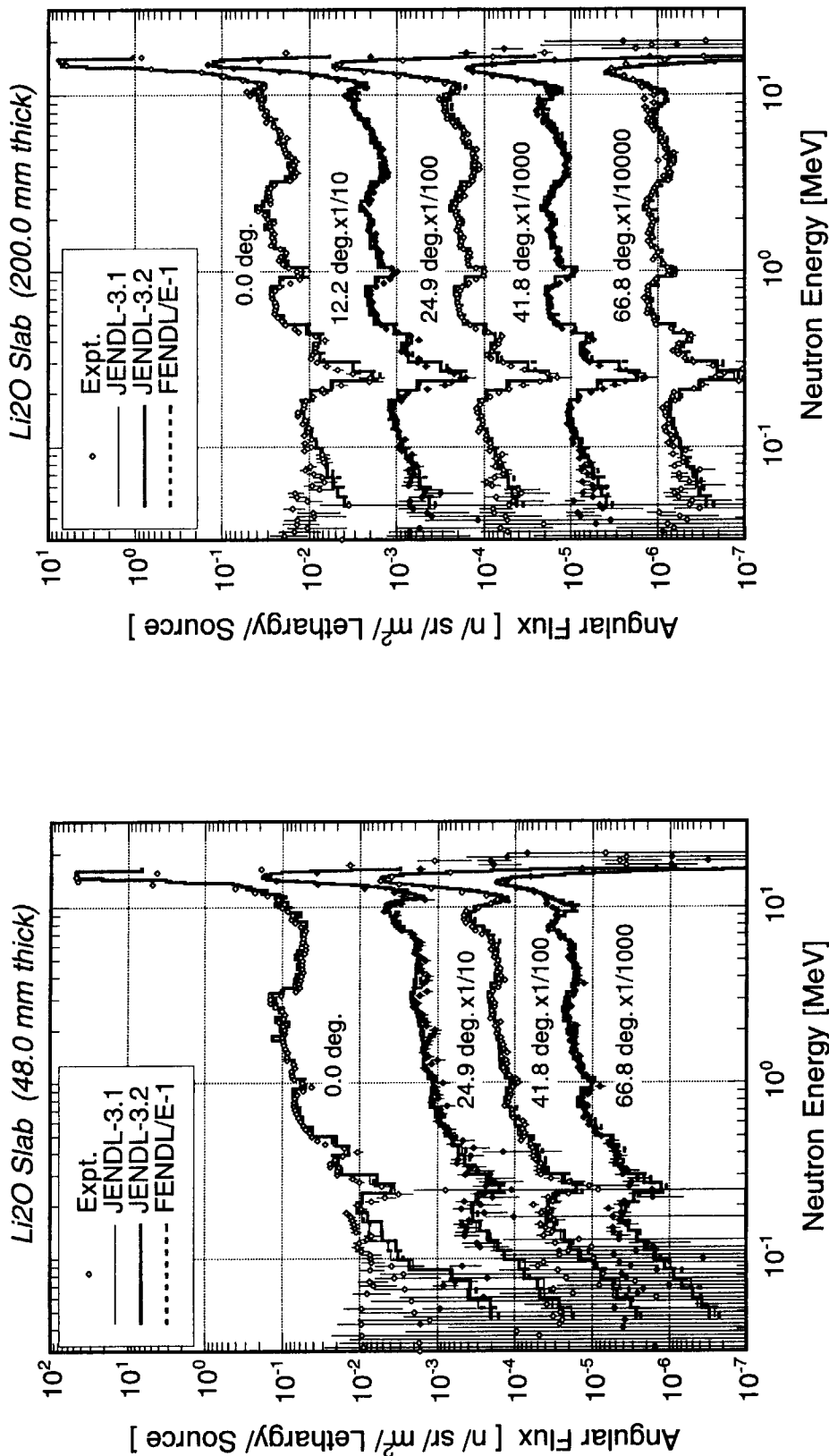


Fig. 3.3.1 Neutron spectra leaking from the lithium oxide slab assembly of 48.0 mm in thickness measured and calculated with JENDL-3.1, JENDL-3.2 and FENDL/E-1.0.

Fig. 3.3.2 Neutron spectra leaking from the lithium oxide slab assembly of 200.0 mm in thickness measured and calculated with JENDL-3.1, JENDL-3.2 and FENDL/E-1.0.

Fig. 3.3.3 Neutron spectra leaking from the lithium oxide slab assembly of 200.0 mm in thickness measured and calculated with JENDL-3.1, JENDL-3.2 and FENDL/E-1.0.

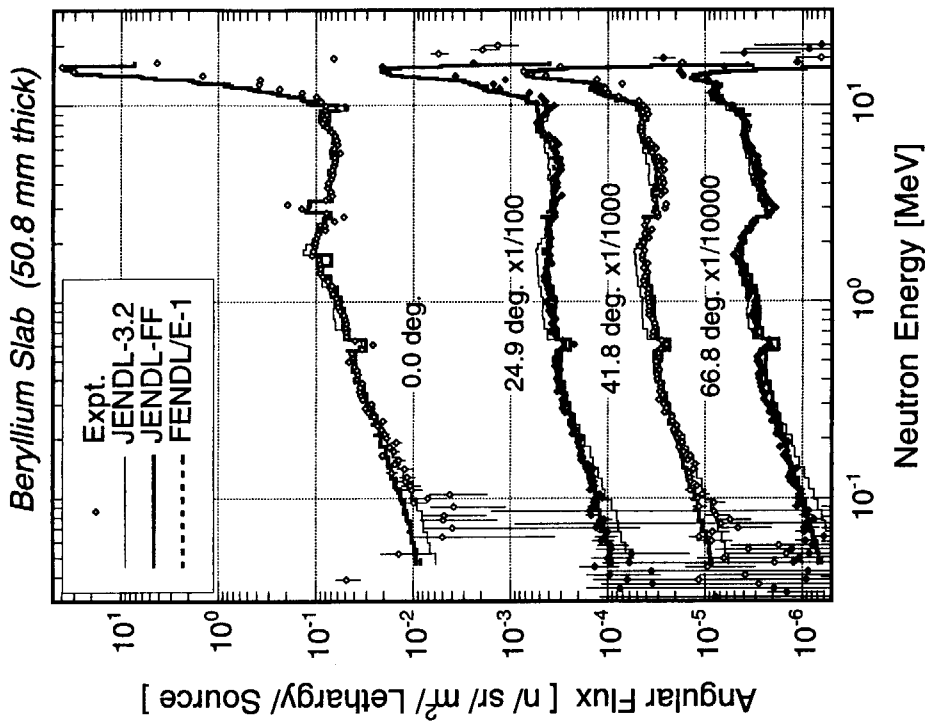


Fig. 3.3.4 Neutron spectra leaking from the beryllium slab assembly of 50.8 mm thickness measured and calculated with JENDL-3.2, JENDL Fusion File and FENDL/E-1.0.

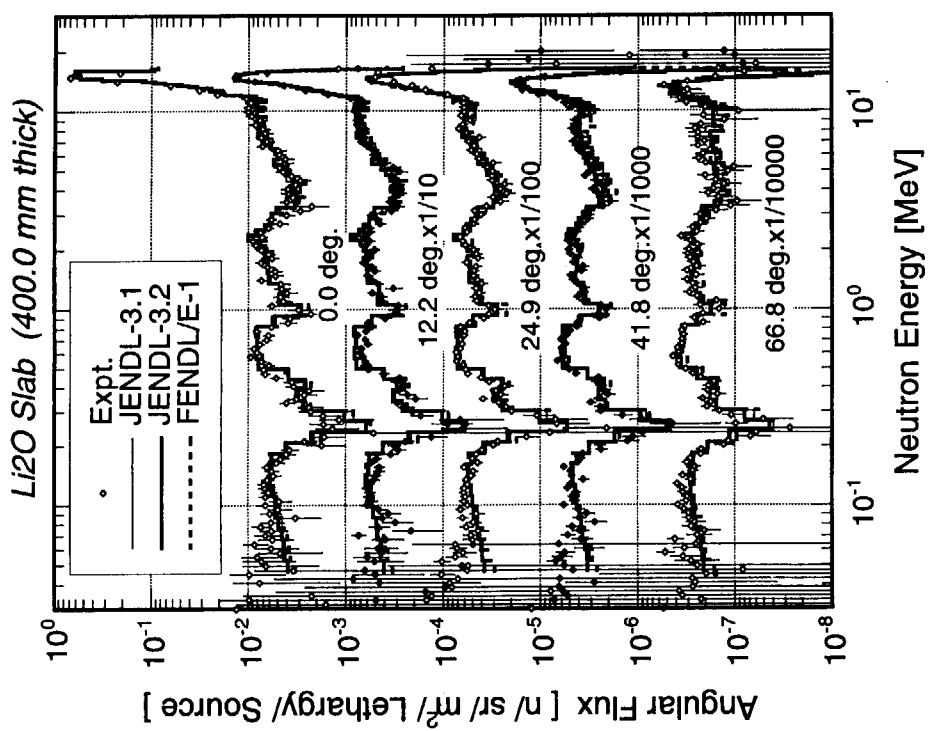


Fig. 3.3.3 Neutron spectra leaking from the lithium oxide slab assembly of 400.0 mm in thickness measured and calculated with JENDL-3.1, JENDL-3.2 and FENDL-E-1.0.

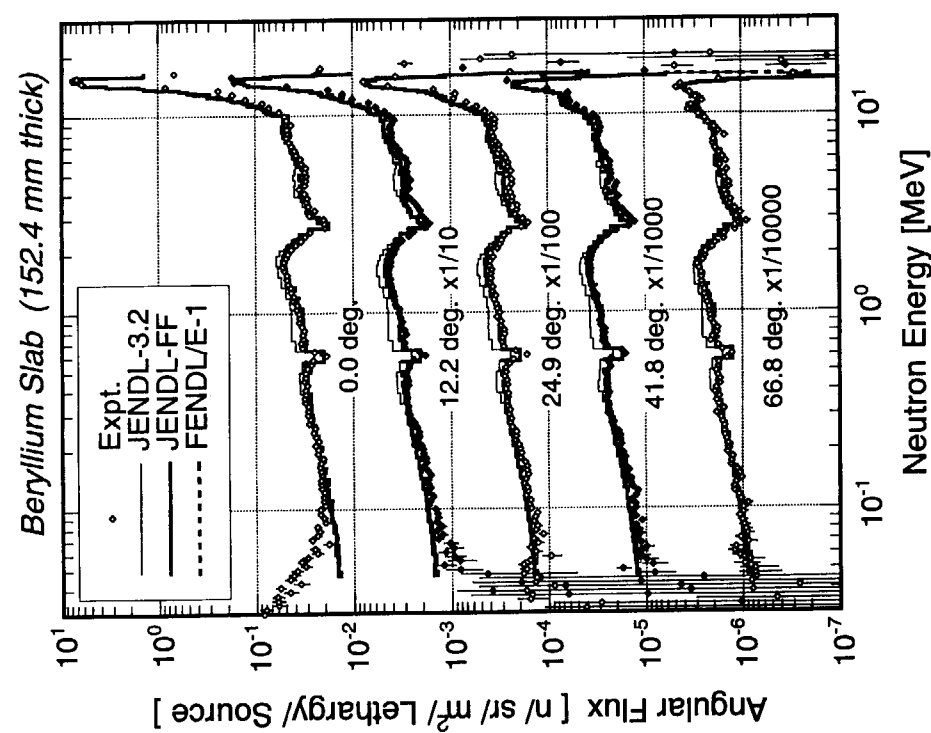


Fig. 3.3.5 Neutron spectra leaking from the beryllium slab assembly of 152.4 mm in thickness measured and calculated with JENDL-3.2, JENDL Fusion File and FENDL/E-1.0.

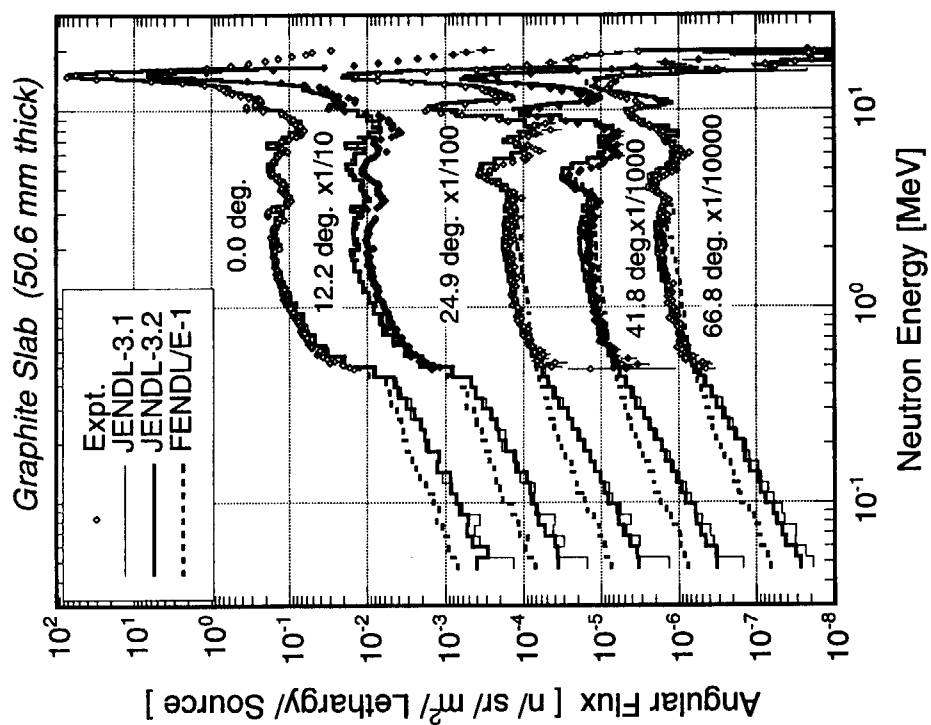


Fig. 3.3.6 Neutron spectra leaking from the graphite slab assembly of 50.6 mm in thickness measured and calculated with JENDL-3.1, JENDL-3.2 and FENDL/E-1.0.

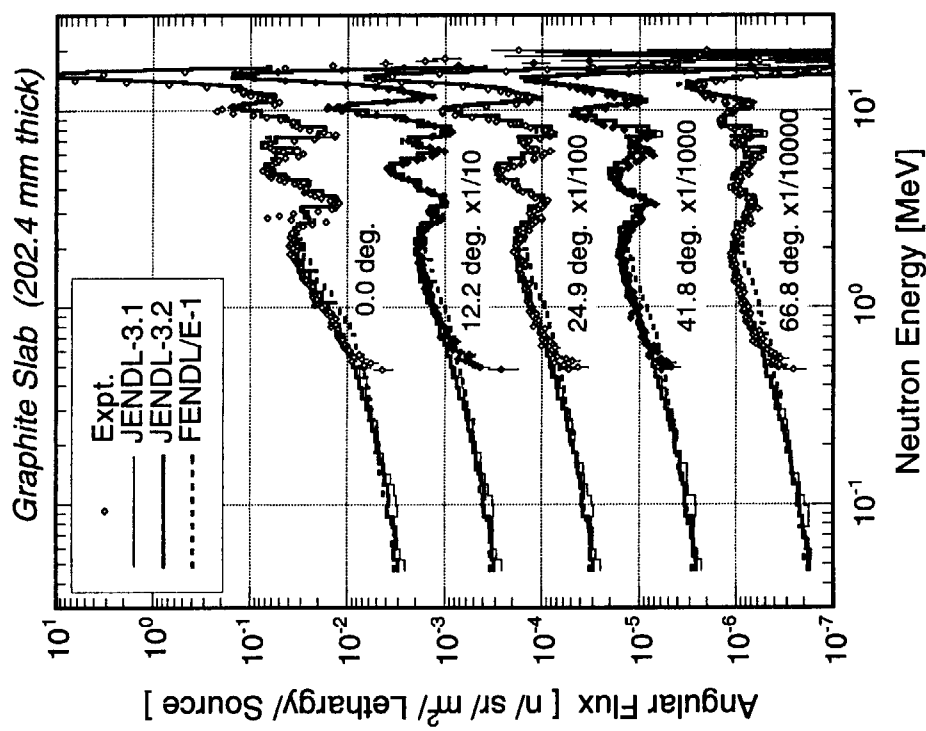


Fig. 3.3.7 Neutron spectra leaking from the graphite slab assembly of 202.4 mm in thickness measured and calculated with JENDL-3.1, JENDL-3.2 and FENDL/E-1.0.

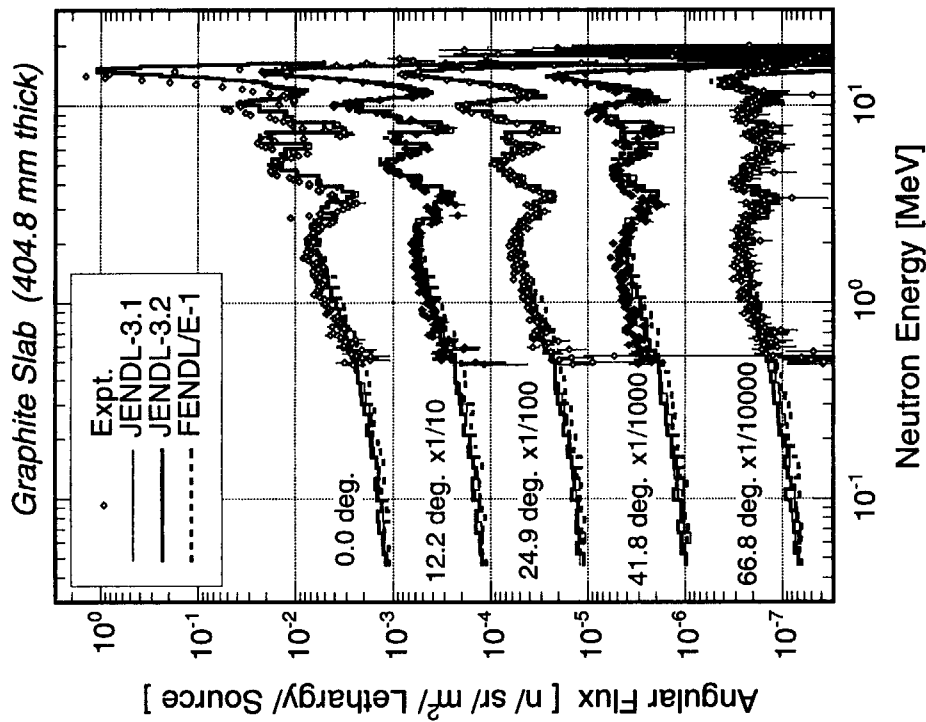


Fig. 3.3.8 Neutron spectra leaking from the graphite slab assembly of 404.8 mm in thickness measured and calculated with JENDL-3.1, JENDL-3.2 and FENDL/E-1.0.

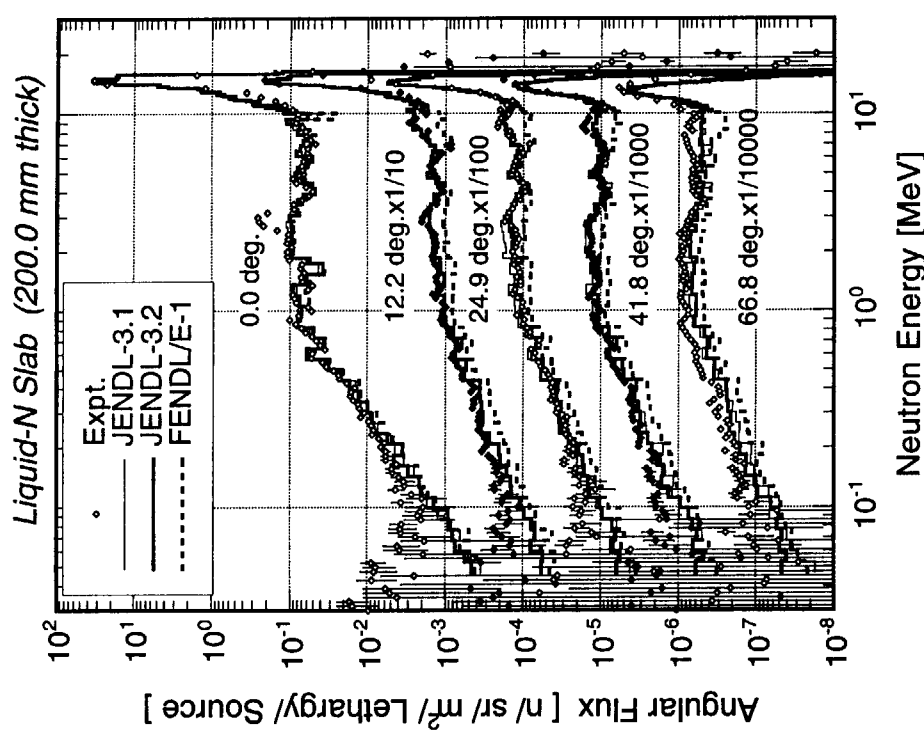


Fig. 3.3.9 Neutron spectra leaking from the liquid-nitrogen slab assembly of 200.0 mm in thickness measured and calculated with JENDL-3.1, JENDL-3.2 and FENDL/E-1.0.

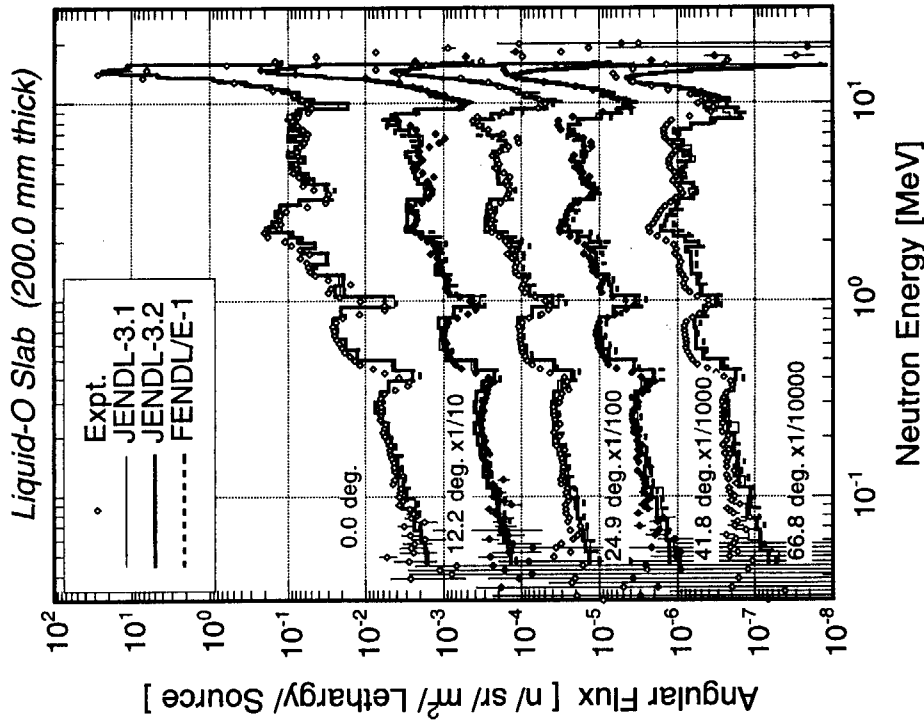


Fig. 3.3.10 Neutron spectra leaking from the liquid-oxygen slab assembly of 200.0 mm in thickness measured and calculated with JENDL-3.1, JENDL-3.2 and FENDL/E-1.0.

Neutron spectra leaking from the liquid-oxygen slab assembly of 200.0 mm in thickness measured and calculated with JENDL-3.1, JENDL-3.2 and FENDL/E-1.0.

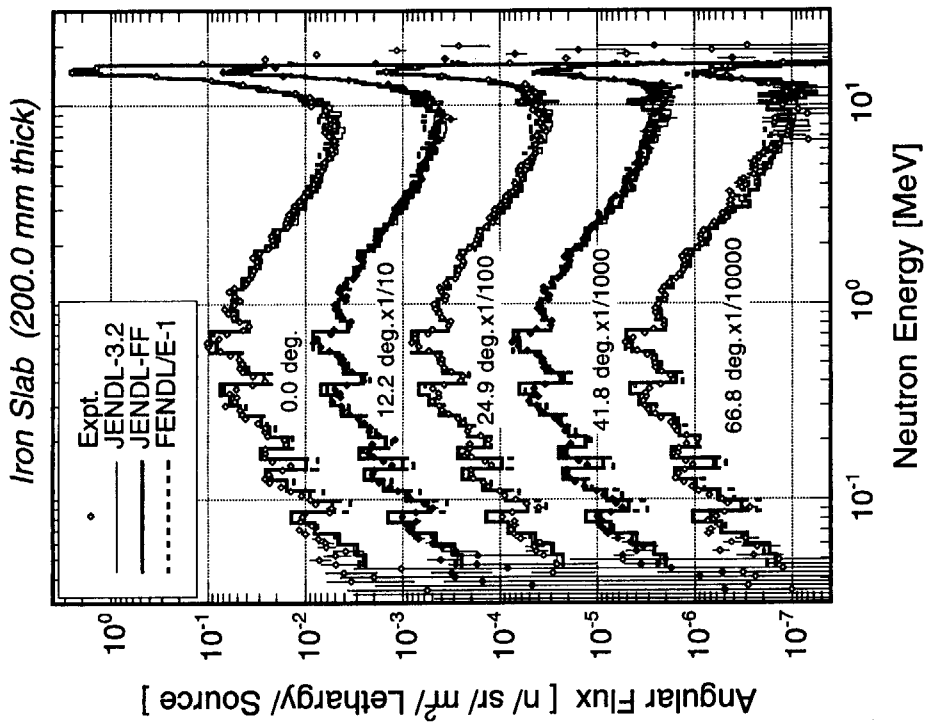


Fig. 3.3.12 Neutron spectra leaking from the iron slab assembly of 200.0 mm in thickness measured and calculated with JENDL-3.2, JENDL Fusion File and FENDL/E-1.0.

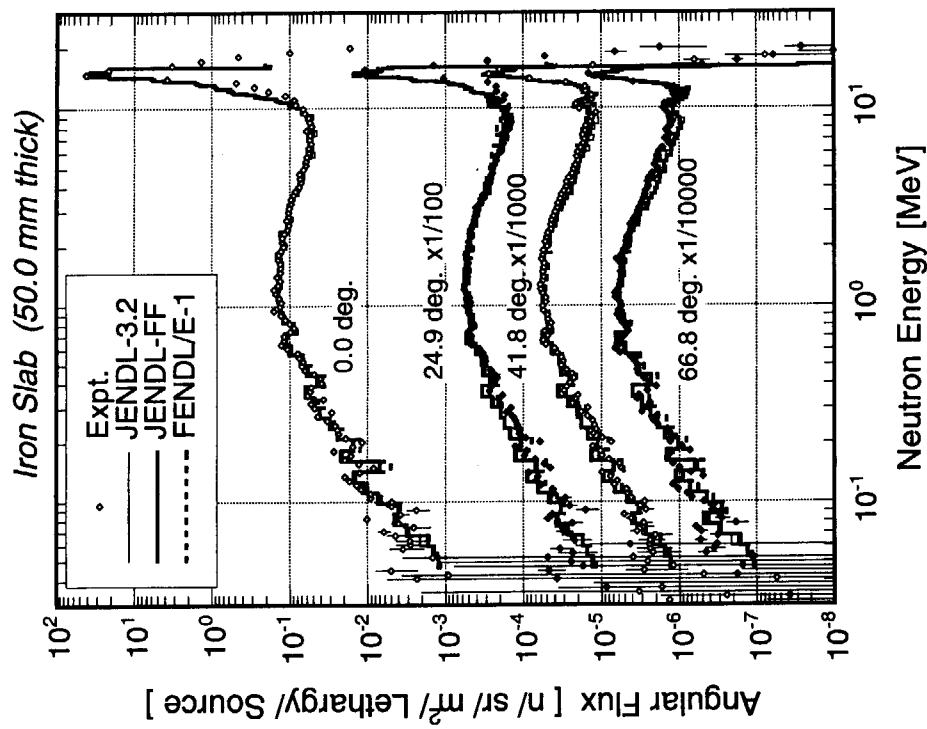


Fig. 3.3.11 Neutron spectra leaking from the iron slab assembly of 50.0 mm in thickness measured and calculated with JENDL-3.2, JENDL Fusion File and FENDL/E-1.0.

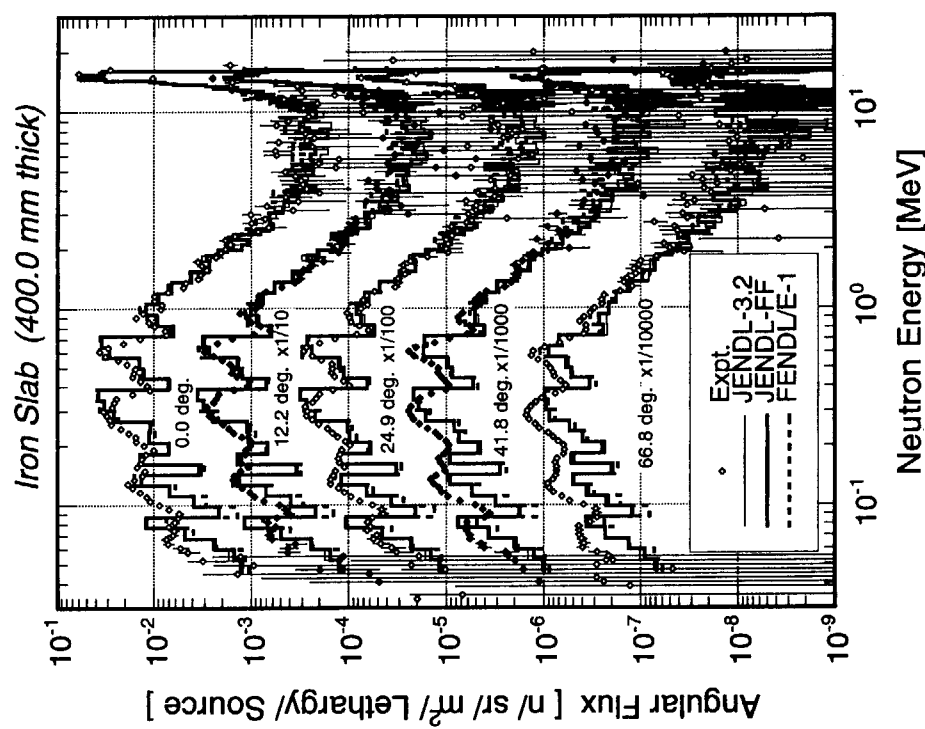


Fig. 3.3.13 Neutron spectra leaking from the iron slab assembly of 400.0 mm in thickness measured and calculated with JENDL-3.2, JENDL Fusion File and FENDL/E-1.0.

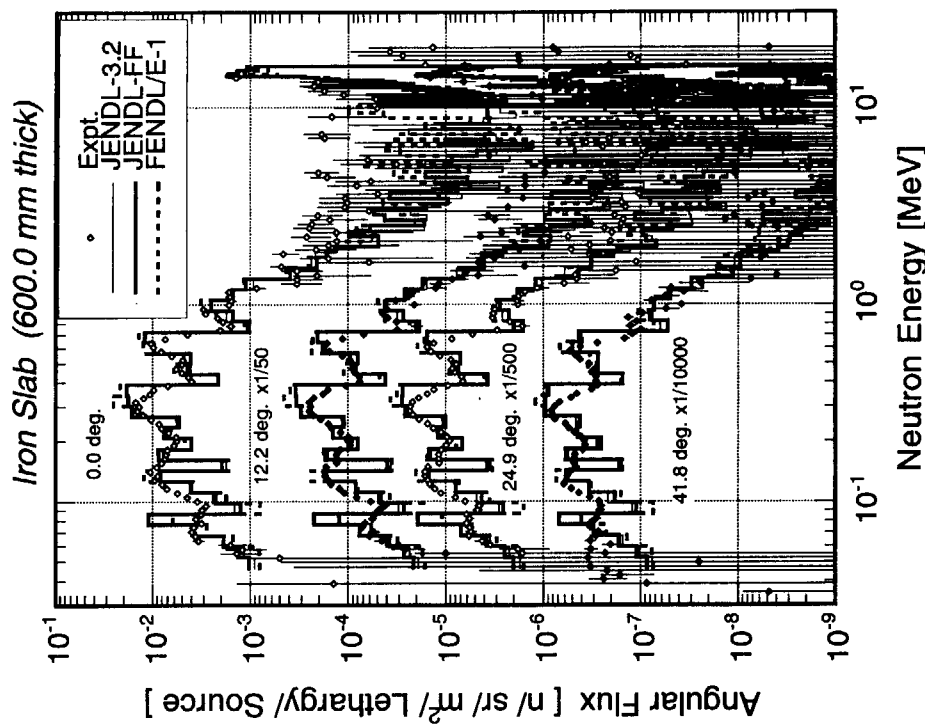


Fig. 3.3.14 Neutron spectra leaking from the iron slab assembly of 600.0 mm in thickness measured and calculated with JENDL-3.2, JENDL Fusion File and FENDL/E-1.0.

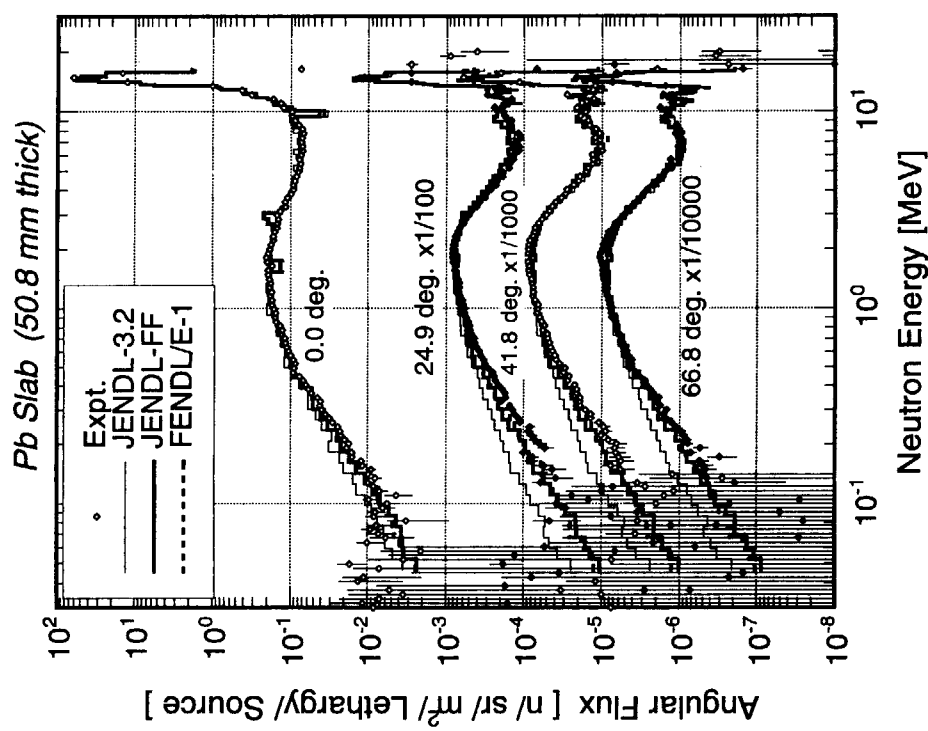


Fig. 3.3.15 Neutron spectra leaking from the lead slab assembly of 50.8 mm in thickness measured and calculated with JENDL-3.2, JENDL Fusion File and FENDL/E-1.0.

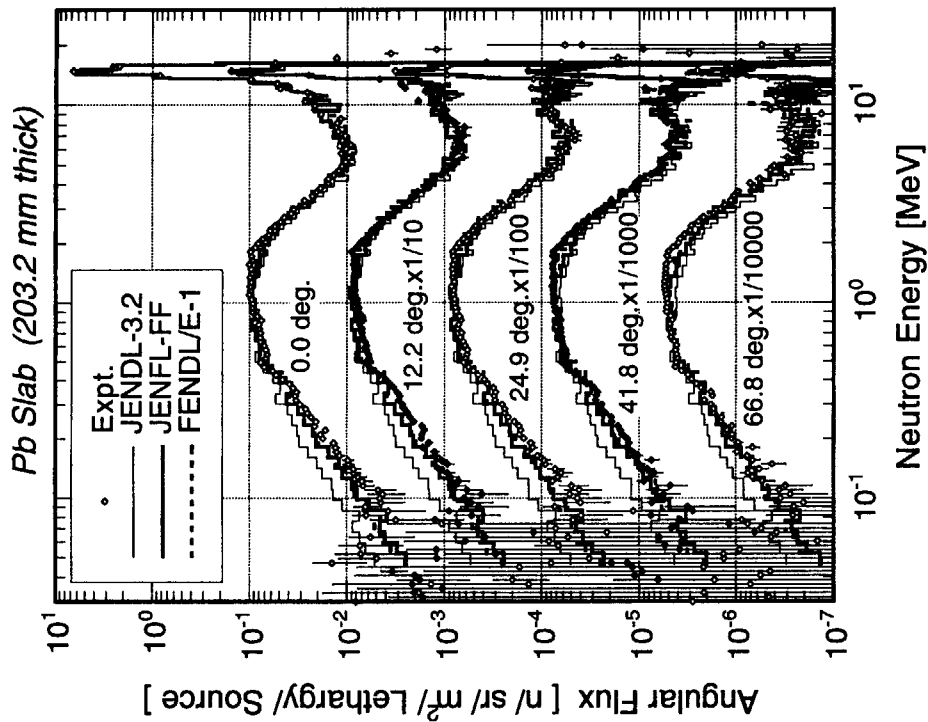


Fig. 3.3.16 Neutron spectra leaking from the lead slab assembly of 203.2 mm in thickness measured and calculated with JENDL-3.2, JENDL Fusion File and FENDL/E-1.0.

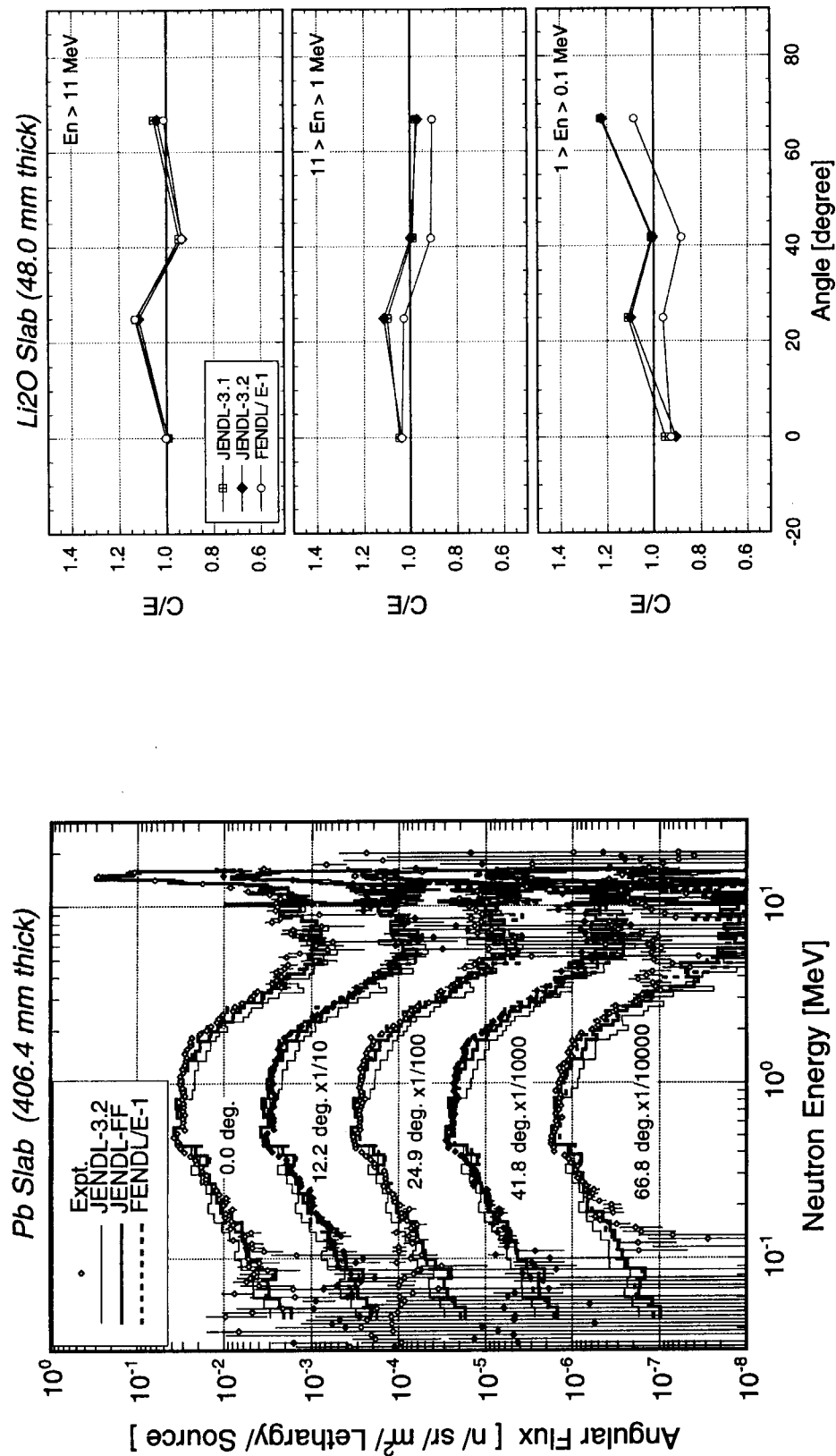


Fig. 3.3.17 Neutron spectra leaking from the lead slab assembly of 406.4 mm in thickness measured and calculated with JENDL-3.2, JENDL Fusion File and FENDL/E-1.0.

Fig. 3.3.18

Calculated to experimental ratios of integral neutron fluxes in several energy intervals for the lithium oxide slab assembly of 48.0 mm in thickness for JENDL-3.1, JENDL-3.2 and FENDL/E-1.0.

Fig. 3.3.19 Calculated to experimental ratios of integral neutron fluxes in several energy intervals for the lithium oxide slab assembly of 48.0 mm in thickness for JENDL-3.1, JENDL-3.2 and FENDL/E-1.0.

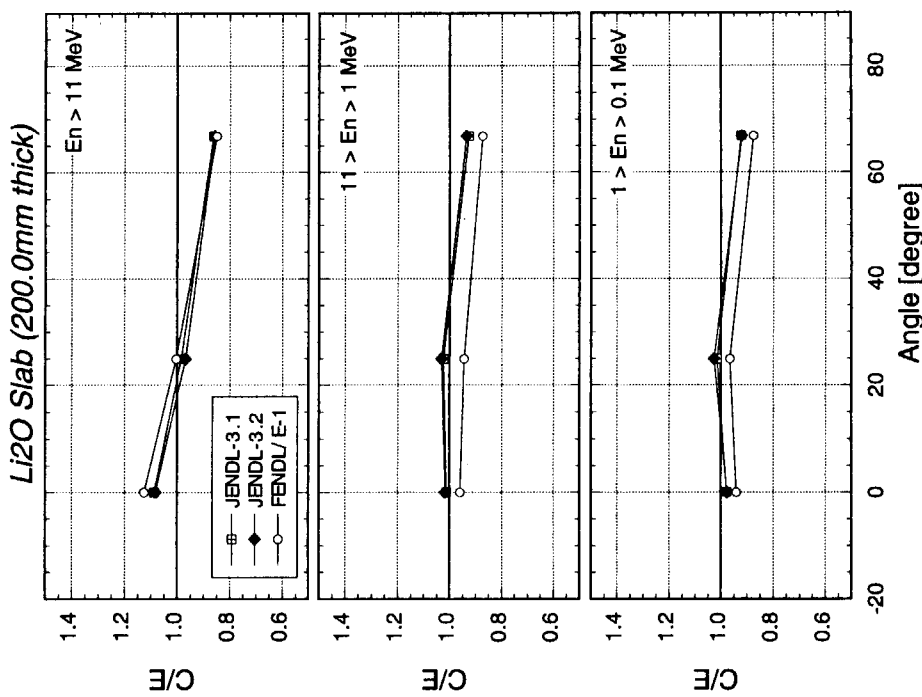


Fig. 3.3.19 Calculated to experimental ratios of integral neutron fluxes in several energy intervals for the lithium oxide slab assembly of 200.0 mm in thickness for JENDL-3.1, JENDL-3.2 and FENDL/E-1.0.

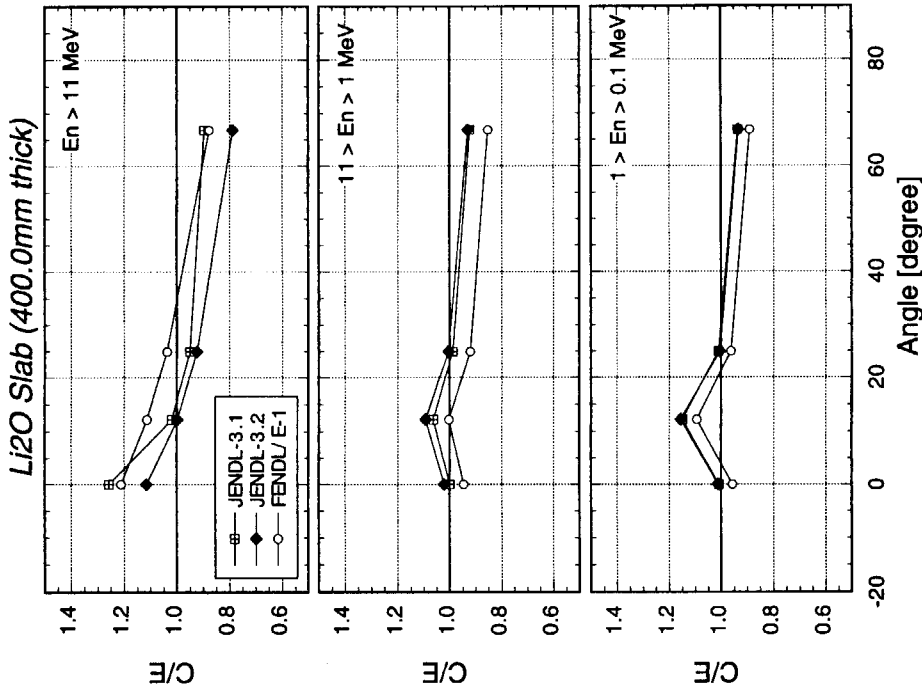


Fig. 3.3.20 Calculated to experimental ratios of integral neutron fluxes in several energy intervals for the lithium oxide slab assembly of 400.0 mm in thickness for JENDL-3.1, JENDL-3.2 and FENDL/E-1.0.

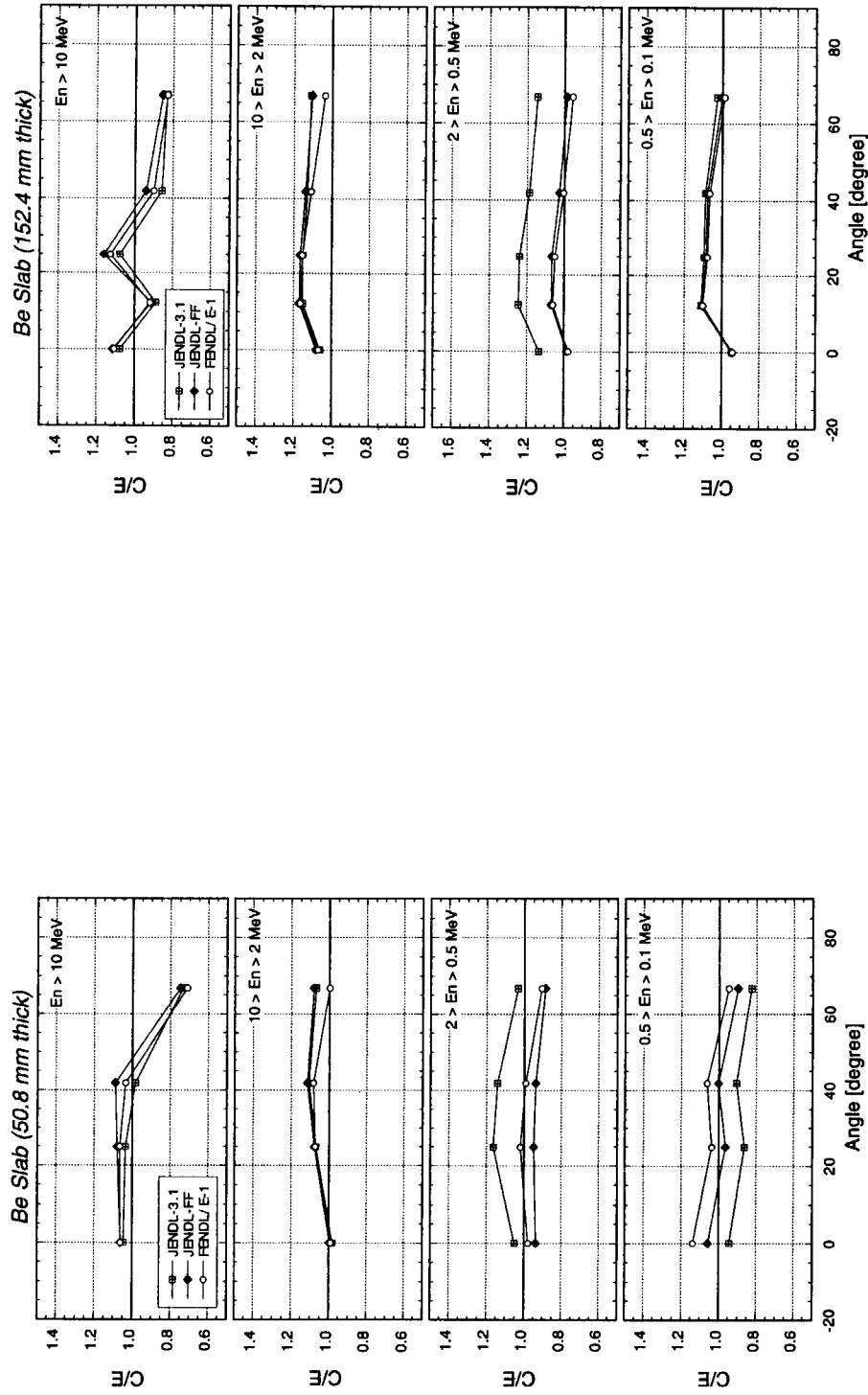


Fig. 3.3.21 Calculated to experimental ratios of integral neutron fluxes in several energy intervals for the beryllium slab assembly of 50.8 mm in thickness for JENDL-3.2, JENDL Fusion File and FENDL-E-1.

Fig. 3.3.22 Calculated to experimental ratios of integral neutron fluxes in several energy intervals for the beryllium slab assembly of 152.4 mm in thickness for JENDL-3.2, JENDL Fusion File and FENDL-E-1.

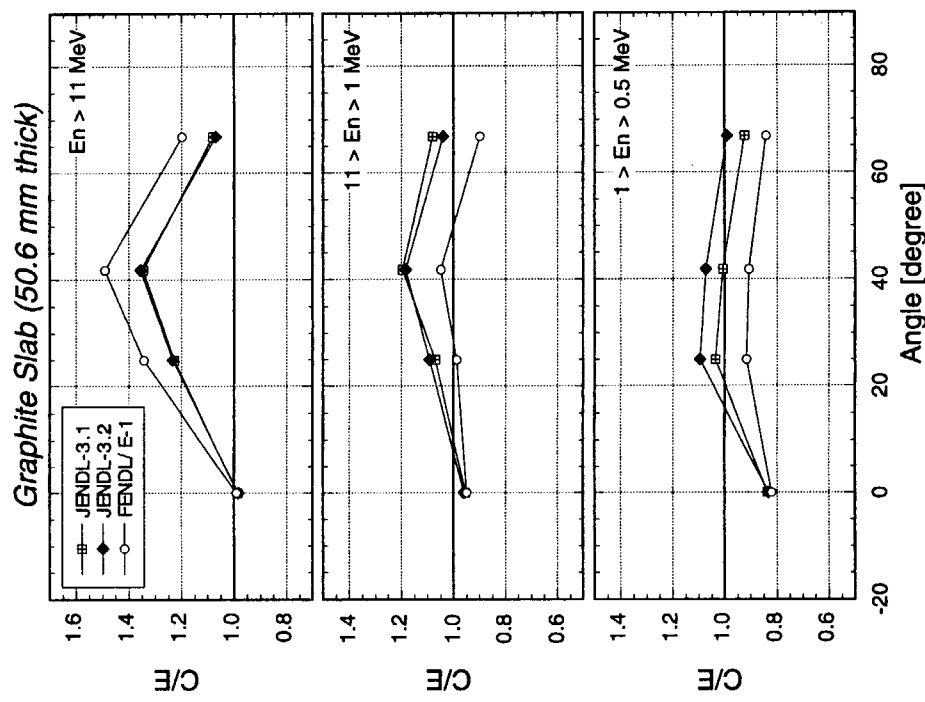


Fig. 3.3.23 Calculated to experimental ratios of integral neutron fluxes in several energy intervals for the graphite slab assembly of 50.6 mm in thickness for JENDL-3.1, JENDL-3.2 and FENDL/E-1.0.

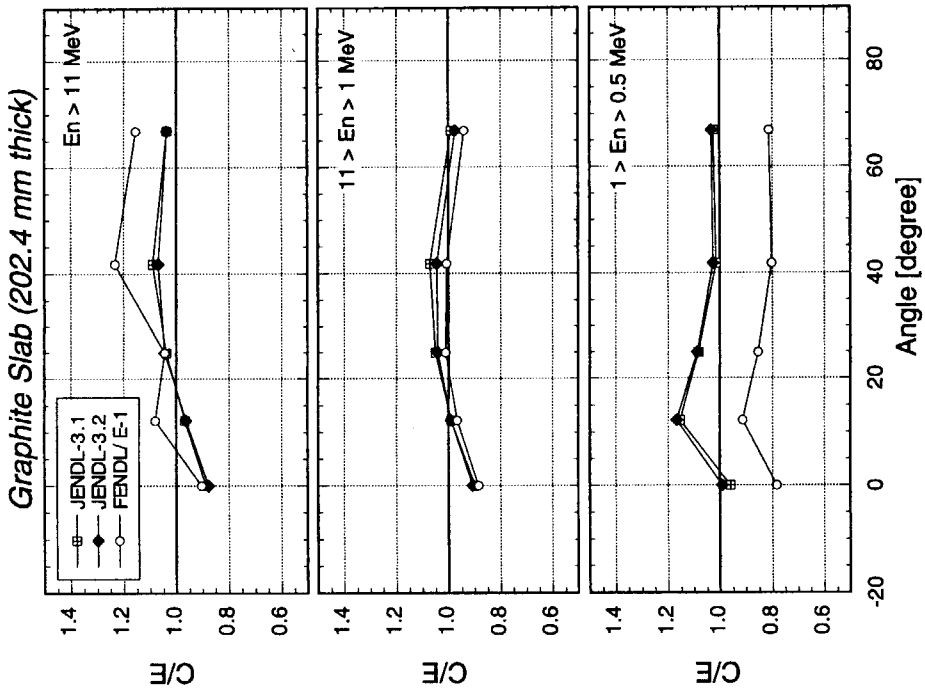


Fig. 3.3.24 Calculated to experimental ratios of integral neutron fluxes in several energy intervals for the graphite slab assembly of 202.4 mm in thickness for JENDL-3.1, JENDL-3.2 and FENDL/E-1.0.

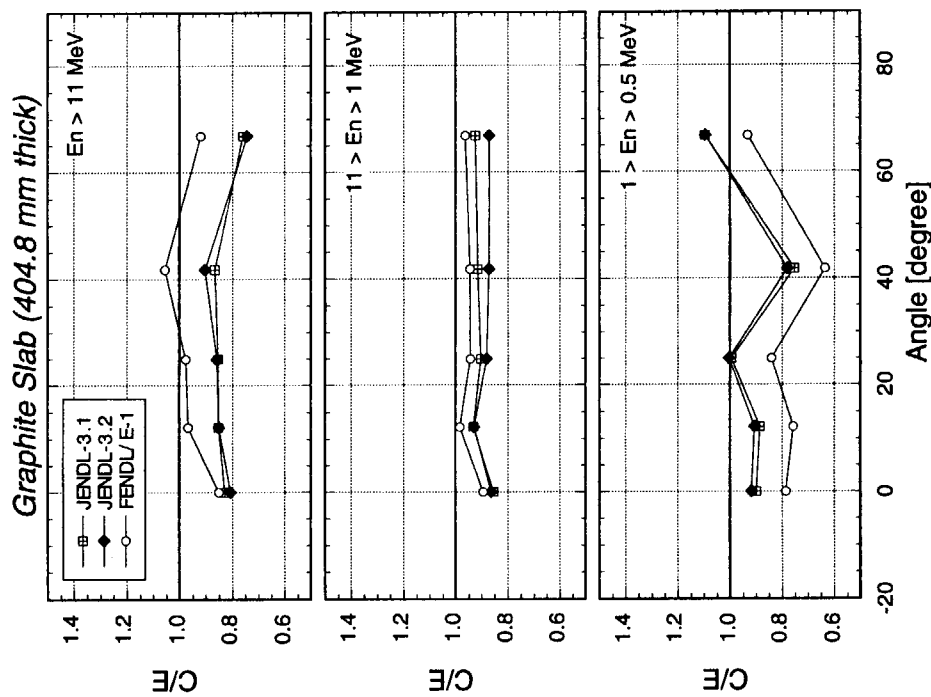


Fig. 3.3.25 Calculated to experimental ratios of integral neutron fluxes in several energy intervals for the graphite slab assembly of 404.8 mm in thickness for JENDL-3.1, JENDL-3.2 and FENDL/E-1.0.

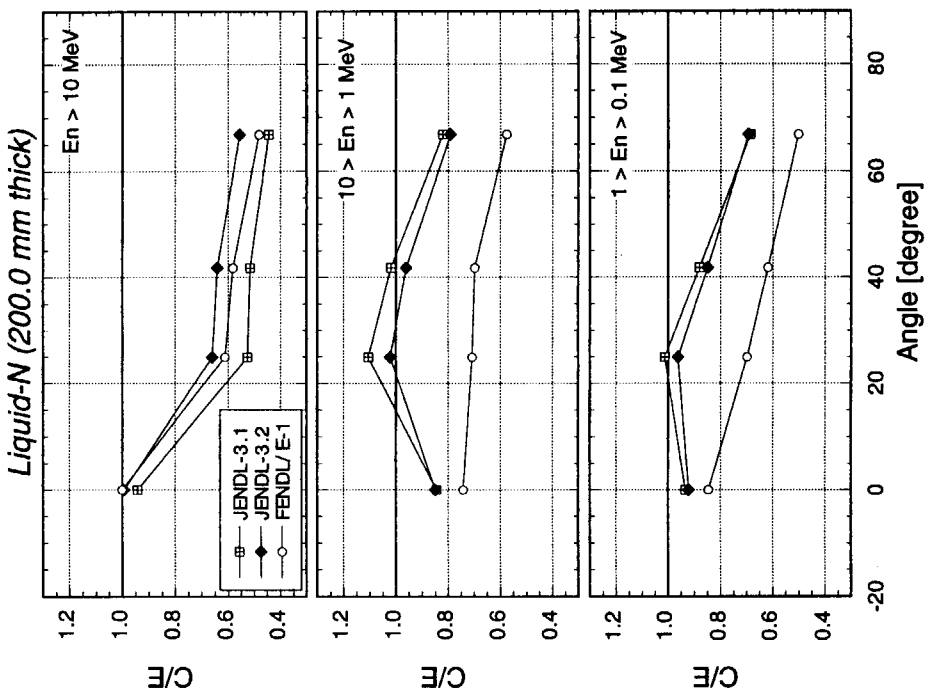


Fig. 3.3.26 Calculated to experimental ratios of integral neutron fluxes in several energy intervals for the liquid-nitrogen slab assembly of 200.0 mm in thickness for JENDL-3.1, JENDL-3.2 and FENDL/E-1.0.

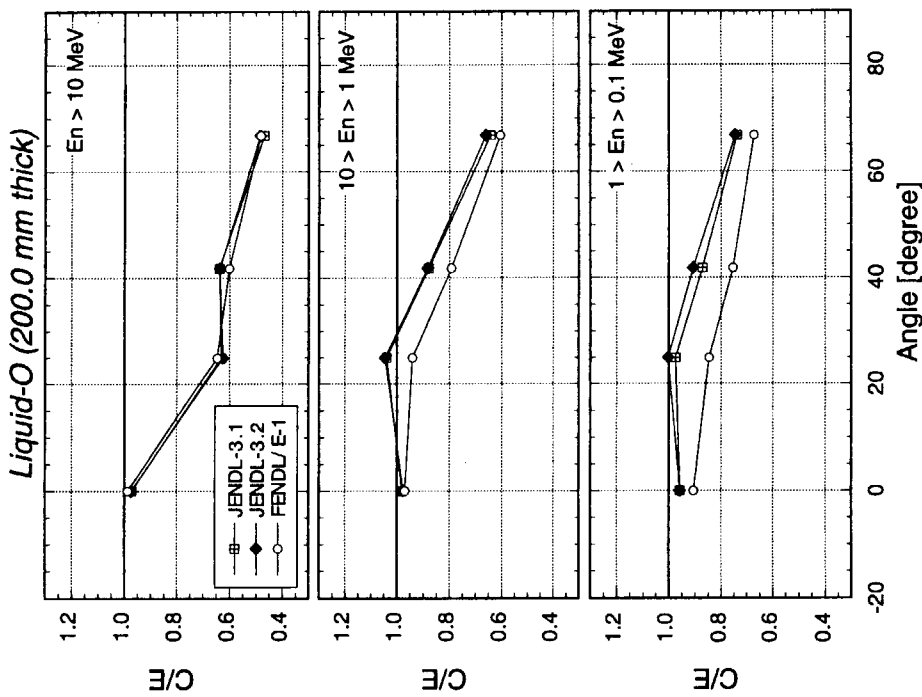


Fig. 3.3.27 Calculated to experimental ratios of integral neutron fluxes in several energy intervals for the liquid-oxygen slab assembly of 200.0 mm in thickness for JENDL-3.1, JENDL-3.2 and FENDL/E-1.0.

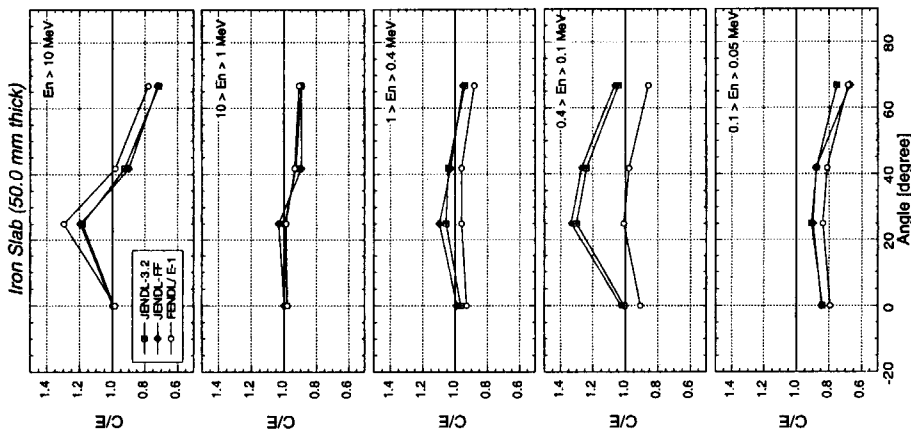


Fig. 3.3.28 Calculated to experimental ratios of integral neutron fluxes in several energy intervals for the iron slab assembly of 50.0 mm in thickness for JENDL-3.2, JENDL Fusion File and FENDL/E-1.0.

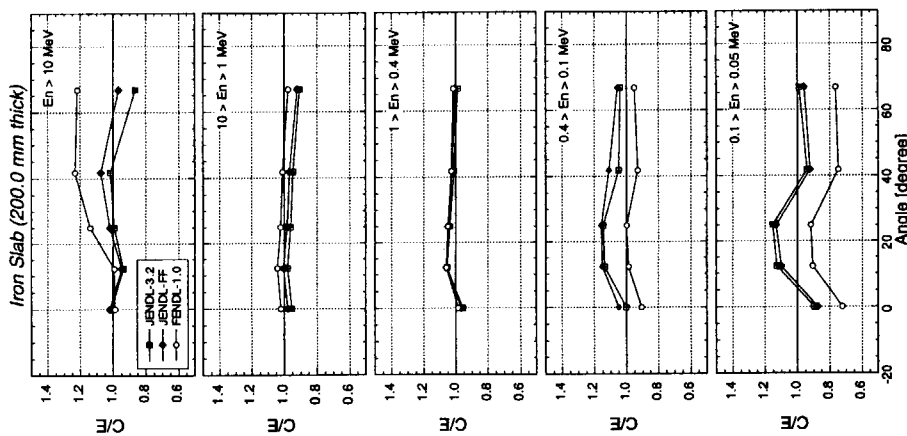


Fig. 3.3.29 Calculated to experimental ratios of integral neutron fluxes in several energy intervals for the iron slab assembly of 200.0 mm in thickness for JENDL-3.2, JENDL Fusion File and FENDL-E1.0.

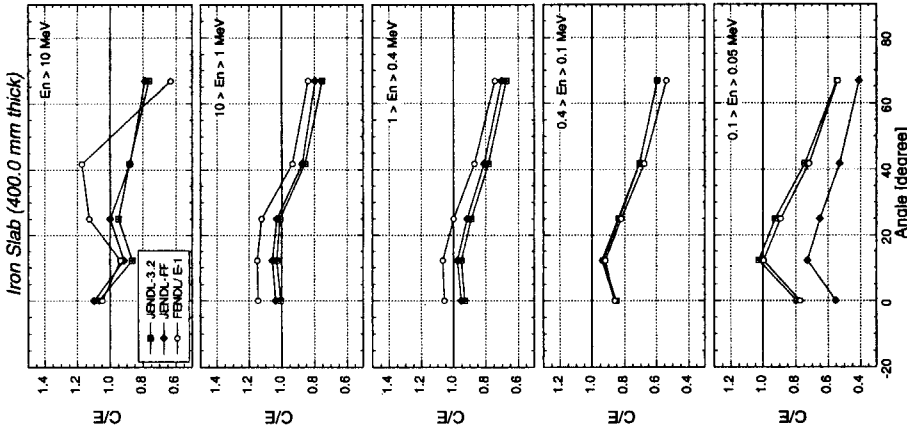


Fig. 3.3.30

Calculated to experimental ratios of integral neutron fluxes in several energy intervals for the iron slab assembly of 400.0 mm in thickness for JENDL-3.2, JENDL Fusion File and FENDL-E1.0.

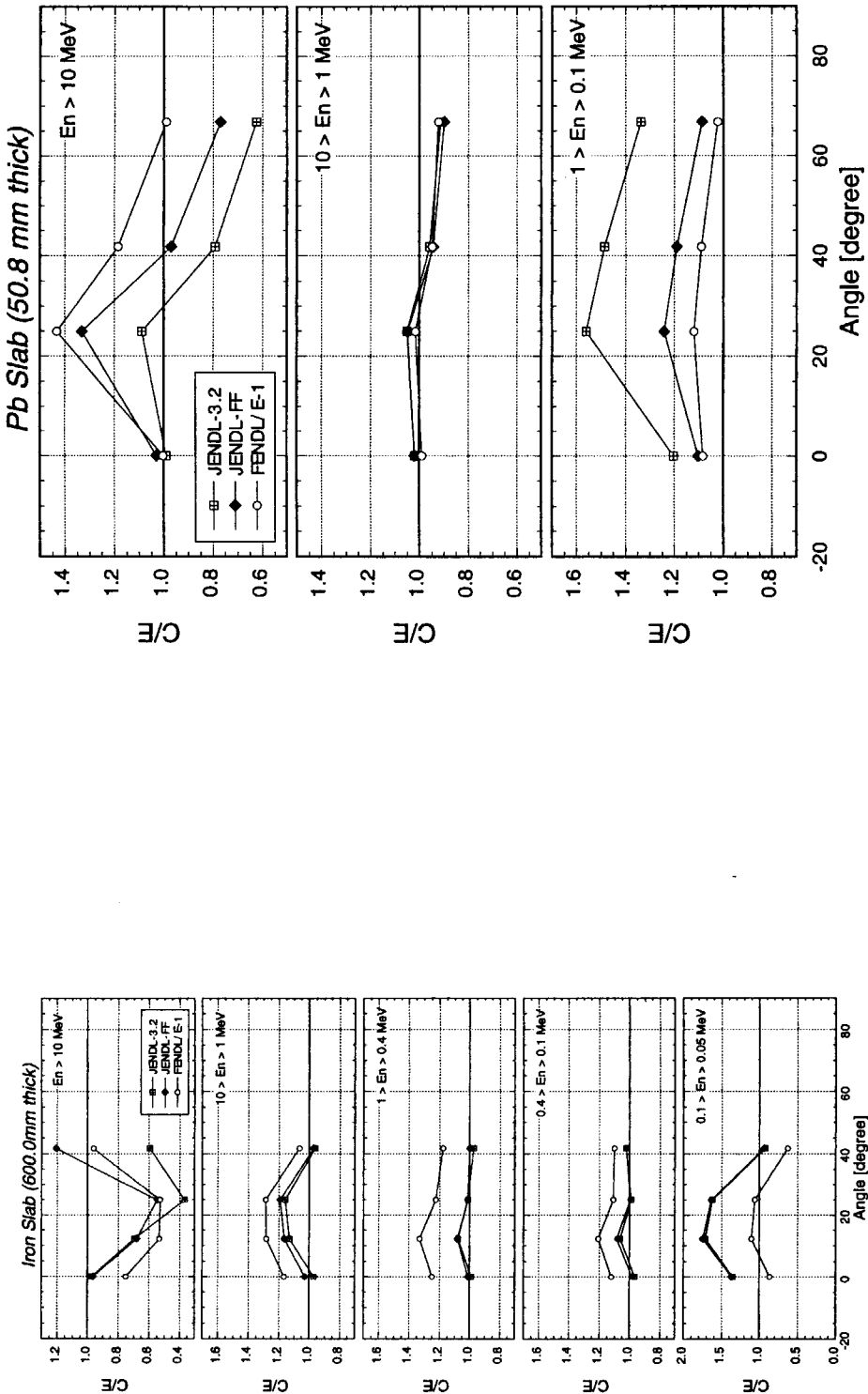


Fig. 3.3.31 Calculated to experimental ratios of integral neutron fluxes in several energy intervals for the iron slab assembly of 600.0 mm in thickness for JENDL-3.2, JENDL Fusion File and FENDL/E-1.0.

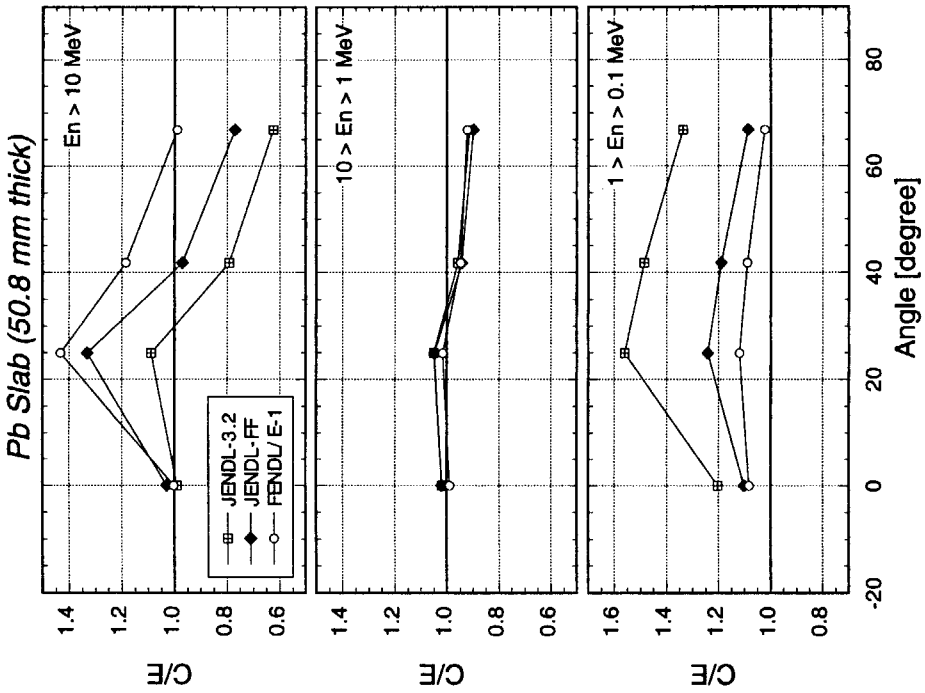


Fig. 3.3.32 Calculated to experimental ratios of integral neutron fluxes in several energy intervals for the lead slab assembly of 50.8 mm in thickness for JENDL-3.2, JENDL Fusion File and FENDL/E-1.0.

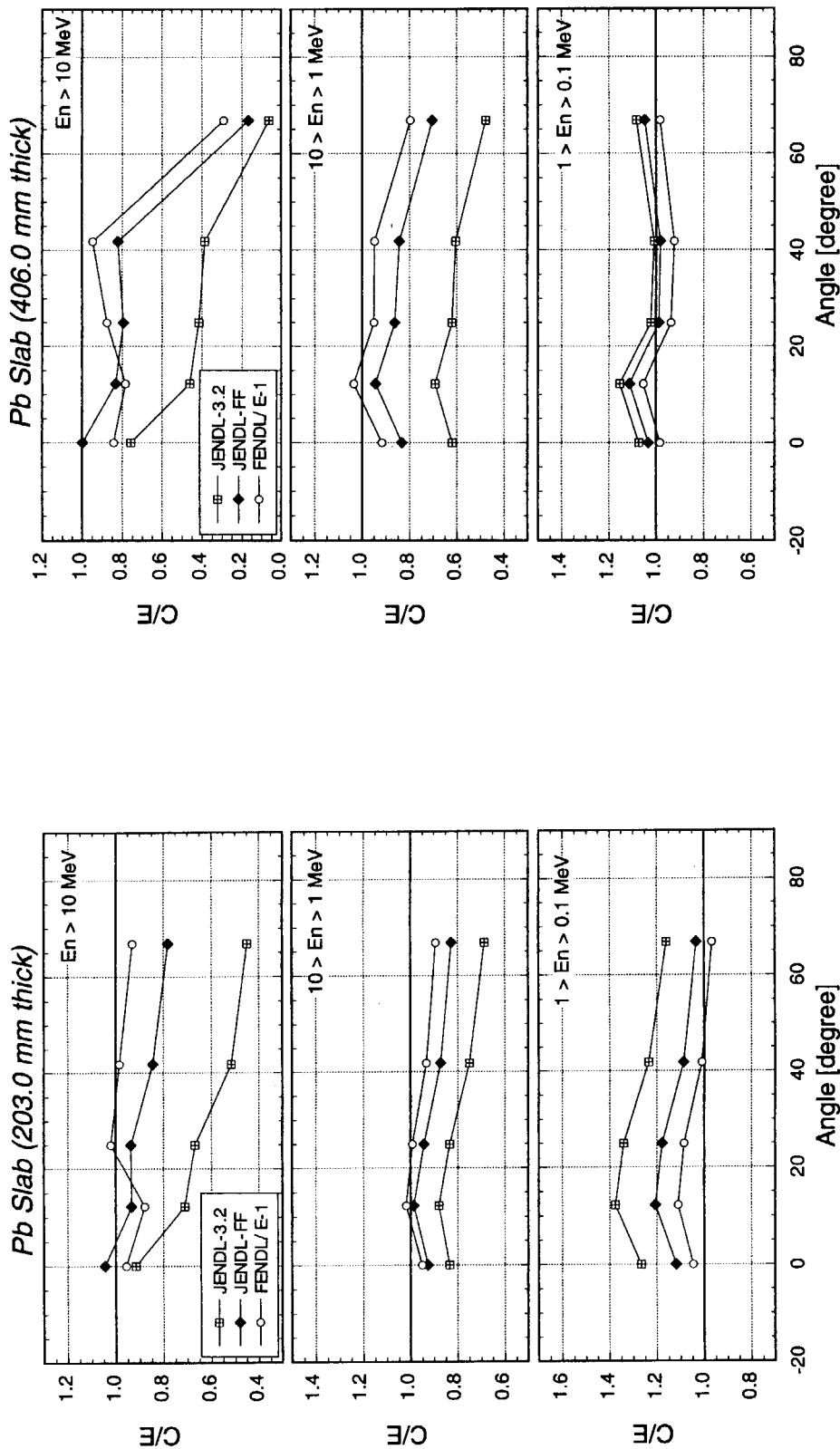


Fig. 3.3.33 Calculated to experimental ratios of integral neutron fluxes in several energy intervals for the lead slab assembly of 203.2 mm in thickness for JENDL-3.2, JENDL Fusion File and FENDL/E-10.

Fig. 3.3.34 Calculated to experimental ratios of integral neutron fluxes in several energy intervals for the lead slab assembly of 406.4 mm in thickness for JENDL-3.2, JENDL Fusion File and FENDL/E-10.

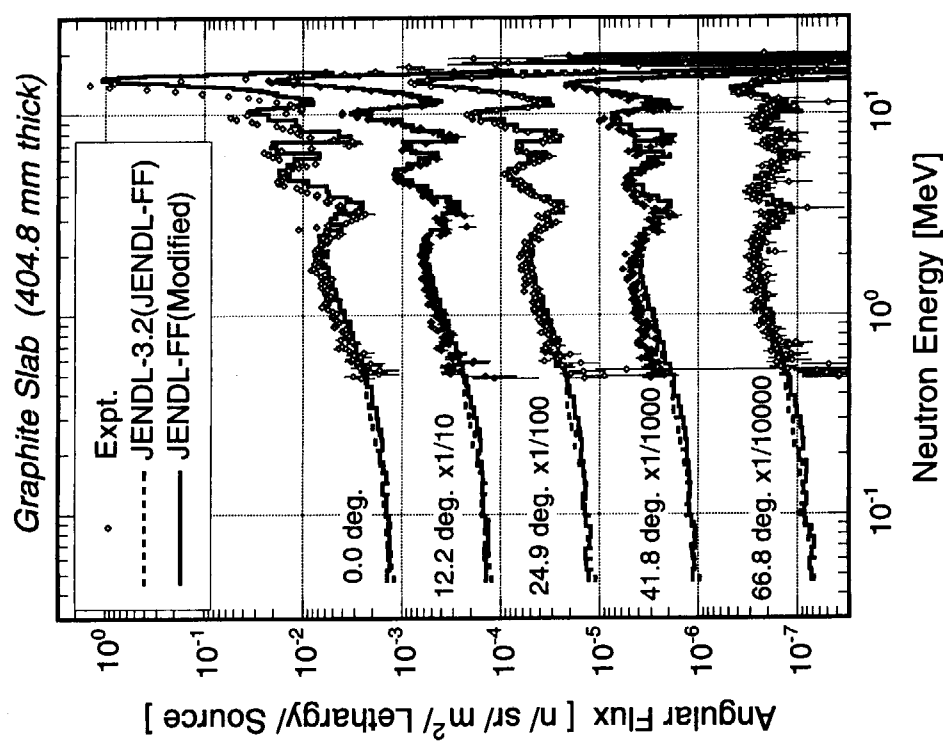


Fig. 3.4.1 Neutron spectra leaking from the graphite slab assembly of 202.4 mm in thickness measured and calculated with JENDL-3.2 (same as JENDL Fusion File) and the modified JENDL Fusion File.

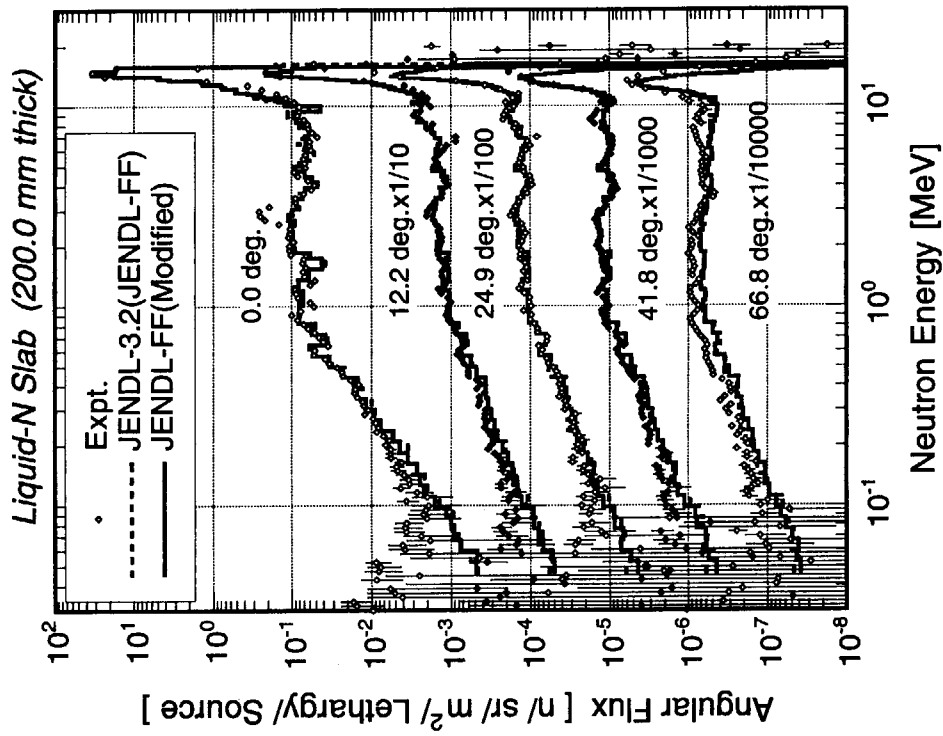


Fig. 3.4.2 Neutron spectra leaking from the liquid-nitrogen slab assembly of 200.0 mm in thickness measured and calculated with JENDL-3.2 (same as JENDL Fusion File) and the modified JENDL Fusion File.

Fig. 3.4.3 Neutron spectra leaking from the liquid-nitrogen slab assembly of 200.0 mm in thickness measured and calculated with JENDL-3.2 (same as JENDL Fusion File) and the modified JENDL Fusion File.

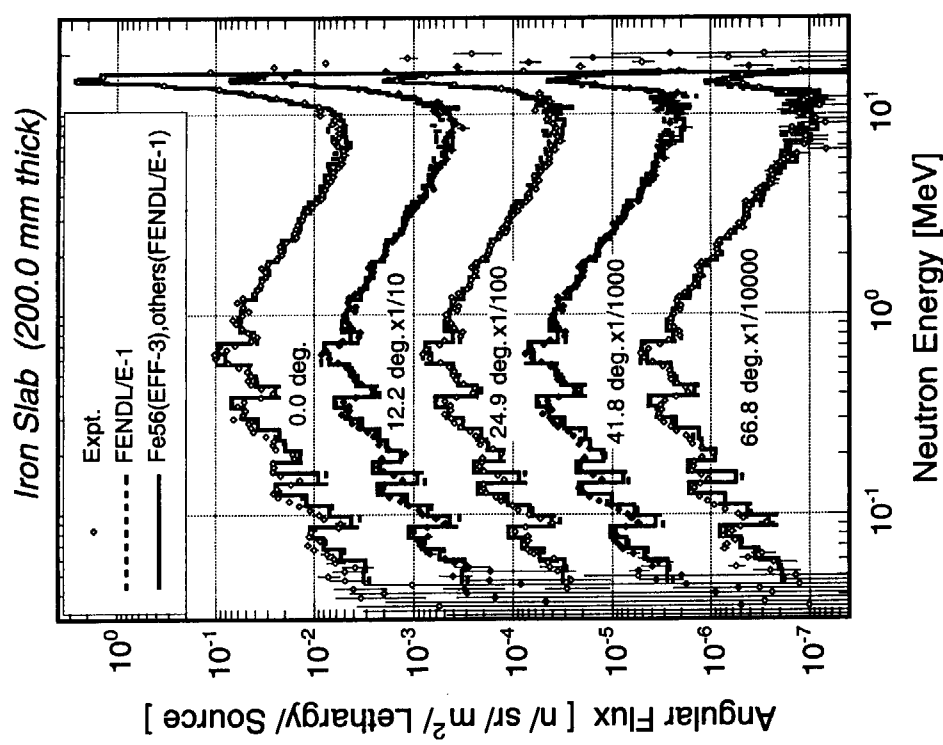


Fig. 3.4.3 Neutron spectra leaking from the iron slab assembly of 200.0 mm in thickness measured and calculated with FENDL/E-1.0, and the combination of EFF-3 (Fe-56) and FENDL/E-1.0 (Fe-54, Fe-57 & Fe-58).

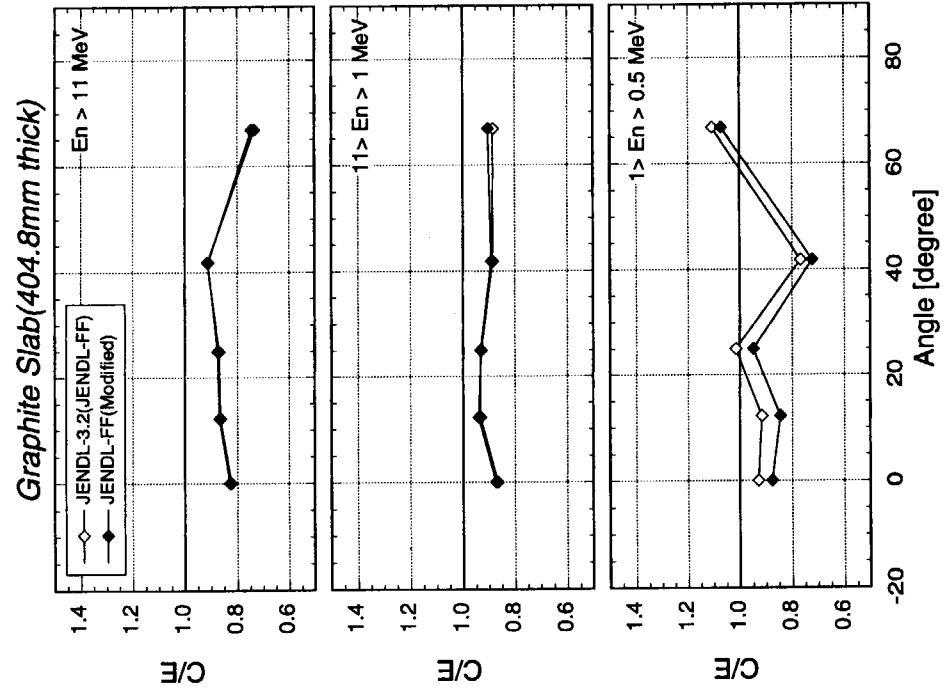


Fig. 3.4.4 Calculated to experimental ratios of integral neutron fluxes in several energy intervals for the graphite slab assembly of 202.4 mm in thickness for JENDL-3.2 (same as JENDL Fusion File) and the modified JENDL Fusion File.

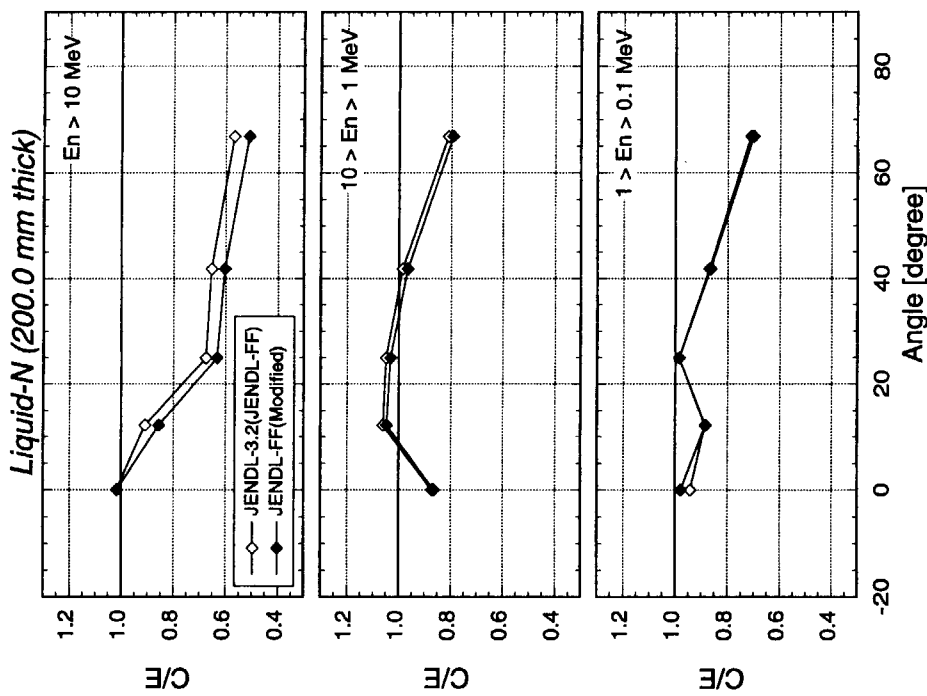


Fig. 3.4.5 Calculated to experimental ratios of integral neutron fluxes in several energy intervals for the liquid-nitrogen slab assembly of 200.0 mm in thickness for JENDL-3.2 (same as JENDL Fusion File) and the modified JENDL Fusion File.

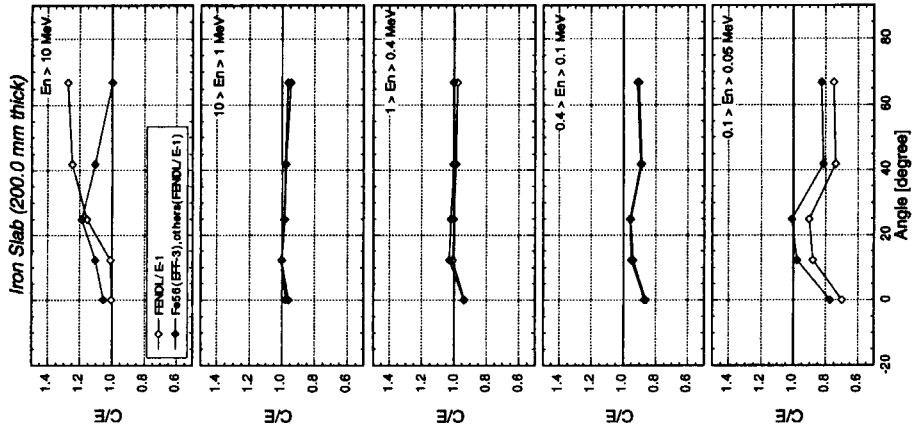


Fig. 3.4.6

Calculated to experimental ratios of integral neutron fluxes in several energy intervals for the iron slab assembly of 200.0 mm in thickness for FENDL/E-1.0, and the combination of BF-3 (Fe-56) and FENDL/E-1.0 (Fe-54, Fe-57 & Fe-58).

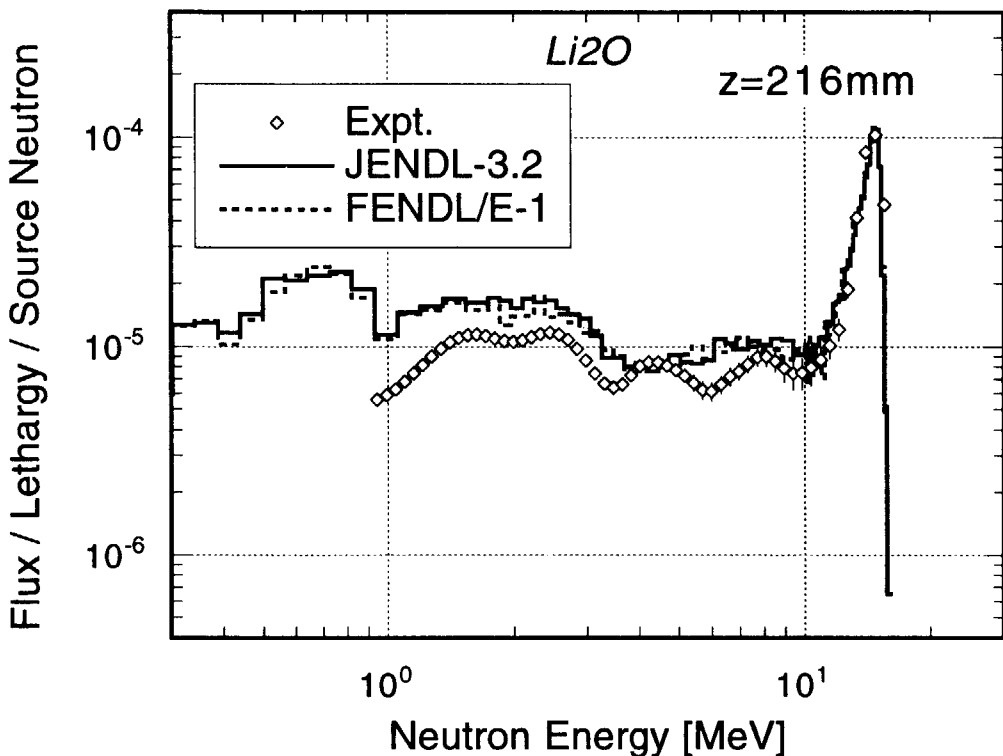


Fig. 4.3.1 Neutron spectra at the 216 mm depth in the cylindrical lithium oxide assembly measured and calculated with JENDL-3.2 and FENDL/E-1.0.

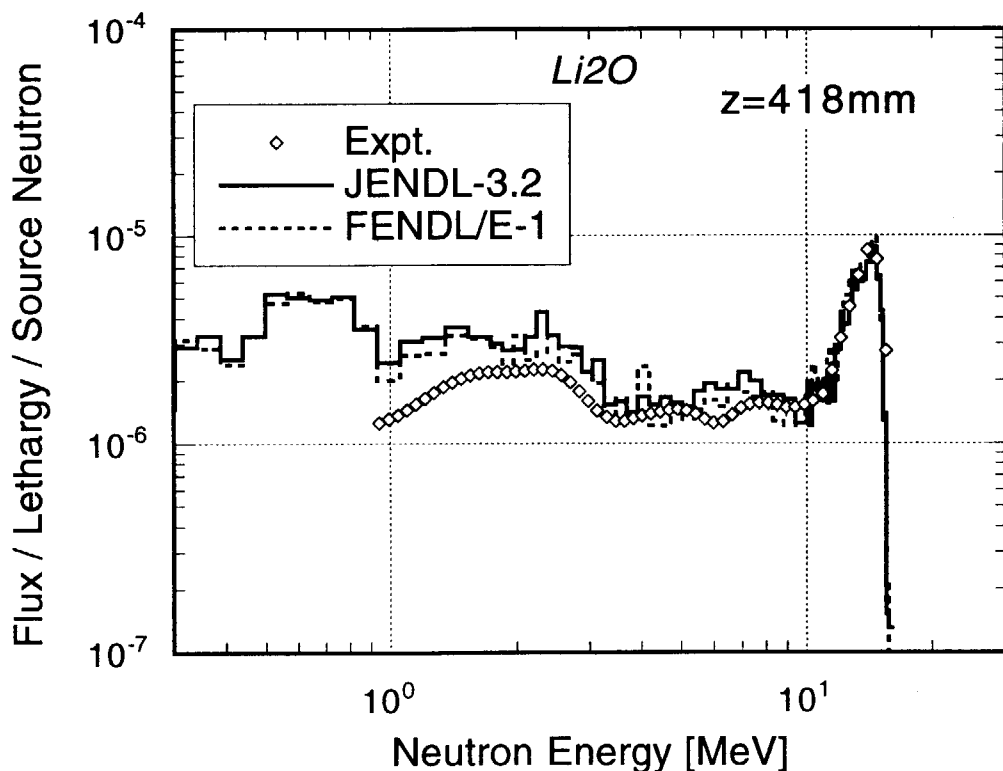


Fig. 4.3.2 Neutron spectra at the 418 mm depth in the cylindrical lithium oxide assembly measured and calculated with JENDL-3.2 and FENDL/E-1.0.

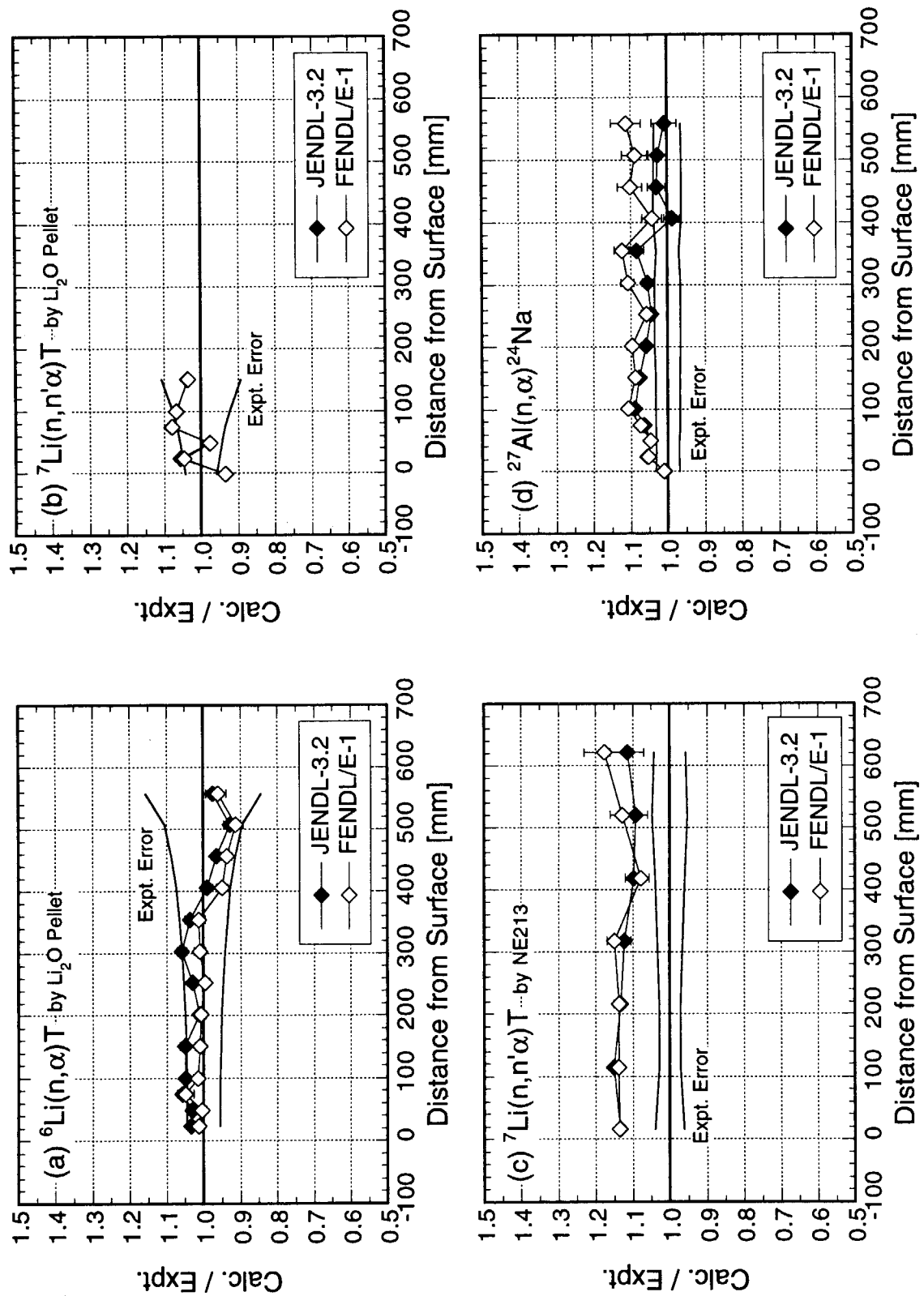


Fig. 4.3.3 Calculated to experimental ratios of dosimetry reaction rates in the cylindrical lithium oxide assembly for JENDL-3.2 and FENDL/E-1.0. (1/3)

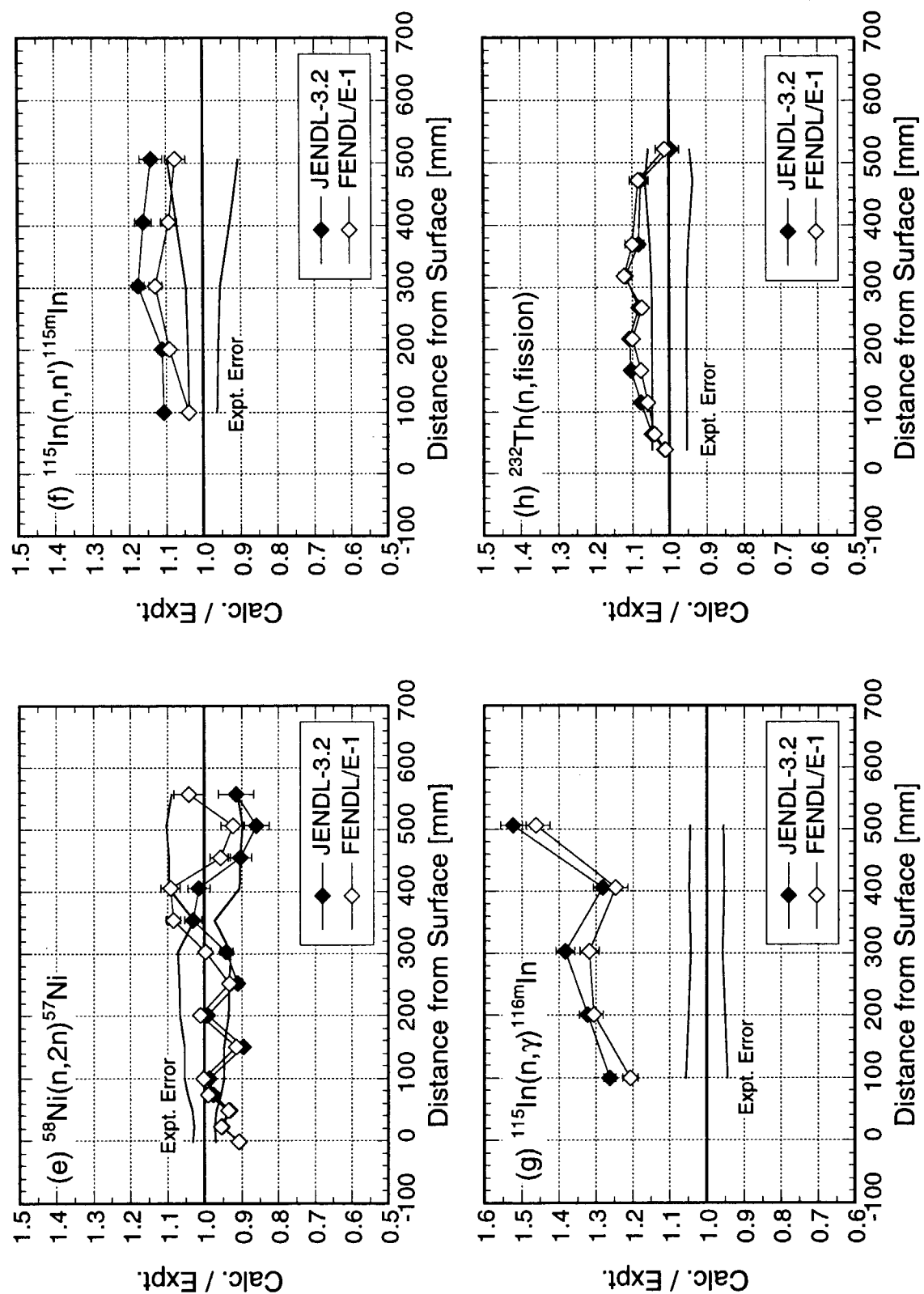


Fig. 4.3.3 Continued. (2/3)

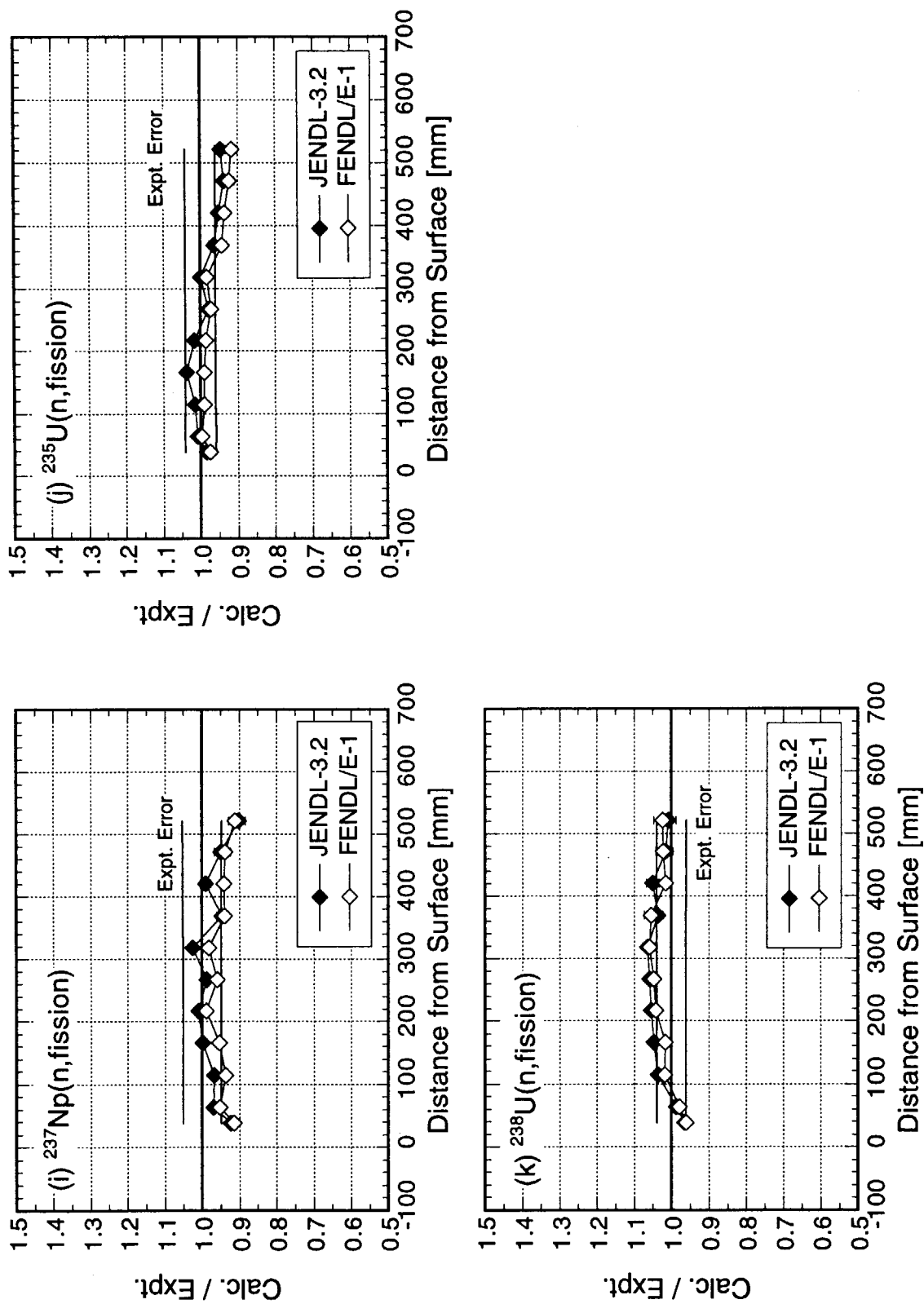
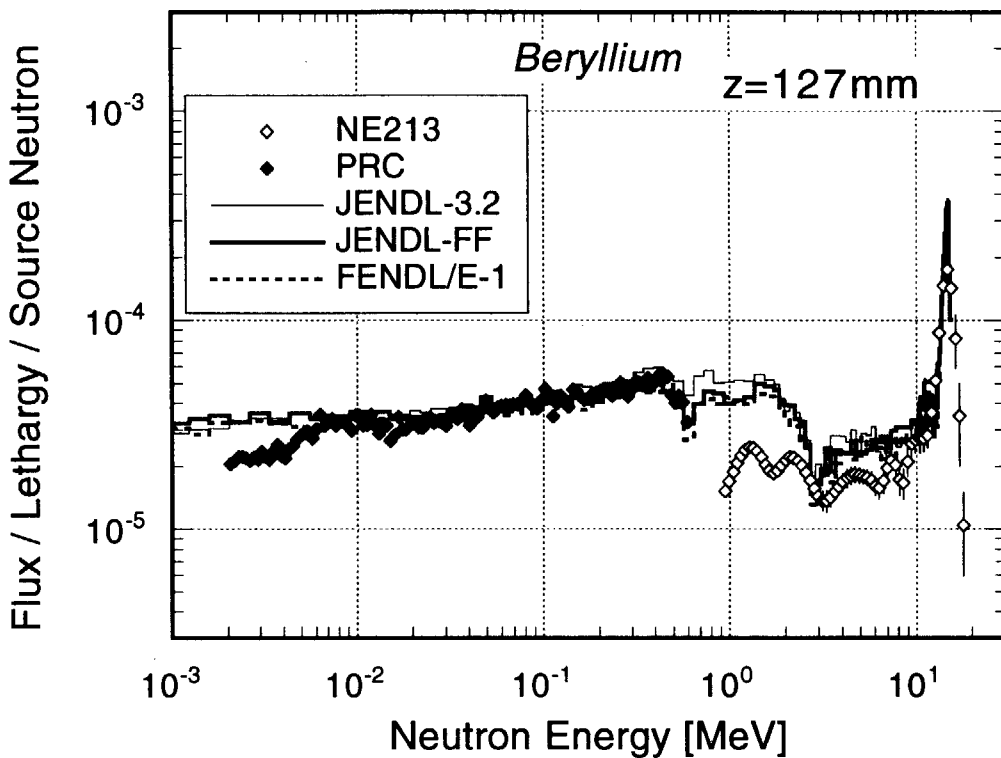


Fig. 4.3.3 Continued. (3/3)



4.3.4 Neutron spectra at the 127 mm depth in the cylindrical beryllium assembly measured and calculated with JENDL-3.2, JENDL Fusion File and FENDL/E-1.0.

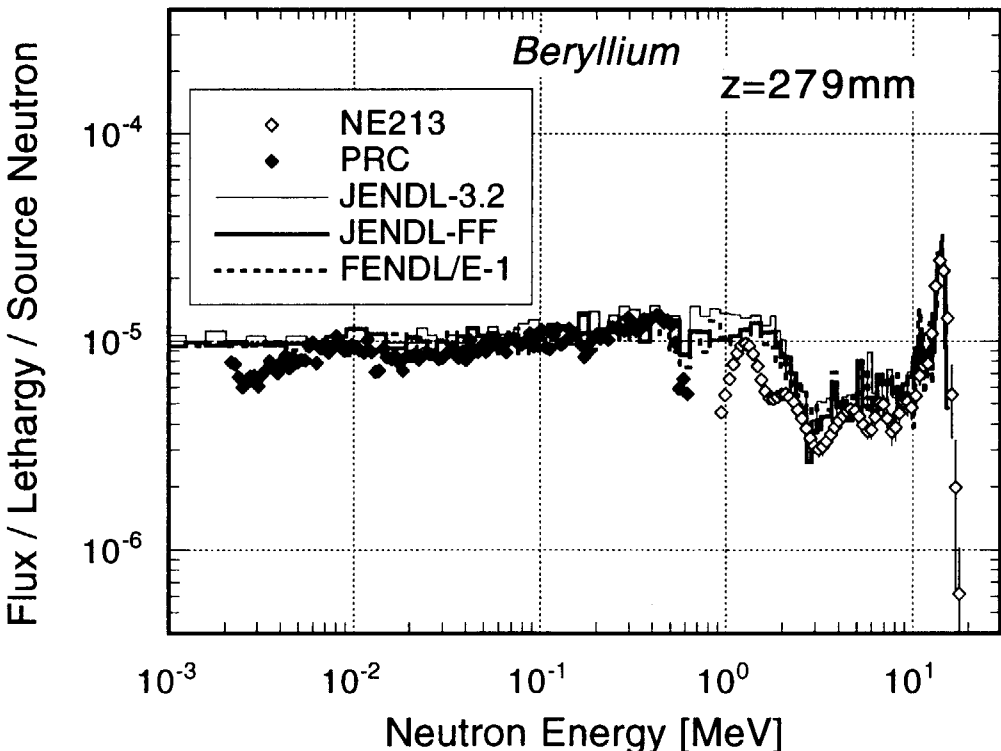


Fig. 4.3.5 Neutron spectra at the 279 mm depth in the cylindrical beryllium assembly measured and calculated with JENDL-3.2, JENDL Fusion File and FENDL/E-1.0.

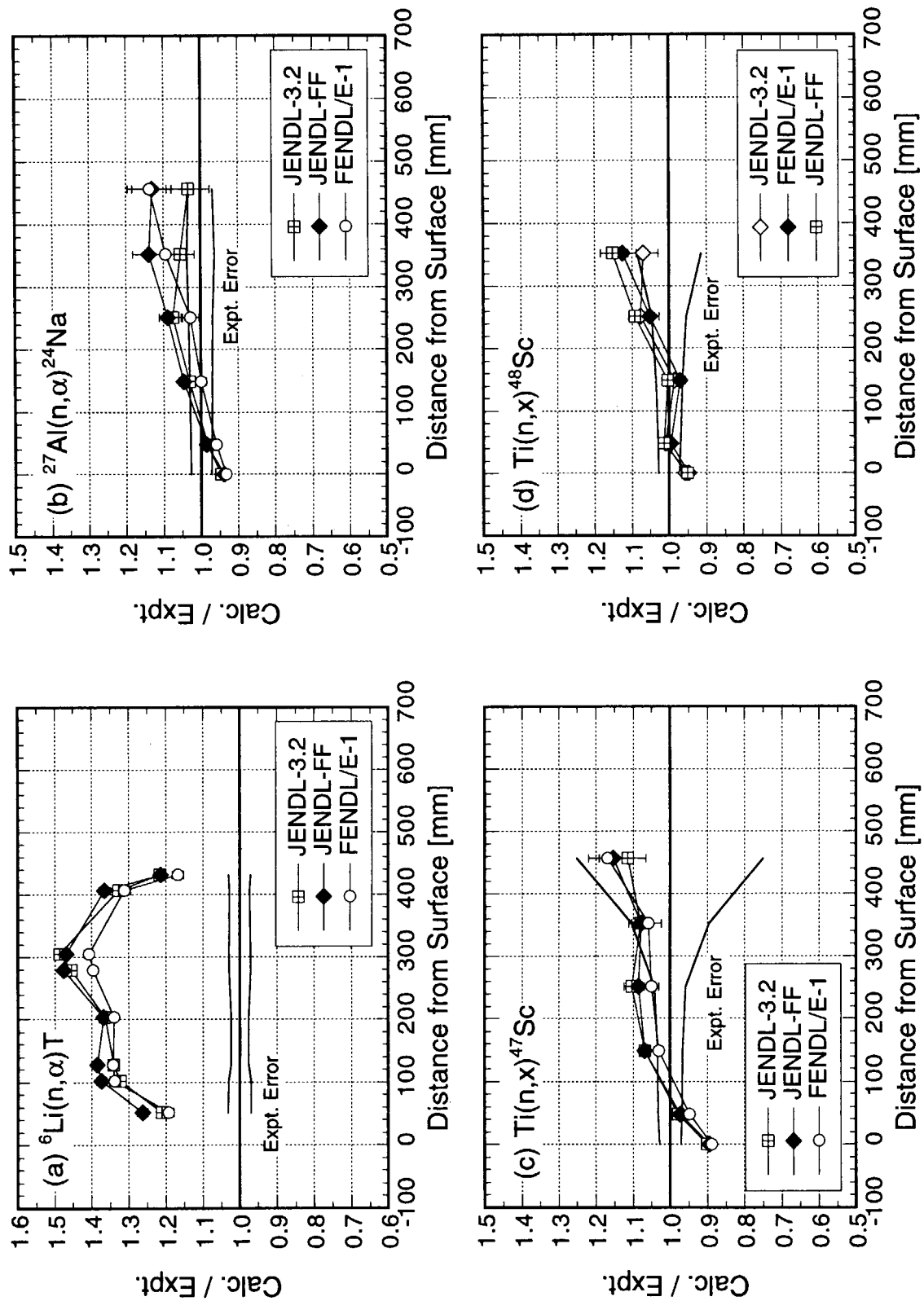


Fig. 4.3.6 Calculated to experimental ratios of dosimetry reaction rates in the cylindrical beryllium assembly for JENDL-3.2, JENDL Fusion File and FENDL/E-1.0. (1/3)

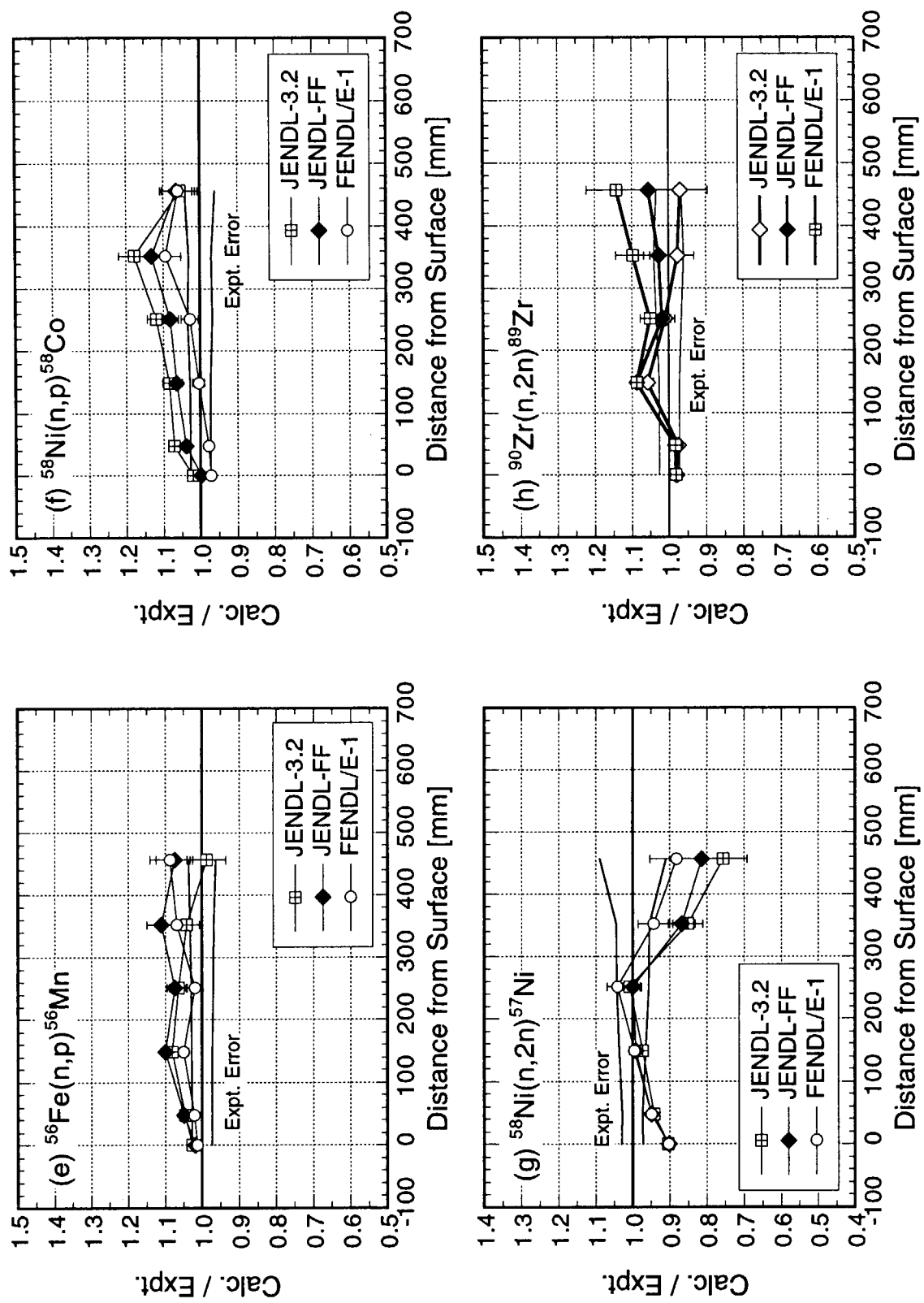


Fig. 4.3.6 Continued. (2/3)

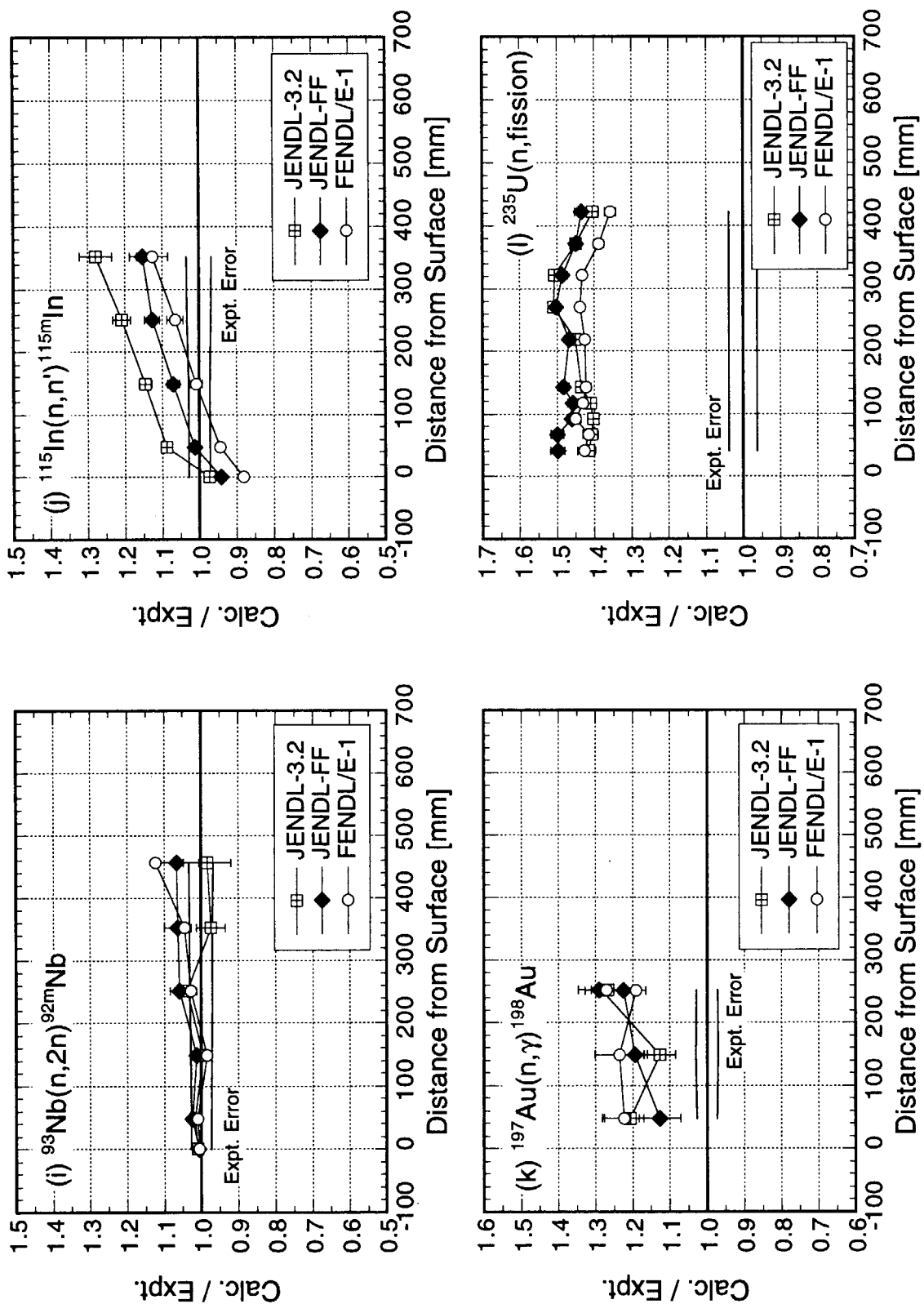


Fig. 4.3.6 Continued. (3/3)

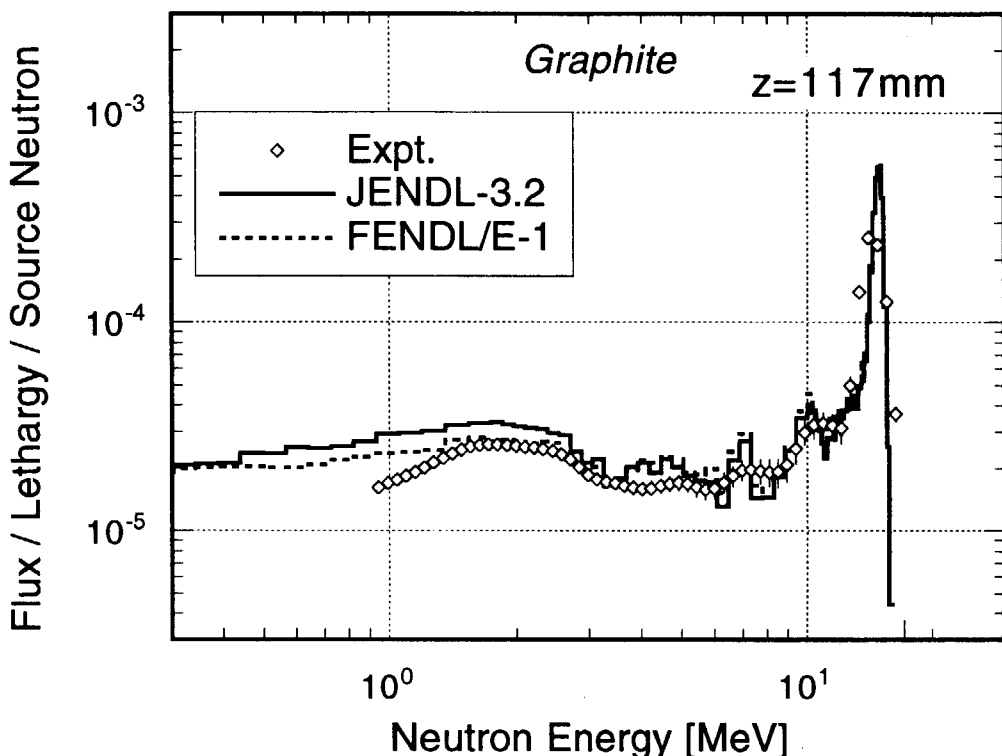


Fig. 4.3.7 Neutron spectra at the 117 mm depth in the cylindrical graphite assembly measured and calculated with JENDL-3.2 and FENDL/E-1.0.

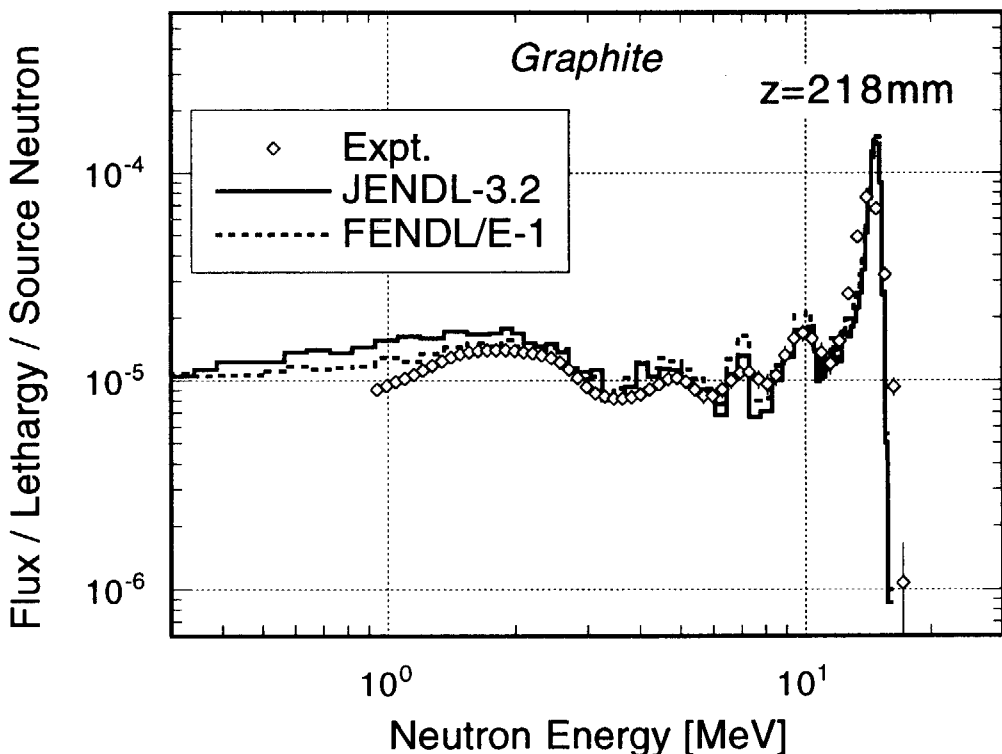


Fig. 4.3.8 Neutron spectra at the 218 mm depth in the cylindrical graphite assembly measured and calculated with JENDL-3.2 and FENDL/E-1.0.

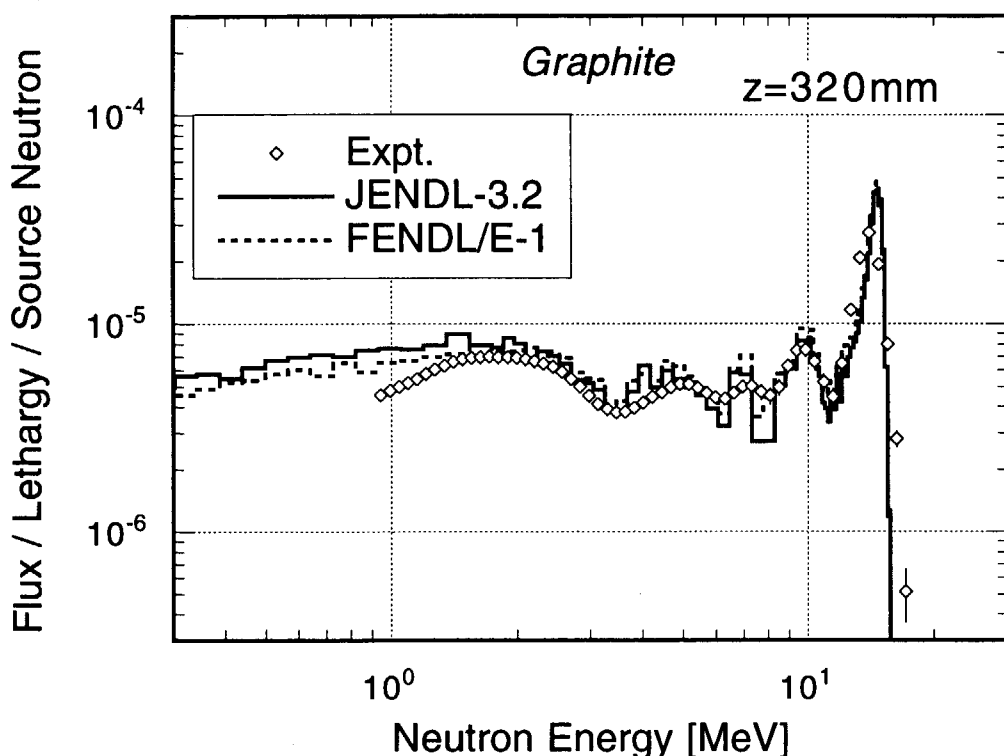


Fig. 4.3.9 Neutron spectra at the 320 mm depth in the cylindrical graphite assembly measured and calculated with JENDL-3.2 and FENDL/E-1.0.

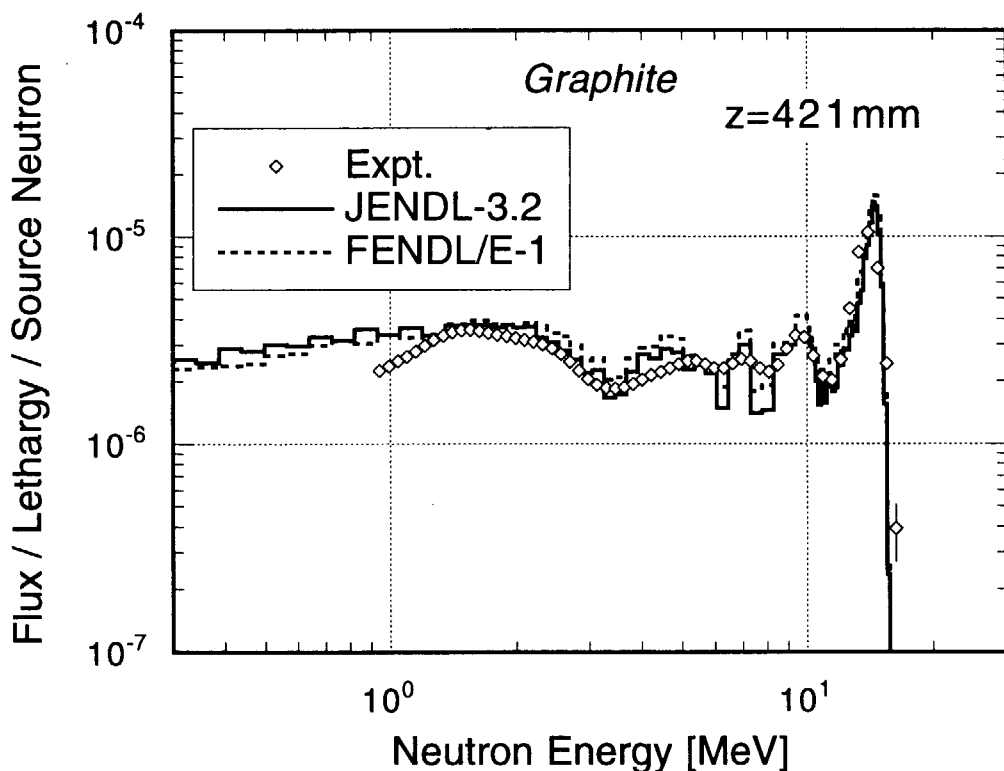


Fig. 4.3.10 Neutron spectra at the 421 mm depth in the cylindrical graphite assembly measured and calculated with JENDL-3.2 and FENDL/E-1.0.

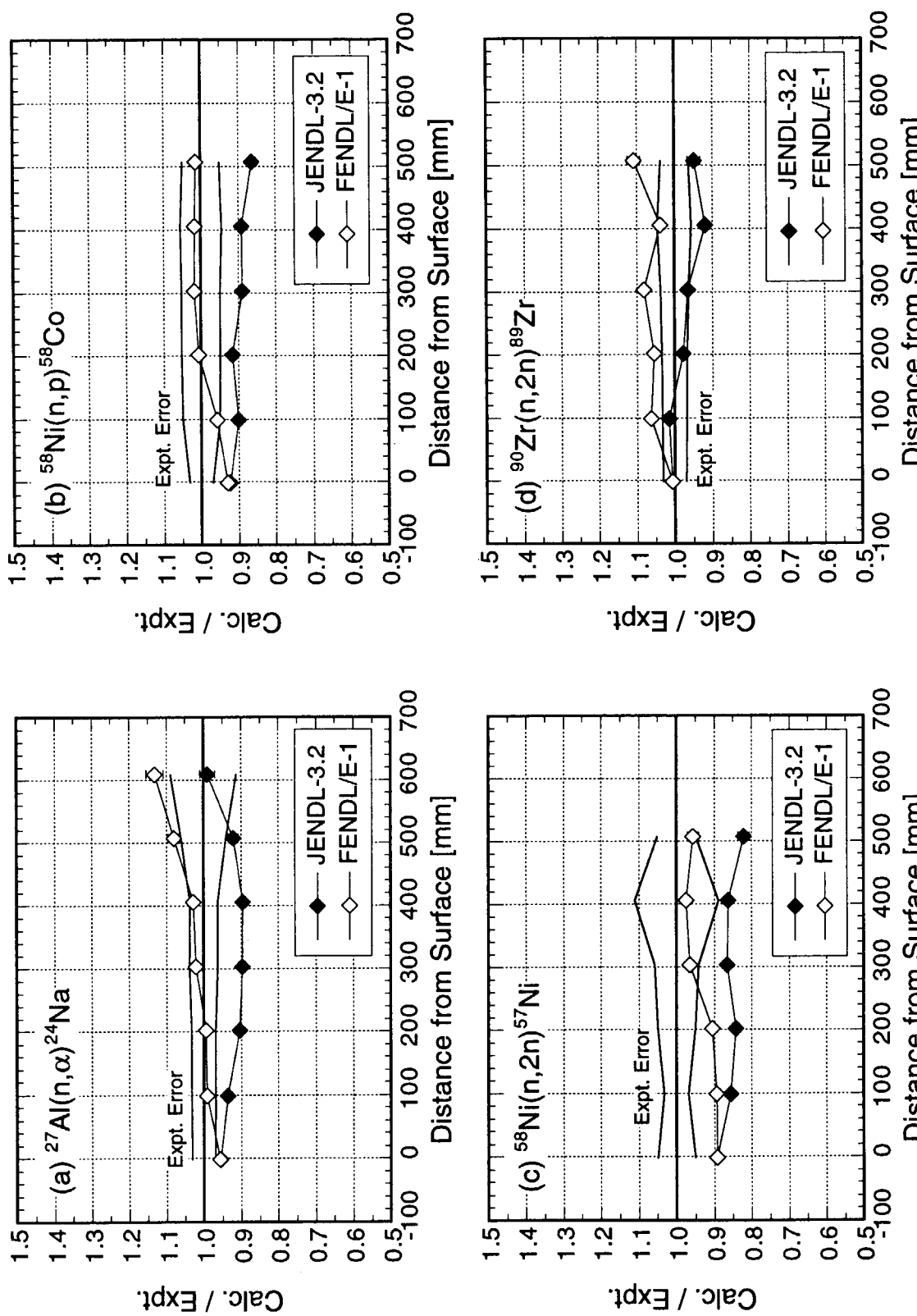


Fig. 4.3.11 Calculated to experimental ratios of dosimetry reaction rates in the cylindrical graphite assembly for JENDL-3.2 and FENDL/E-1.0. (1/2)

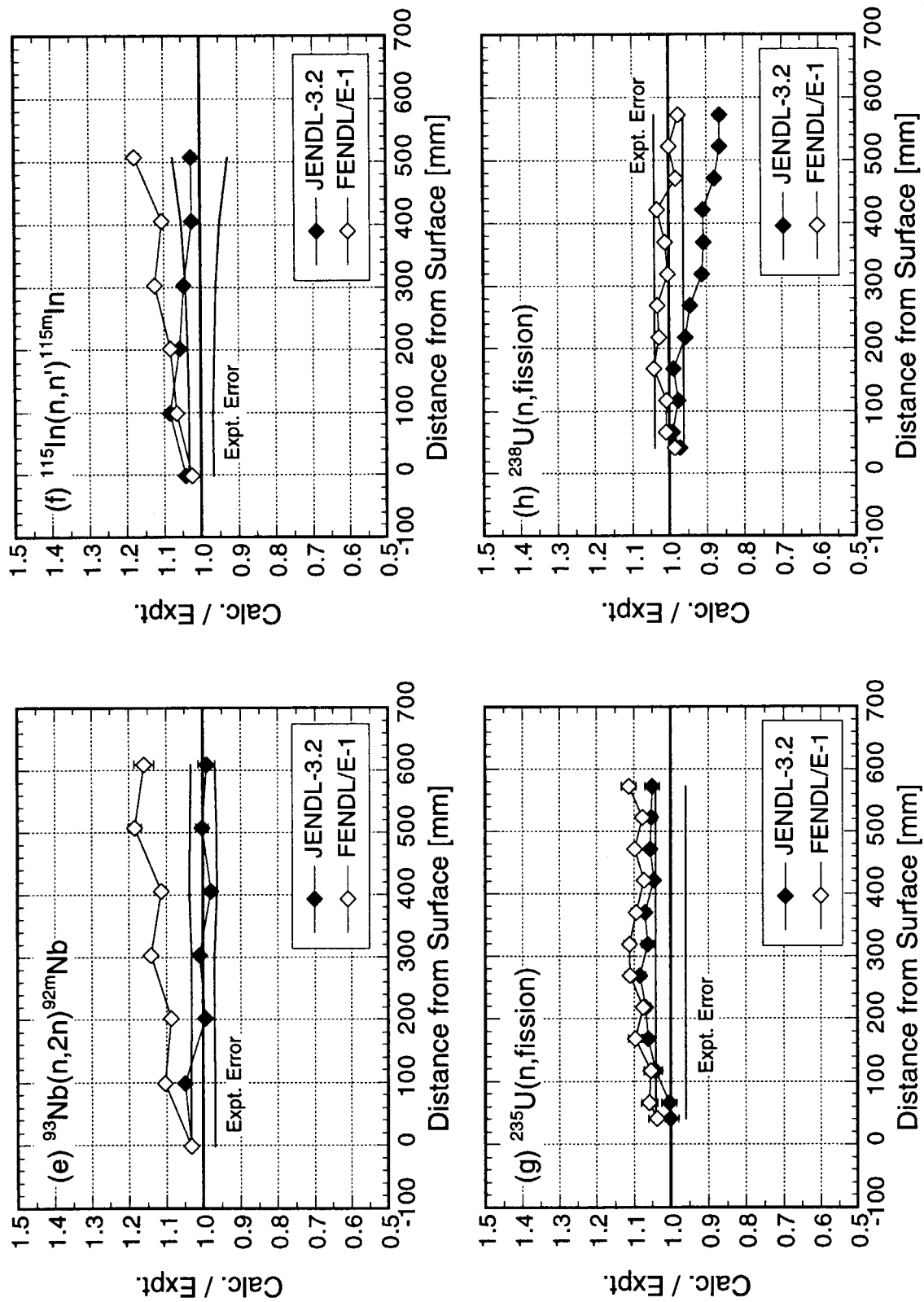


Fig. 4.3.11 Continued. (2/2)

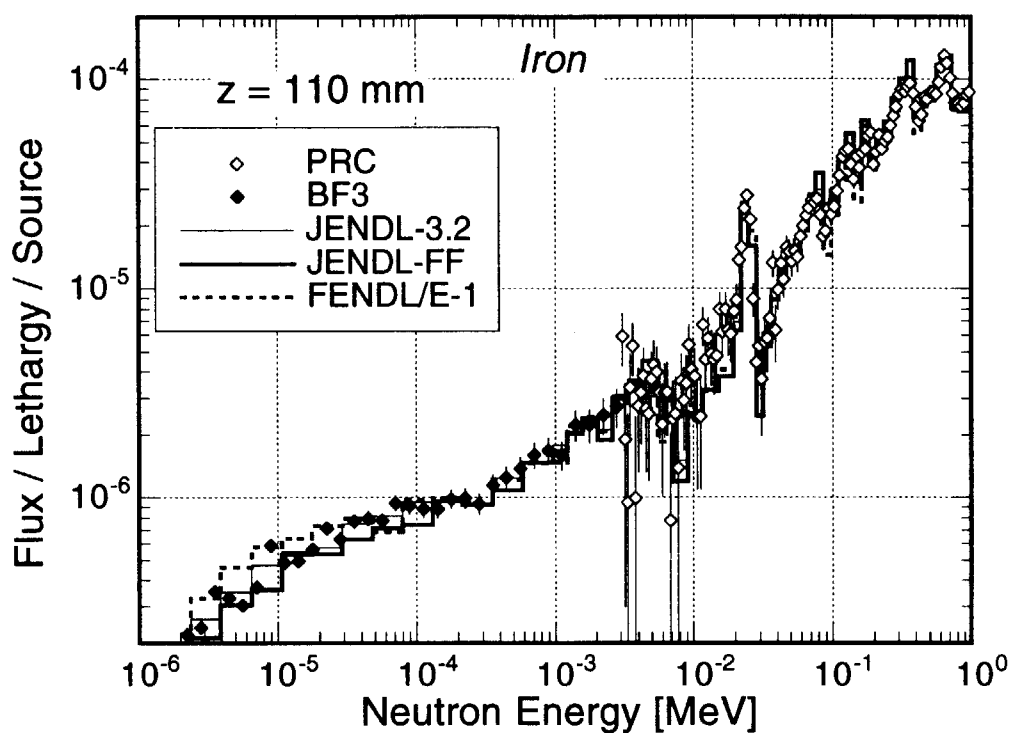


Fig. 4.3.12 Neutron spectra at the 110 mm depth in the cylindrical iron assembly measured and calculated with JENDL-3.2, JENDL Fusion File and FENDL/E-1.0.

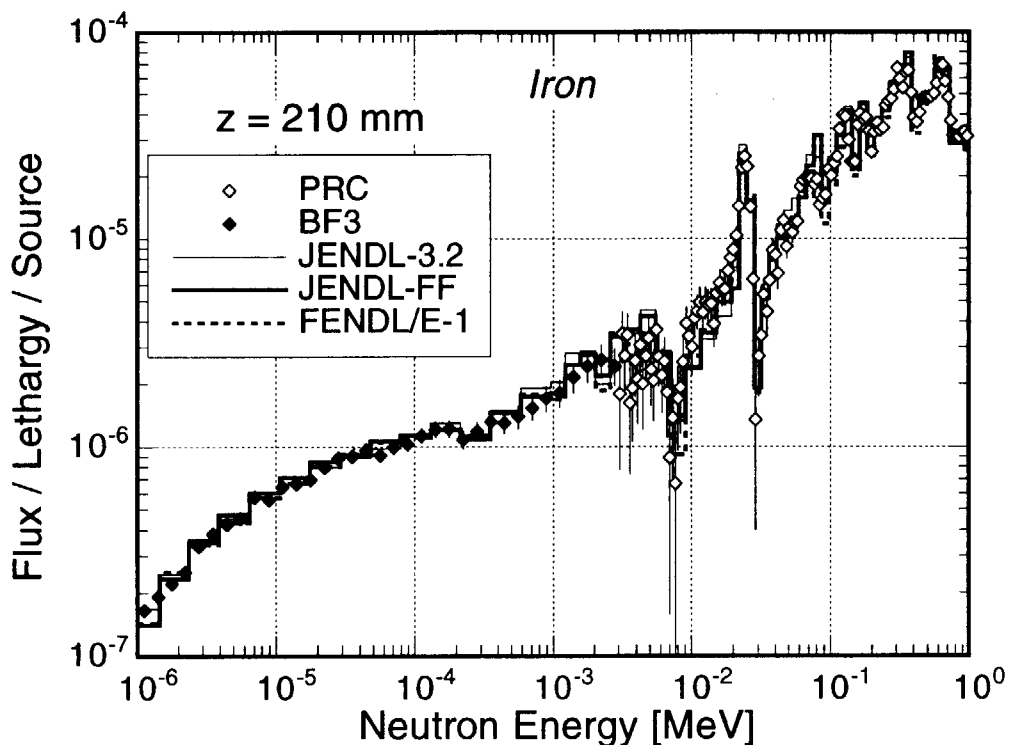


Fig. 4.3.13 Neutron spectra at the 210 mm depth in the cylindrical iron assembly measured and calculated with JENDL-3.2, JENDL Fusion File and FENDL/E-1.0.

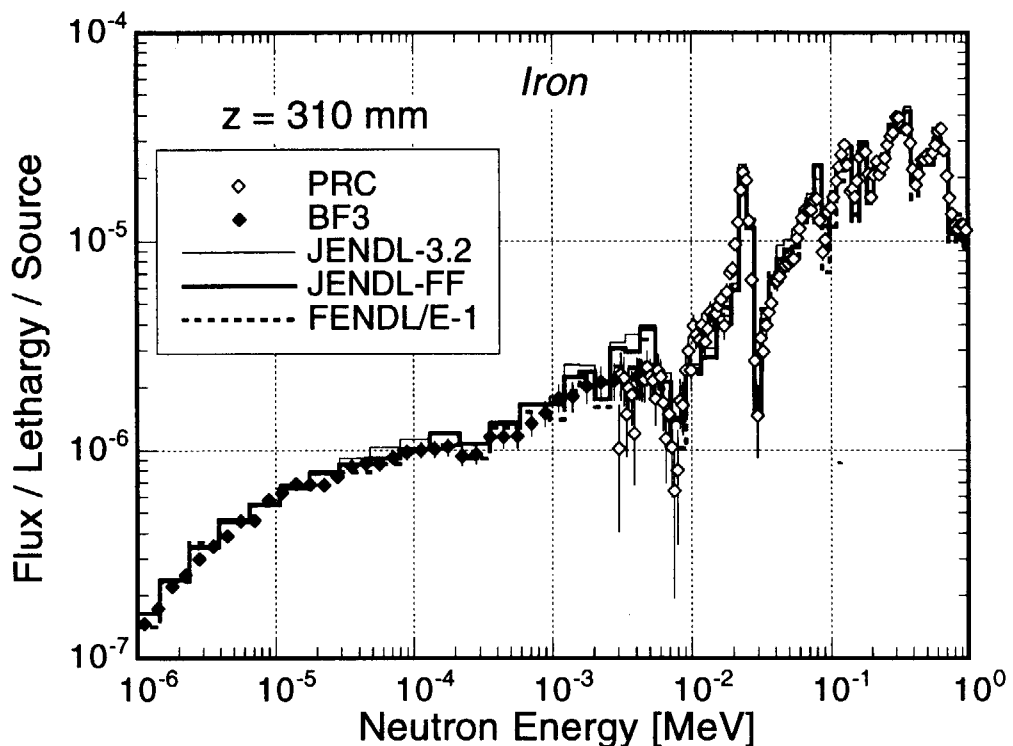


Fig. 4.3.14 Neutron spectra at the 310 mm depth in the cylindrical iron assembly measured and calculated with JENDL-3.2, JENDL Fusion File and FENDL/E-1.0.

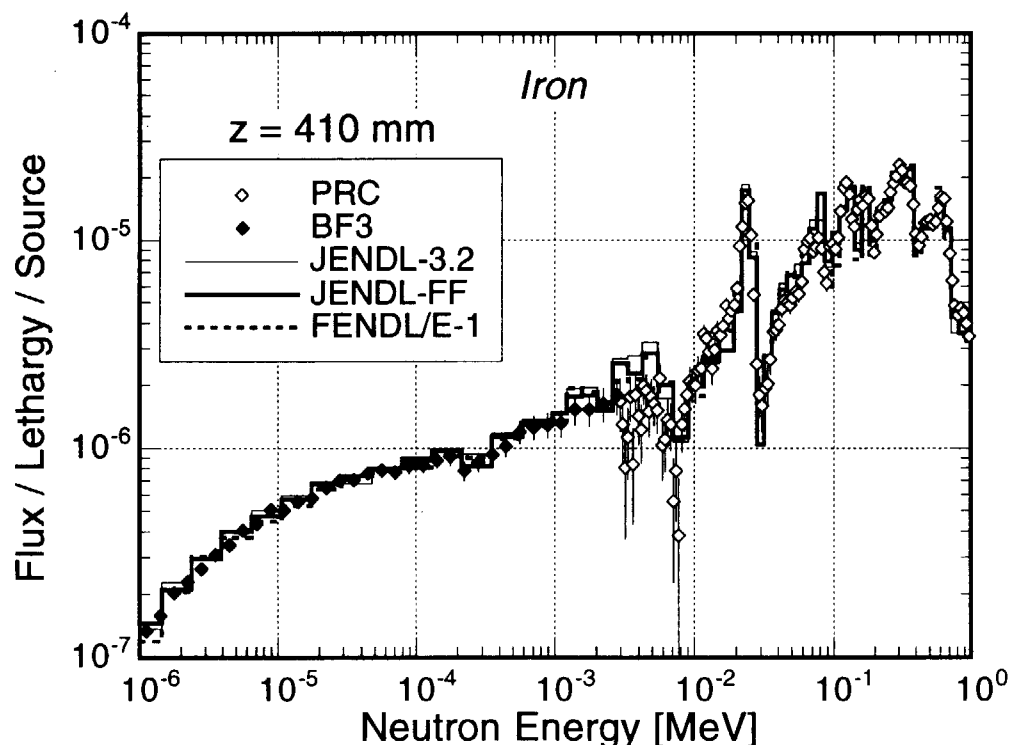


Fig. 4.3.15 Neutron spectra at the 410 mm depth in the cylindrical iron assembly measured and calculated with JENDL-3.2, JENDL Fusion File and FENDL/E-1.0.

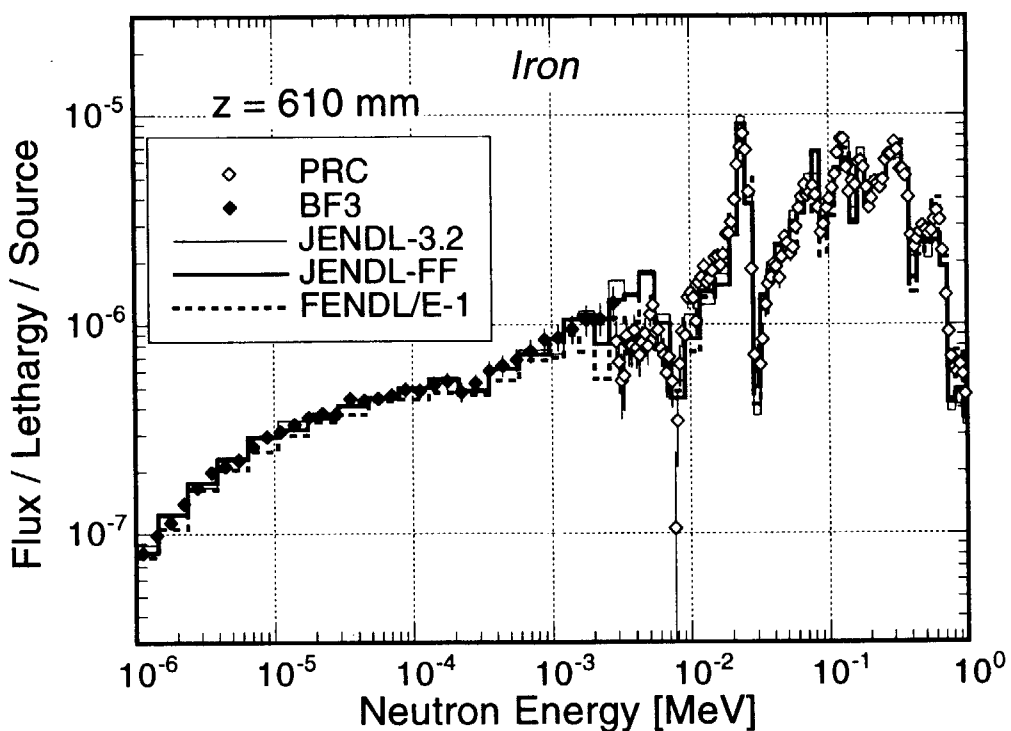


Fig. 4.3.16 Neutron spectra at the 610 mm depth in the cylindrical iron assembly measured and calculated with JENDL-3.2, JENDL Fusion File and FENDL/E-1.0.

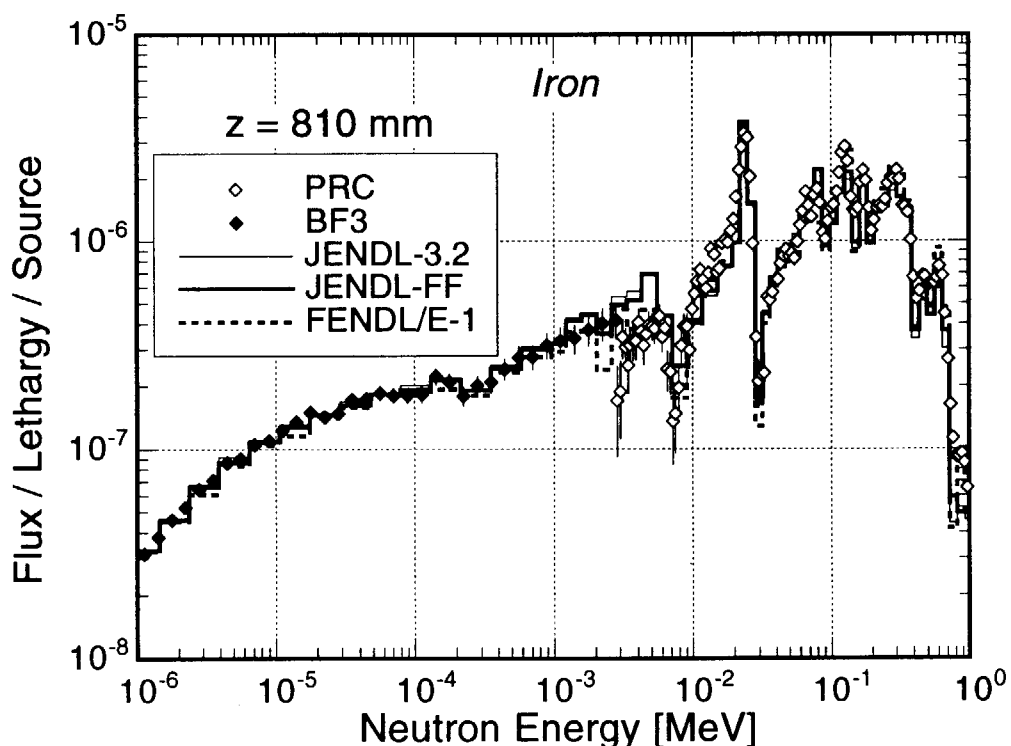


Fig. 4.3.17 Neutron spectra at the 810 mm depth in the cylindrical iron assembly measured and calculated with JENDL-3.2, JENDL Fusion File and FENDL/E-1.0.

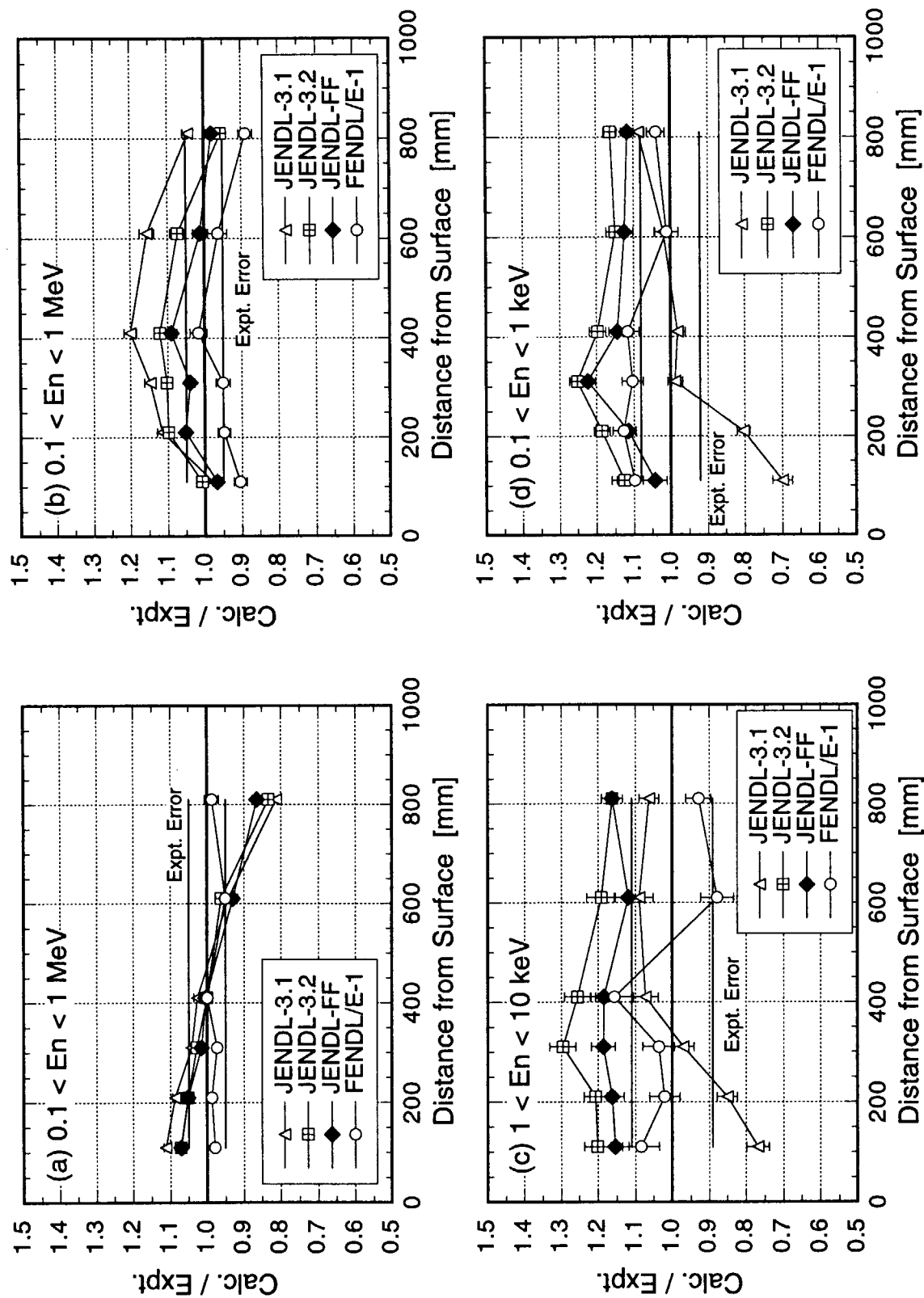


Fig. 4.3.18 Calculated to experimental ratios of neutron fluxes integrated in the six energy intervals in the cylindrical iron assembly for JENDL-3.1, JENDL-3.2, JENDL-Fusion File and FENDL/E-1.0. (1/2)

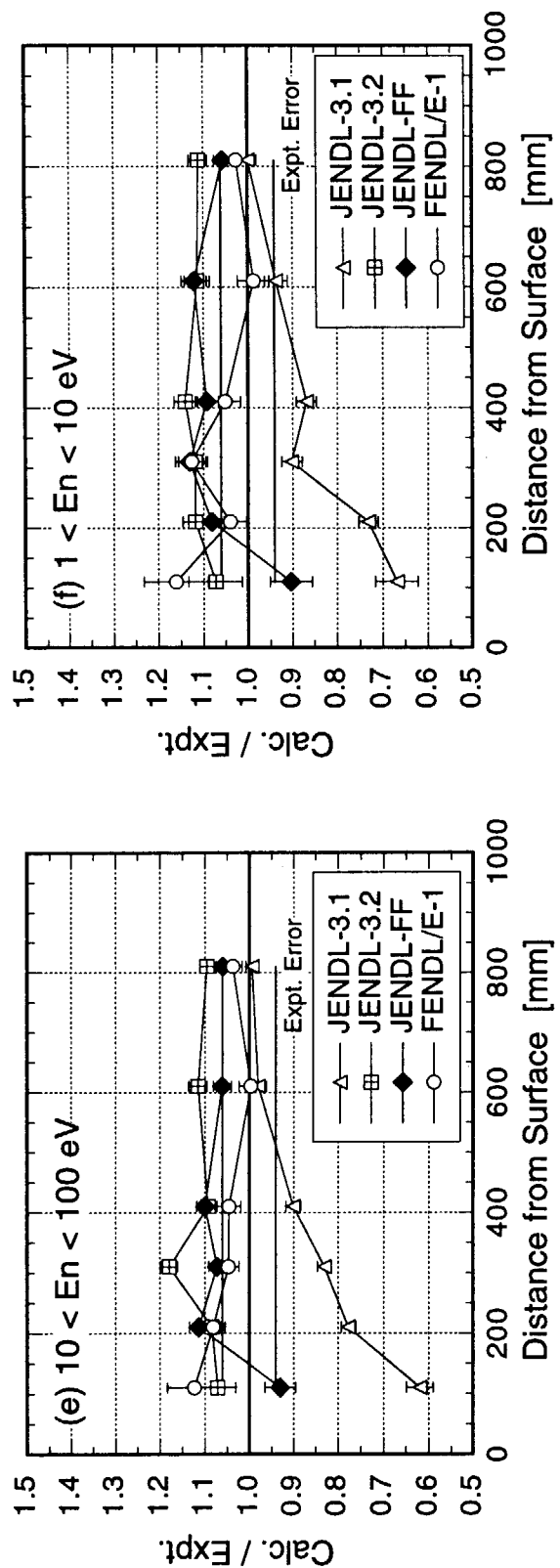


Fig. 4.3.18 Continued. (2/2)

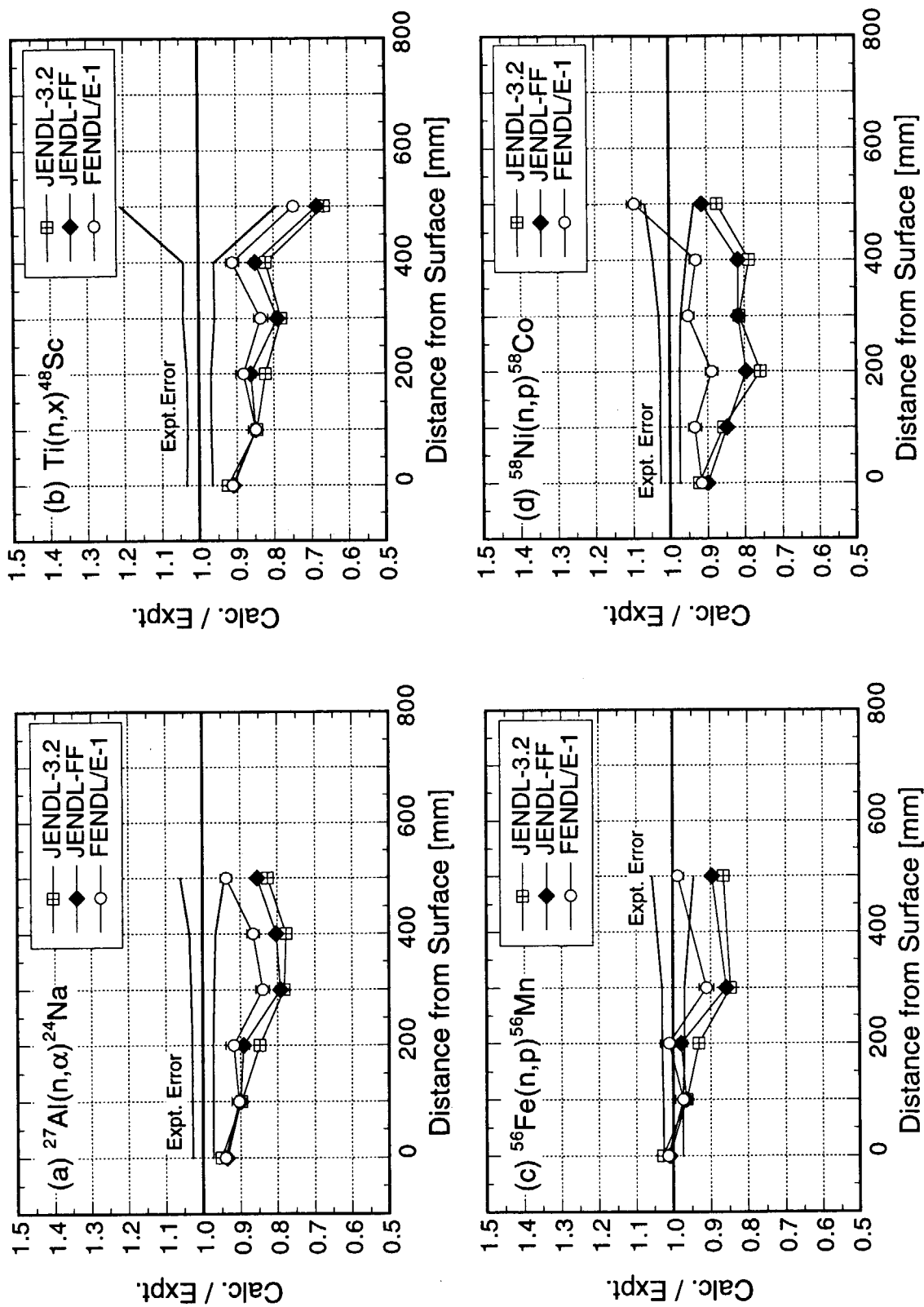


Fig. 4.3.19 Calculated to experimental ratios of dosimetry reaction rates in the cylindrical iron assembly for JENDL-3.2, JENDL Fusion File and FENDL/E-1.0. (1/3)

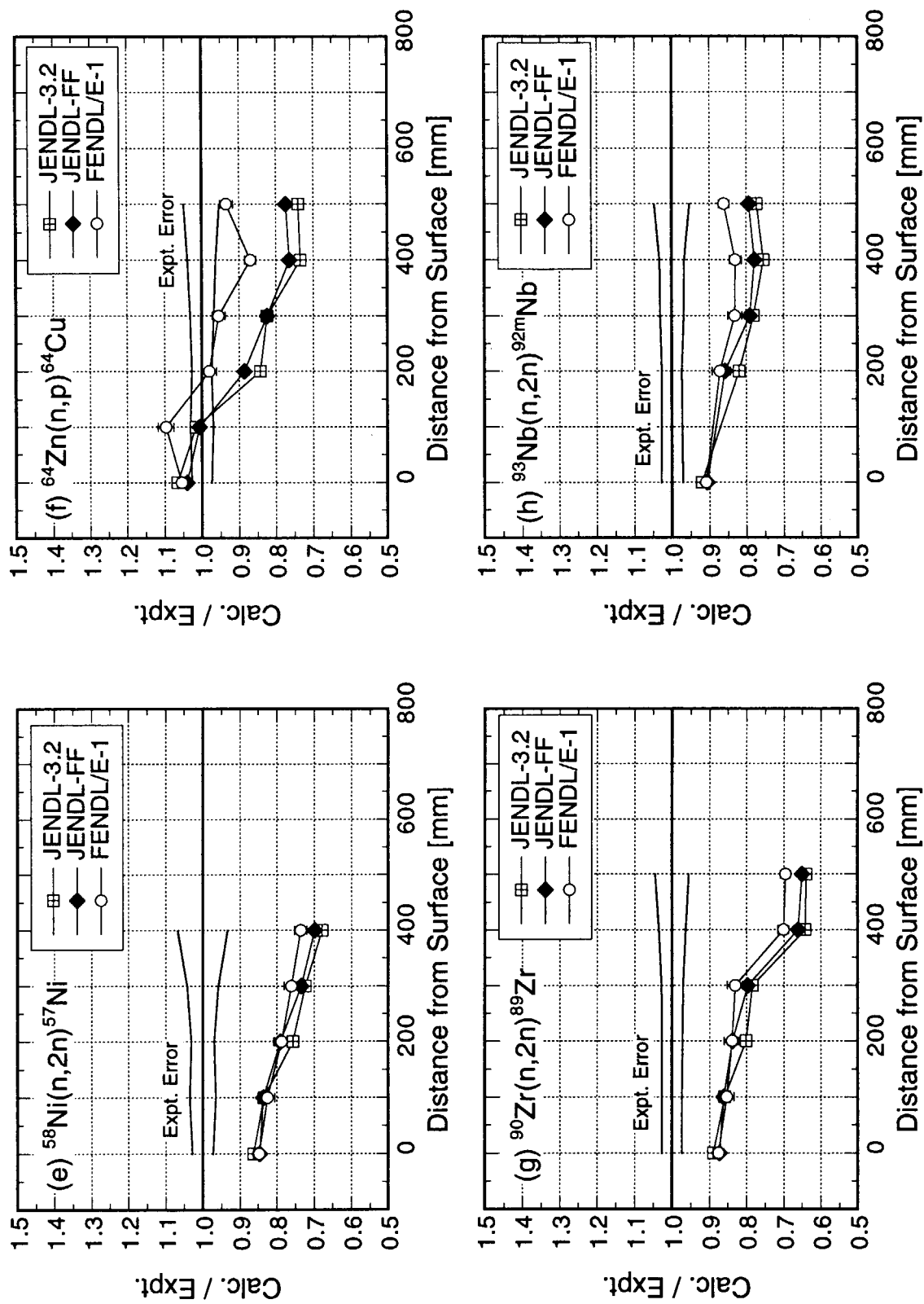


Fig. 4.3.19 Continued. (2/3)

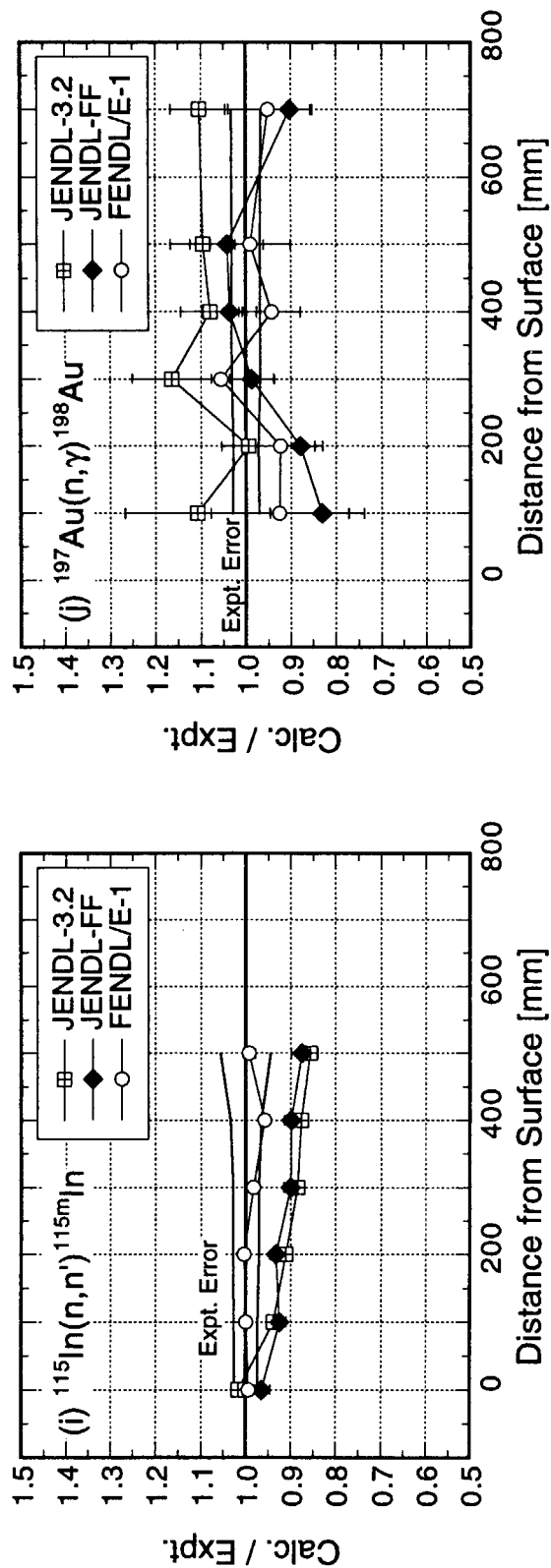


Fig. 4.3.19 Continued. (3/3)

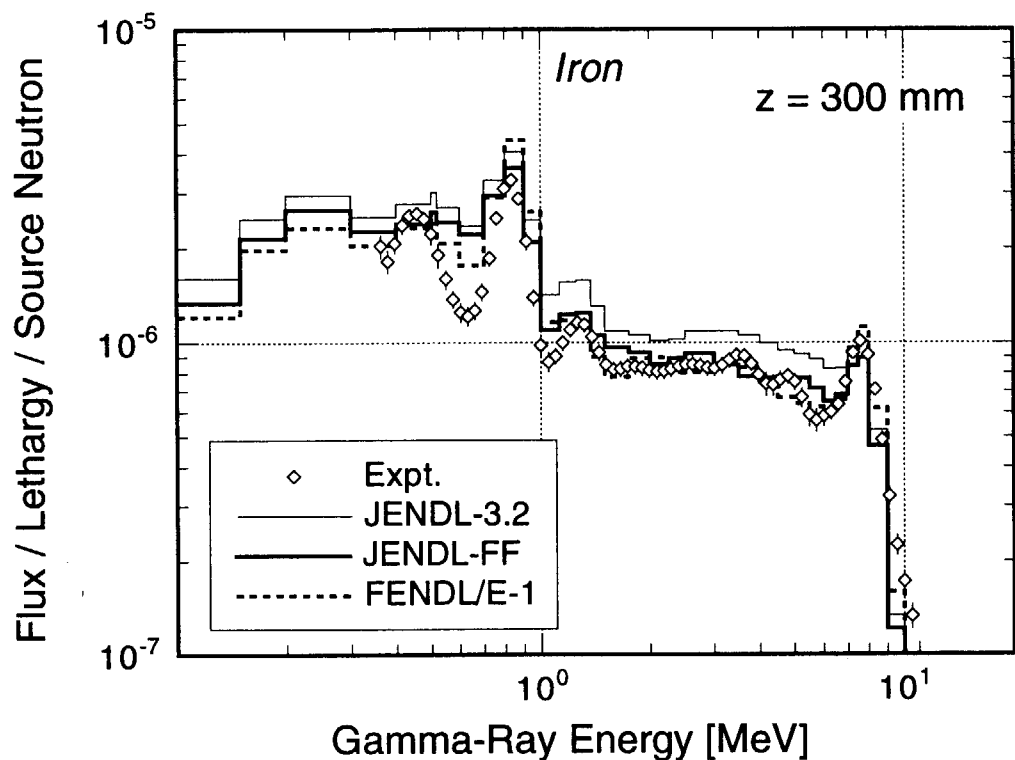


Fig. 4.3.20 Gamma-ray spectra at the 300 mm depth in the cylindrical iron assembly measured and calculated with JENDL-3.2, JENDL Fusion File and FENDL/E-1.0.

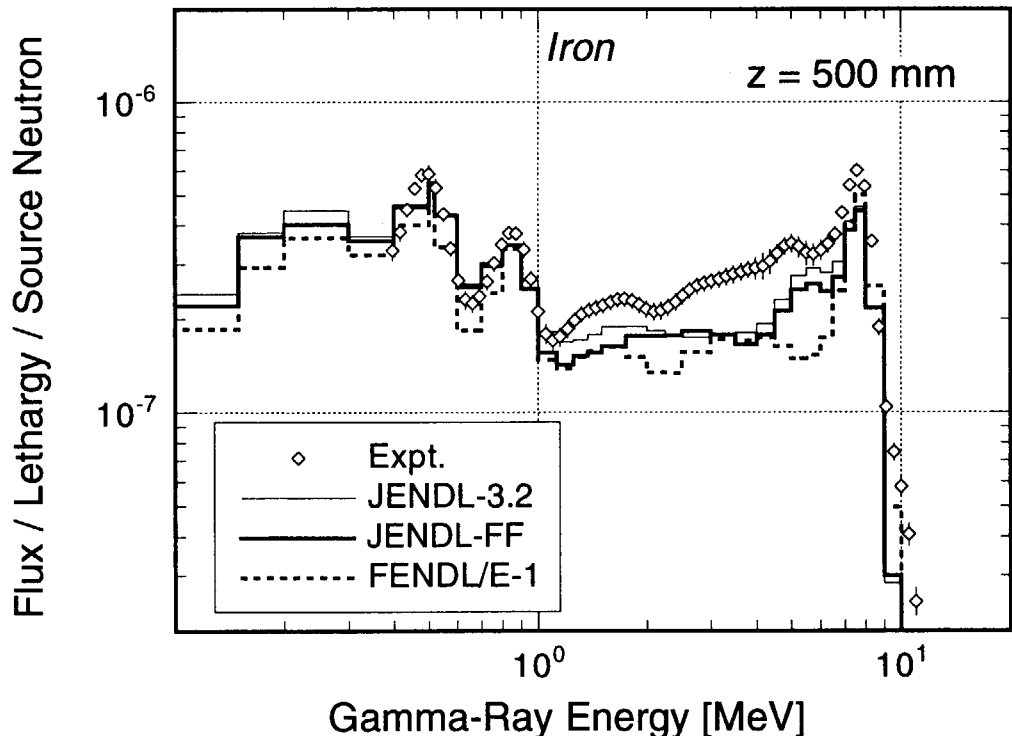


Fig. 4.3.21 Gamma-ray spectra at the 500 mm depth in the cylindrical iron assembly measured and calculated with JENDL-3.2, JENDL Fusion File and FENDL/E-1.0.

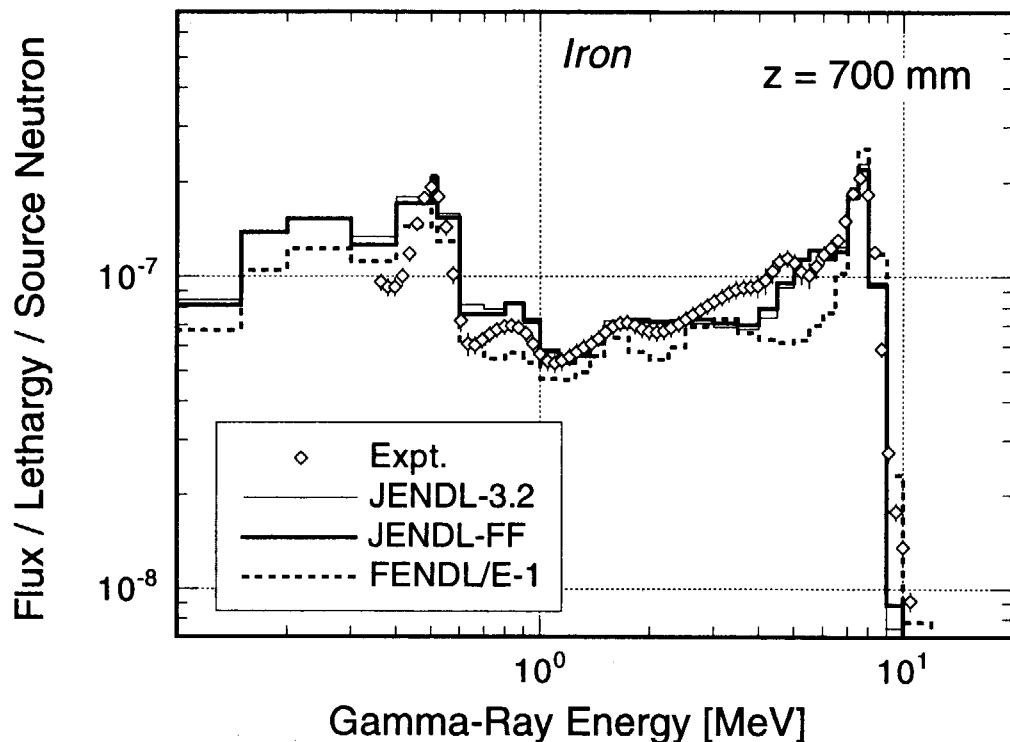


Fig. 4.3.22 Gamma-ray spectra at the 700 mm depth in the cylindrical iron assembly measured and calculated with JENDL-3.2, JENDL Fusion File and FENDL/E-1.0.

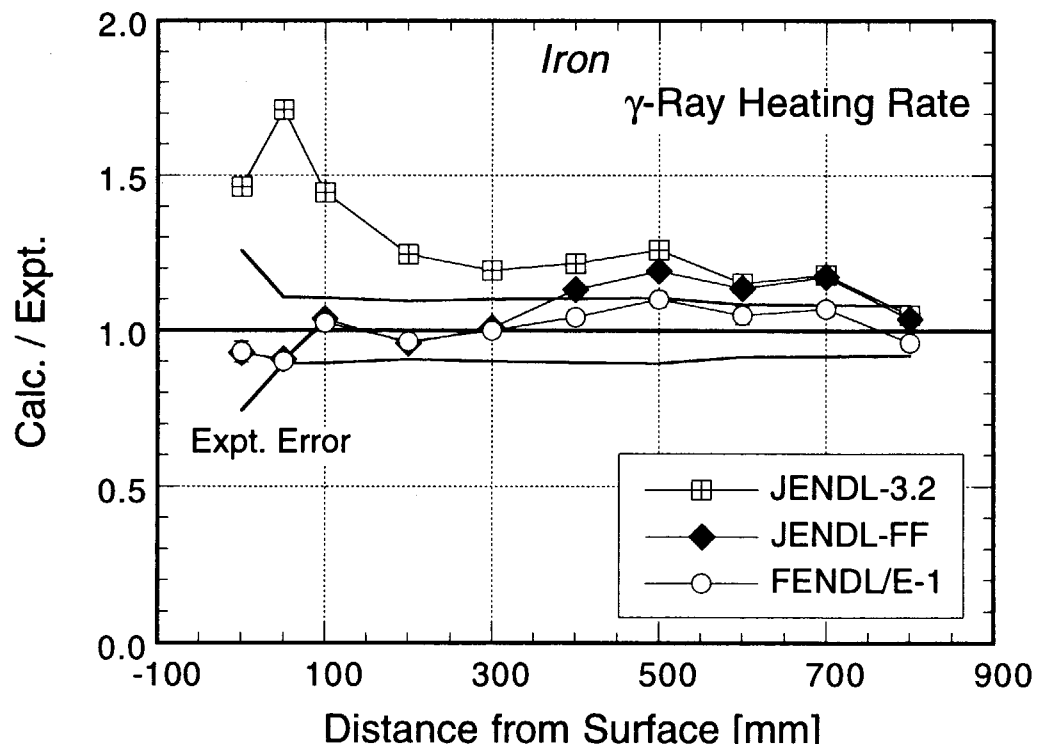


Fig. 4.3.23 Calculated to experimental ratios of gamma-ray heating rates in the cylindrical iron assembly for JENDL-3.2, JENDL Fusion File and FENDL/E-1.0.

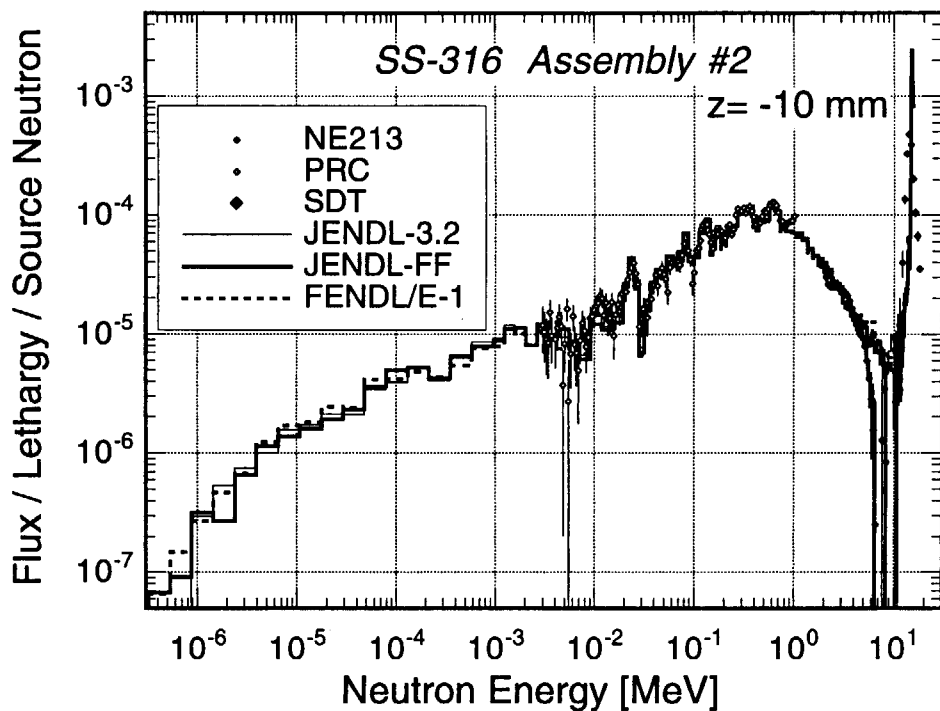


Fig. 4.3.24 Neutron spectra at the front surface of the cylindrical SS316 assembly measured and calculated with JENDL-3.2, JENDL Fusion File and FENDL/E-1.0.

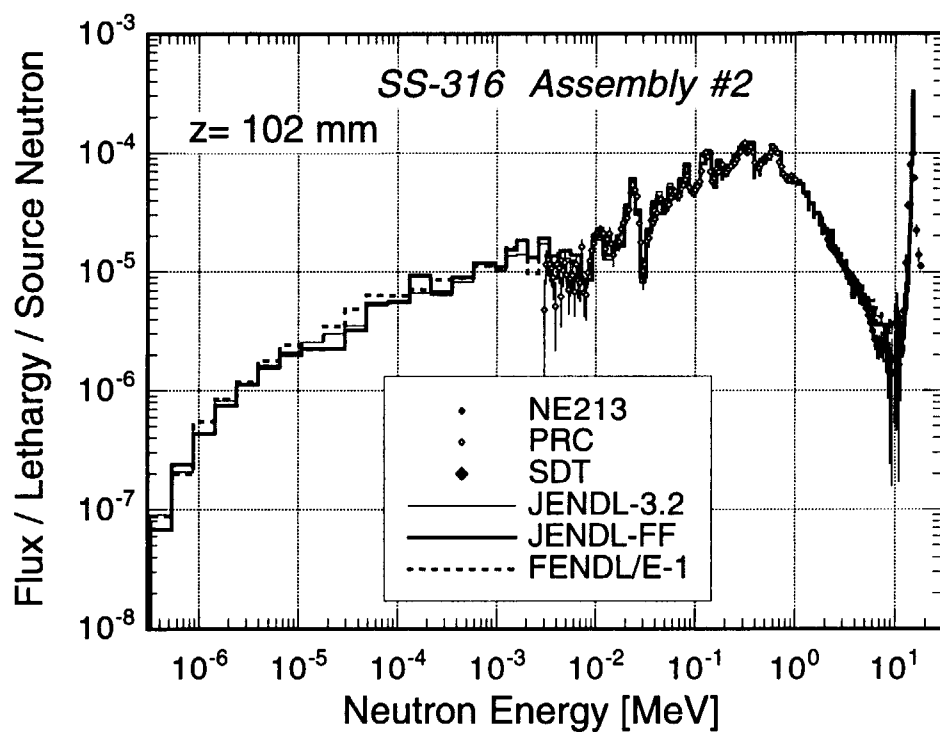


Fig. 4.3.25 Neutron spectra at the 102 mm depth in the cylindrical SS316 assembly measured and calculated with JENDL-3.2, JENDL Fusion File and FENDL/E-1.0.

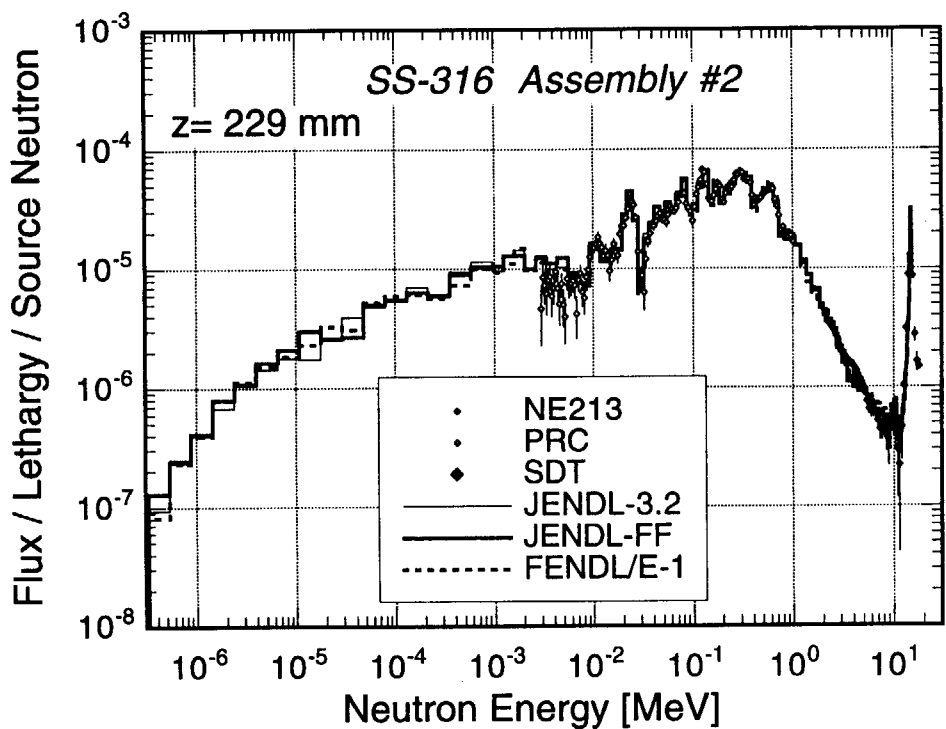


Fig. 4.3.26 Neutron spectra at the 229 mm depth in the cylindrical SS316 assembly measured and calculated with JENDL-3.2, JENDL Fusion File and FENDL/E-1.0.

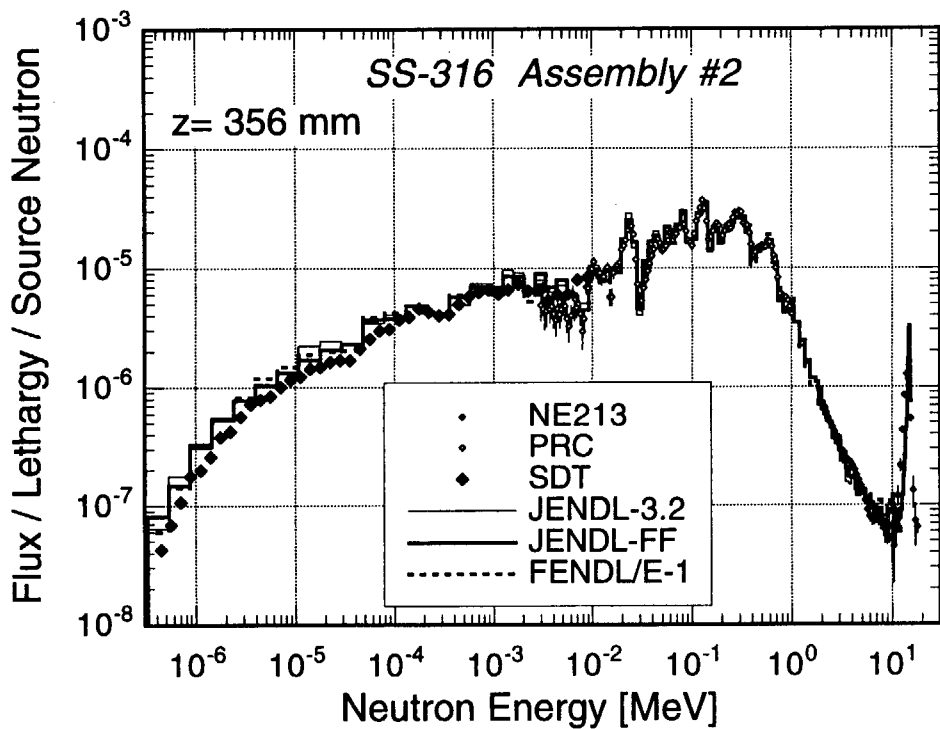


Fig. 4.3.27 Neutron spectra at the 356 mm depth in the cylindrical SS316 assembly measured and calculated with JENDL-3.2, JENDL Fusion File and FENDL/E-1.0.

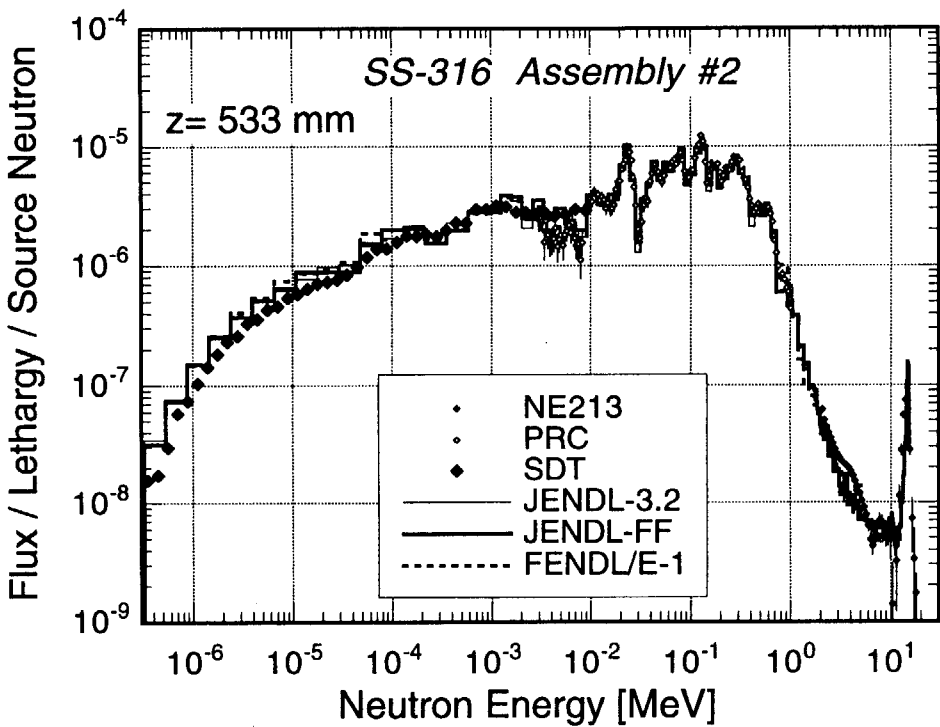


Fig. 4.3.28 Neutron spectra at the 533 mm depth in the cylindrical SS316 assembly measured and calculated with JENDL-3.2, JENDL Fusion File and FENDL/E-1.0.

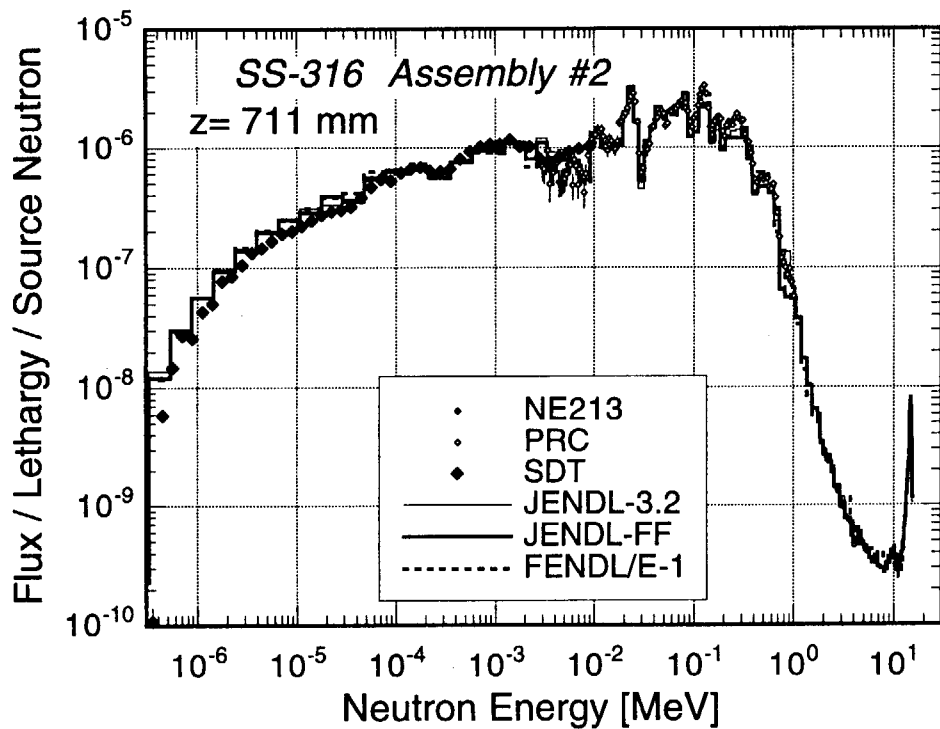


Fig. 4.3.29 Neutron spectra at the 711 mm depth in the cylindrical SS316 assembly measured and calculated with JENDL-3.2, JENDL Fusion File and FENDL/E-1.0.

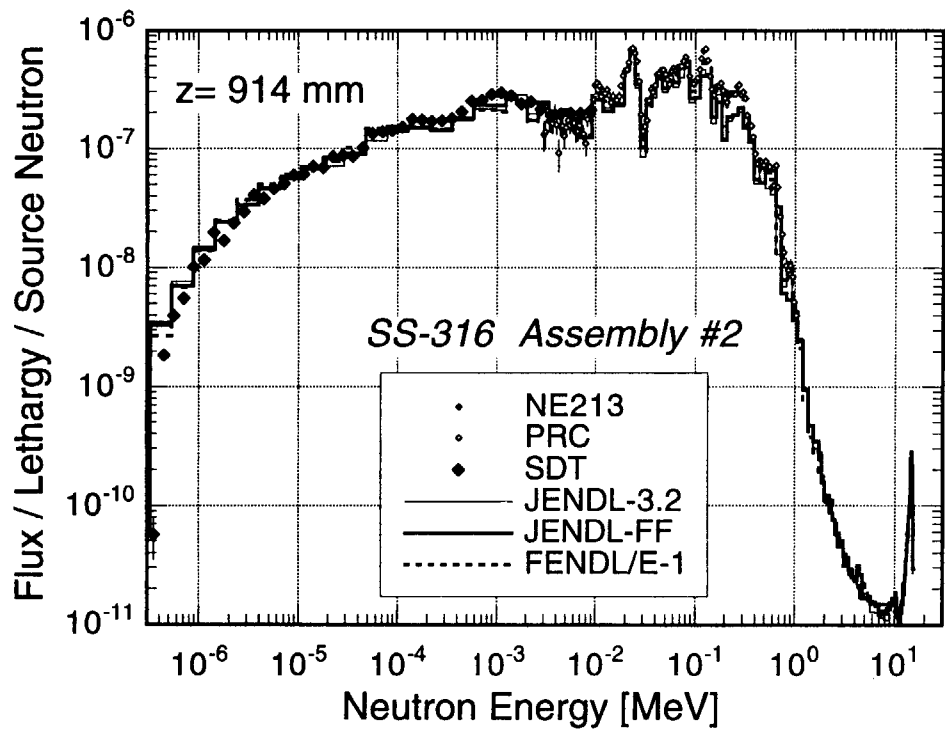


Fig. 4.3.30 Neutron spectra at the 914 mm depth in the cylindrical SS316 assembly measured and calculated with JENDL-3.2, JENDL Fusion File and FENDL/E-1.0.

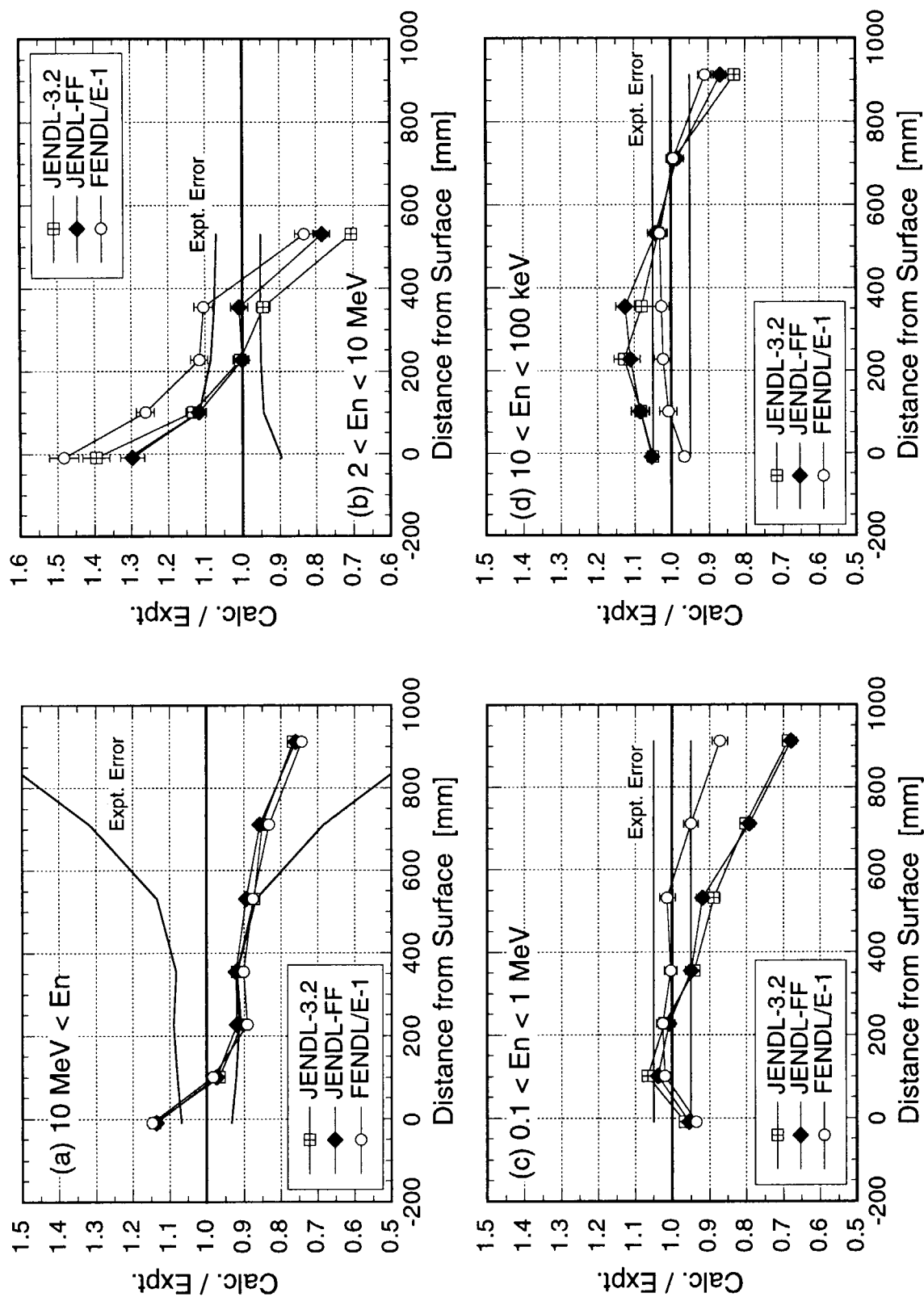


Fig. 4.3.31 Calculated to experimental ratios of neutron fluxes integrated in the eight energy intervals in the cylindrical SS316 assembly for JENDL-3.2, JENDL Fusion File and FENDL/E-1.0. (1/2)

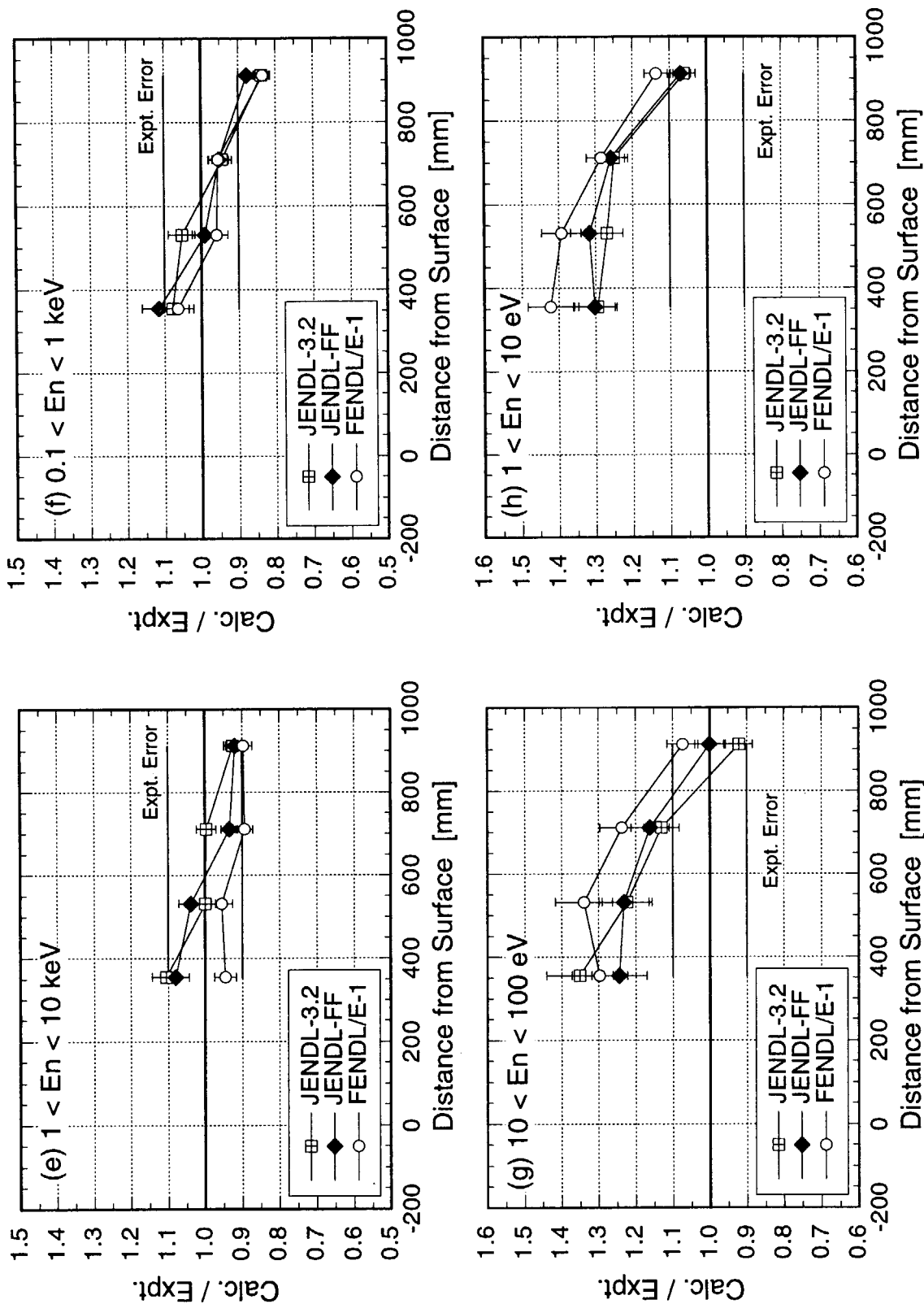


Fig. 4.3.31 Continued. (2/2)

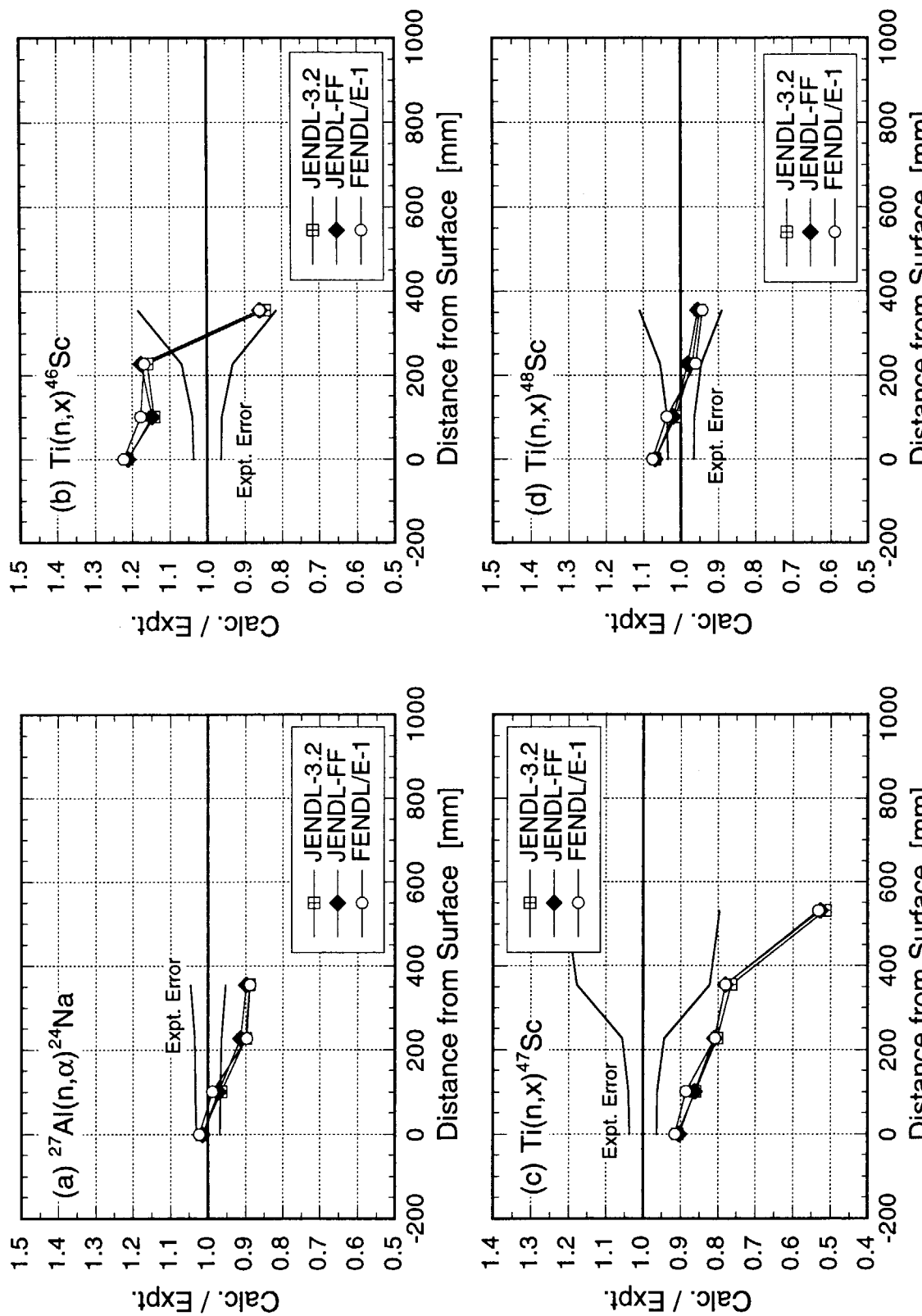


Fig. 4.3.32 Calculated to experimental ratios of dosimetry reaction rates in the cylindrical SS316 assembly for JENDL-3.2, JENDL Fusion File and FENDL/E-1.0. (1/4)

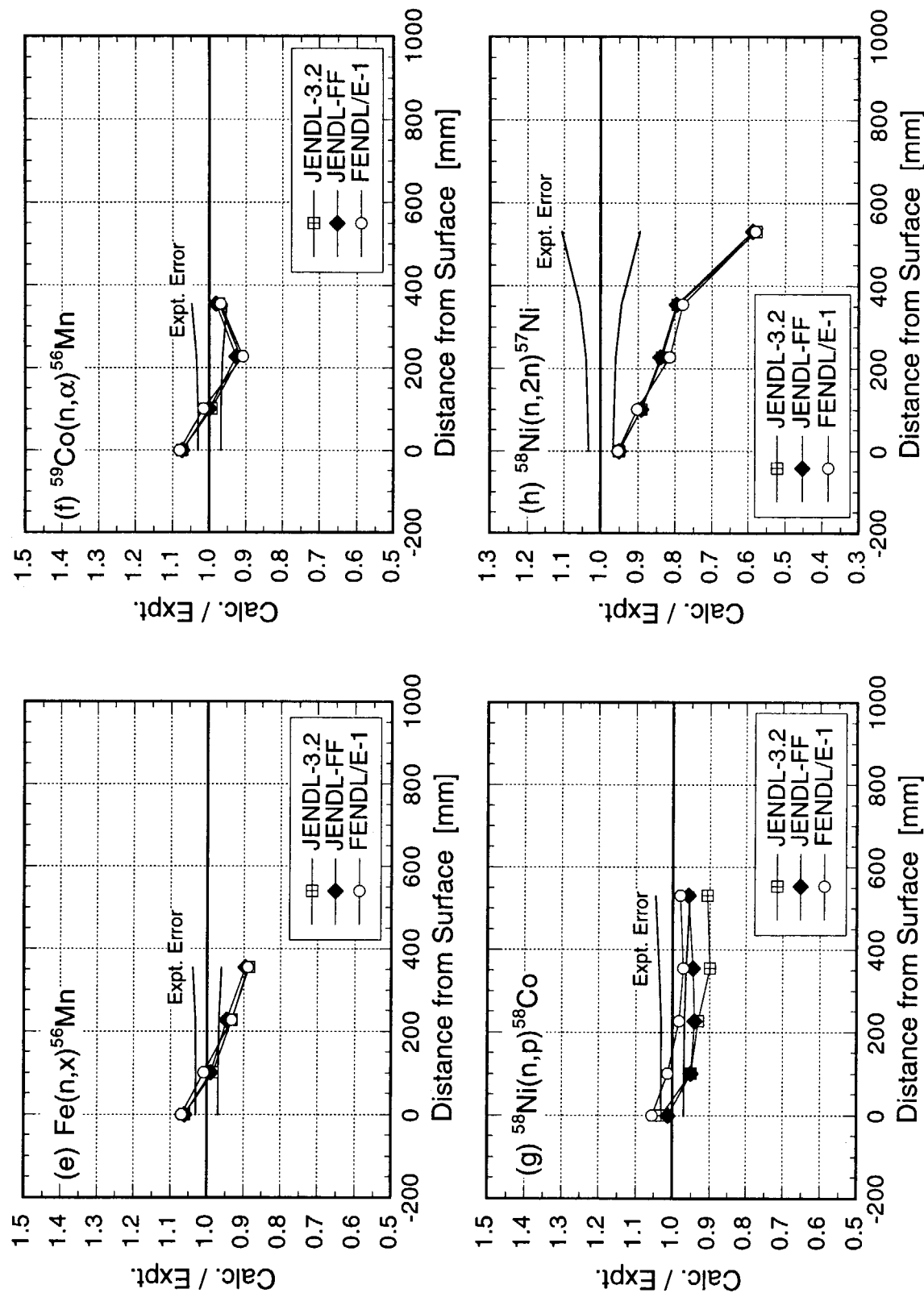


Fig. 4.3.32 Continued. (2/4)

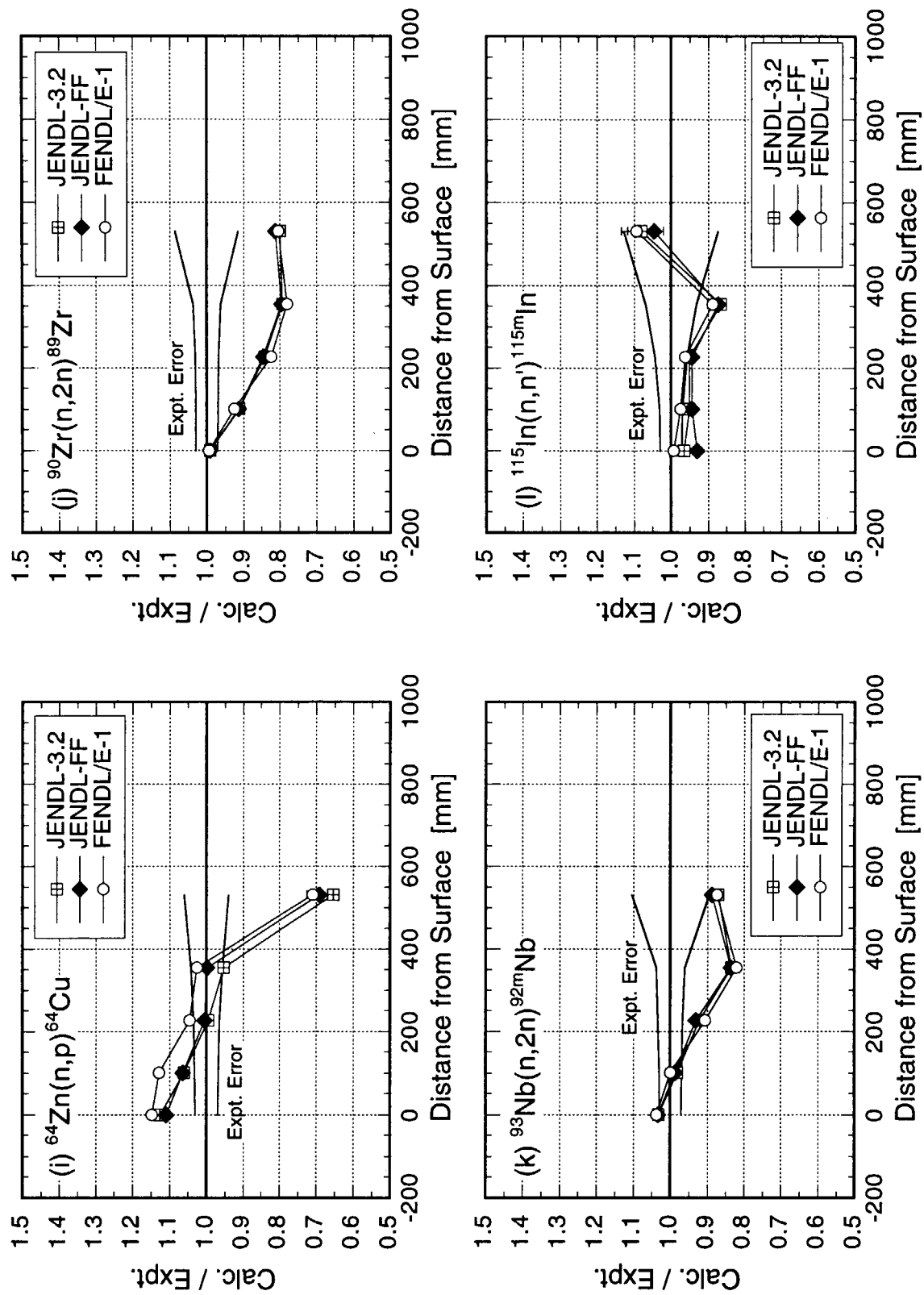


Fig. 4.3.32 Continued. (3/4)

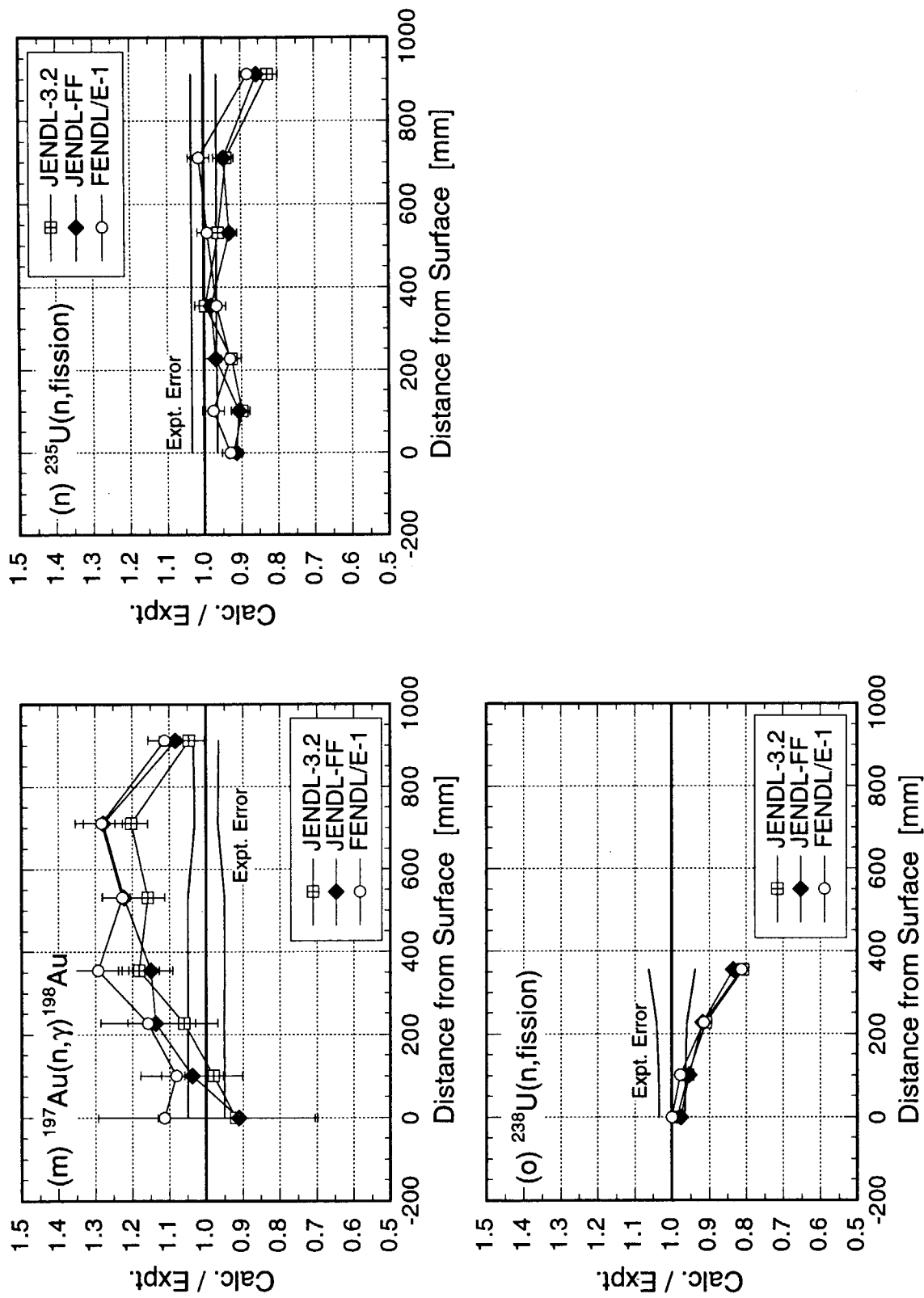


Fig. 4.3.32 Continued. (4/4)

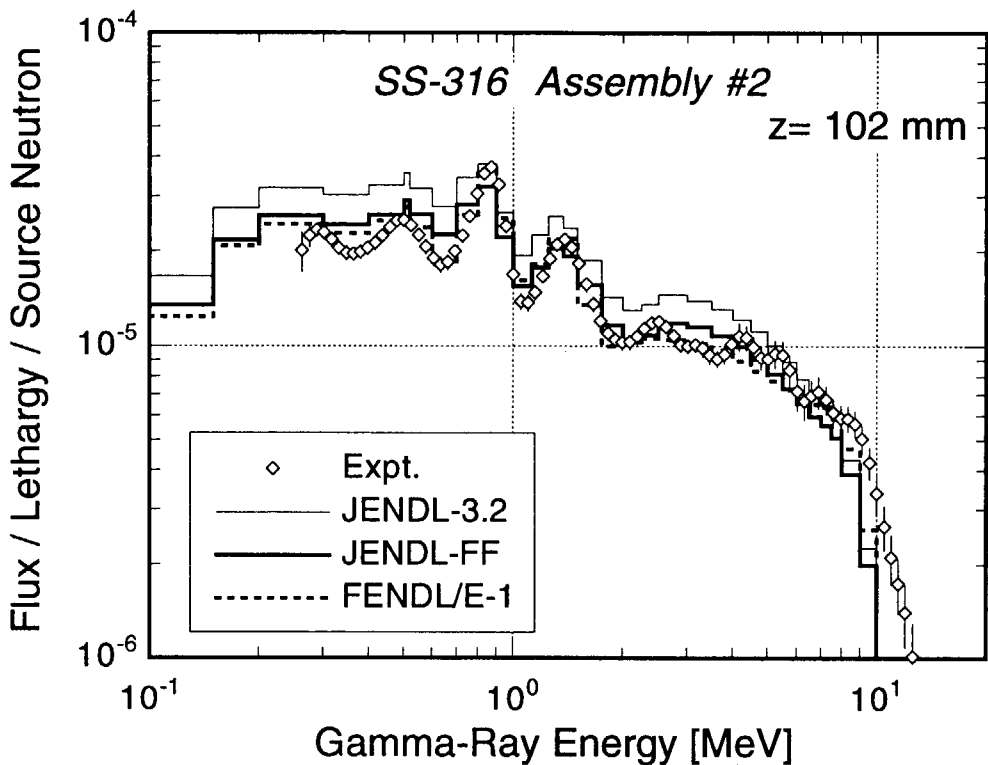


Fig. 4.3.33 Gamma-ray spectra at the 102 mm depth in the cylindrical SS316 assembly measured and calculated with JENDL-3.2, JENDL Fusion File and FENDL/E-1.0.

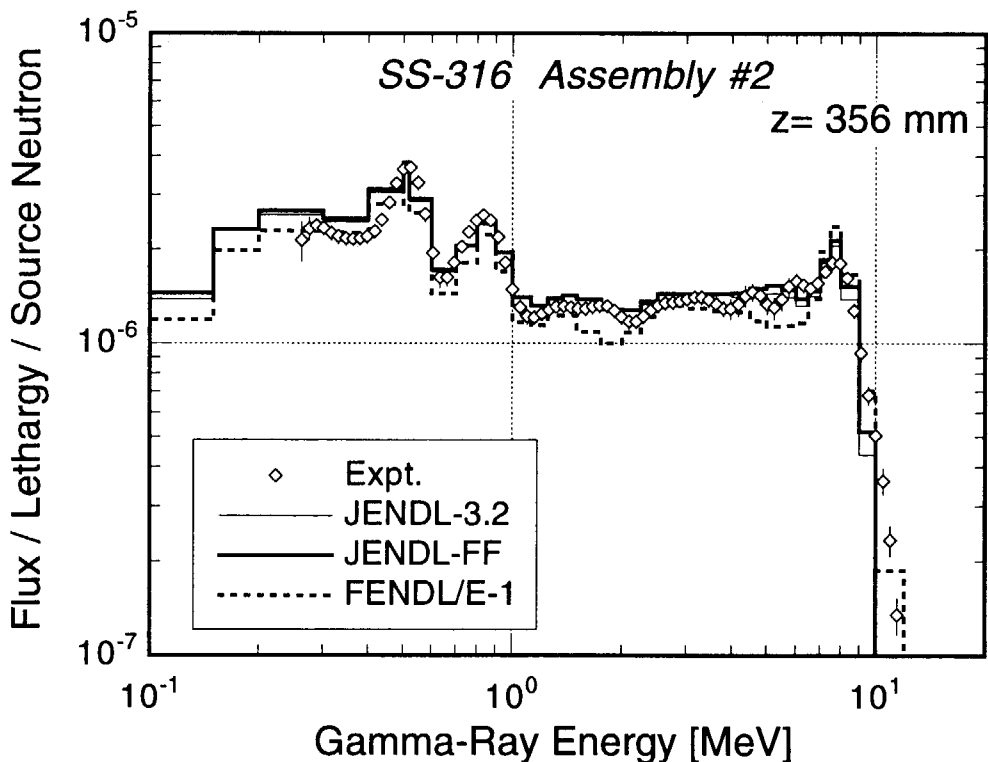


Fig. 4.3.34 Gamma-ray spectra at the 356 mm depth in the cylindrical SS316 assembly measured and calculated with JENDL-3.2, JENDL Fusion File and FENDL/E-1.0.

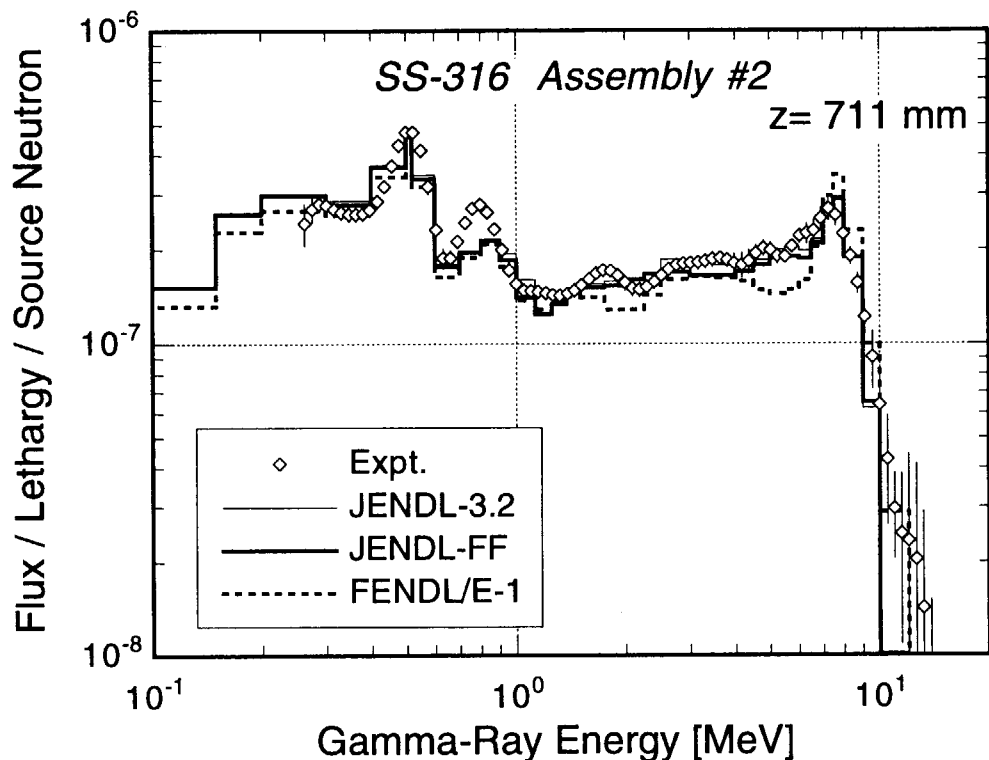


Fig. 4.3.35 Gamma-ray spectra at the 711 mm depth in the cylindrical SS316 assembly measured and calculated with JENDL-3.2, JENDL Fusion File and FENDL/E-1.0.

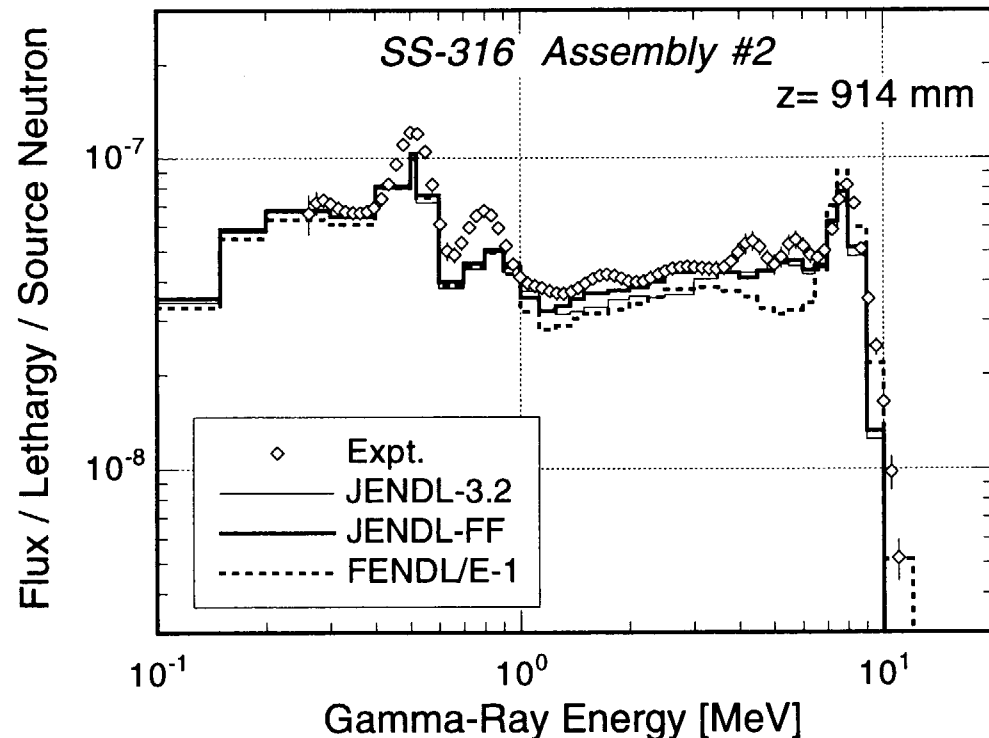


Fig. 4.3.36 Gamma-ray spectra at the 914 mm depth in the cylindrical SS316 assembly measured and calculated with JENDL-3.2, JENDL Fusion File and FENDL/E-1.0.

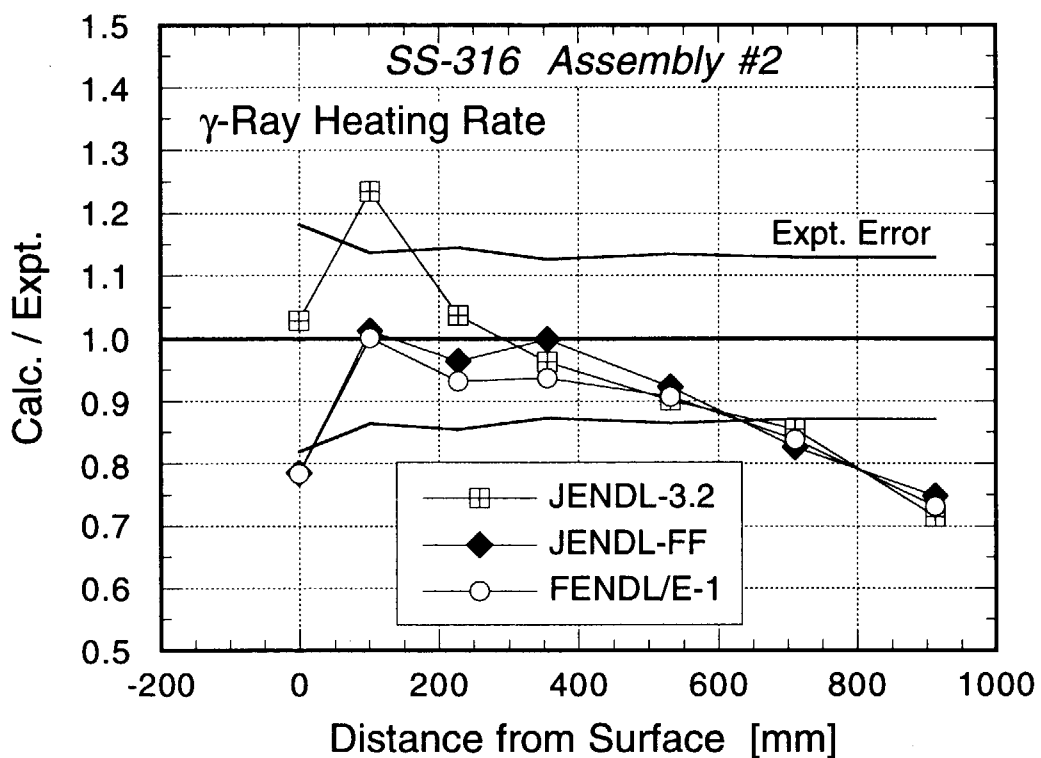


Fig. 4.3.37 Calculated to experimental ratios of gamma-ray heating rates in the cylindrical SS316 assembly for JENDL-3.2, JENDL Fusion File and FENDL/E-1.0.

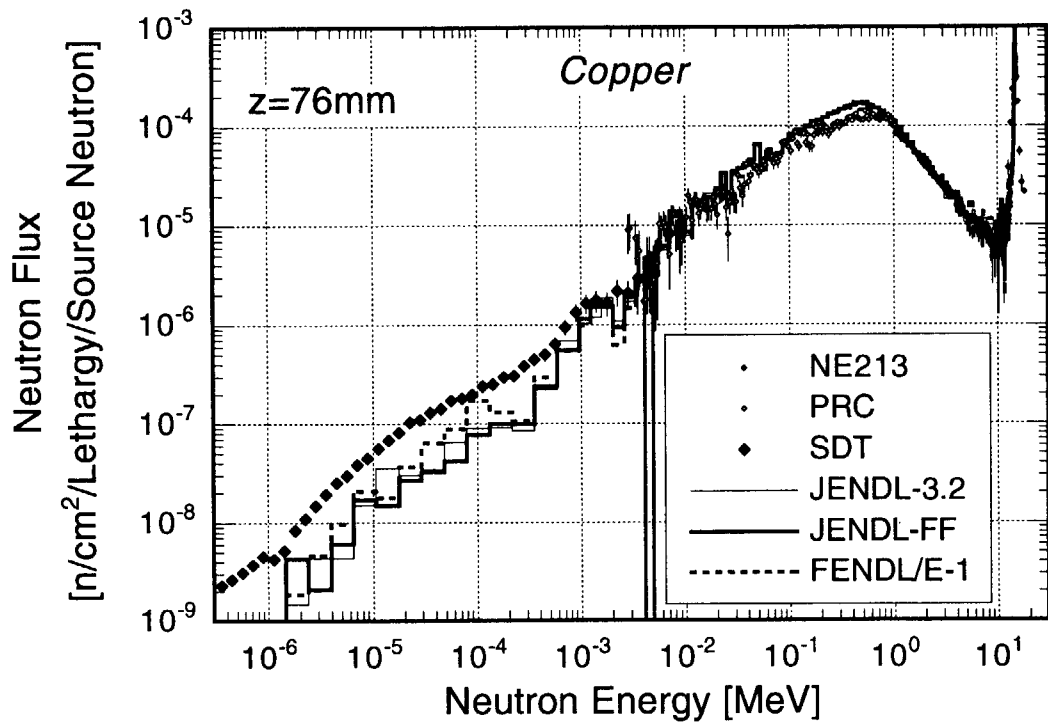


Fig. 4.3.38 Neutron spectra at the 76 mm depth in the cylindrical copper assembly measured and calculated with JENDL-3.2, JENDL Fusion File and FENDL/E-1.0.

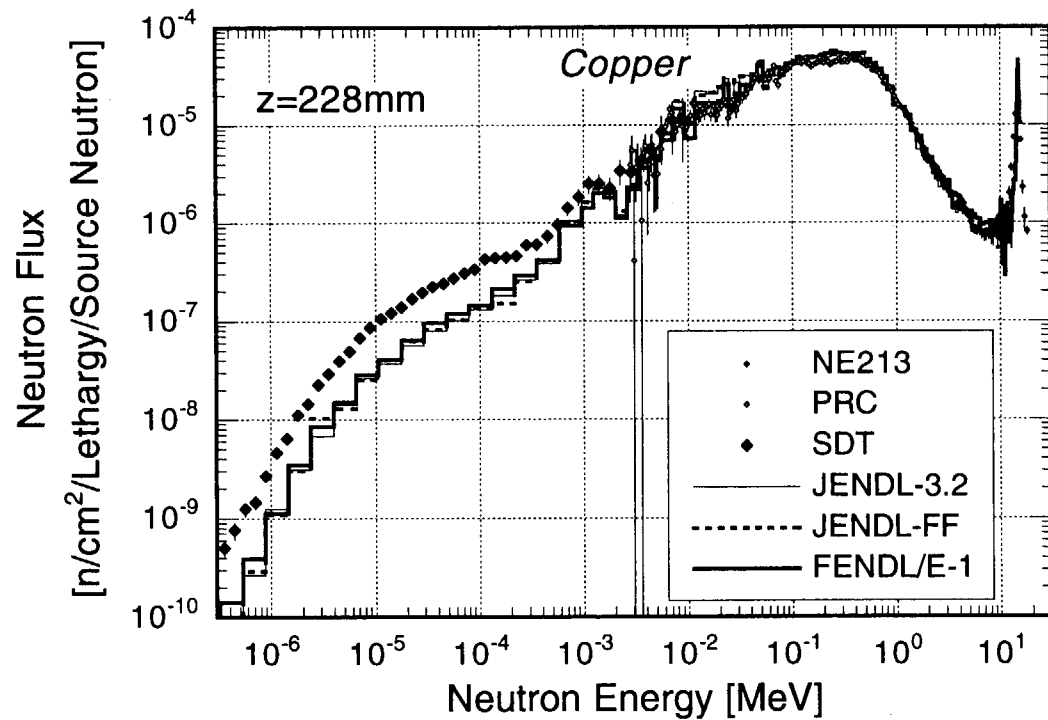


Fig. 4.3.39 Neutron spectra at the 228 mm depth in the cylindrical copper assembly measured and calculated with JENDL-3.2, JENDL Fusion File and FENDL/E-1.0.

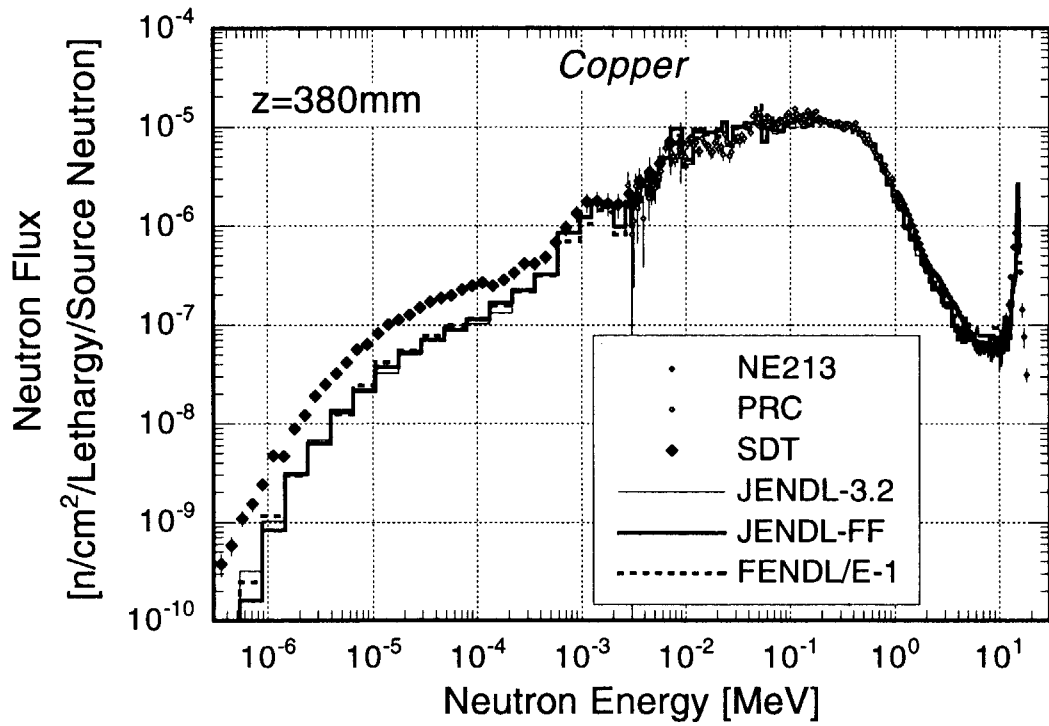


Fig. 4.3.40 Neutron spectra at the 380 mm depth in the cylindrical copper assembly measured and calculated with JENDL-3.2, JENDL Fusion File and FENDL/E-1.0.

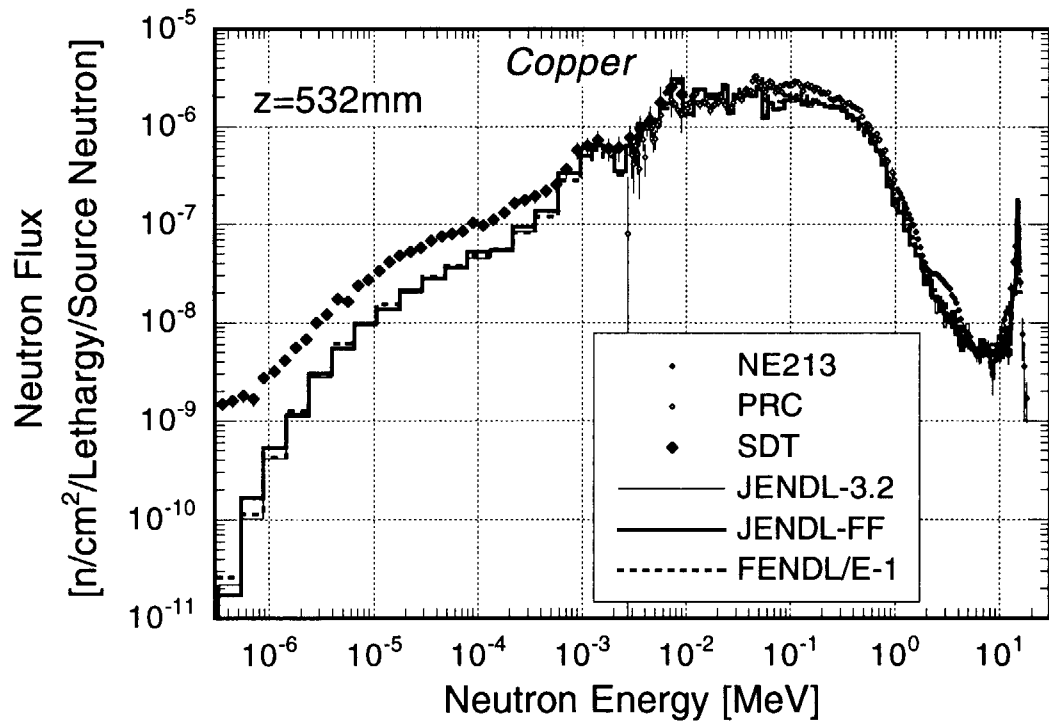


Fig. 4.3.41 Neutron spectra at the 532 mm depth in the cylindrical copper assembly measured and calculated with JENDL-3.2, JENDL Fusion File and FENDL/E-1.0.

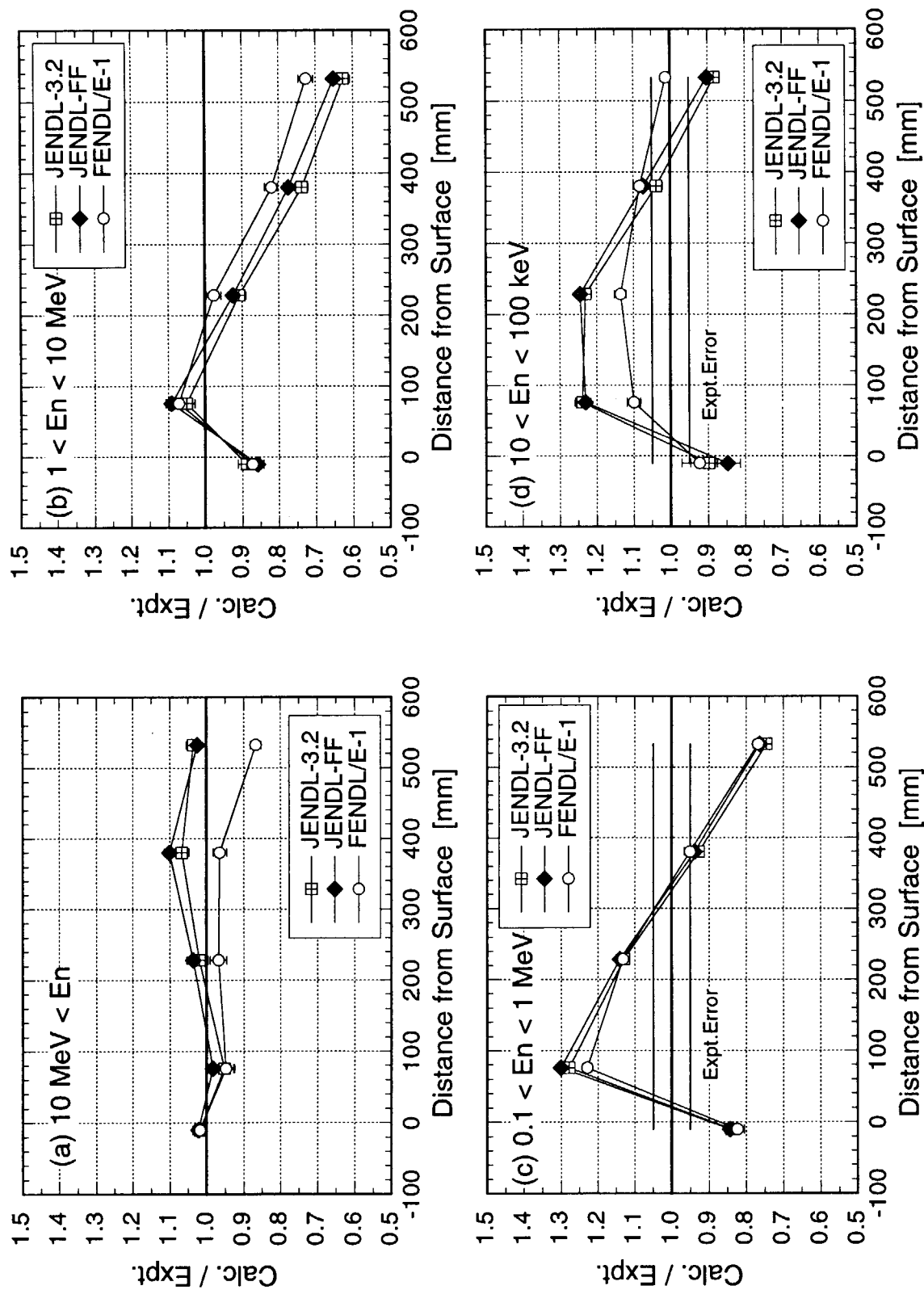


Fig. 4.3.42 Calculated to experimental ratios of neutron fluxes integrated in the eight energy intervals in the cylindrical copper assembly for JENDL-3.2, JENDL Fusion File and FENDL/E-1.0. (1/2)

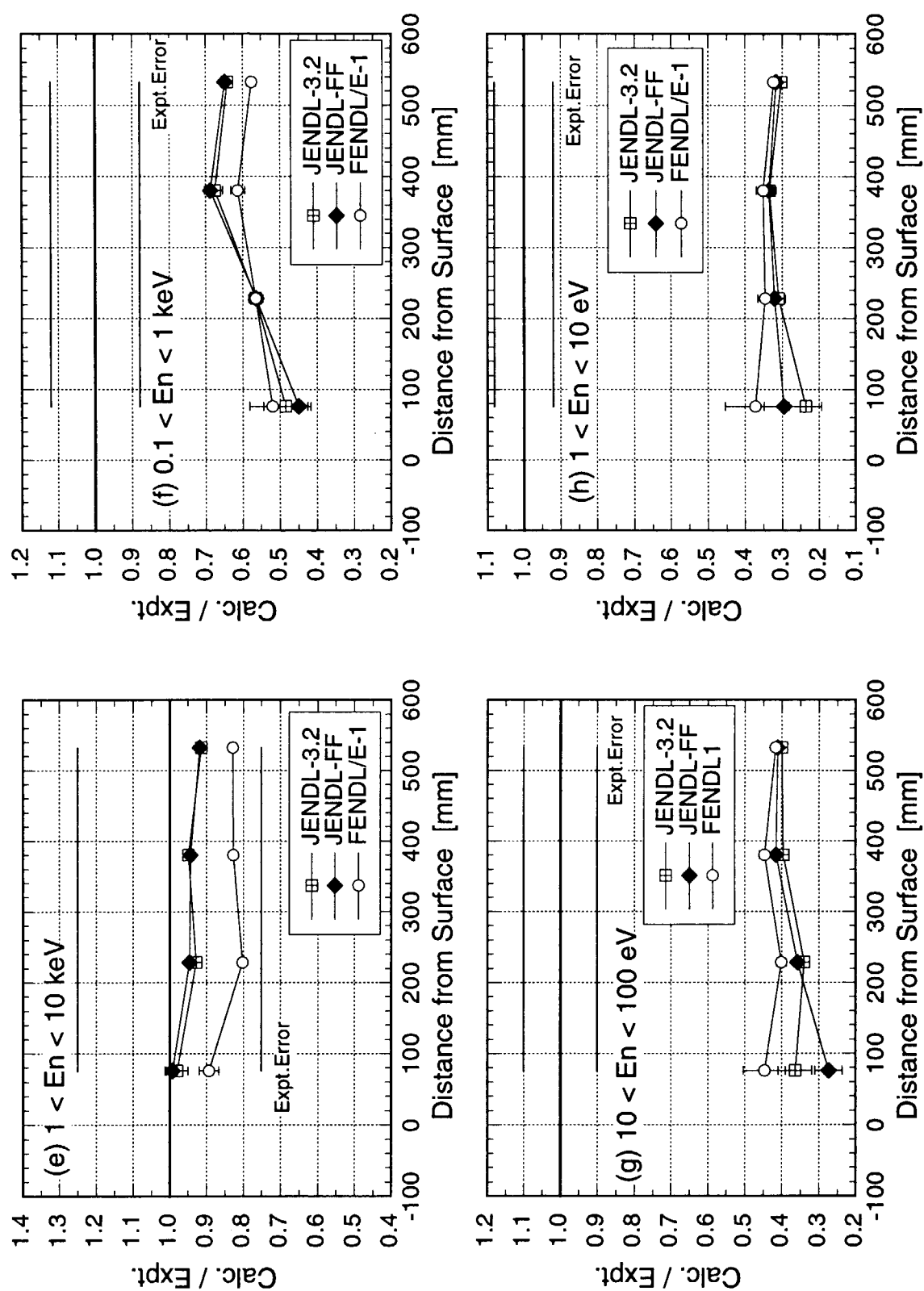


Fig. 4.3.42 Continued. (2/2)

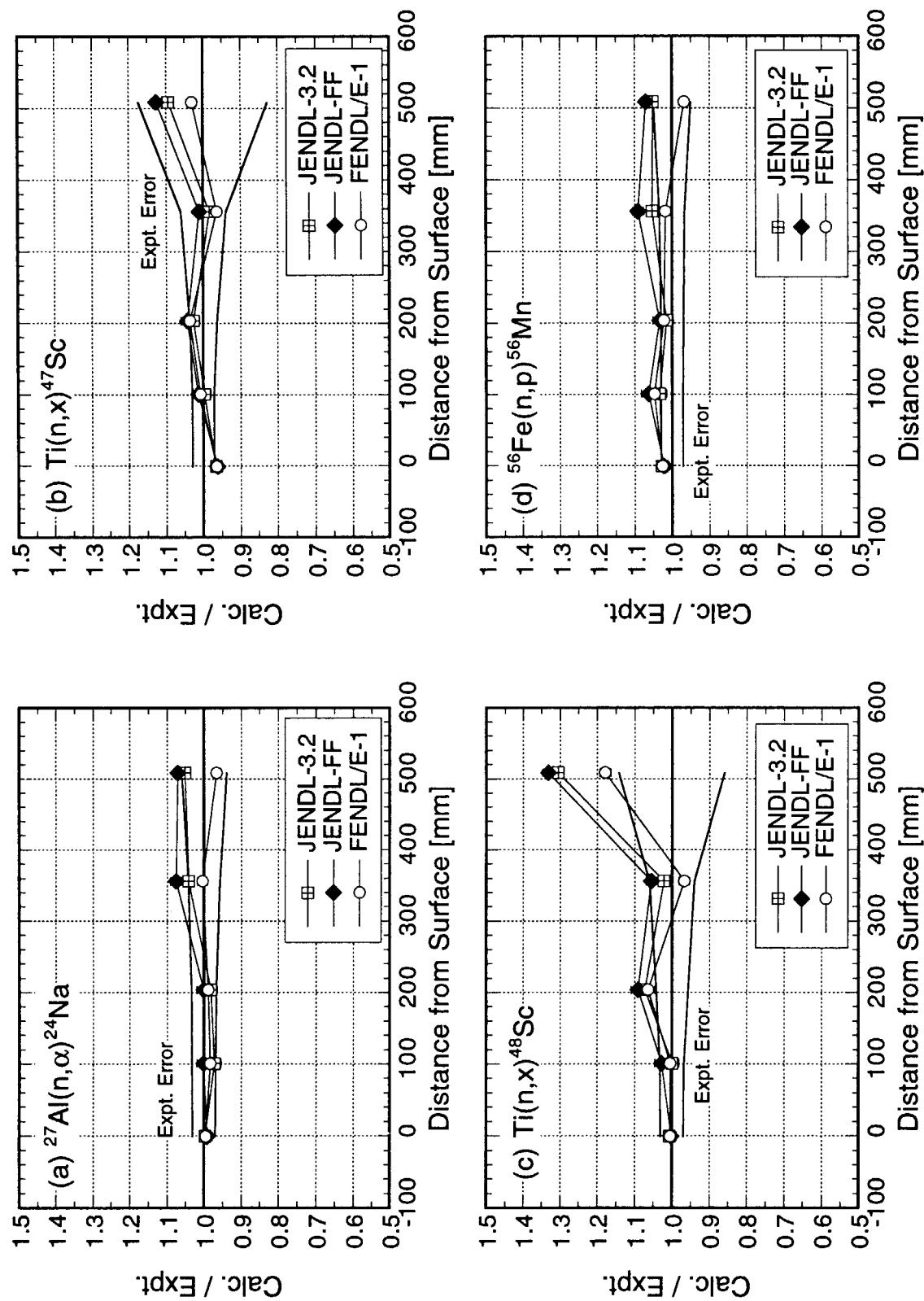


Fig. 4.3.43 Calculated to experimental ratios of dosimetry reaction rates in the cylindrical copper assembly for JENDL-3.2, JENDL Fusion File and FENDL/E-1.0. (13)

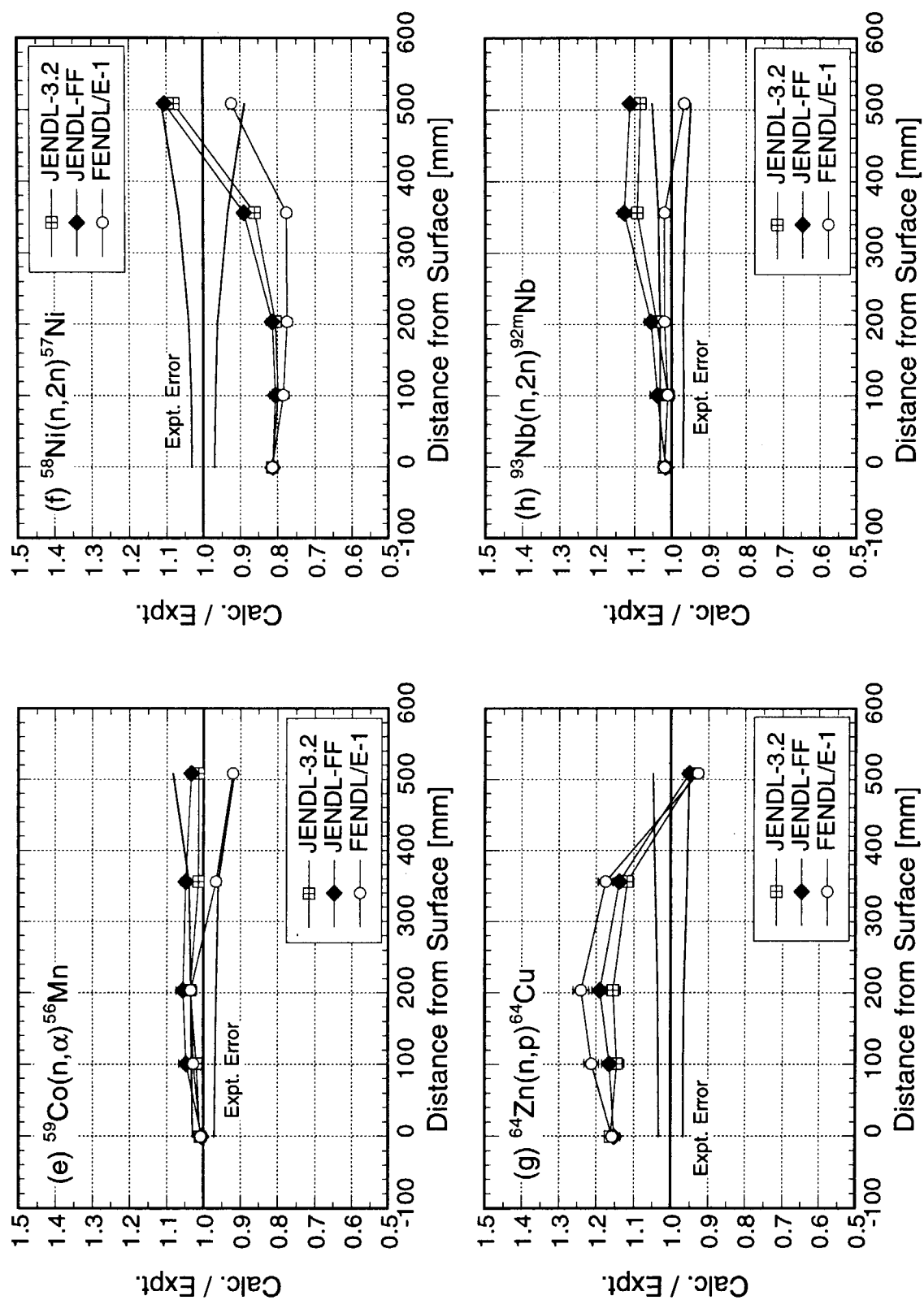


Fig. 4.3.43 Continued. (2/3)

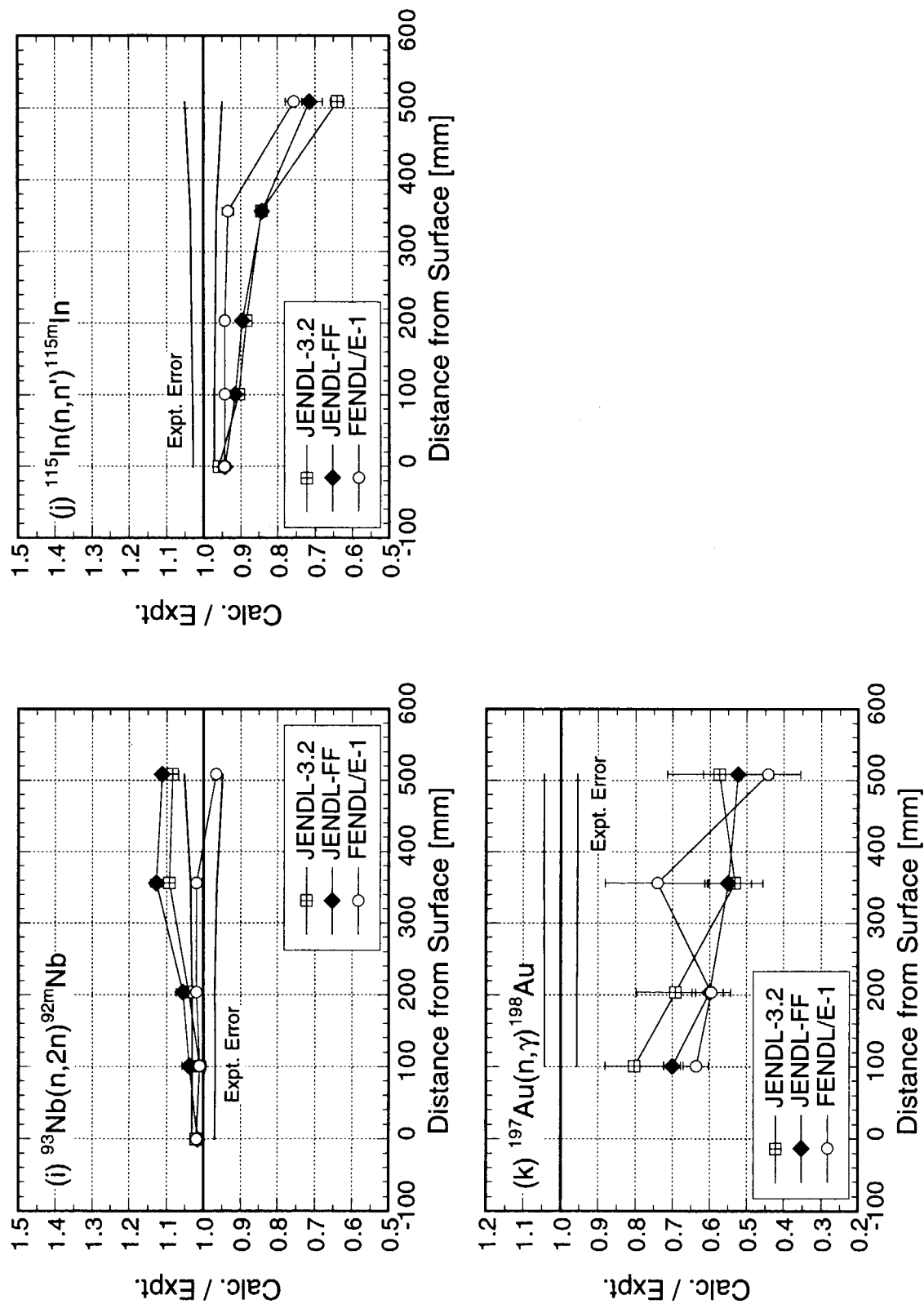


Fig. 4.3.43 Continued. (3/3)

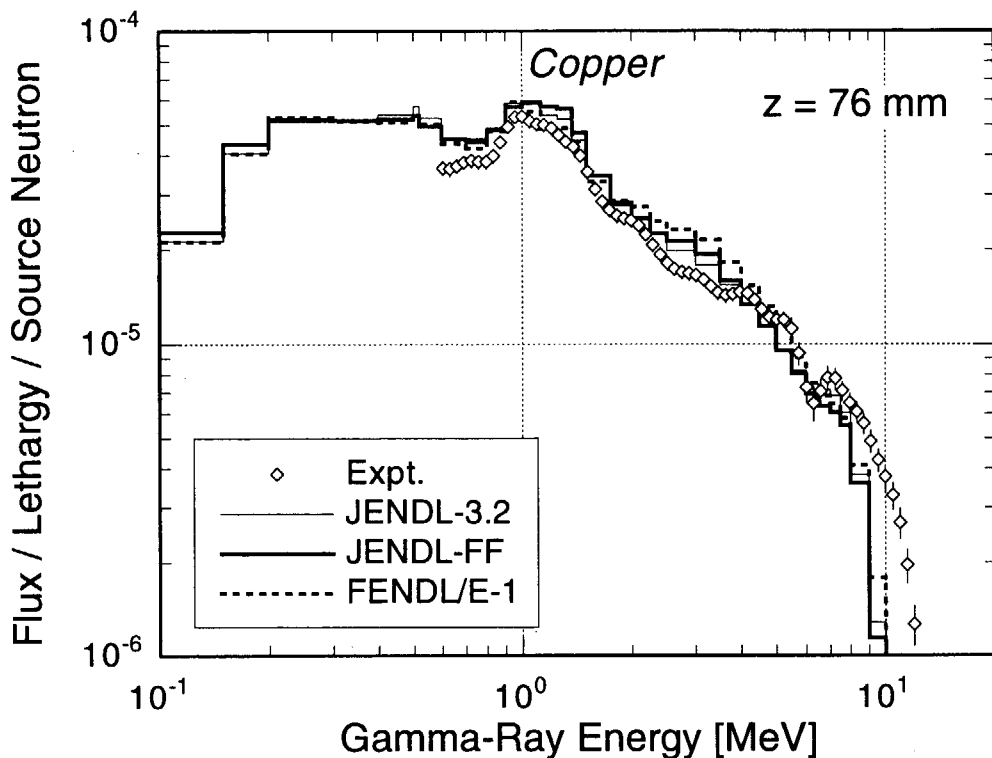


Fig. 4.3.44 Gamma-ray spectra at the 76 mm depth in the cylindrical copper assembly measured and calculated with JENDL-3.2, JENDL Fusion File and FENDL/E-1.0.

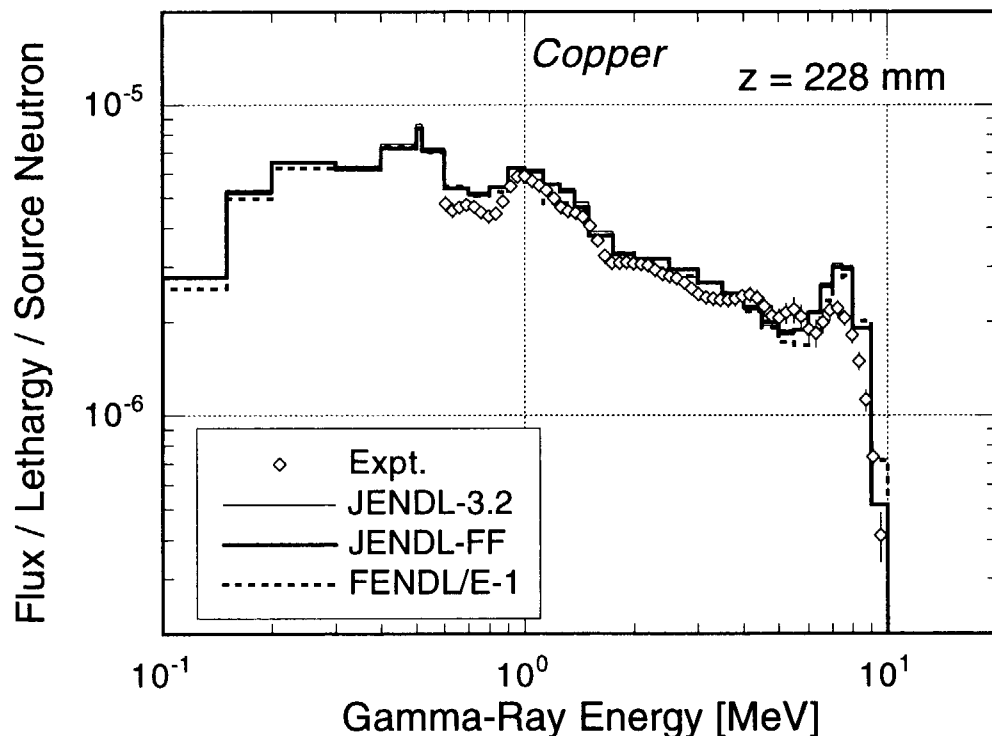


Fig. 4.3.45 Gamma-ray spectra at the 228 mm depth in the cylindrical copper assembly measured and calculated with JENDL-3.2, JENDL Fusion File and FENDL/E-1.0.

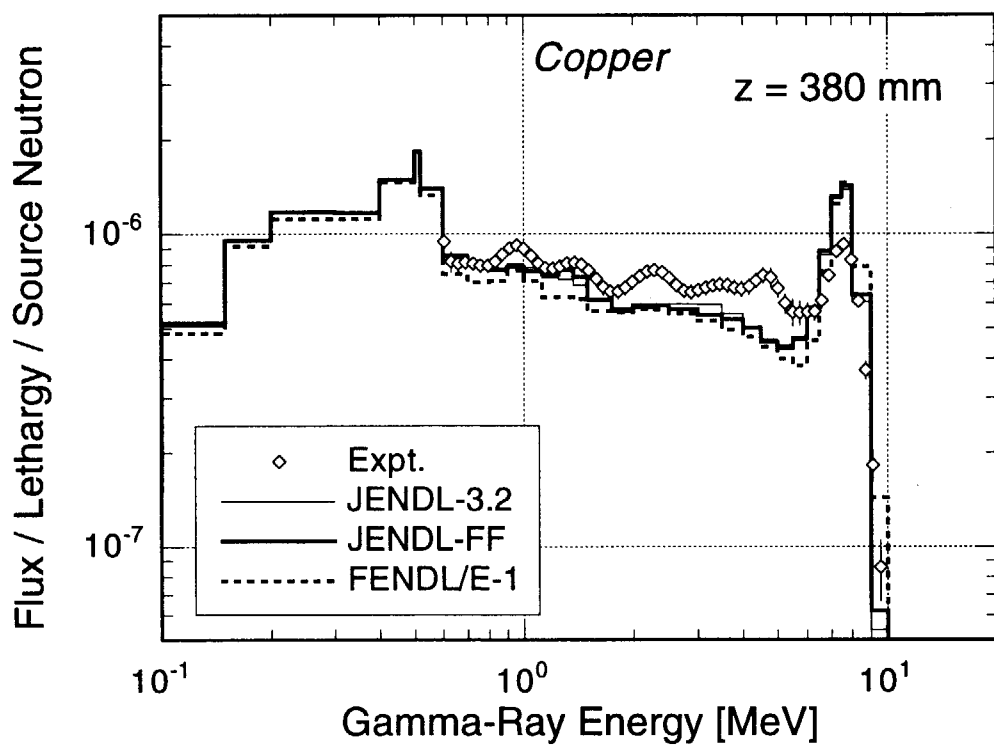


Fig. 4.3.46 Gamma-ray spectra at the 380 mm depth in the cylindrical copper assembly measured and calculated with JENDL-3.2, JENDL Fusion File and FENDL/E-1.0.

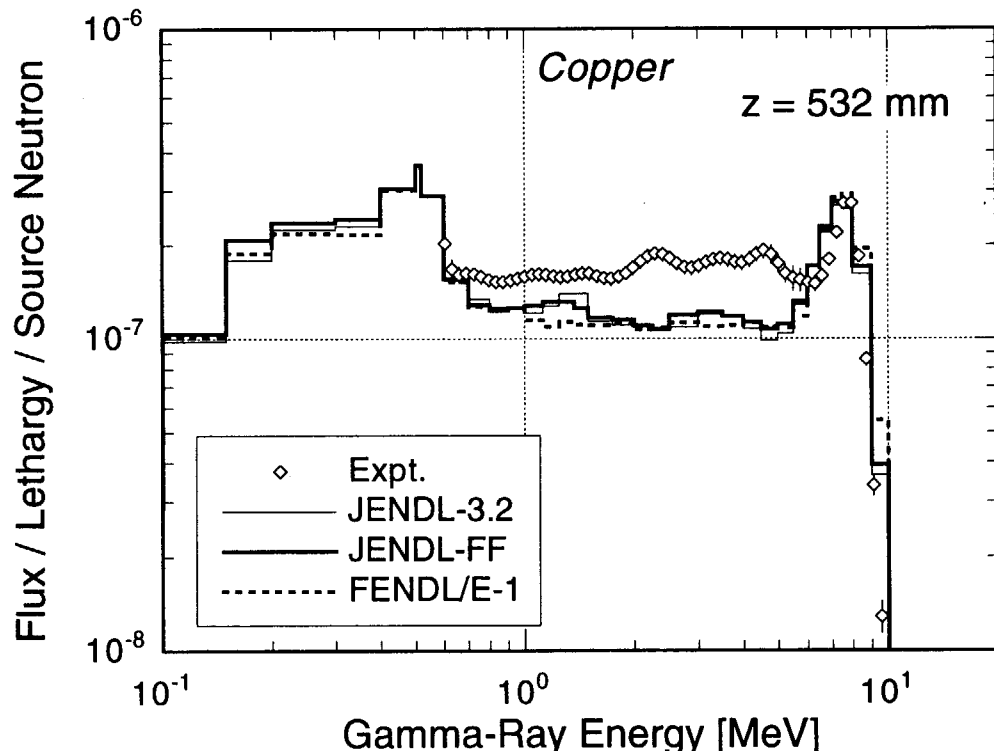


Fig. 4.3.47 Gamma-ray spectra at the 532 mm depth in the cylindrical copper assembly measured and calculated with JENDL-3.2, JENDL Fusion File and FENDL/E-1.0.

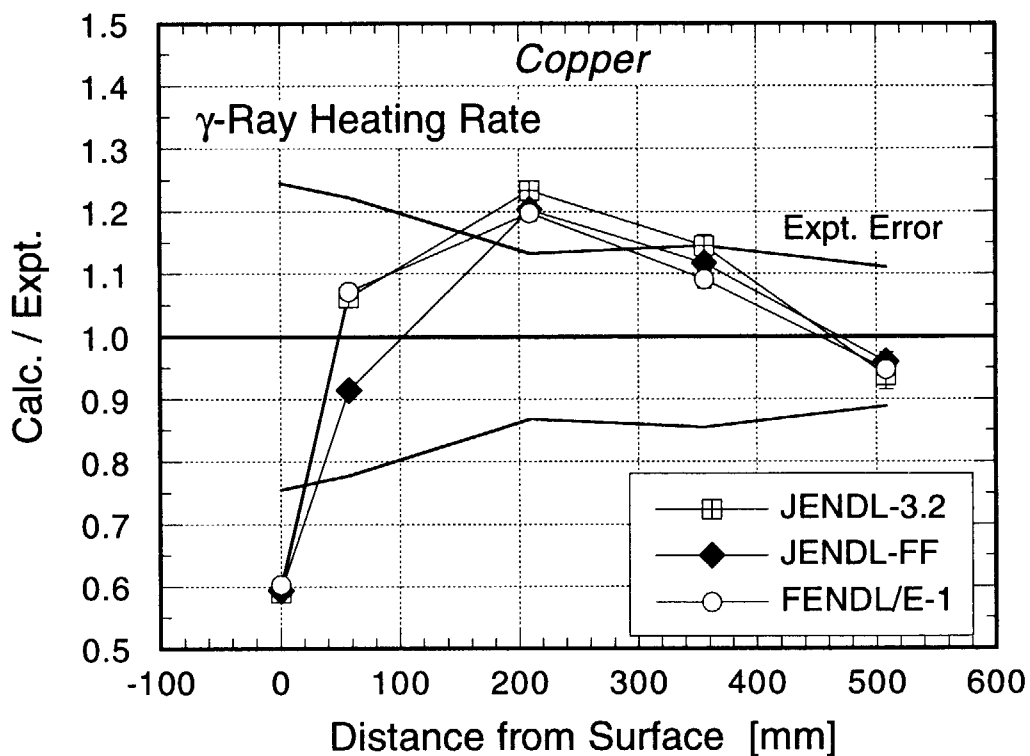


Fig. 4.3.48 Calculated to experimental ratios of gamma-ray heating rates in the cylindrical copper assembly for JENDL-3.2, JENDL Fusion File and FENDL/E-1.0.

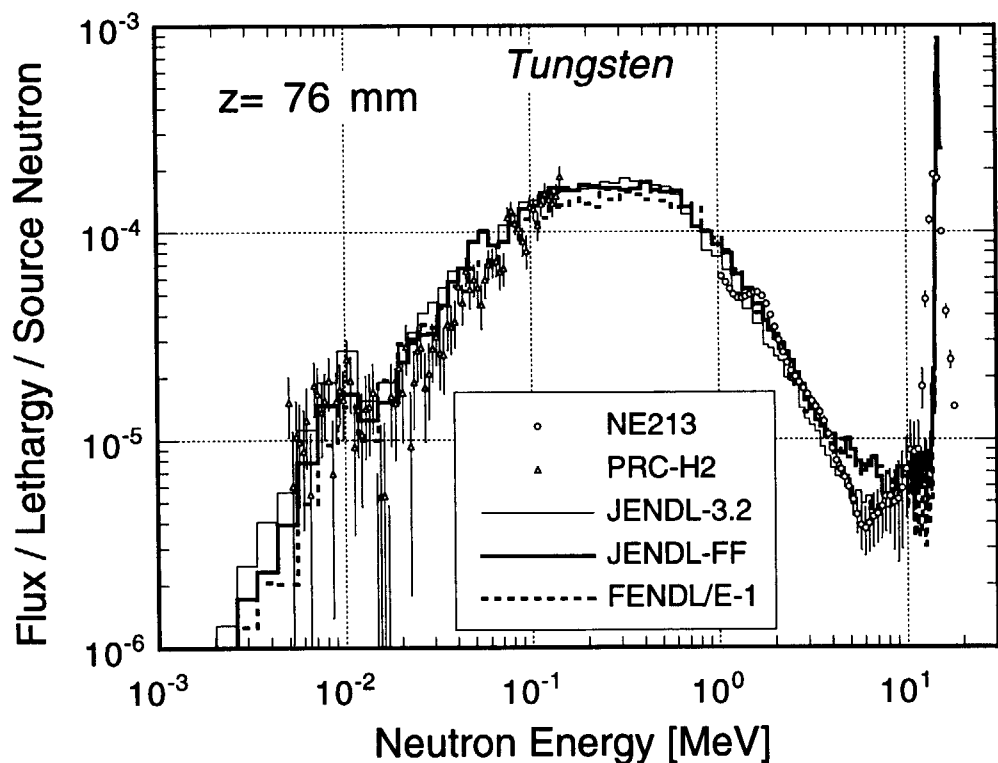


Fig. 4.3.49 Neutron spectra at the 76 mm depth in the cylindrical tungsten assembly measured and calculated with JENDL-3.2, JENDL Fusion File and FENDL/E-1.0.

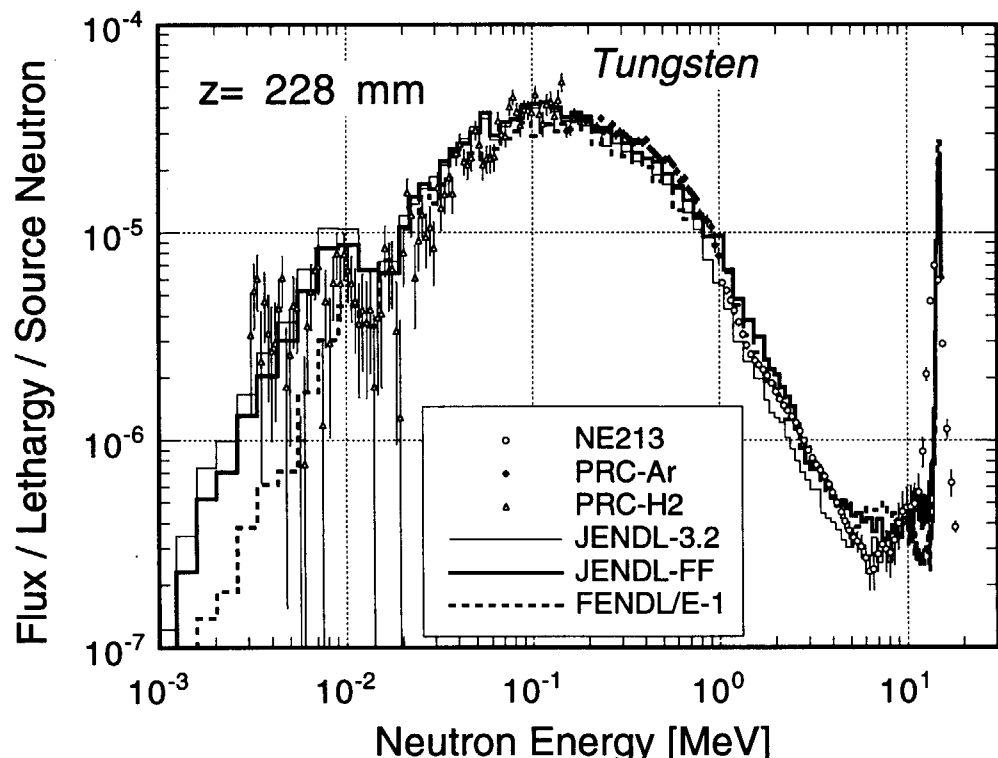


Fig. 4.3.50 Neutron spectra at the 228 mm depth in the cylindrical tungsten assembly measured and calculated with JENDL-3.2, JENDL Fusion File and FENDL/E-1.0.

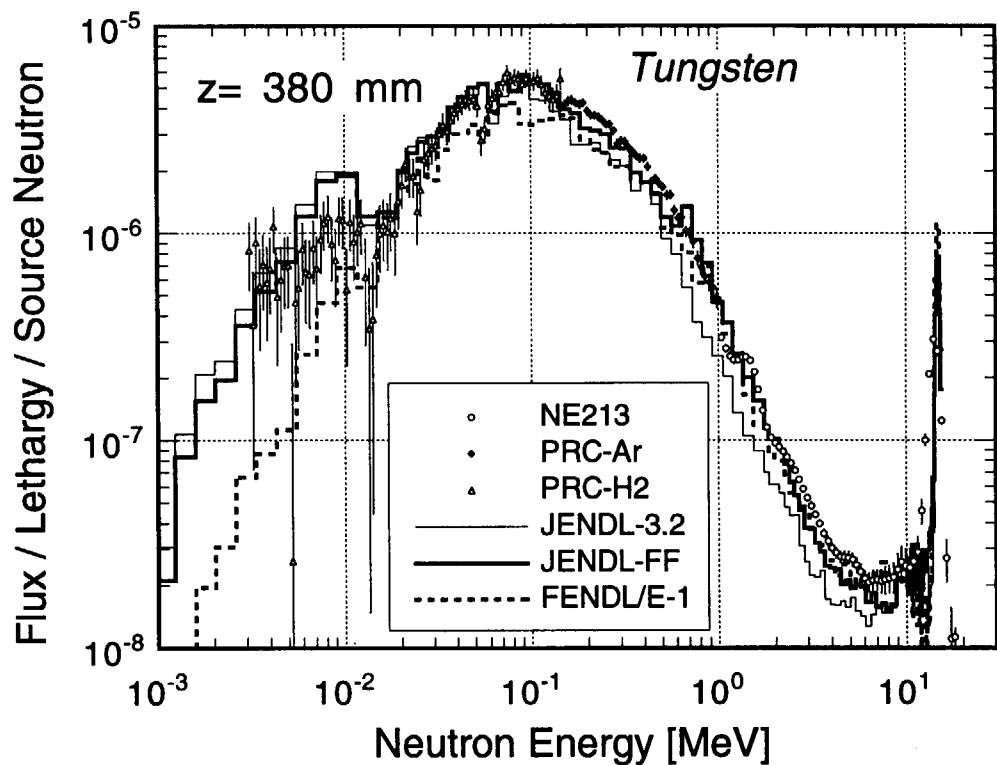


Fig. 4.3.51 Neutron spectra at the 380 mm depth in the cylindrical tungsten assembly measured and calculated with JENDL-3.2, JENDL Fusion File and FENDL/E-1.0.

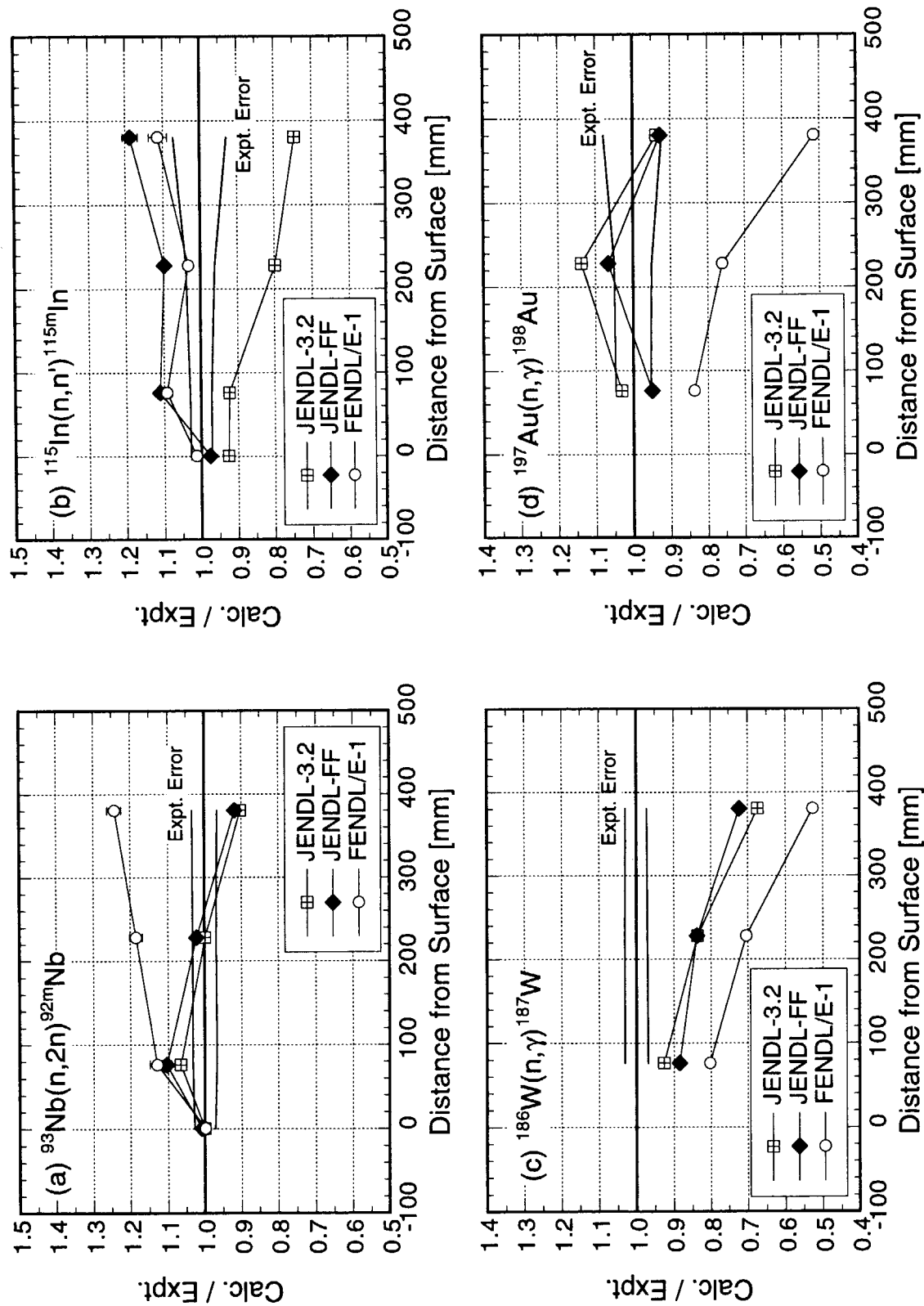


Fig. 4.3.52 Calculated to experimental ratios of dosimetry reaction rates in the cylindrical tungsten assembly for JENDL-3.2, JENDL Fusion File and FENDL/E-1.0.

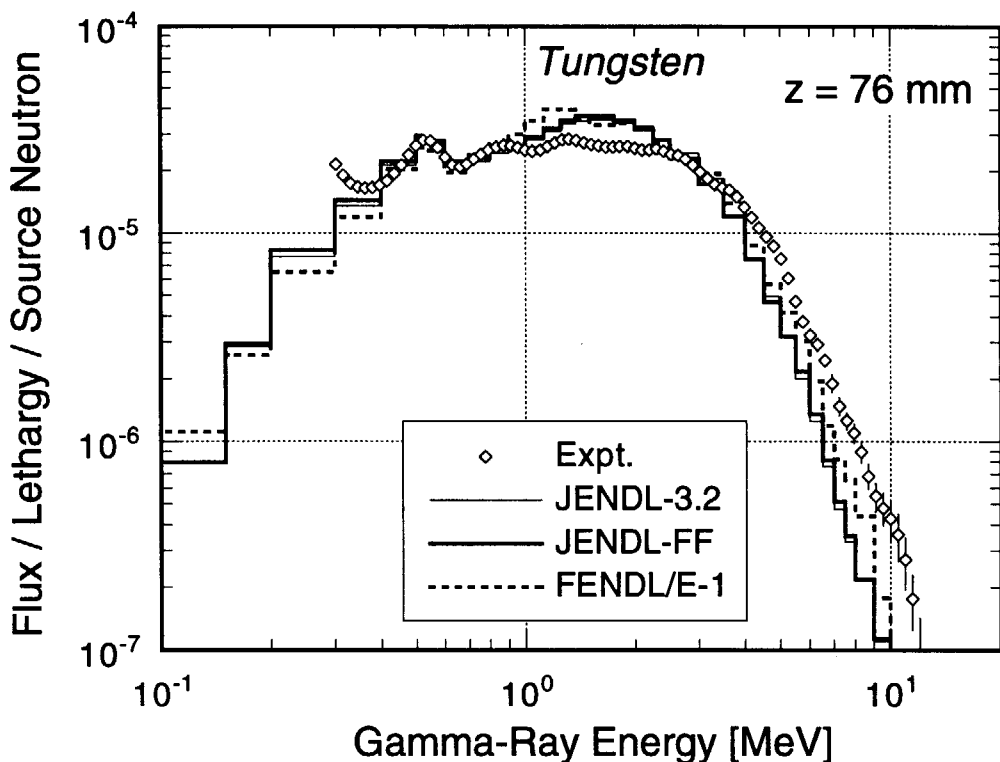


Fig. 4.3.53 Gamma-ray spectra at the 76 mm depth in the cylindrical tungsten assembly measured and calculated with JENDL-3.2, JENDL Fusion File and FENDL/E-1.0.

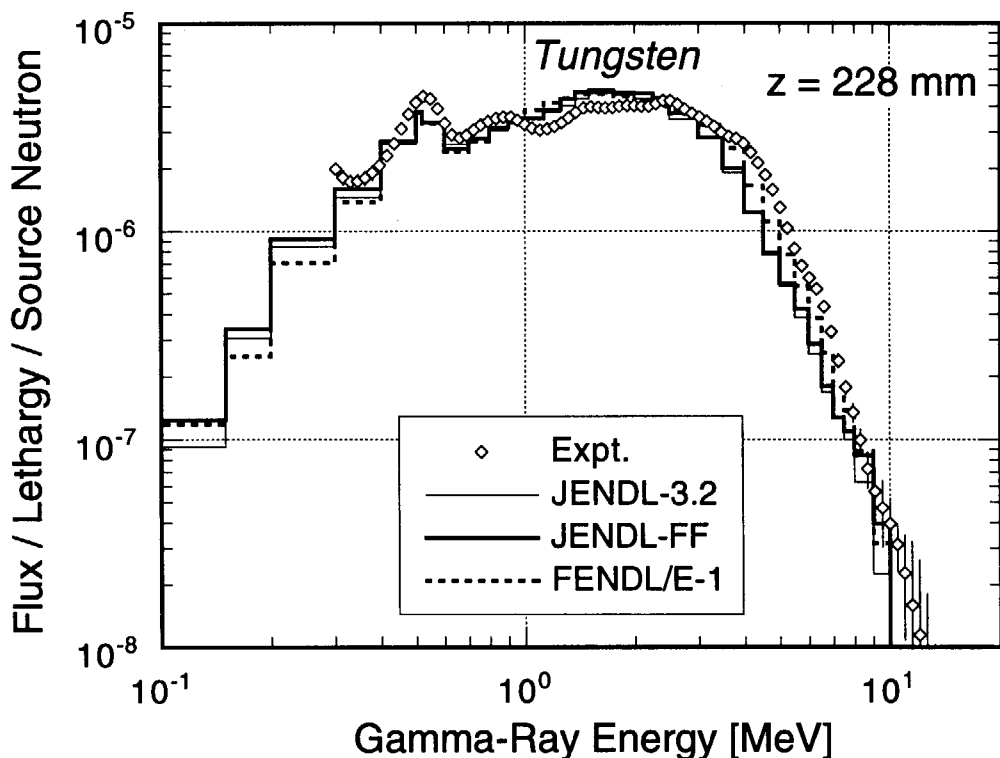


Fig. 4.3.54 Gamma-ray spectra at the 228 mm depth in the cylindrical tungsten assembly measured and calculated with JENDL-3.2, JENDL Fusion File and FENDL/E-1.0.

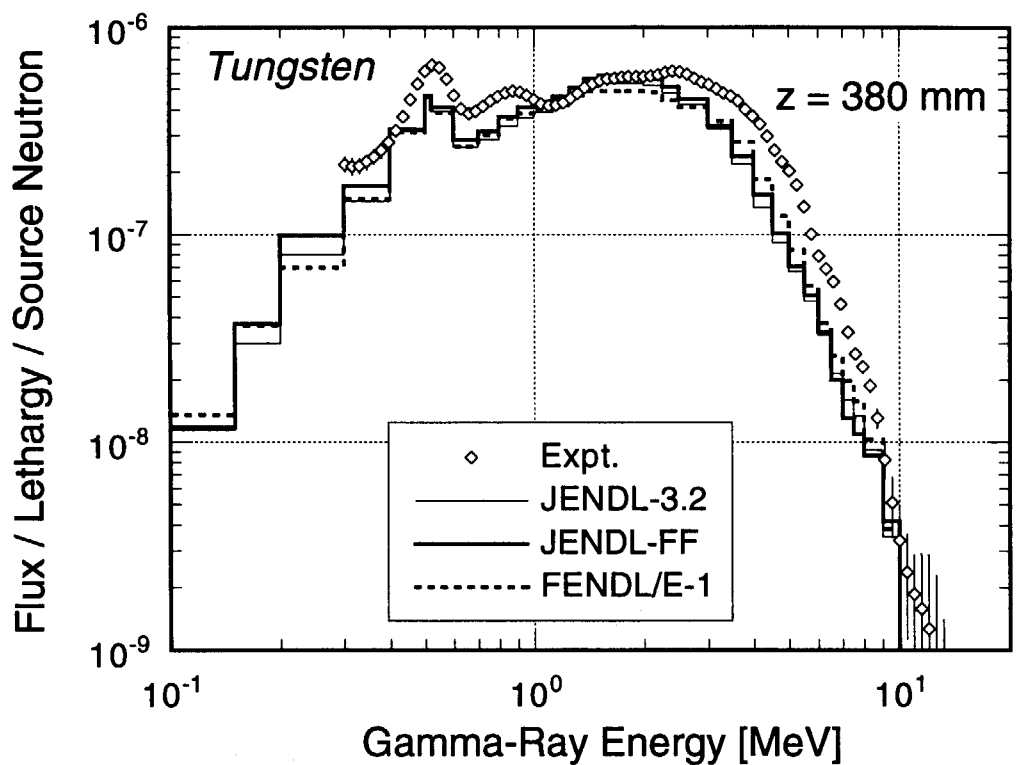


Fig. 4.3.55 Gamma-ray spectra at the 380 mm depth in the cylindrical tungsten assembly measured and calculated with JENDL-3.2, JENDL Fusion File and FENDL/E-1.0.

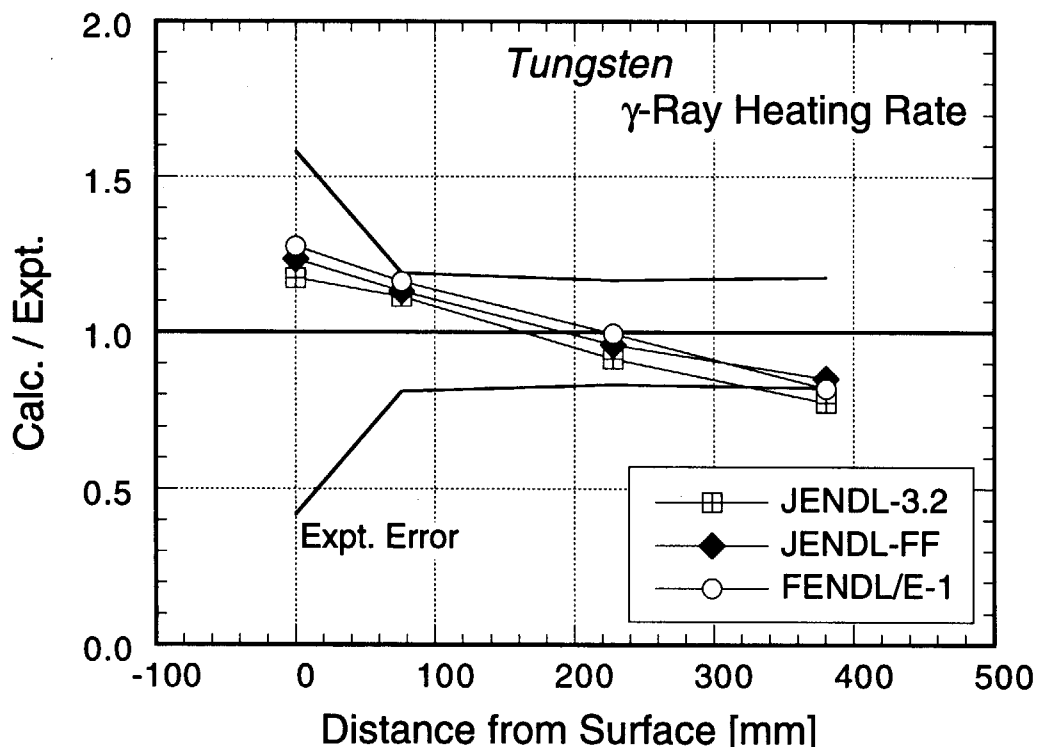


Fig. 4.3.56 Calculated to experimental ratios of gamma-ray heating rates in the cylindrical tungsten assembly for JENDL-3.2, JENDL Fusion File and FENDL/E-1.0.

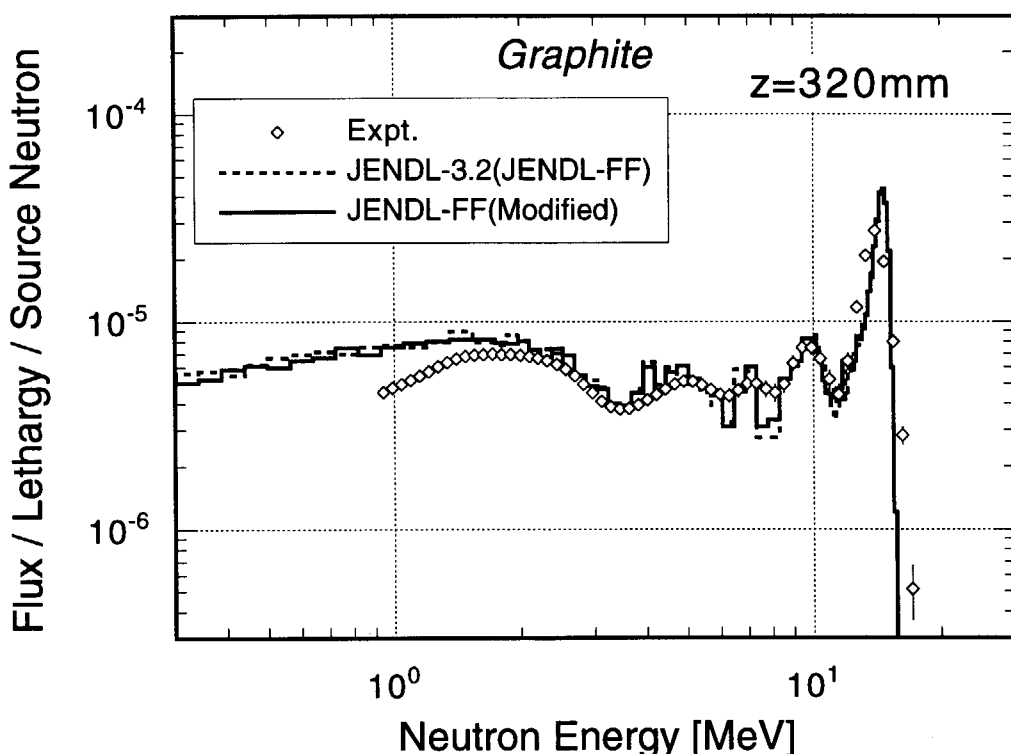


Fig. 4.4.1 Neutron spectra at the 320 mm depth in the cylindrical graphite assembly measured and calculated with JENDL-3.2 (same as JENDL-FF) and the modified JENDL Fusion File.

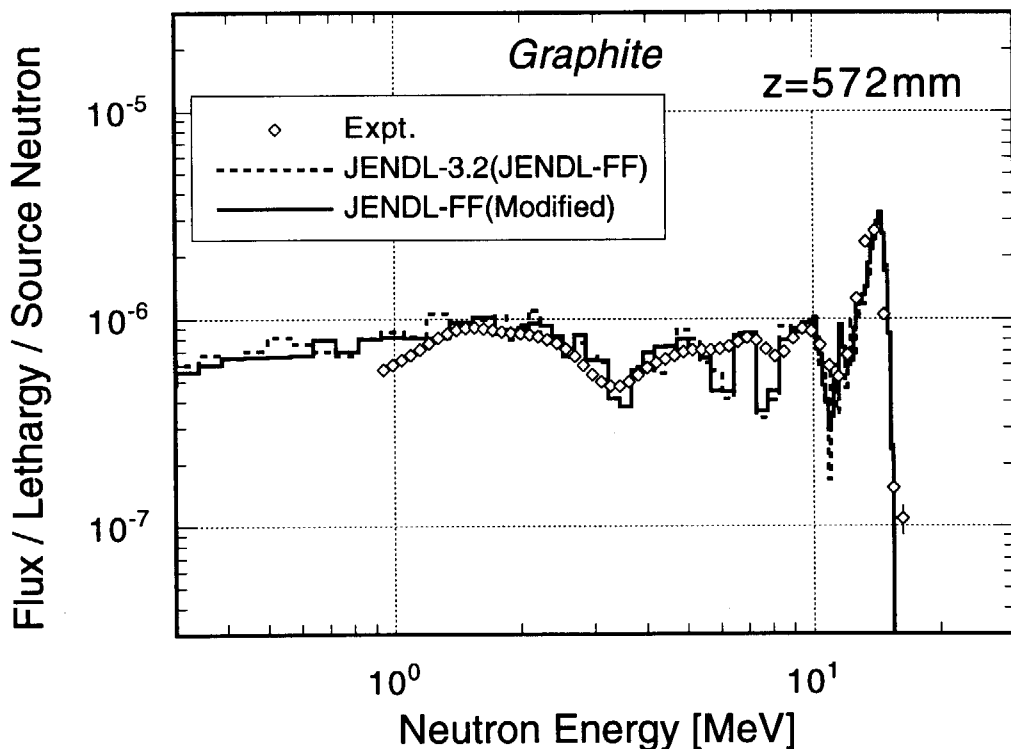


Fig. 4.4.2 Neutron spectra at the 572 mm depth in the cylindrical graphite assembly measured and calculated with JENDL-3.2 (same as JENDL-FF) and the modified JENDL Fusion File.

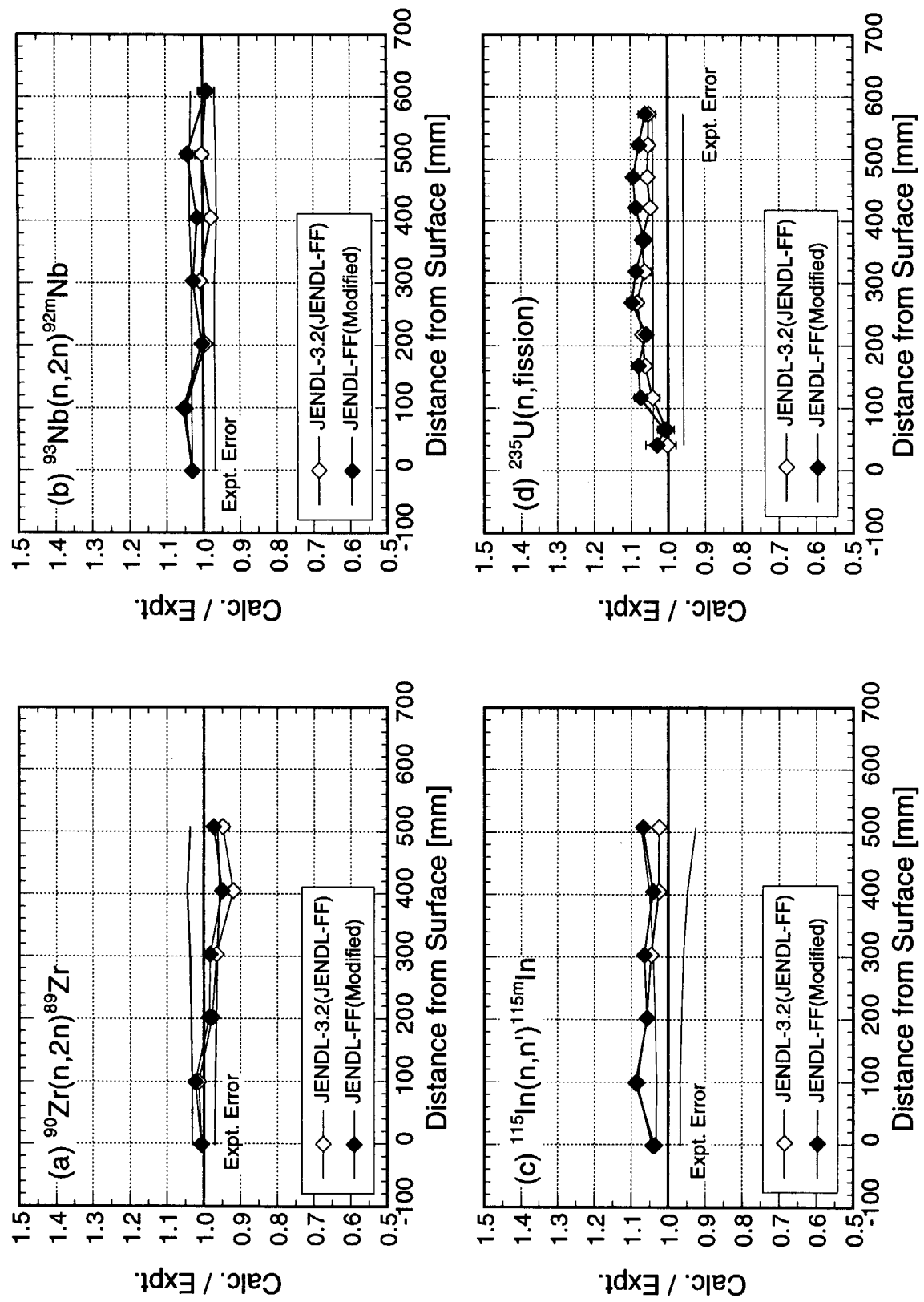


Fig. 4.4.3 Calculated to experimental ratios of dosimetry reaction rates in the cylindrical graphite assembly for JENDL-3.2 (same as JENDL-FF) and the modified JENDL Fusion File.

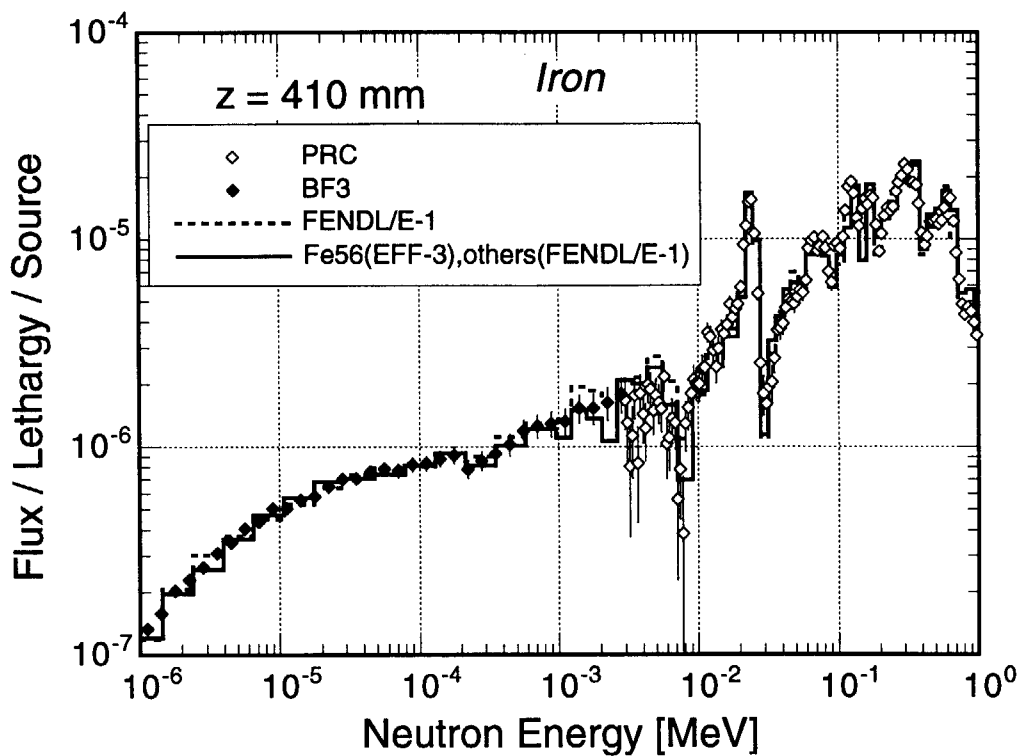


Fig. 4.4.4 Neutron spectra at the 410 mm depth in the cylindrical iron assembly measured and calculated with FENDL/E-1.0, and the combination of EFF-3 (Fe-56) and FENDL/E-1.0 (Fe-54, Fe-57 & Fe-58).

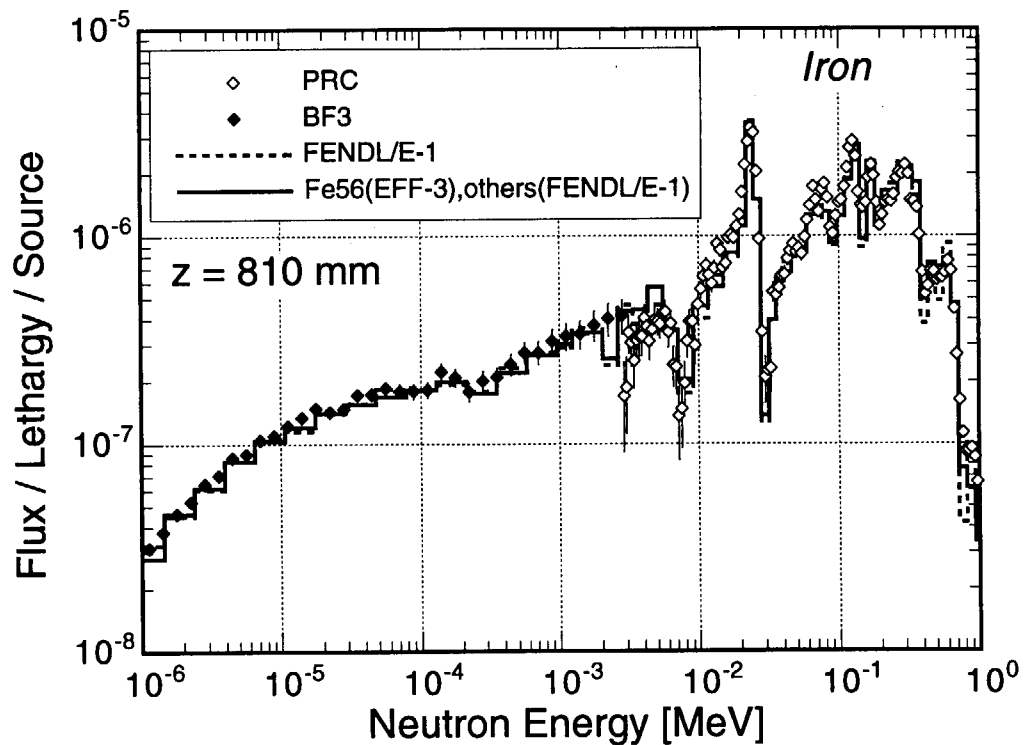


Fig. 4.4.5 Neutron spectra at the 810 mm depth in the cylindrical iron assembly measured and calculated with FENDL/E-1.0, and the combination of EFF-3 (Fe-56) and FENDL/E-1.0 (Fe-54, Fe-57 & Fe-58).

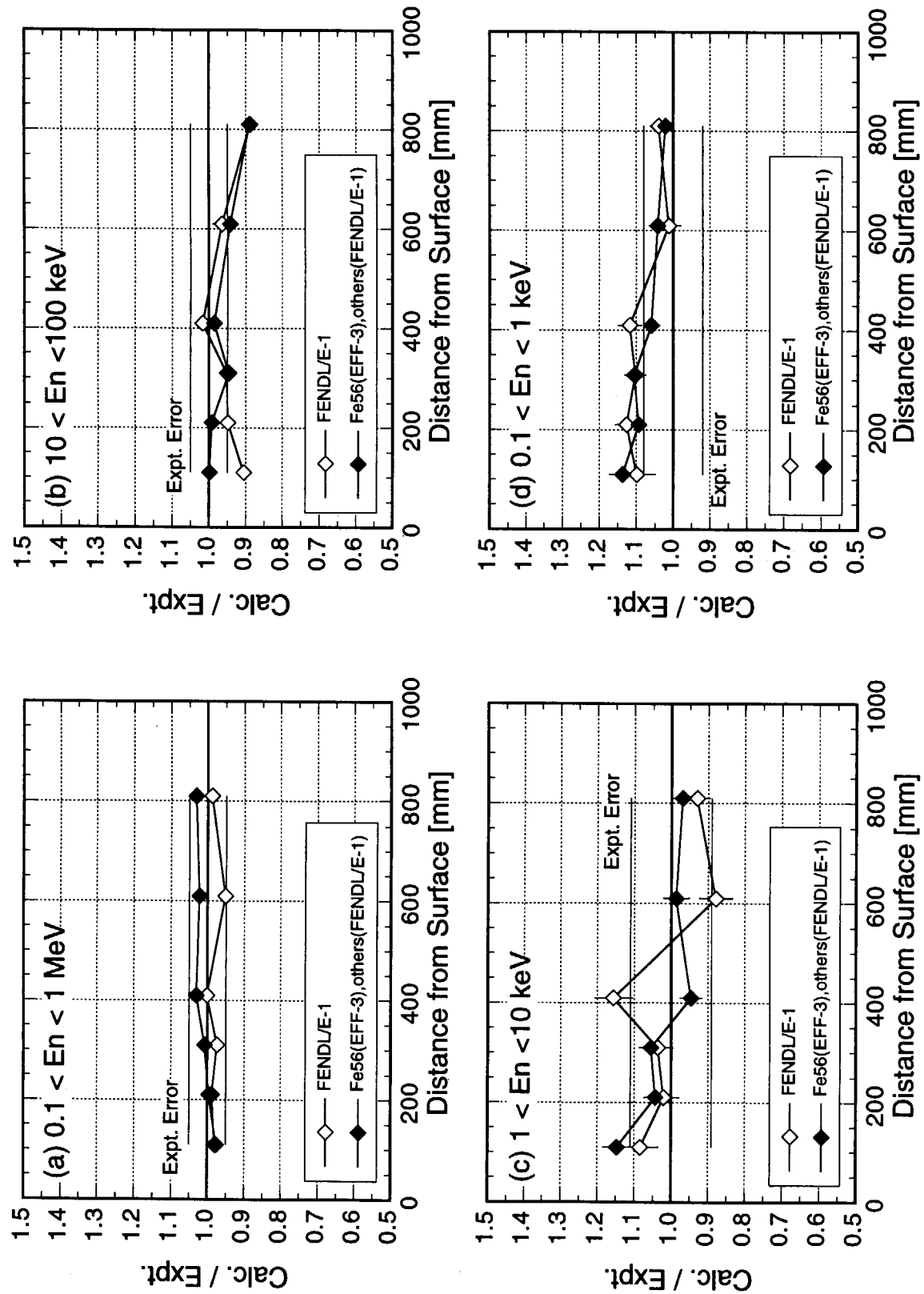


Fig. 4.4.6 Calculated to experimental ratios of neutron fluxes integrated in the six energy intervals in the cylindrical iron assembly for FENDL/E-1.0, and the combination of EFF-3 (Fe-56) and FENDL/E-1.0 (Fe-54, Fe-57 & Fe-58). (1/2)

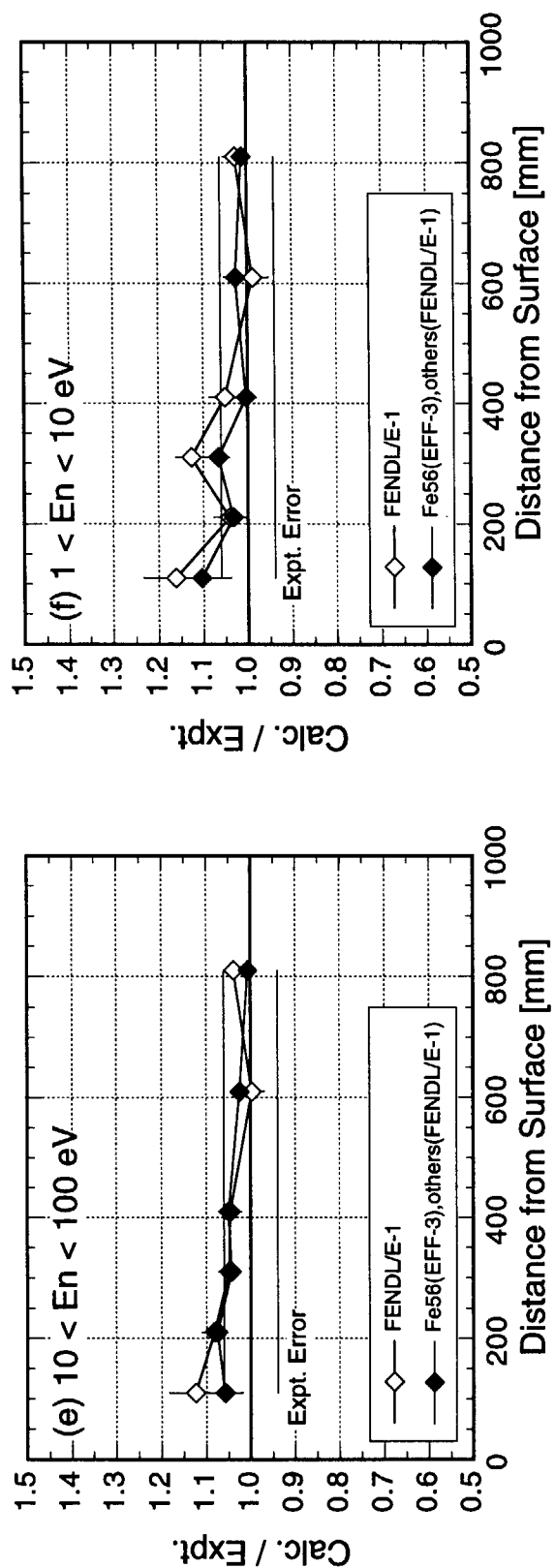


Fig. 4.4.6 Continued. (2/2)

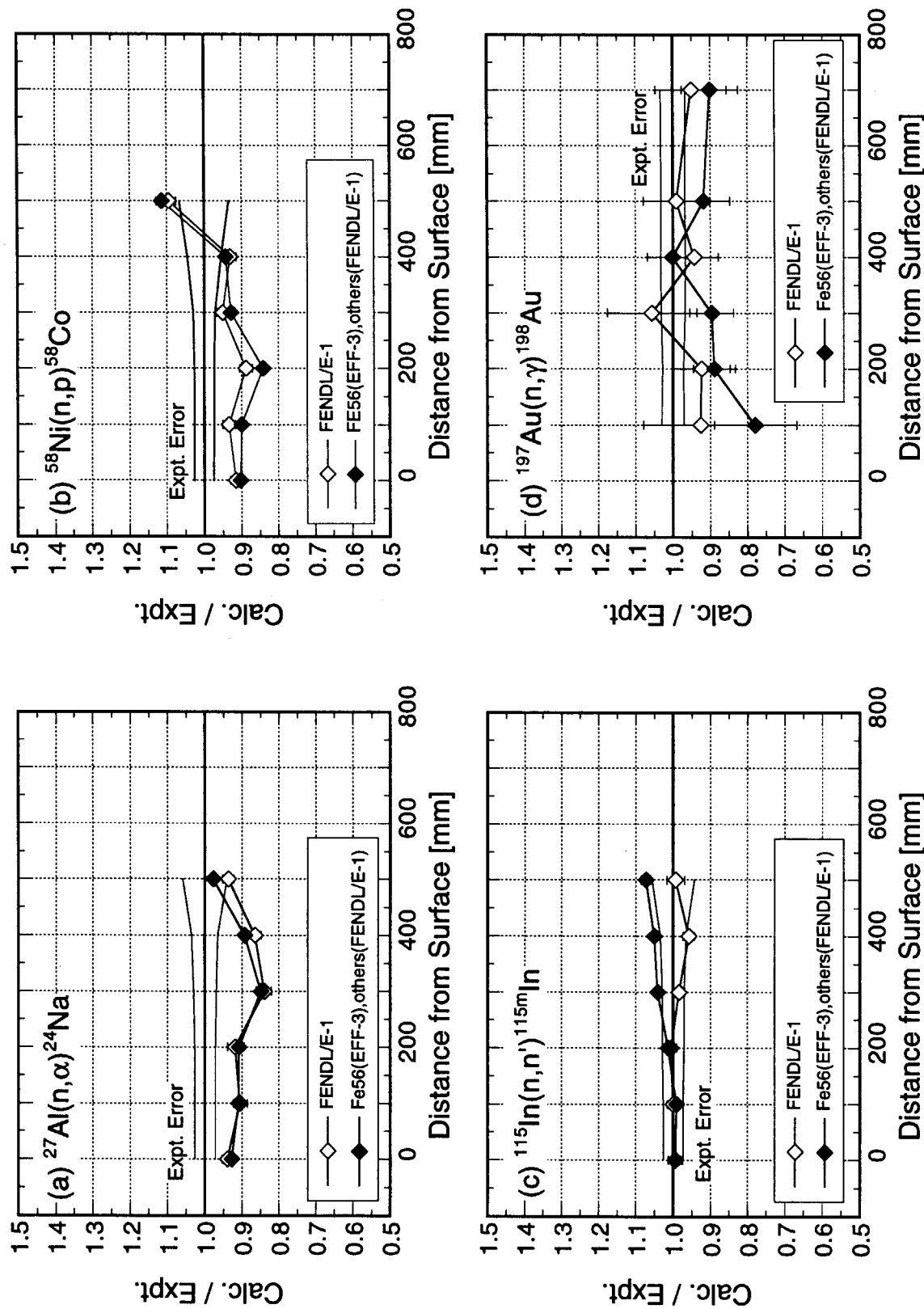


Fig. 4.4.7 Calculated to experimental ratios of dosimetry reaction rates in the cylindrical iron assembly for FENDL/E-1.0, and the combination of EFF-3 (Fe-56) and FENDL/E-1.0 (Fe-54, Fe-57 & Fe-58).

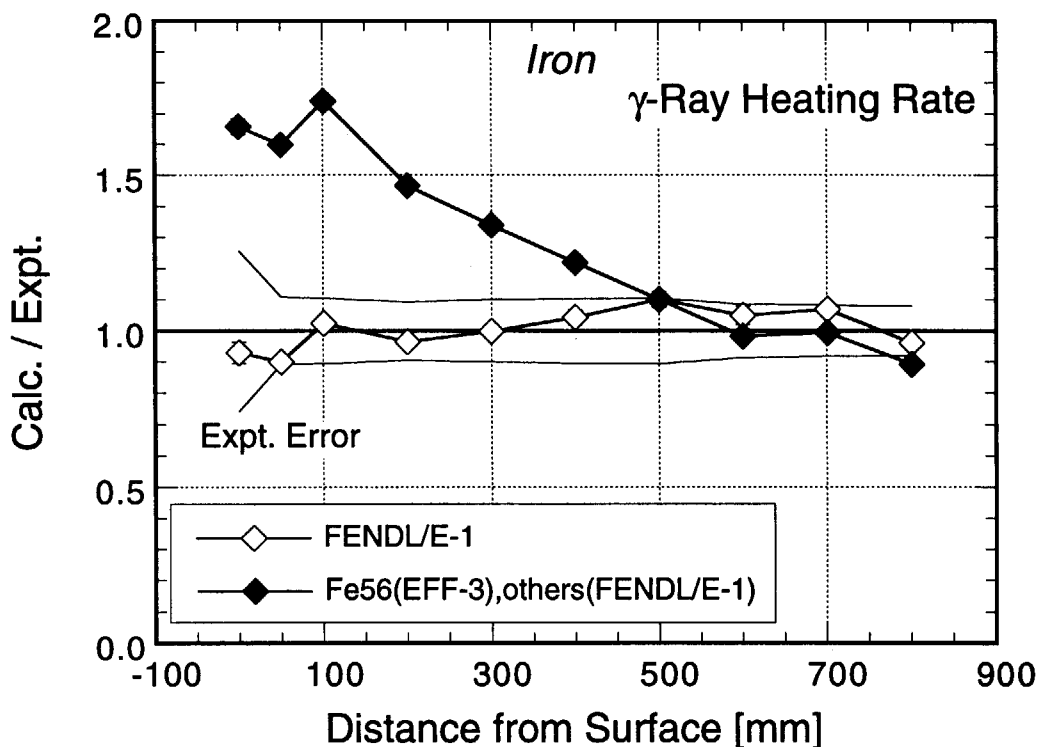


Fig. 4.4.8 Gamma-ray spectra at the 700 mm depth in the cylindrical iron assembly measured and calculated with FENDL/E-1.0, and the combination of EFF-3 (Fe-56) and FENDL/E-1.0 (Fe-54, Fe-57 & Fe-58).

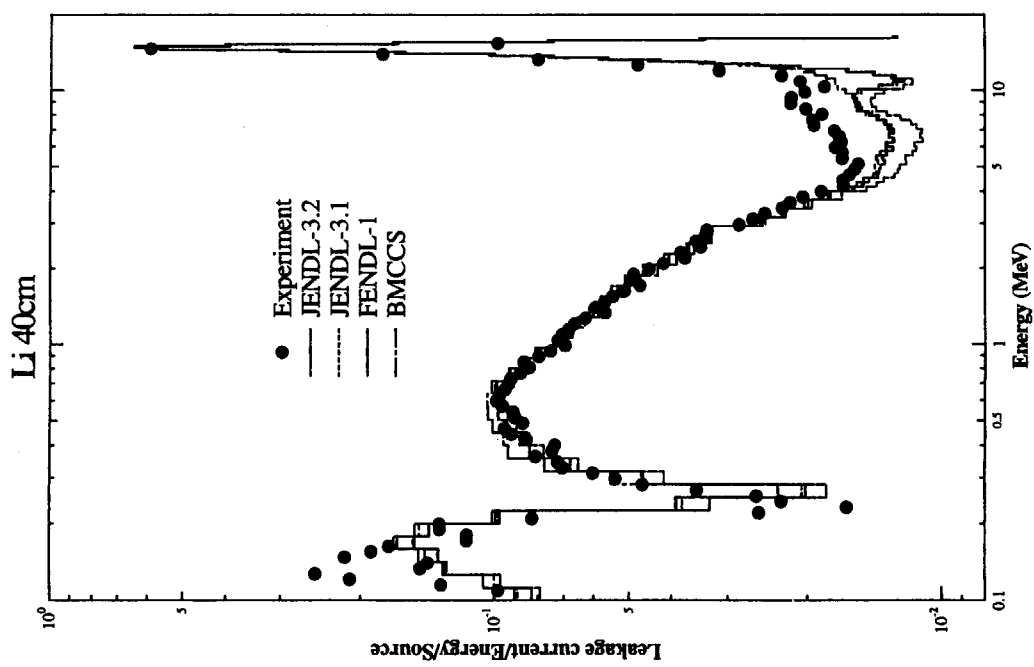


Fig. 5.3.1 Neutron spectra leaking from the spherical lithium pile measured and calculated with various nuclear data files.

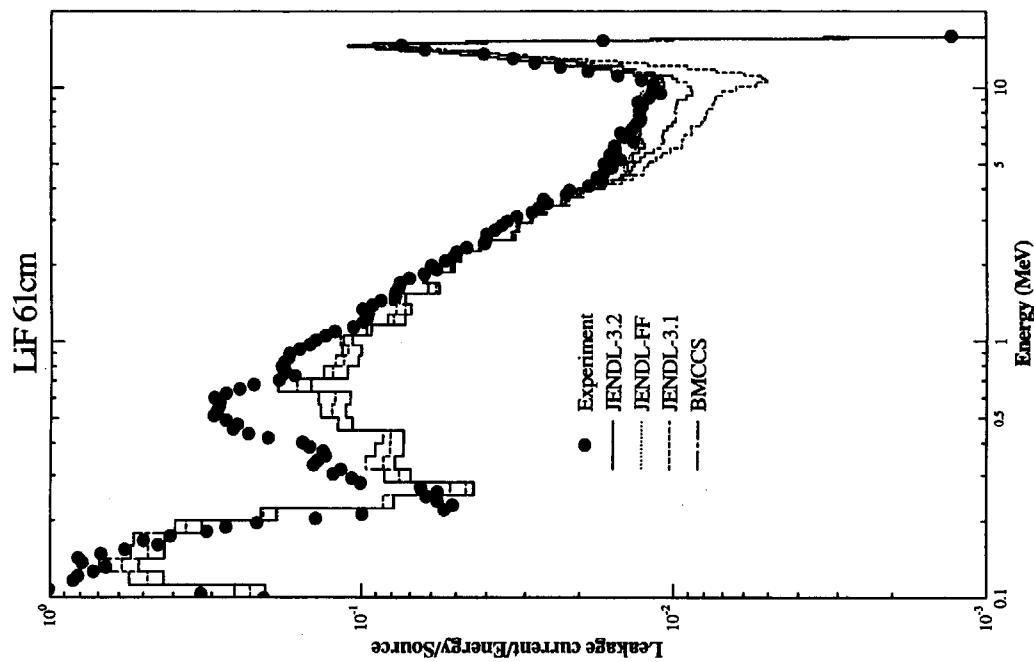


Fig. 5.3.2 Neutron spectra leaking from the spherical lithium fluoride pile measured and calculated with various nuclear data files.

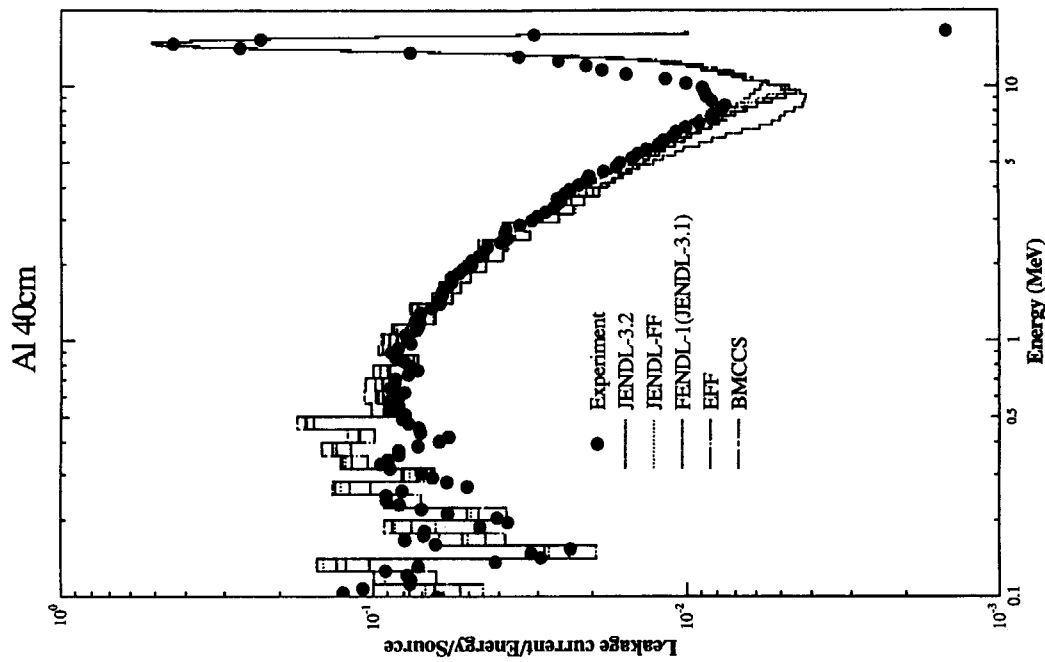


Fig. 5.3.4 Neutron spectra leaking from the spherical aluminum pile measured and calculated with various nuclear data files.

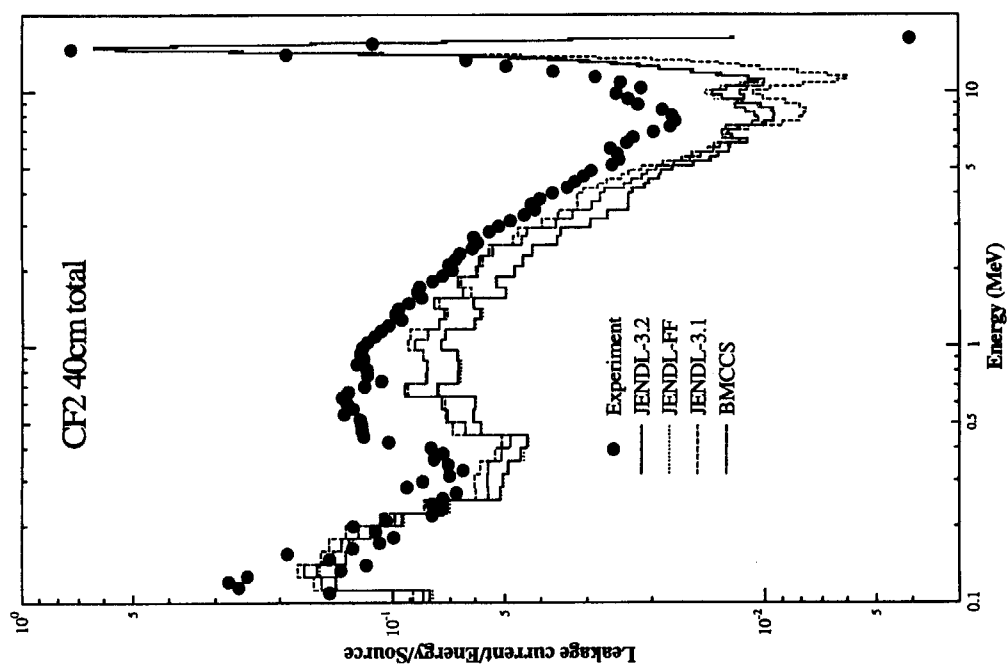


Fig. 5.3.3 Neutron spectra leaking from the spherical Teflon (CF<sub>2</sub>) pile measured and calculated with various nuclear data files.

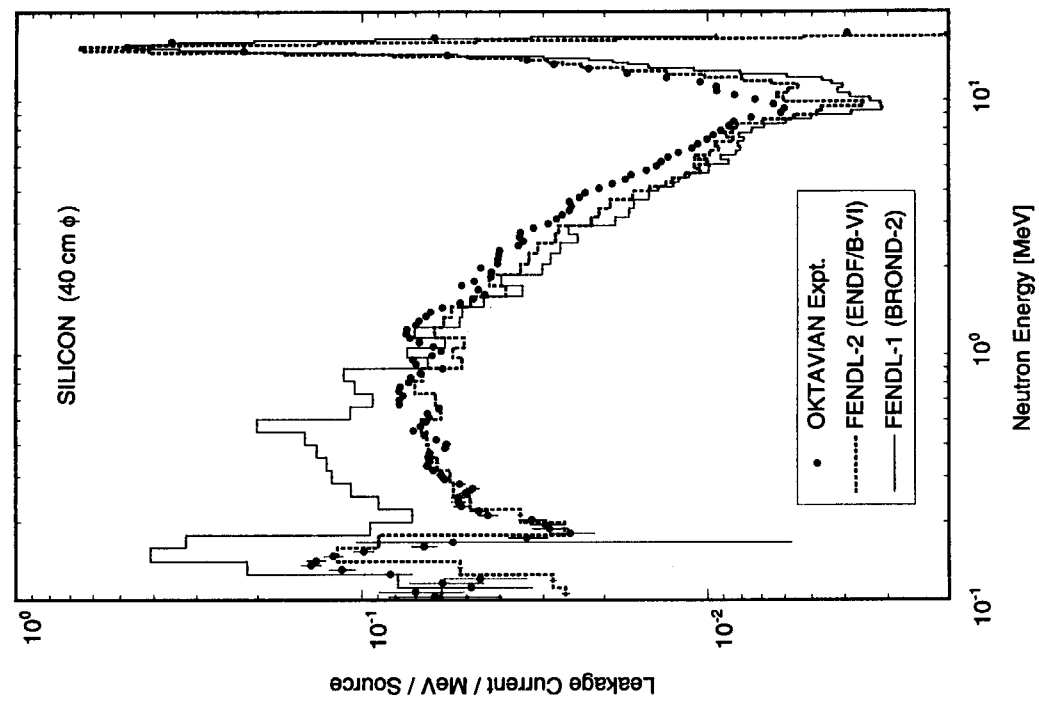


Fig. 5.3.5 Neutron spectra leaking from the spherical silicon (40 cm diam.) pile measured and calculated with various nuclear data files.

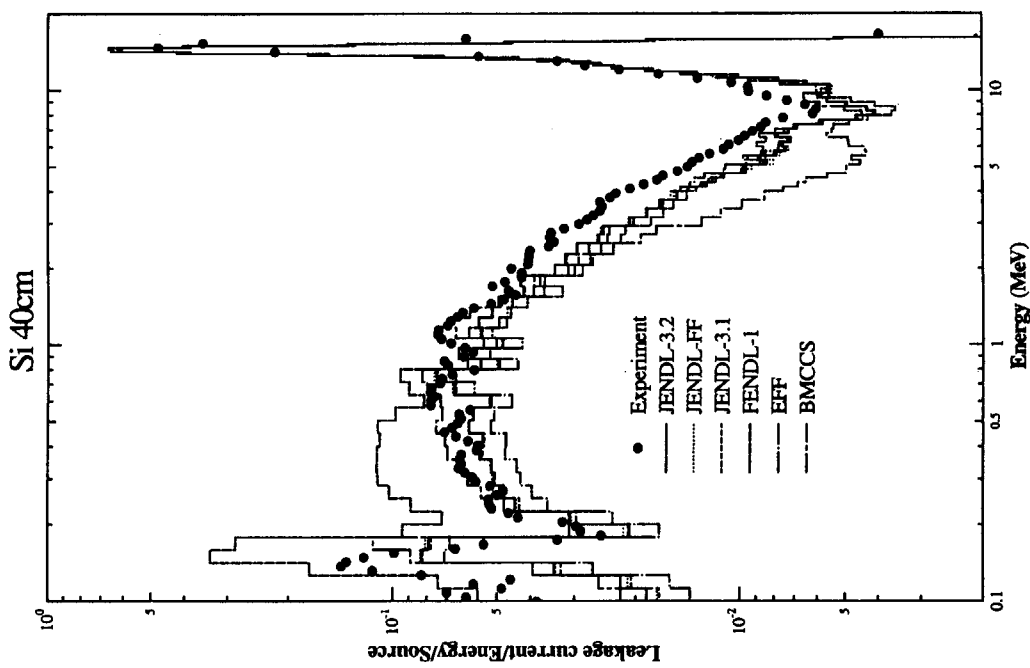


Fig. 5.3.6 Neutron spectra leaking from the spherical silicon (40 cm diam.) pile measured and calculated with FENDL-1 and FENDL-2.

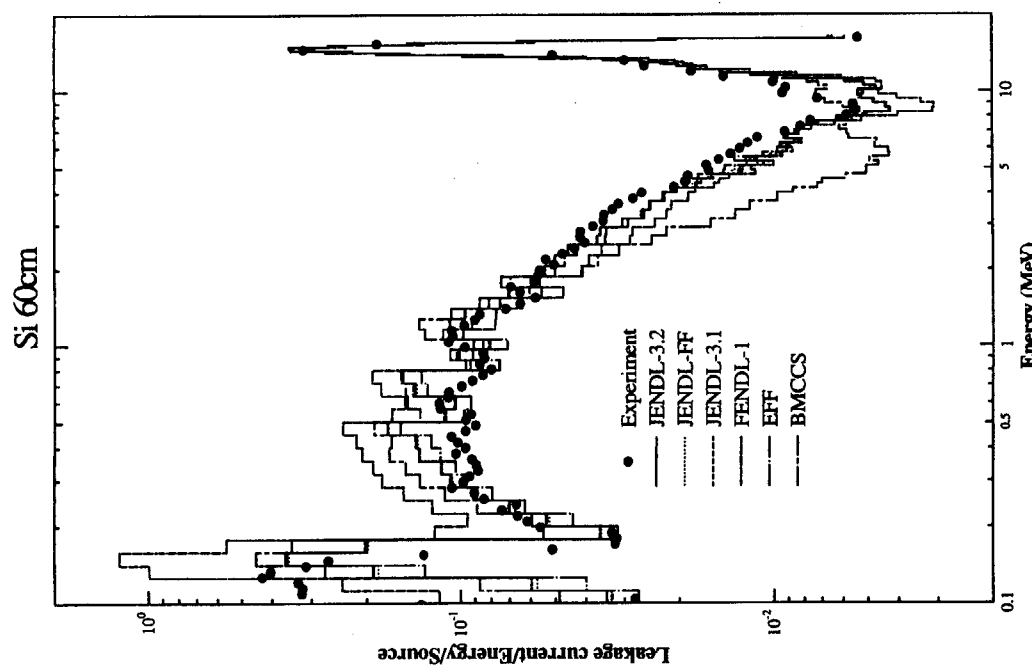
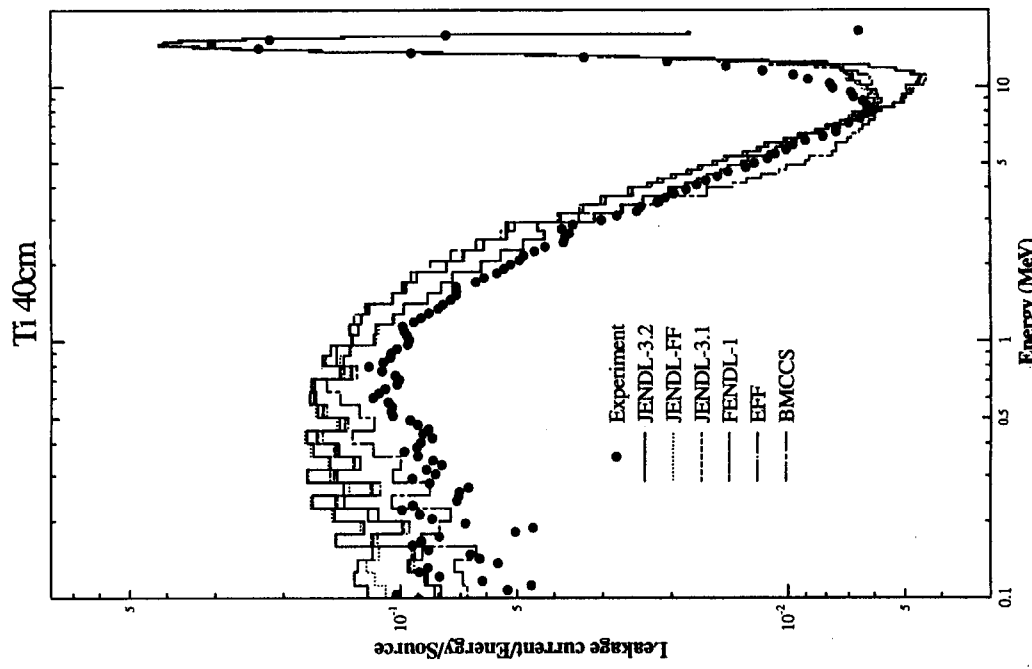


Fig. 5.3.7 Neutron spectra leaking from the spherical silicon (60 cm diam.) pile measured and calculated with various nuclear data files.

Fig. 5.3.8 Neutron spectra leaking from the spherical titanium pile measured and calculated with various nuclear data files.

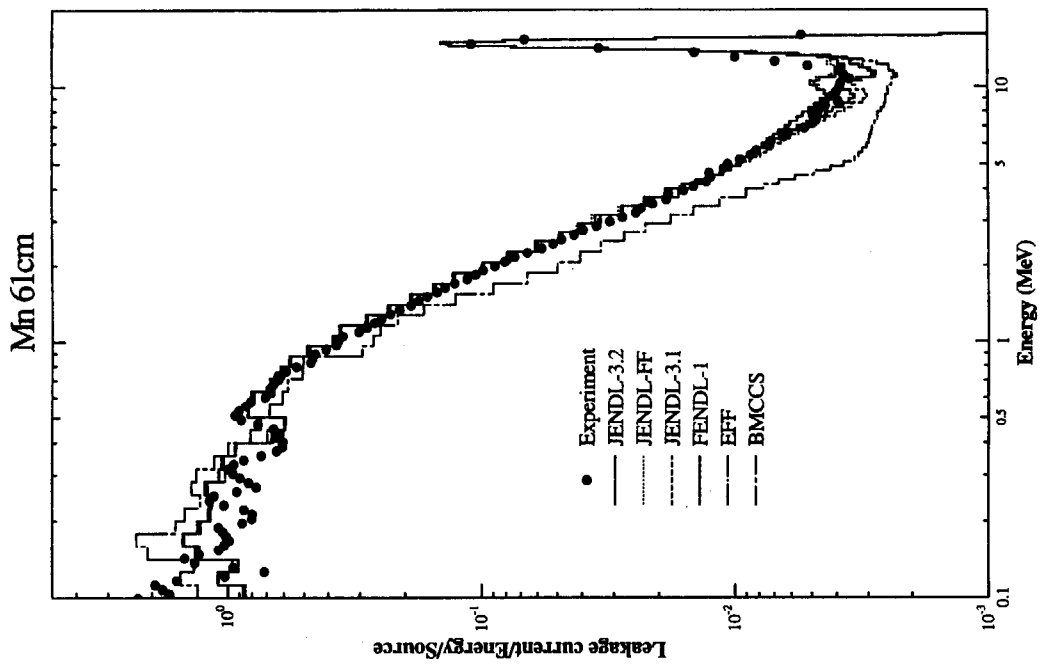


Fig. 5.3.10 Neutron spectra leaking from the spherical manganese pile measured and calculated with various nuclear data files.

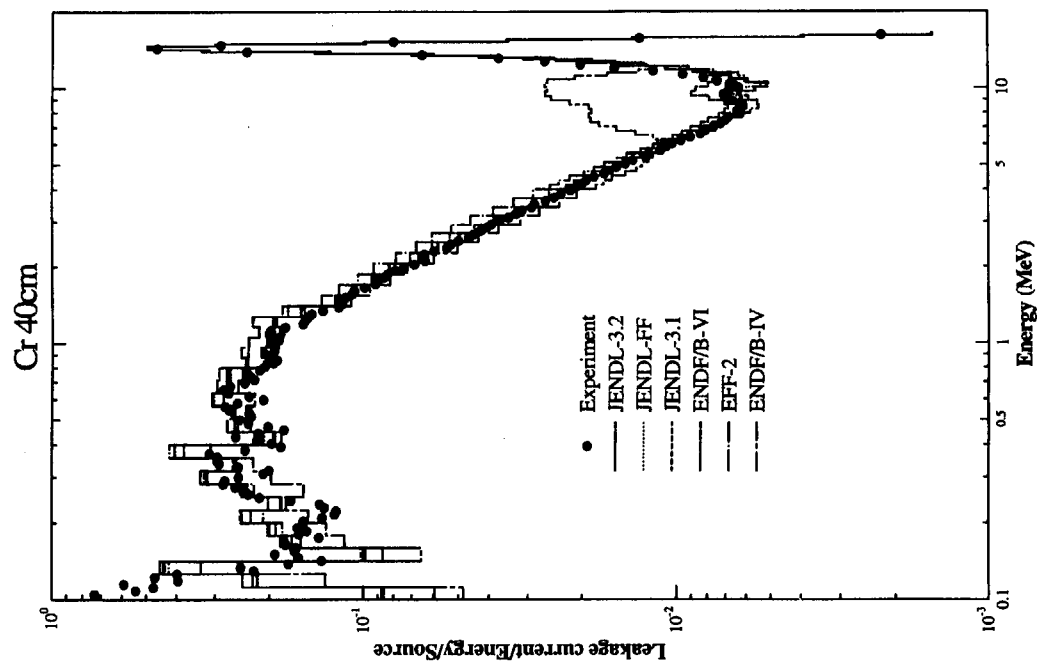


Fig. 5.3.9 Neutron spectra leaking from the spherical chromium pile measured and calculated with various nuclear data files.

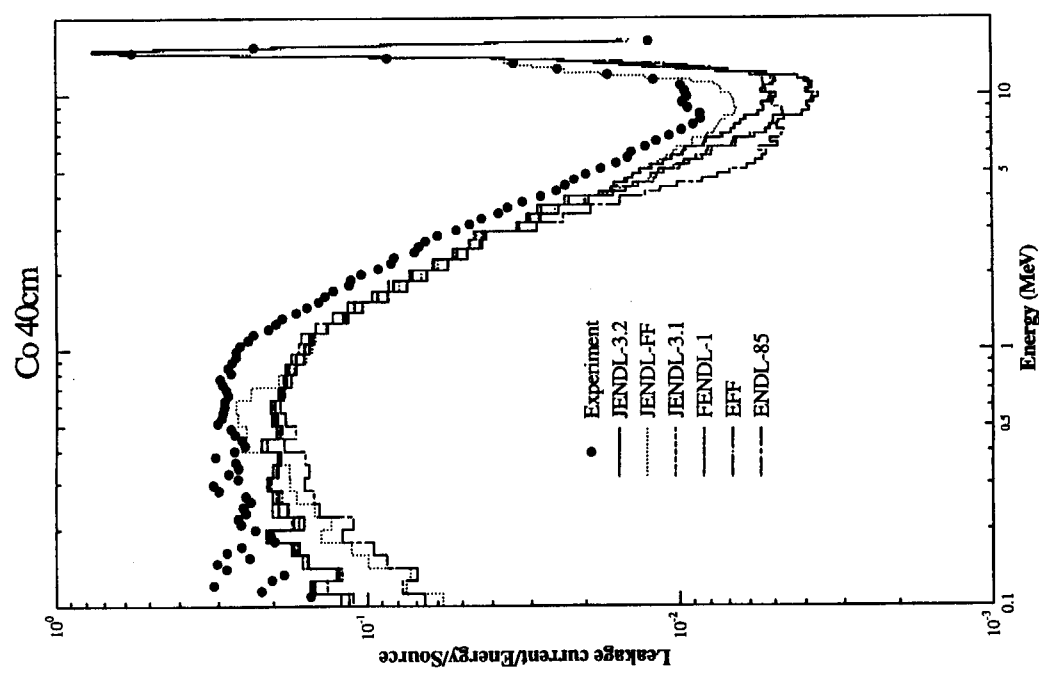


Fig. 5.3.11 Neutron spectra leaking from the spherical cobalt pile measured and calculated with various nuclear data files.

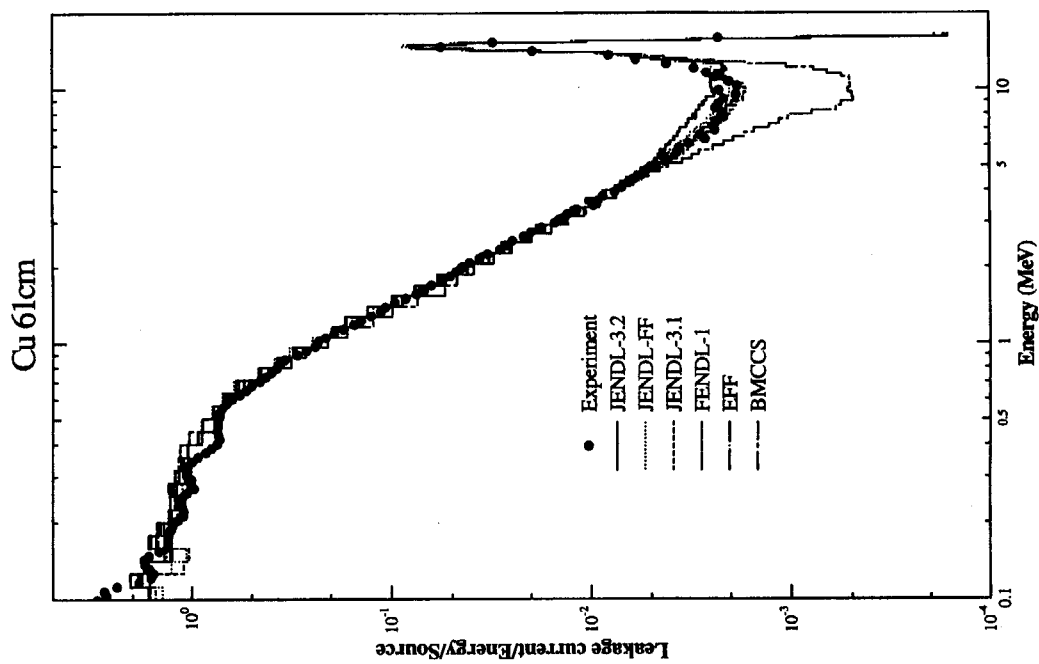


Fig. 5.3.12 Neutron spectra leaking from the spherical copper pile measured and calculated with various nuclear data files.

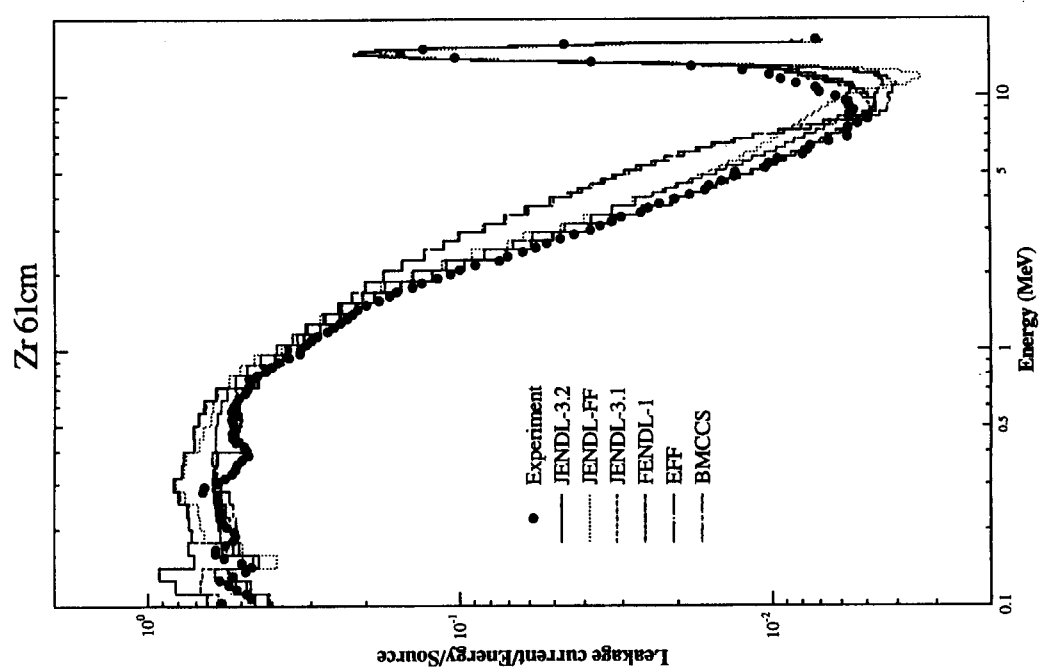


Fig. 5.3.13 Neutron spectra leaking from the spherical zirconium pile measured and calculated with various nuclear data files.

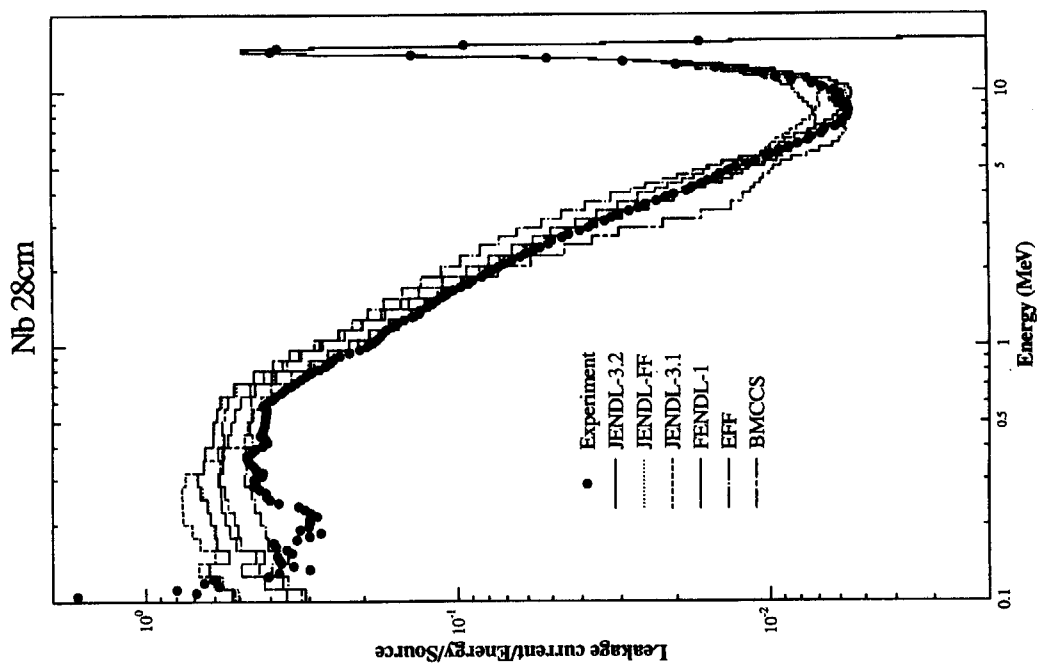


Fig. 5.3.14 Neutron spectra leaking from the spherical niobium pile measured and calculated with various nuclear data files.

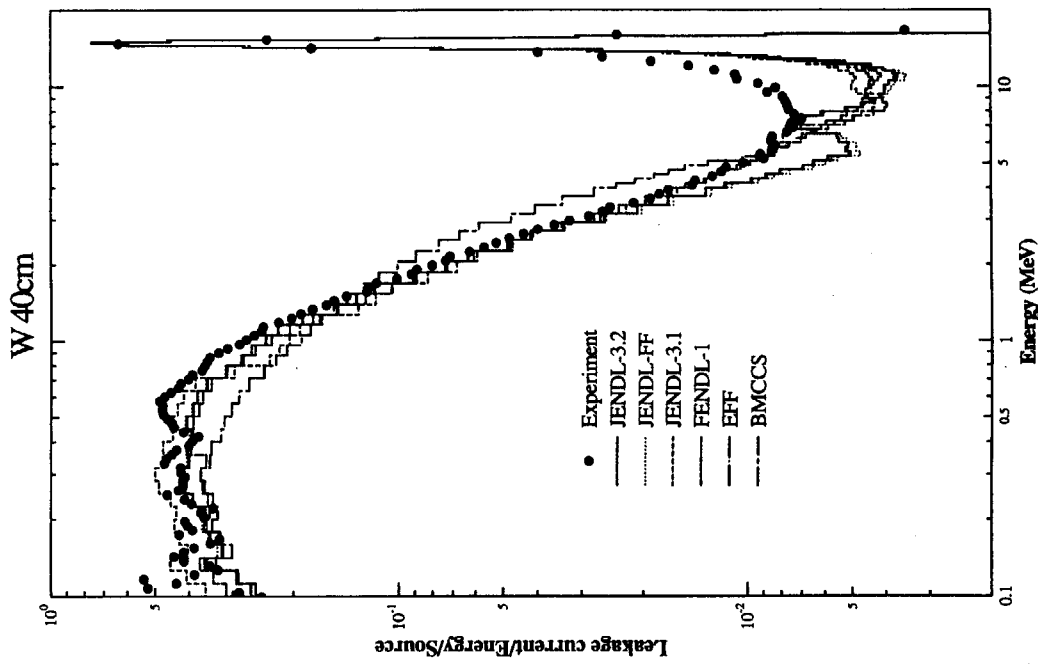


Fig. 5.3.15 Neutron spectra leaking from the spherical molybdenum pile measured and calculated with various nuclear data files.

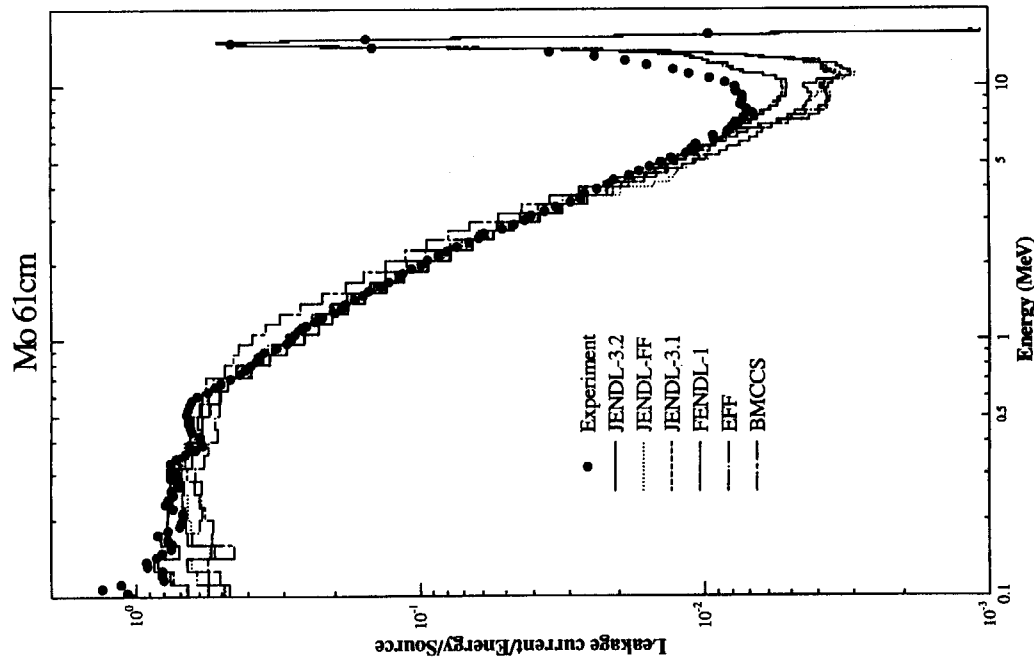


Fig. 5.3.16 Neutron spectra leaking from the spherical tungsten pile measured and calculated with various nuclear data files.

Neutron spectra leaking from the spherical tungsten pile measured and calculated with various nuclear data files.

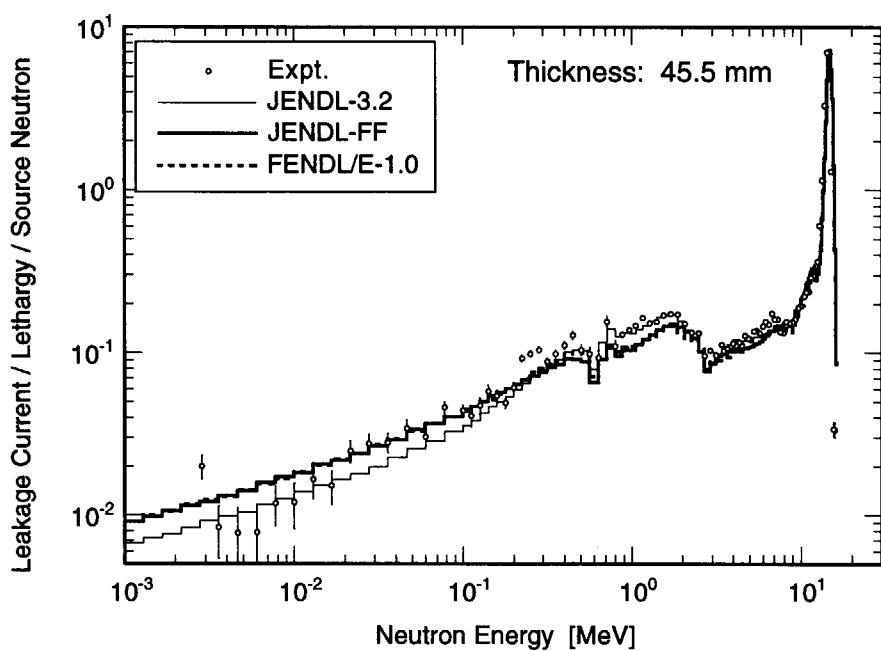


Fig. 5.3.17 Neutron spectra leaking from the spherical beryllium pile of 45.5 mm in thickness measured and calculated with various nuclear data files.

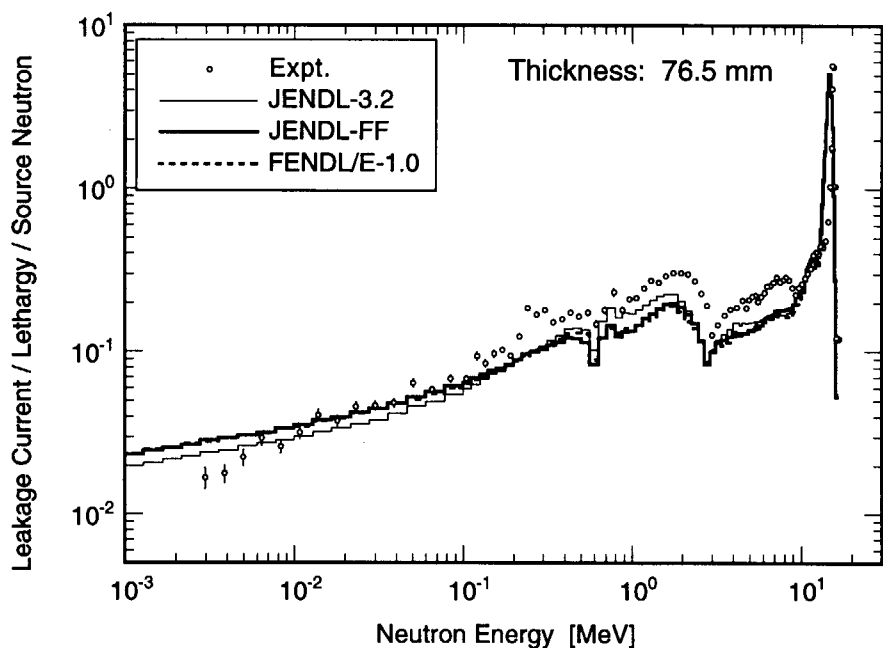


Fig. 5.3.18 Neutron spectra leaking from the spherical beryllium pile of 76.5 mm in thickness measured and calculated with various nuclear data files.

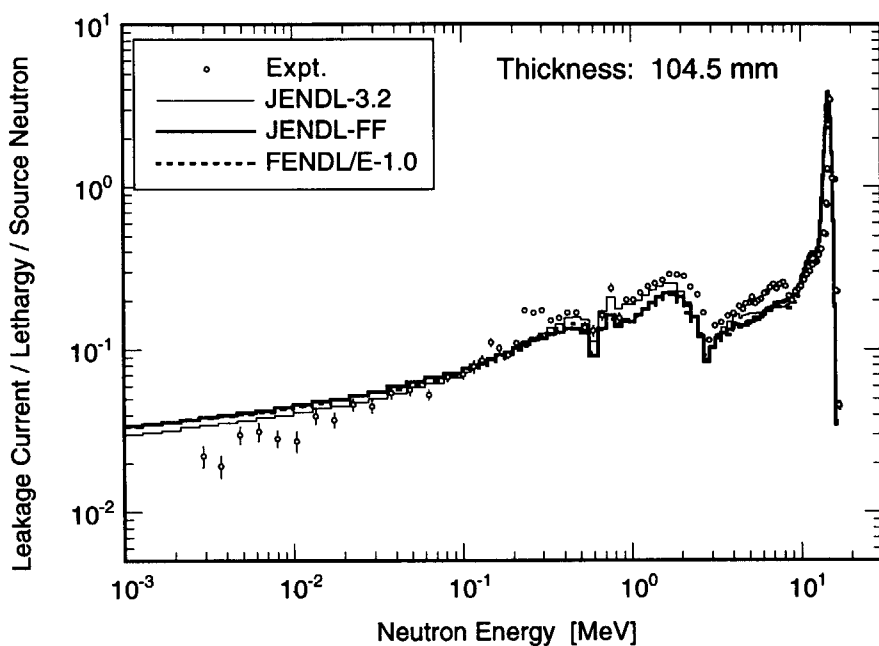


Fig. 5.3.19 Neutron spectra leaking from the spherical beryllium pile of 104.5 mm in thickness measured and calculated with various nuclear data files.

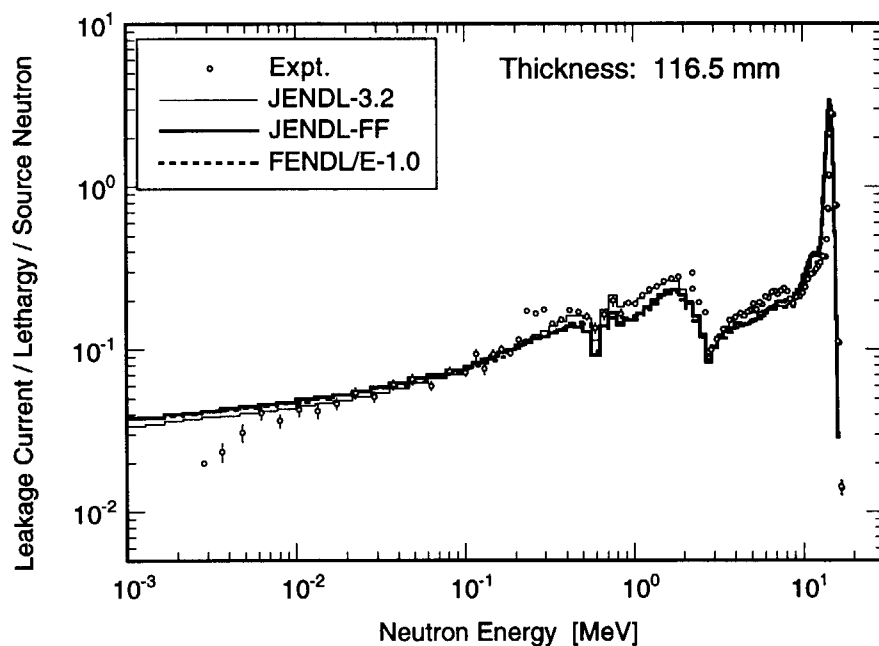


Fig. 5.3.20 Neutron spectra leaking from the spherical beryllium pile of 116.5 mm in thickness measured and calculated with various nuclear data files.

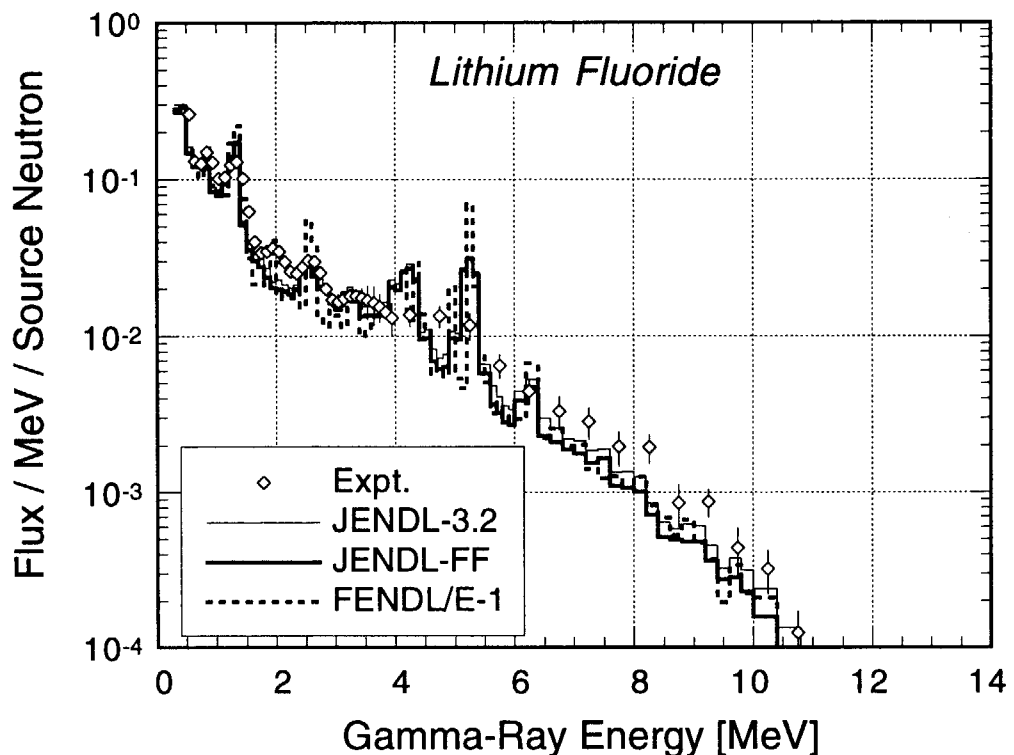


Fig. 5.4.1 Gamma-ray spectra leaking from the spherical lithium fluoride pile measured and calculated with JENDL-3.2, JENDL Fusion File and FENDL/E-1.0.

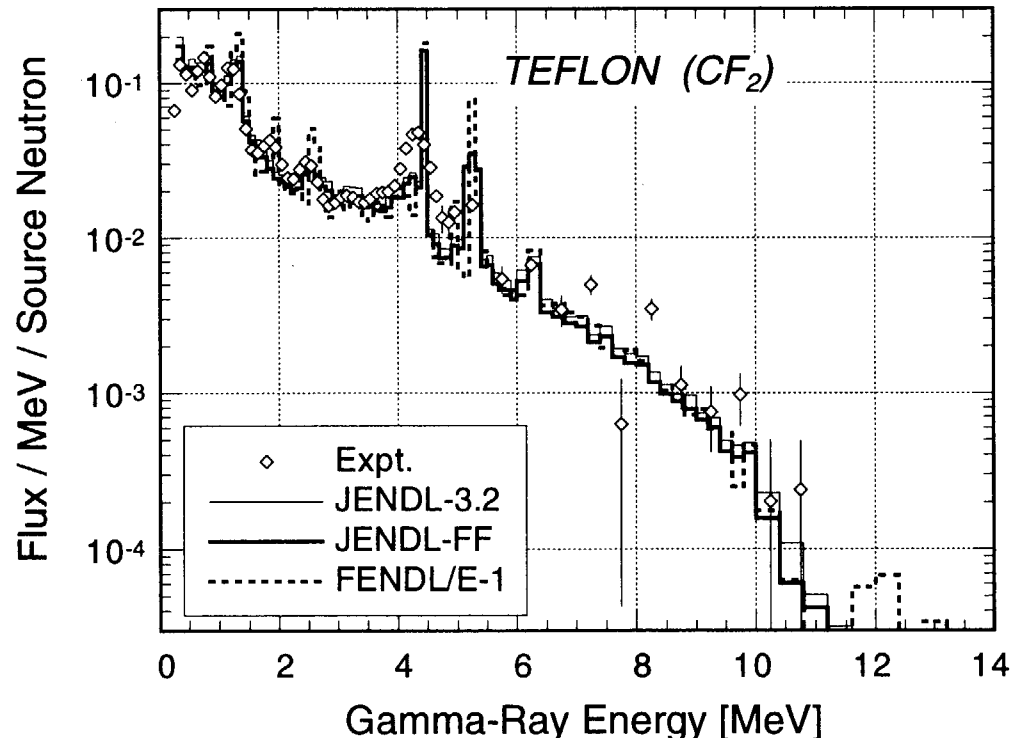


Fig. 5.4.2 Gamma-ray spectra leaking from the spherical Teflon ( $CF_2$ ) pile measured and calculated with JENDL-3.2, JENDL Fusion File and FENDL/E-1.0.

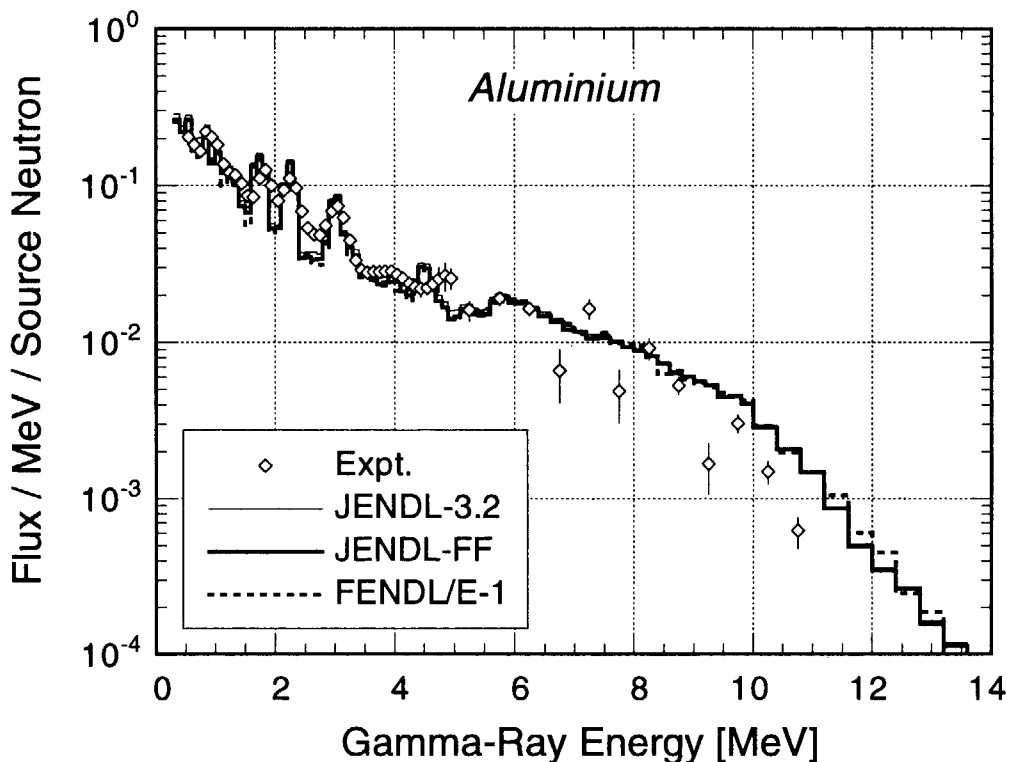


Fig. 5.4.3 Gamma-ray spectra leaking from the spherical aluminum pile measured and calculated with JENDL-3.2, JENDL Fusion File and FENDL/E-1.0.

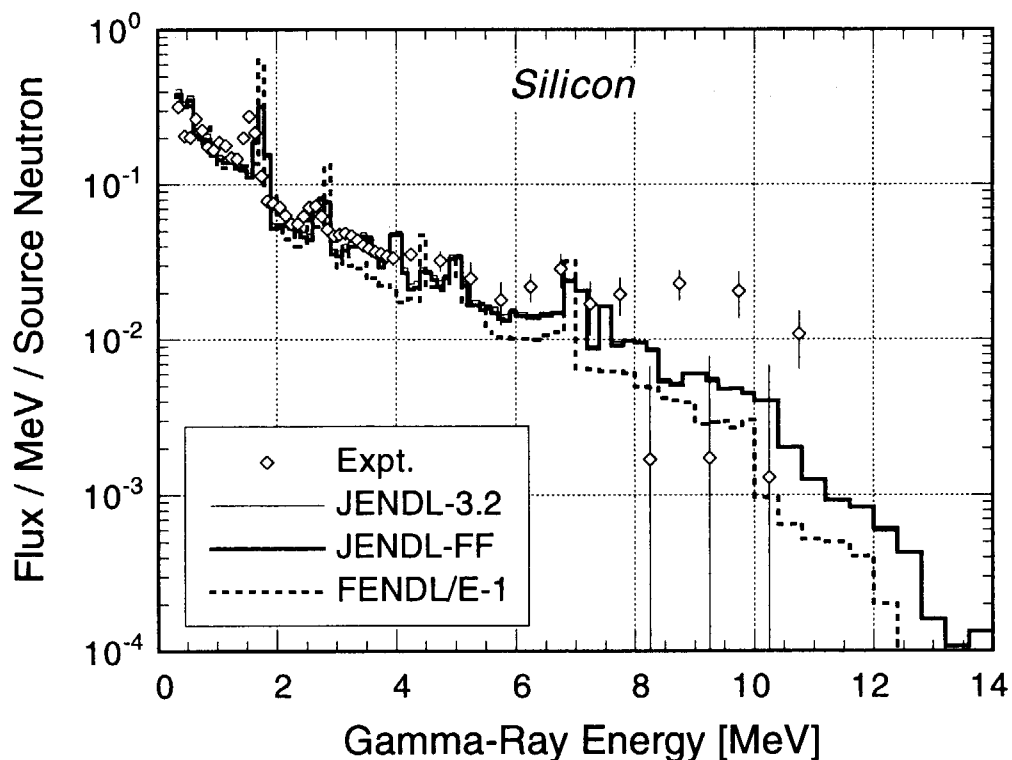


Fig. 5.4.4 Gamma-ray spectra leaking from the spherical silicon pile measured and calculated with JENDL-3.2, JENDL Fusion File and FENDL/E-1.0.

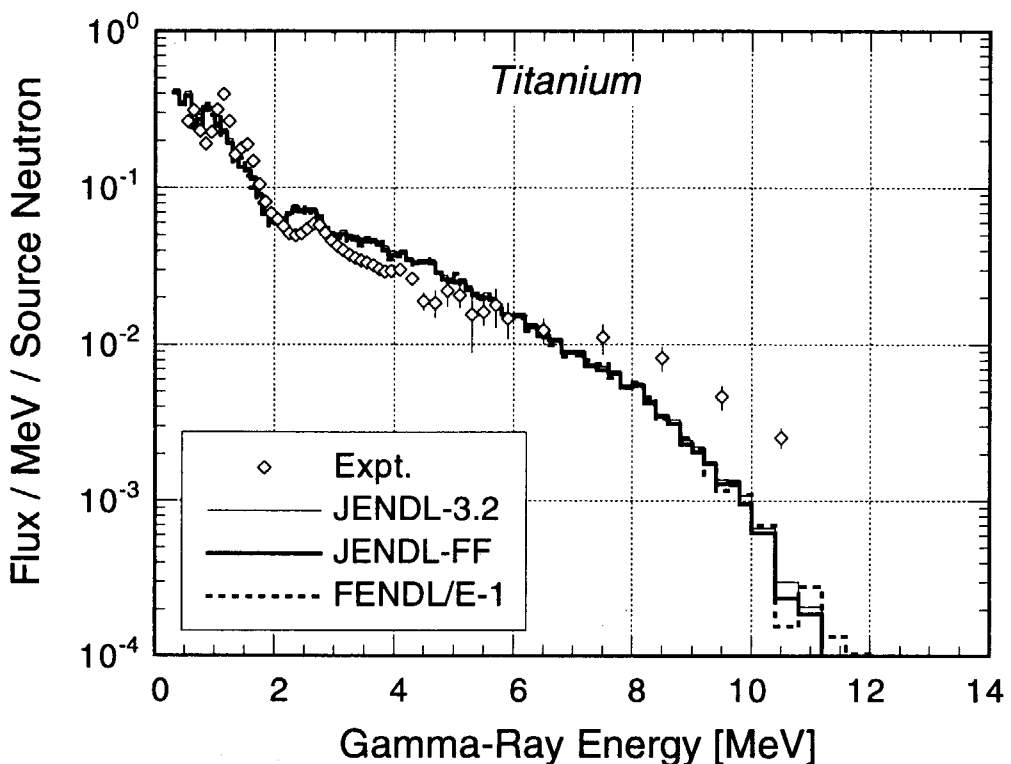


Fig. 5.4.5 Gamma-ray spectra leaking from the spherical titanium pile measured and calculated with JENDL-3.2, JENDL Fusion File and FENDL/E-1.0.

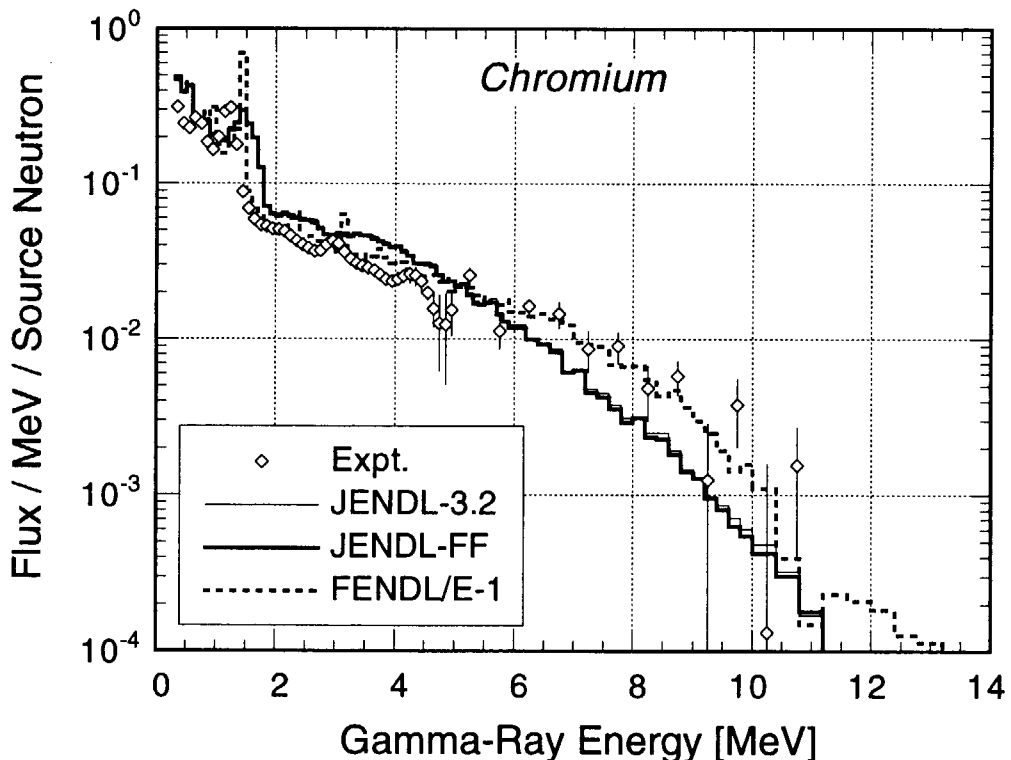


Fig. 5.4.6 Gamma-ray spectra leaking from the spherical chromium pile measured and calculated with JENDL-3.2, JENDL Fusion File and FENDL/E-1.0.

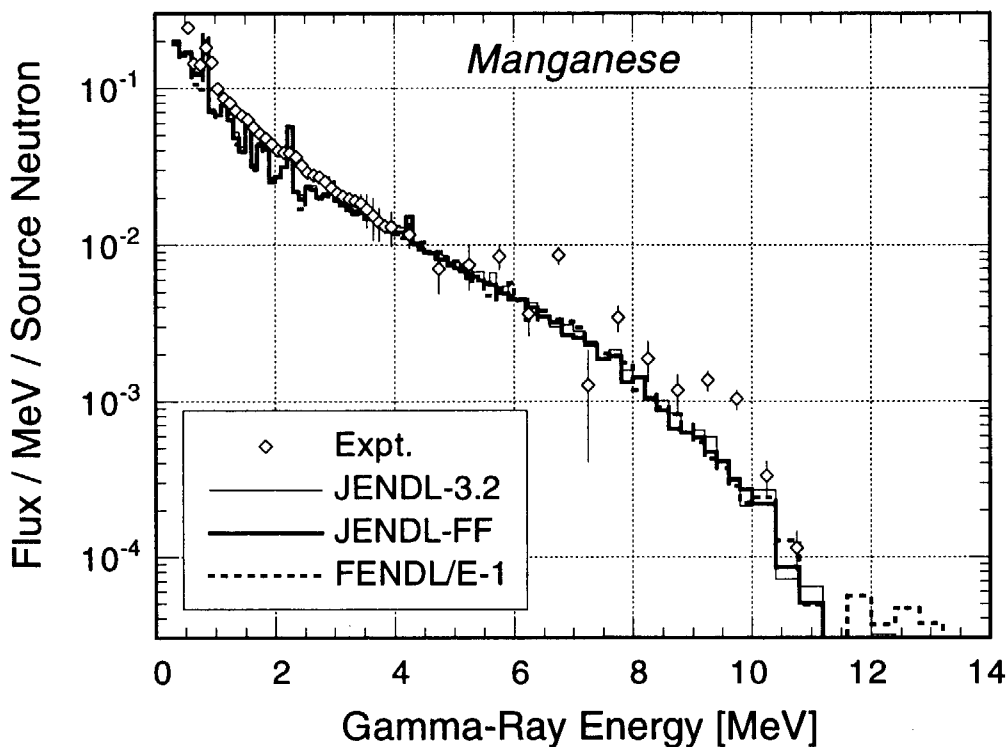


Fig. 5.4.7    Gamma-ray spectra leaking from the spherical manganese pile measured and calculated with JENDL-3.2, JENDL Fusion File and FENDL/E-1.0.

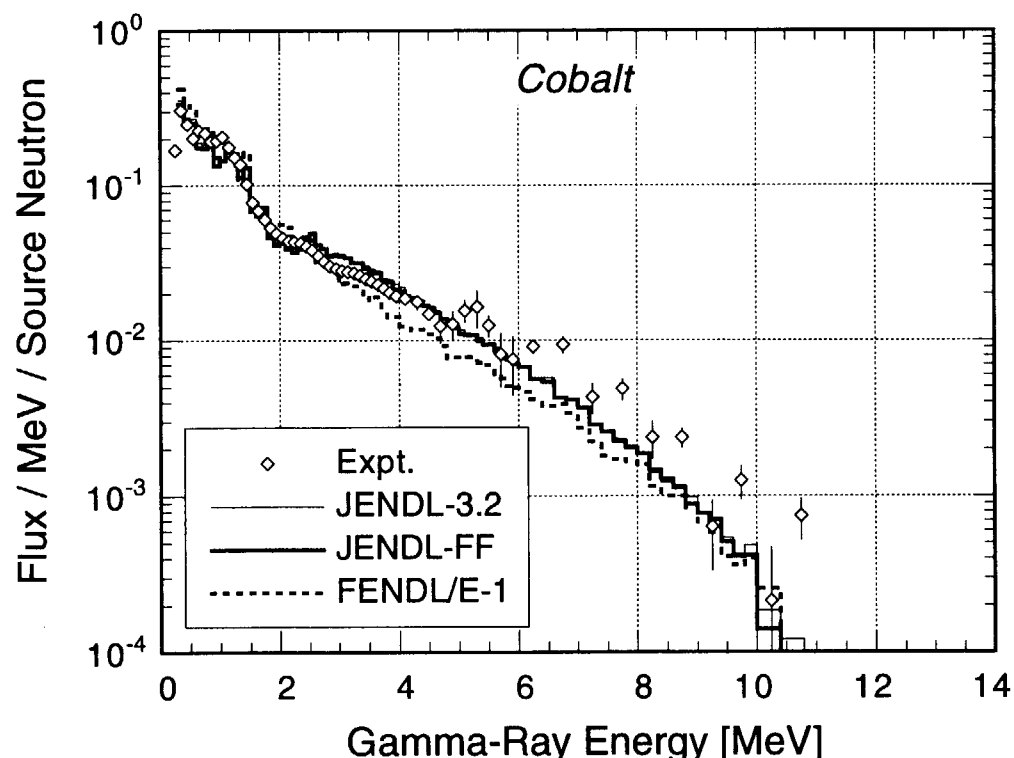


Fig. 5.4.8    Gamma-ray spectra leaking from the spherical cobalt pile measured and calculated with JENDL-3.2, JENDL Fusion File and FENDL/E-1.0.

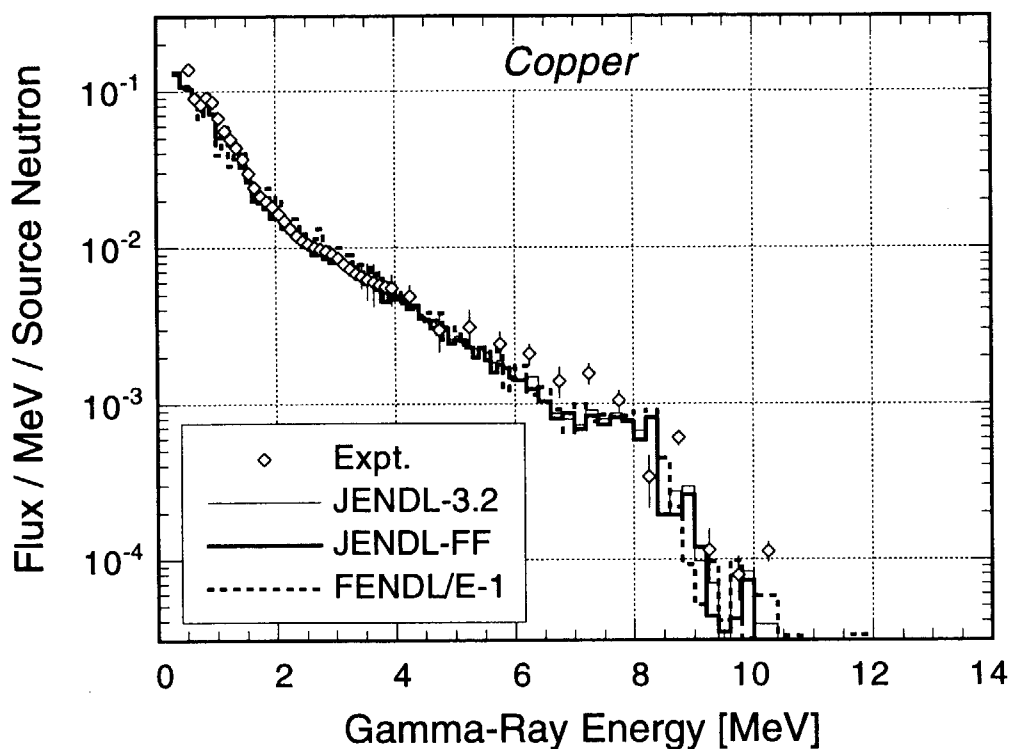


Fig. 5.4.9 Gamma-ray spectra leaking from the spherical copper pile measured and calculated with JENDL-3.2, JENDL Fusion File and FENDL/E-1.0.

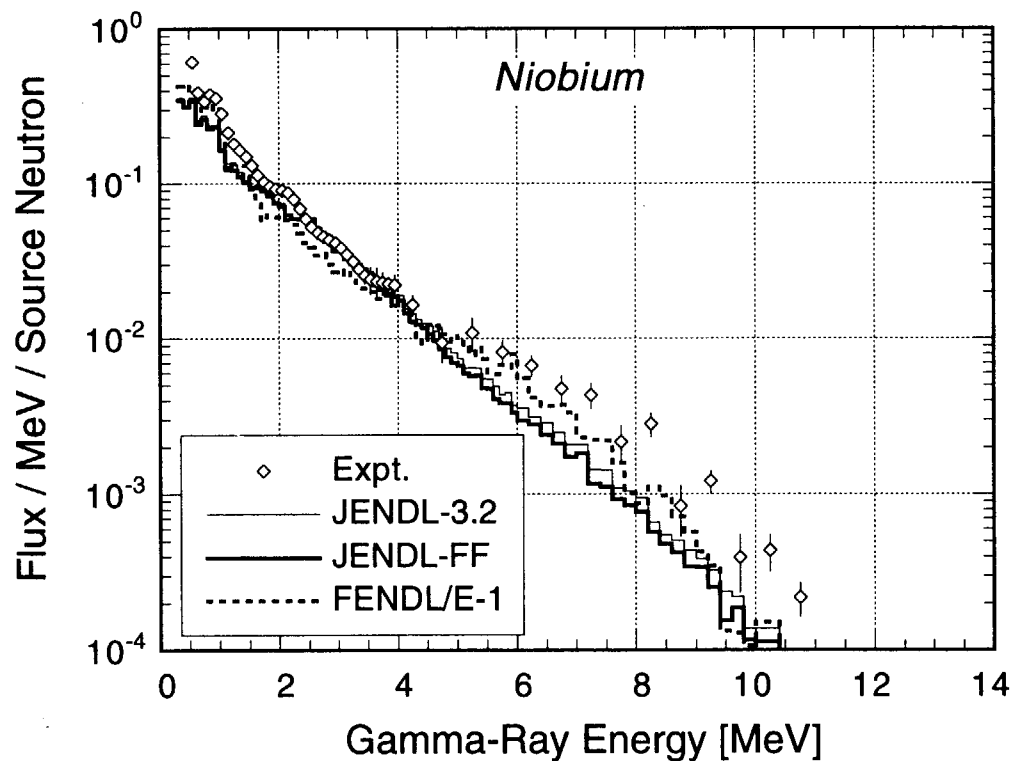


Fig. 5.4.10 Gamma-ray spectra leaking from the spherical niobium pile measured and calculated with JENDL-3.2, JENDL Fusion File and FENDL/E-1.0.

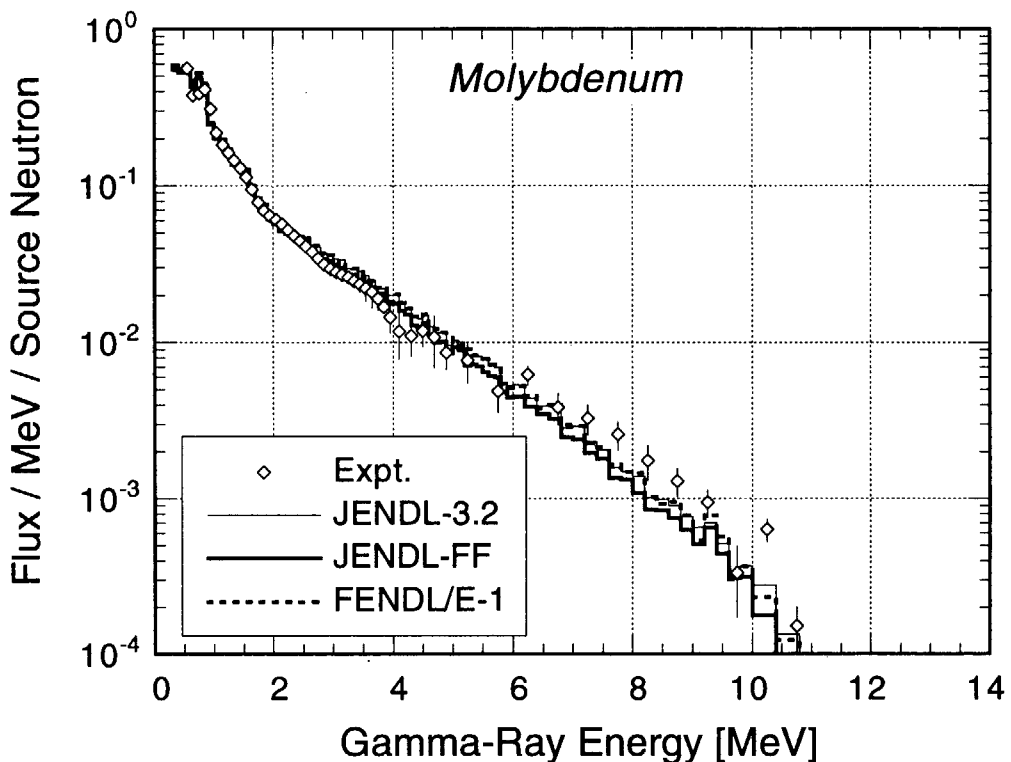


Fig. 5.4.11 Gamma-ray spectra leaking from the spherical molybdenum pile measured and calculated with JENDL-3.2, JENDL Fusion File and FENDL/E-1.0.

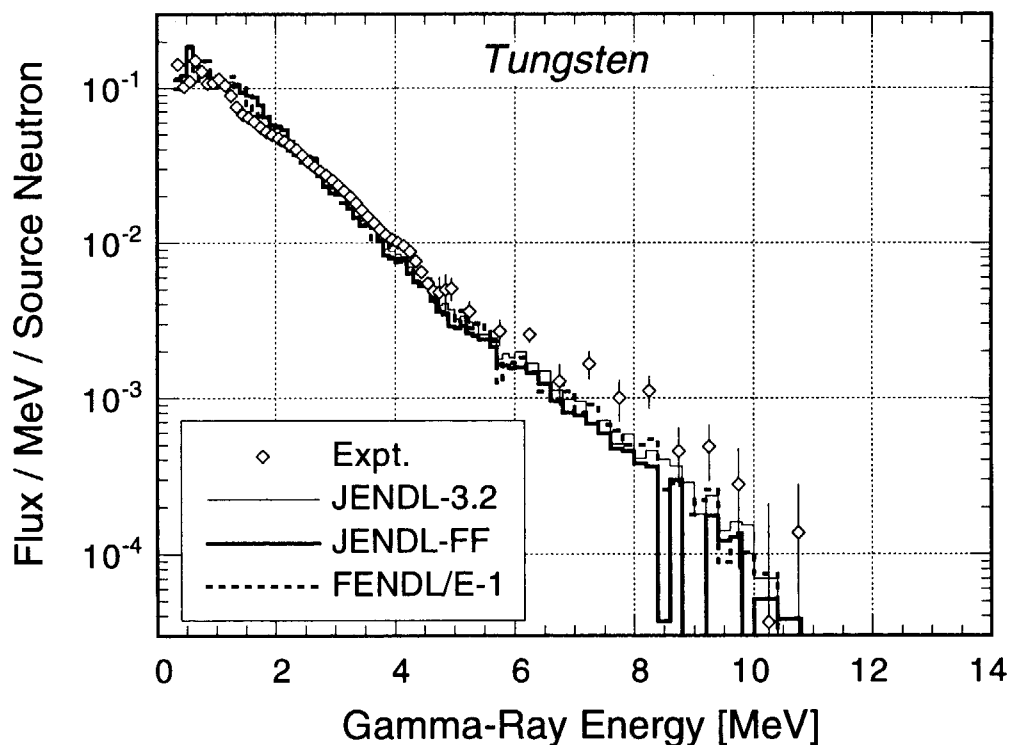


Fig. 5.4.12 Gamma-ray spectra leaking from the spherical tungsten pile measured and calculated with JENDL-3.2, JENDL Fusion File and FENDL/E-1.0.

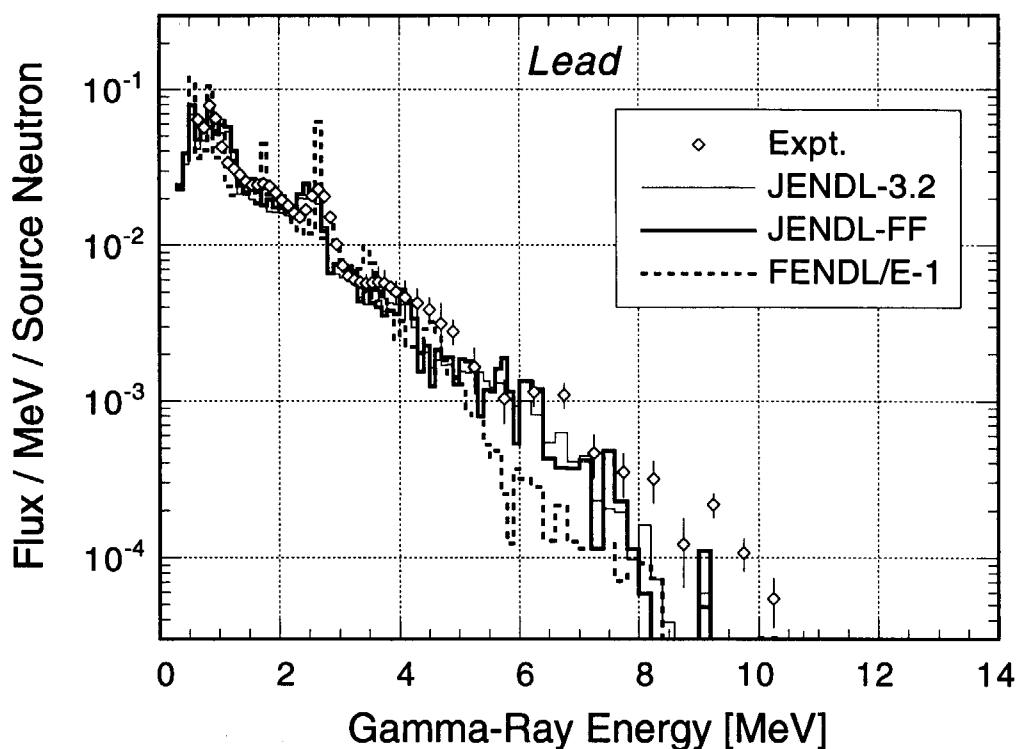


Fig. 5.4.13 Gamma-ray spectra leaking from the spherical lead pile measured and calculated with JENDL-3.2, JENDL Fusion File and FENDL/E-1.0.

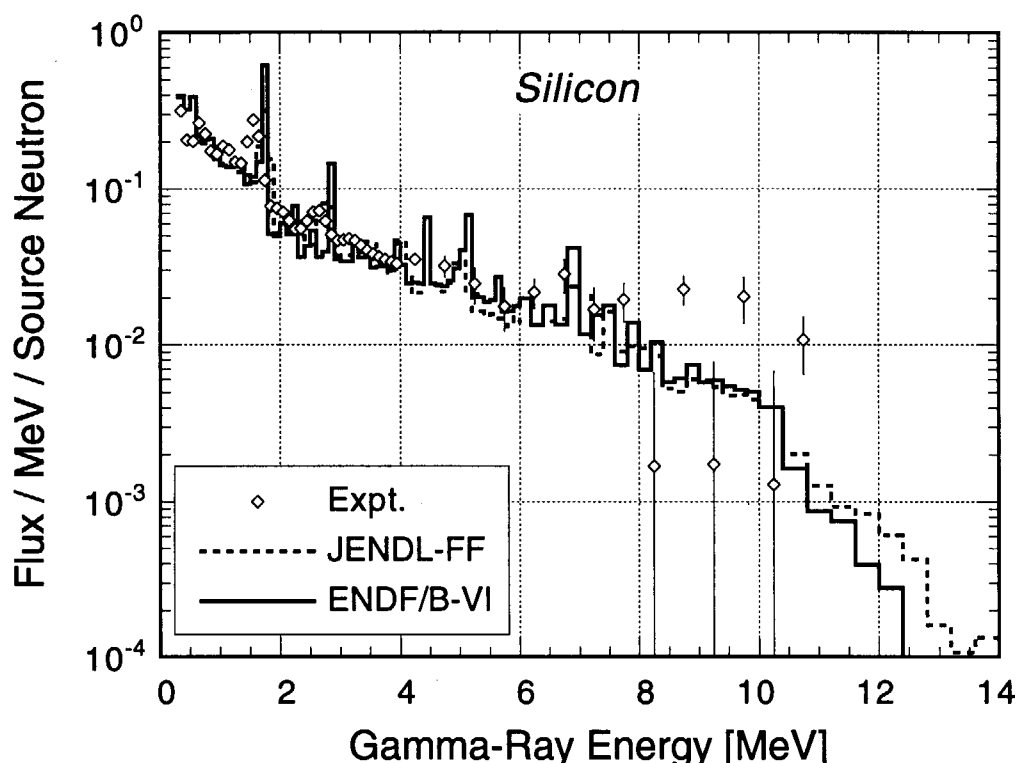


Fig. 5.4.14 Gamma-ray spectra leaking from the spherical silicon pile measured and calculated with ENDF/B-VI and JENDL Fusion File.

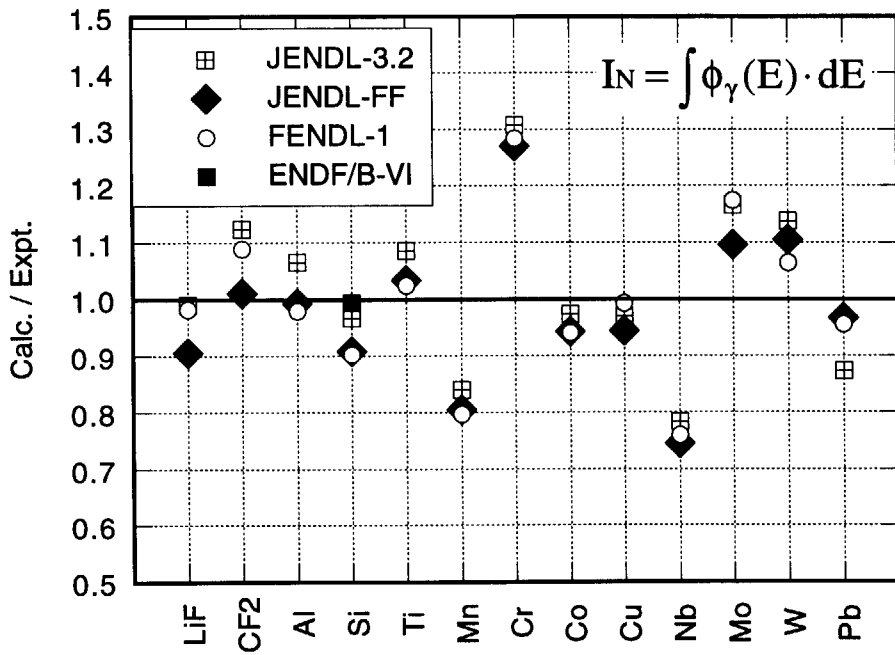


Fig. 5.4.15 Calculated to experimental ratios of the total number of gamma-rays ( $I_N$ ) for the thirteen materials for JENDL-3.2, JENDL Fusion File and FENDL/E-1.0.

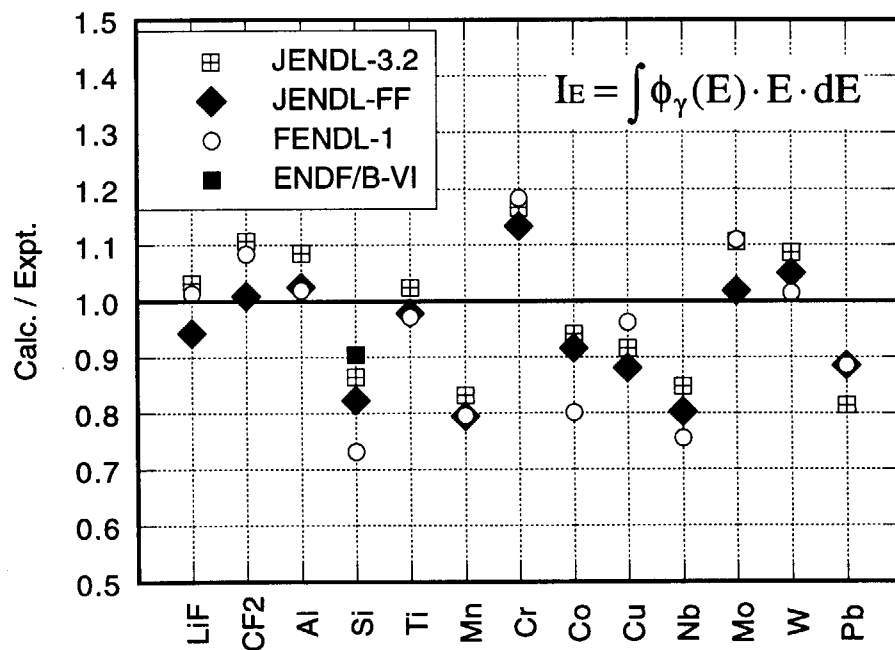


Fig. 5.4.16 Calculated to experimental ratios of the total gamma-ray energy ( $I_E$ ) for the thirteen materials for JENDL-3.2, JENDL Fusion File and FENDL/E-1.0.

## APPENDIX Input Data of MCNP

Some examples of input data for the MCNP-4A code used in the benchmark calculations are attached in the following figures.

### FNS TOF Experiment

Lithium Oxide	Fig. A-1
Beryllium	Fig. A-2
Graphite	Fig. A-3
Nitrogen	Fig. A-4
Oxygen	Fig. A-5
Iron	Fig. A-6
Lead	Fig. A-7

### FNS Clean Benchmark Experiment

Lithium oxide	Fig. A-8
Beryllium	Fig. A-9
Graphite	Fig. A-10
Iron	Fig. A-11
SS316	Fig. A-12
Copper	Fig. A-13
Tungsten	Fig. A-14

### OKTAVIAN Pulsed Sphere Experiment

Neutron spectrum	Fig. A-15
Secondary gamma-ray spectrum with D-T neutron source	Fig. A-16
Secondary gamma-ray spectrum with target gamma-ray source	Fig. A-17

```

fns-tof/31.4 cm(r)*4.80 cm(z)-li2o cyl./fixed cone JENDL-3.2
c   ****
c   * cell carad      *
c   ****
c   ***** external void *****
1    0      -4 : +4 -2 +3 : +10 : +2 -10 +5 +6 +7 +8 +9
c   ***** source vacuum region *****
2    0      -3 +4 -1
c   ***** material region *****
3    1     8.86823-2 -3 +1 -2
c   ***** detector vacuum region *****
4    0 +2 -10 -5 : +2 -10 -6 : +2 -10 -7 : +2 -10 -8 : +2 -10 -9
c   ----- the following is a blank delimiter

c   ****
c   * surface card      *
c   ****
1      pz      -4.80
2      pz      0
3      cz      31.4
4      pz      -50
5      cz      5.2283
6      1 cz      5.2332
7      2 cz      5.2451
8      3 cz      5.2716
9      4 cz      5.3304
10     so      1000
c   ----- the following is a blank delimiter

c   ****
c   * mode card      - neutron only      *
c   ****
mode n
c   ****
c   * transformation cards      *
c   * rotation about the y axis by theta*
c   ****
*tr1  0 0 0      12.2 90 102.2 90 0 90
      77.8 90 12.2 +1
*tr2  0 0 0      24.9 90 114.9 90 0 90
      65.1 90 24.9 +1
*tr3  0 0 0      41.8 90 131.8 90 0 90
      48.2 90 41.8 +1
*tr4  0 0 0      66.8 90 156.8 90 0 90
      23.2 90 66.8 +1
c   ****
c   * cell parameter cards      *
c   ****
imp:n 0 1 1 1
c   ****
c   * source specification cards      *
c   * src1=point isotropic option      *
c   * sdir dirc. biasing - height reduction considered*
c   * si(eng.) and sp(prob.) taken from betof source      *
c   * expt. data      *
c   ****
sdef erg=d1 pos=0 0 -24.80 vec=0 0 1 dir=d2 wgt=1.0
sb2 -31 4.0
si1 4.6308-02
      5.2474-02 5.9461-02 6.7378-02 7.6349-02 8.6515-02
      9.8035-02 1.1109-01 1.2588-01 1.4264-01 1.6163-01
      1.8315-01 2.0754-01 2.3517-01 2.6649-01 3.0197-01
      3.4217-01 3.8774-01 4.3936-01 4.9786-01 5.6415-01
      6.3927-01 7.2438-01 8.2084-01 9.3013-01 1.0540+00
      1.1943+00 1.3533+00 1.5335+00 1.7377+00 1.8498+00
      1.9691+00 2.0961+00 2.2313+00 2.3752+00 2.5284+00
      2.6914+00 2.8650+00 3.0498+00 3.2465+00 3.4559+00
      3.6787+00 3.9160+00 4.1686+00 4.4374+00 4.7236+00
      5.0282+00 5.3525+00 5.6978+00 6.0652+00 6.4564+00
      6.8728+00 7.3161+00 7.7879+00 8.2902+00 8.8249+00
      9.3940+00 9.9999+00 1.0157+01 1.0317+01 1.0480+01
      1.0645+01 1.0812+01 1.0983+01 1.1156+01 1.1331+01
      1.1510+01 1.1691+01 1.1875+01 1.2062+01 1.2252+01
      1.2445+01 1.2641+01 1.2840+01 1.3042+01 1.3248+01

```

**Fig. A-1** A typical example of input data of MCNP for the analysis of the FNS/TOF experiment on lithium oxide.

```

1.3456+01 1.3668+01 1.3883+01 1.4102+01 1.4324+01
1.4550+01 1.4779+01 1.5012+01 1.5248+01 1.5488+01
1.5732+01 1.5980+01 1.6231+01 1.6487+01
sp1 0
0 0 0 0 0
4.600-05 6.959-05 8.399-05 1.727-04 1.554-04
1.932-04 2.512-04 3.390-04 4.520-04 5.189-04
6.487-04 7.450-04 8.417-04 9.862-04 1.215-03
1.421-03 1.591-03 1.810-03 1.933-03 2.203-03
2.353-03 2.397-03 2.468-03 2.501-03 1.255-03
1.238-03 1.243-03 1.162-03 1.164-03 1.193-03
1.185-03 1.448-03 1.718-03 2.186-03 1.653-03
1.040-03 9.251-04 8.761-04 8.385-04 7.505-04
7.832-04 7.368-04 6.683-04 6.248-04 5.473-04
5.120-04 4.928-04 4.124-04 3.956-04 4.339-04
4.881-04 6.196-04 1.714-04 2.017-04 2.109-04
2.134-04 2.369-04 2.547-04 2.576-04 2.685-04
2.849-04 2.881-04 3.445-04 5.177-04 5.260-04
5.417-04 7.421-04 7.535-04 7.649-04 9.229-04
9.597-04 9.782-04 5.512-03 8.224-03 8.337-03
6.554-02 1.400-01 1.424-01 1.440-01 1.456-01
1.480-01 1.454-01 2.054-02 2.095-02
*****
c * material specification cards *
c -----
c ---- li2o/ss cover -----
m1 3006.37c 4.27817-3 3007.37c 5.33792-2 8016.37c 2.88287-2
26000.37c 1.55712-3 28000.37c 1.83687-4 24000.37c 4.22314-4
25055.37c 3.30907-5
c drxs
c -----
c * tally specification cards *
c -----
fc5 --- fluxes at 5 pt dts(th=0.0, 12.2, 24.9, 41.8, 66.8 deg)
f5:n 0.0 0 738.2000 1
      156.1056 0 722.017 1
      311.7349 0 671.5754 1
      496.03346 0 554.7832 1
      691.8332 0 296.5201 1
dd 0.5 100
e0 4.6308-02
      5.2474-02 5.9461-02 6.7378-02 7.6349-02 8.6515-02
      9.8035-02 1.1109-01 1.2588-01 1.4264-01 1.6163-01
      1.8315-01 2.0754-01 2.3517-01 2.6649-01 3.0197-01
      3.4217-01 3.8774-01 4.3936-01 4.9786-01 5.6415-01
      6.3927-01 7.2438-01 8.2084-01 9.3013-01 1.0540+00
      1.1943+00 1.3533+00 1.5335+00 1.7377+00 1.8498+00
      1.9691+00 2.0961+00 2.2313+00 2.3752+00 2.5284+00
      2.6914+00 2.8650+00 3.0498+00 3.2465+00 3.4559+00
      3.6787+00 3.9160+00 4.1686+00 4.4374+00 4.7236+00
      5.0282+00 5.3525+00 5.6978+00 6.0652+00 6.4564+00
      6.8728+00 7.3161+00 7.7879+00 8.2902+00 8.8249+00
      9.3940+00 9.9999+00 1.0157+01 1.0317+01 1.0480+01
      1.0645+01 1.0812+01 1.0983+01 1.1156+01 1.1331+01
      1.1510+01 1.1691+01 1.1875+01 1.2062+01 1.2252+01
      1.2445+01 1.2641+01 1.2840+01 1.3042+01 1.3248+01
      1.3456+01 1.3668+01 1.3883+01 1.4102+01 1.4324+01
      1.4550+01 1.4779+01 1.5012+01 1.5248+01 1.5488+01
      1.5732+01 1.5980+01 1.6231+01 1.6487+01
fq0 e f
c -----
c * problem cutoff cards *
c -----
cut:n 0 4.6308-02 -10 -0.01
nps 2000000
ctme 180
c -----
c * peripheral crads *
c -----
prdmp 1000000 1000000
lost 10 10
print

```

Fig. A-1 Continued (2/2).

```

fns-tof/31.4 cm(r)*5.06 cm(z)-be cyl./fixed cone bias/JENDL-3.2
c   ****
c   * cell carad      *
c   ****
c   ***** external void ****
1    0      -4 : +4 -2 +3 : +10 : +2 -10 +5 +6 +7 +8 +9
c   ***** source vacuum region ****
2    0      -3 +4 -1
c   ***** material region ****
3    1      1.215-1 -3 +1 -2
c   ***** detector vacuum region ****
4    0      +2 -10 -5 : +2 -10 -6 : +2 -10 -7 : +2 -10 -8 : +2 -10 -9
c   ----- the following is a blank delimiter

c   ****
c   * surface card      *
c   ****
1      pz      -5.06
2      pz      0
3      cz      31.4
4      pz      -50
5      cz      5.228
6      1 cz      5.235
7      2 cz      5.242
8      3 cz      5.270
9      4 cz      5.332
10     so      1000
c   ----- the following is a blank delimiter

c   ****
c   * mode card      - neutron only      *
c   ****
mode n
c   ****
c   * transformation cards      *
c   * rotation about the y axis by theta*
c   ****
*tr1  0 0 0      12.2 90 102.2 90 0 90
*tr2  0 0 0      77.8 90 12.2 +1
*tr2  0 0 0      24.9 90 114.9 90 0 90
*tr2  0 0 0      65.1 90 24.9 +1
*tr3  0 0 0      41.8 90 131.8 90 0 90
*tr3  0 0 0      48.2 90 41.8 +1
*tr4  0 0 0      66.8 90 156.8 90 0 90
*tr4  0 0 0      23.2 90 66.8 +1
c   ****
c   * cell parameter cards      *
c   ****
imp:n 0 1 1 1
c   ****
c   * source specification cards      *
c   * srcl=point isotropic option      *
c   * sdir dirc. biasing - height reduction considered*
c   * si(eng.) and sp(prob.) taken from betof source      *
c   * expt. data      *
c   ****
sdef erg=d1 pos=0 0 -25.06 vec=0 0 1 dir=d2 wgt=1.0
sb2 -31 4.0
sil 4.6308-02
5.2474-02 5.9461-02 6.7378-02 7.6349-02 8.6515-02
9.8035-02 1.1109-01 1.2588-01 1.4264-01 1.6163-01
1.8315-01 2.0754-01 2.3517-01 2.6649-01 3.0197-01
3.4217-01 3.8774-01 4.3936-01 4.9786-01 5.6415-01
6.3927-01 7.2438-01 8.2084-01 9.3013-01 1.0540+00
1.1943+00 1.3533+00 1.5335+00 1.7377+00 1.8498+00
1.9691+00 2.0961+00 2.2313+00 2.3752+00 2.5284+00
2.6914+00 2.8650+00 3.0498+00 3.2465+00 3.4559+00
3.6787+00 3.9160+00 4.1686+00 4.4374+00 4.7236+00
5.0282+00 5.3525+00 5.6978+00 6.0652+00 6.4564+00
6.8728+00 7.3161+00 7.7879+00 8.2902+00 8.8249+00
9.3940+00 9.9999+00 1.0157+01 1.0317+01 1.0480+01
1.0645+01 1.0812+01 1.0983+01 1.1156+01 1.1331+01
1.1510+01 1.1691+01 1.1875+01 1.2062+01 1.2252+01
1.2445+01 1.2641+01 1.2840+01 1.3042+01 1.3248+01

```

Fig. A-2 A typical example of input data of MCNP for the analysis of the FNS/TOF experiment on beryllium.

```

1.3456+01 1.3668+01 1.3883+01 1.4102+01 1.4324+01
1.4550+01 1.4779+01 1.5012+01 1.5248+01 1.5488+01
1.5732+01 1.5980+01 1.6231+01 1.6487+01
sp1 0
0 0 0 0 0
0 5.045-05 1.197-04 1.745-04 2.433-04
2.511-04 3.572-04 4.063-04 5.016-04 6.489-04
7.416-04 8.517-04 1.041-03 1.208-03 1.454-03
1.694-03 1.851-03 2.077-03 2.229-03 2.337-03
2.381-03 2.537-03 2.614-03 1.386-03 1.362-03
1.333-03 1.278-03 1.262-03 1.267-03 1.326-03
1.757-03 2.744-03 4.302-03 2.974-03 1.100-03
1.072-03 1.009-03 8.938-04 8.675-04 8.483-04
7.534-04 6.830-04 6.709-04 6.652-04 6.191-04
5.136-04 4.860-04 5.057-04 5.266-04 6.163-04
7.539-04 2.027-04 2.446-04 2.567-04 2.599-04
3.287-04 3.745-04 3.789-04 5.094-04 6.856-04
6.933-04 8.102-04 1.166-03 1.184-03 1.248-03
2.430-03 2.467-03 2.504-03 5.970-03 6.696-03
6.824-03 1.731-02 2.364-02 2.396-02 6.401-02
1.159-01 1.180-01 1.271-01 1.538-01 1.564-01
1.535-01 2.881-02 2.918-02 0
*****
c * material specification cards *
c -----
c ---- beryllium -----
m1 4009.37c 1.215-1
c drxs
c -----
c * tally specification cards *
c -----
fc5 --- fluxes at 5 pt dts(th=0.0, 12.2, 24.9, 41.8, 66.8 deg)
f5:n 0.0 0 738.0000 1
      156.16903 0 722.31035 1
      311.5665 0 671.21257 1
      495.90016 0 554.63414 1
      692.10891 0 296.63826 1
dd 0.5 100
e0 4.6308-02
5.2474-02 5.9461-02 6.7378-02 7.6349-02 8.6515-02
9.8035-02 1.1109-01 1.2588-01 1.4264-01 1.6163-01
1.8315-01 2.0754-01 2.3517-01 2.6649-01 3.0197-01
3.4217-01 3.8774-01 4.3936-01 4.9786-01 5.6415-01
6.3927-01 7.2438-01 8.2084-01 9.3013-01 1.0540+00
1.1943+00 1.3533+00 1.5335+00 1.7377+00 1.8498+00
1.9691+00 2.0961+00 2.2313+00 2.3752+00 2.5284+00
2.6914+00 2.8650+00 3.0498+00 3.2465+00 3.4559+00
3.6787+00 3.9160+00 4.1686+00 4.4374+00 4.7236+00
5.0282+00 5.3525+00 5.6978+00 6.0652+00 6.4564+00
6.8728+00 7.3161+00 7.7879+00 8.2902+00 8.8249+00
9.3940+00 9.9999+00 1.0157+01 1.0317+01 1.0480+01
1.0645+01 1.0812+01 1.0983+01 1.1156+01 1.1331+01
1.1510+01 1.1691+01 1.1875+01 1.2062+01 1.2252+01
1.2445+01 1.2641+01 1.2840+01 1.3042+01 1.3248+01
1.3456+01 1.3668+01 1.3883+01 1.4102+01 1.4324+01
1.4550+01 1.4779+01 1.5012+01 1.5248+01 1.5488+01
1.5732+01 1.5980+01 1.6231+01 1.6487+01
fq0 e f
*****
c * problem cutoff cards *
c -----
cut:n 0 4.6308-02 -10 -0.01
nps 2000000
ctme 180
*****
c * peripheral crads *
c -----
prdmp 1000000 1000000
lost 10 10
print

```

Fig. A-2 Continued (2/2).

```

fns-tof/31.4 cm(r)*5.06 cm(z)-c cyl./JENDL-3.2/5 pt detectors
c   **** cell carad   *
c   **** material region *****
c   ***** external void *****
1    0      -4 : +4 -2 +3 : +10 : +2 -10 +5 +6 +7 +8 +9
c   ***** source vacuum region *****
2    0      -3 +4 -1
c   ***** detector vacuum region *****
3    1     8.694-2 -3 +1 -2
4    0 +2 -10 -5 : +2 -10 -6 : +2 -10 -7 : +2 -10 -8 : +2 -10 -9
c   ----- the following is a blank delimiter

c   **** surface card *****
c   * mode card - neutron only *
c   ****
mode n ****
c   * transformation cards   *
c   * rotation about the y axis by theta*
c   ****
*tr1  0 0 0    12.2 90 102.2 90 0 90
      77.8 90 12.2 +1
*tr2  0 0 0    24.9 90 114.9 90 0 90
      65.1 90 24.9 +1
*tr3  0 0 0    41.8 90 131.8 90 0 90
      48.2 90 41.8 +1
*tr4  0 0 0    66.8 90 156.8 90 0 90
      23.2 90 66.8 +1
c   **** cell parameter cards ***
c   ****
imp:n 0 1 1 1 ****
c   * source specification cards   *
c   * src1=point isotropic option   *
c   * sdir dirc. biasing - height reduction considered*
c   * si(eng.) and sp(prob.) taken from betof source   *
c   * expt. data   *
c   ****
sdef erg=d1 pos=0 0 -25.06 vec=0 0 1 dir=d2 wgt=1.0
sb2 -31 4.0
sil 4.6308-02
      5.2474-02 5.9461-02 6.7378-02 7.6349-02 8.6515-02
      9.8035-02 1.1109-01 1.2588-01 1.4264-01 1.6163-01
      1.8315-01 2.0754-01 2.3517-01 2.6649-01 3.0197-01
      3.4217-01 3.8774-01 4.3936-01 4.9786-01 5.6415-01
      6.3927-01 7.2438-01 8.2084-01 9.3013-01 1.0540+00
      1.1943+00 1.3533+00 1.5335+00 1.7377+00 1.8498+00
      1.9691+00 2.0961+00 2.2313+00 2.3752+00 2.5284+00
      2.6914+00 2.8650+00 3.0498+00 3.2465+00 3.4559+00
      3.6787+00 3.9160+00 4.1686+00 4.4374+00 4.7236+00
      5.0282+00 5.3525+00 5.6978+00 6.0652+00 6.4564+00
      6.8728+00 7.3161+00 7.7879+00 8.2902+00 8.8249+00
      9.3940+00 9.9999+00 1.0157+01 1.0317+01 1.0480+01
      1.0645+01 1.0812+01 1.0983+01 1.1156+01 1.1331+01
      1.1510+01 1.1691+01 1.1875+01 1.2062+01 1.2252+01
      1.2445+01 1.2641+01 1.2840+01 1.3042+01 1.3248+01

```

**Fig. A-3** A typical example of input data of MCNP for the analysis of the FNS/TOF experiment on graphite.

```

1.3456+01 1.3668+01 1.3883+01 1.4102+01 1.4324+01
1.4550+01 1.4779+01 1.5012+01 1.5248+01 1.5488+01
1.5732+01 1.5980+01 1.6231+01 1.6487+01
sp1 0
0 0 0 0 0
0 0 0 0 0
0 0 0 0 0
0 0 0 2.1438-04 9.1563-04
1.5388-03 2.1627-03 2.5871-03 2.9698-03 3.3277-03
3.7304-03 3.9914-03 4.1831-03 4.3067-03 2.2786-03
2.1176-03 2.1039-03 2.0513-03 2.1117-03 2.0411-03
2.0591-03 2.1096-03 2.1281-03 2.4053-03 2.0935-03
1.8313-03 1.8008-03 1.7868-03 1.6668-03 1.6064-03
1.5991-03 1.6805-03 1.6701-03 1.5432-03 1.2904-03
1.2595-03 1.0310-03 9.2870-04 8.9403-04 8.8635-04
8.7646-04 9.5094-04 2.2846-04 2.2733-04 2.9803-04
3.5343-04 4.2411-04 4.5049-04 4.8501-04 5.7358-04
6.6128-04 7.2272-04 1.0292-03 1.1708-03 1.3518-03
1.5306-03 1.6062-03 1.6985-03 1.7860-03 1.8887-03
2.6840-03 4.0301-03 5.7679-03 1.2112-02 2.2014-02
5.0048-02 1.4342-01 1.9945-01 2.1655-01 1.6617-01
9.8846-02 2.5913-02 9.2423-03 1.2696-03
*****
c * material specification cards *
c ****
c ----- carbon -----
m1 6012.37c 8.694-2
c drxs
c ****
c * tally specification cards *
c ****
fc5 --- fluxes at 5 pt dts(th=0.0, 12.2, 24.9, 41.8, 66.8 deg)
f5:n 0.0 0 738.0000 1
      156.16903 0 722.31035 1
      311.5665 0 671.21257 1
      495.90016 0 554.63414 1
      692.10891 0 296.63826 1
dd 0.5 100
e0 4.6308-02
      5.2474-02 5.9461-02 6.7378-02 7.6349-02 8.6515-02
      9.8035-02 1.1109-01 1.2588-01 1.4264-01 1.6163-01
      1.8315-01 2.0754-01 2.3517-01 2.6649-01 3.0197-01
      3.4217-01 3.8774-01 4.3936-01 4.9786-01 5.6415-01
      6.3927-01 7.2438-01 8.2084-01 9.3013-01 1.0540+00
      1.1943+00 1.3533+00 1.5335+00 1.7377+00 1.8498+00
      1.9691+00 2.0961+00 2.2313+00 2.3752+00 2.5284+00
      2.6914+00 2.8650+00 3.0498+00 3.2465+00 3.4559+00
      3.6787+00 3.9160+00 4.1686+00 4.4374+00 4.7236+00
      5.0282+00 5.3525+00 5.6978+00 6.0652+00 6.4564+00
      6.8728+00 7.3161+00 7.7879+00 8.2902+00 8.8249+00
      9.3940+00 9.9999+00 1.0157+01 1.0317+01 1.0480+01
      1.0645+01 1.0812+01 1.0983+01 1.1156+01 1.1331+01
      1.1510+01 1.1691+01 1.1875+01 1.2062+01 1.2252+01
      1.2445+01 1.2641+01 1.2840+01 1.3042+01 1.3248+01
      1.3456+01 1.3668+01 1.3883+01 1.4102+01 1.4324+01
      1.4550+01 1.4779+01 1.5012+01 1.5248+01 1.5488+01
      1.5732+01 1.5980+01 1.6231+01 1.6487+01
fq0 e f
c ****
c * problem cutoff cards *
c ****
cut:n 0 4.6308-02 -10 -0.01
nps 3000000
ctme 180
c ****
c * peripheral crads *
c ****
prdmp 1000000 1000000
lost 10 10
print

```

Fig. A-3 Continued (2/2).

```

fns-tof/ n2 slab-tof          JENDL-3.2      '94-08-18
c   ****
c   *           cell carad      *
c   ****
c   ***** external void *****
1   0       -13 : +13 -2 +14 : +34 : +2 -34 +29 +30 +31 +32 +33
2   0       -21 -2 -19
c   ***** source vacuum region *****
3   1 4.9210-5    -14 +13 -1 : -27 +1 -20
c   ***** material region *****
c   ----sus316
4   2 8.5979-2    +1 -3 -14 +20 : +4 -2 -14 +19 : +3 -4 -14 +15
5   2 8.5979-2    +27 -28 -20    : +21 -22 -19
6   2 8.5979-2    +9 -11 -17 +20 : +12 -10 -17 +20 : +11 -12 -17 +18
7   2 8.5979-2    +25 -26 -20    : +23 -24 -20
c   ---- vacuum
8   0       +3 -5 -15 +20 : +6 -4 -15 +19 : +5 -6 -15 +16
9   0       +28 -5 -20    : +22 +6 -19
10  0       +7 -9 -17 +20 : +10 -8 -17 +20
11  0       +26 +7 -20    : +24 -8 -20
c   ---- al
12  3 3.6244-3    +5 -7 -16    : +8 -6 -16    : +7 -8 -16 +17
c   ---- n
13  4 3.4756-2    +11 -12 -18    : -25 -11 -20    : -23 +12 -20
c   ***** detector vacuum region *****
14  0 +2 -34 -29 : +2 -34 -30 : +2 -34 -31 : +2 -34 -32 : +2 -34
     -33
c   ----- the following is a blank delimiter
c   ****
c   * surface card             *
c   ****
1   pz      -28.0
2   pz      0.0
3   pz      -27.5
4   pz      -0.5
5   pz      -25.90
6   pz      -2.10
7   pz      -25.20
8   pz      -2.80
9   pz      -24.80
10  pz      -3.20
11  pz      -24.0
12  pz      -4.0
13  pz      -70.0
c   -----
14  cz      35.0
15  cz      34.7
16  cz      30.8
17  cz      30.0
18  cz      29.8
19  cz      23.25
20  cz      15.0
c   ----- test
21  sz      134.146 136.146
22  sz      134.096 136.146
23  sz      -105.7227 102.8227
24  sz      -105.6727 102.8227
25  sz      77.7227 102.8227
26  sz      77.6727 102.8227
27  sz      -129.7227 102.8227
28  sz      -129.6727 102.8227
c   21      pz      -0.05
c   22      pz      -0.10
c   23      sz      -105.7227 102.8227
c   24      sz      -105.6727 102.8227
c   25      pz      -24.05
c   26      pz      -24.10
c   27      sz      -129.7227 102.8227
c   28      sz      -129.6727 102.8227
c   -----
29      cz      4.977
30      1 cz     4.985
31      2 cz     5.012

```

Fig. A-4 A typical example of input data of MCNP for the analysis of the FNS/TOF experiment on liquid nitrogen.

```

32      3 cz      5.074
33      4 cz      5.212
34      so      1000.0
c ----- the following is a blank delimiter
c ****
c * mode card      - neutron only *
c ****
mode n
c ****
c * transformation cards   *
c * rotation about the y axis by theta*
c ****
*tr1  0 0 0    12.2 90 102.2 90 0 90
      77.8 90 12.2 +1
*tr2  0 0 0    24.9 90 114.9 90 0 90
      65.1 90 24.9 +1
*tr3  0 0 0    41.8 90 131.8 90 0 90
      48.2 90 41.8 +1
*tr4  0 0 0    66.8 90 156.8 90 0 90
      23.2 90 66.8 +1
c ****
c * cell parameter cards   *
c ****
imp:n 0 1 1 1 1 1 1
      1 1 1 1 1 1 1
c ****
c * source specification cards   *
c * srcl=point isotropic option   *
c * sdir dirc. biasing - height reduction considered*
c * si(eng.) and sp(prob.) taken from betof source   *
c * expt. data   *
c ****
sdef erg=d1 pos=0 0 -44.0 vec=0 0 1 dir=d2 wgt=1.0
sb2 -31 4.0
sil 4.6308-02
      5.2474-02 5.9461-02 6.7378-02 7.6349-02 8.6515-02
      9.8035-02 1.1109-01 1.2588-01 1.4264-01 1.6163-01
      1.8315-01 2.0754-01 2.3517-01 2.6649-01 3.0197-01
      3.4217-01 3.8774-01 4.3936-01 4.9786-01 5.6415-01
      6.3927-01 7.2438-01 8.2084-01 9.3013-01 1.0540+00
      1.1943+00 1.3533+00 1.5335+00 1.7377+00 1.8498+00
      1.9691+00 2.0961+00 2.2313+00 2.3752+00 2.5284+00
      2.6914+00 2.8650+00 3.0498+00 3.2465+00 3.4559+00
      3.6787+00 3.9160+00 4.1686+00 4.4374+00 4.7236+00
      5.0282+00 5.3525+00 5.6978+00 6.0652+00 6.4564+00
      6.8728+00 7.3161+00 7.7879+00 8.2902+00 8.8249+00
      9.3940+00 9.9999+00 1.0157+01 1.0317+01 1.0480+01
      1.0645+01 1.0812+01 1.0983+01 1.1156+01 1.1331+01
      1.1510+01 1.1691+01 1.1875+01 1.2062+01 1.2252+01
      1.2445+01 1.2641+01 1.2840+01 1.3042+01 1.3248+01
      1.3456+01 1.3668+01 1.3883+01 1.4102+01 1.4324+01
      1.4550+01 1.4779+01 1.5012+01 1.5248+01 1.5488+01
      1.5732+01 1.5980+01 1.6231+01 1.6487+01
sp1 0
      0 0 2.672-05 3.767-05 9.514-05
      1.678-04 1.993-04 2.518-04 2.852-04 3.690-04
      4.198-04 5.345-04 5.945-04 7.769-04 8.991-04
      1.156-03 1.328-03 1.535-03 1.828-03 2.088-03
      2.322-03 2.639-03 2.993-03 3.203-03 3.468-03
      3.648-03 3.690-03 3.809-03 2.043-03 1.989-03
      1.975-03 2.005-03 2.033-03 1.963-03 1.941-03
      1.903-03 1.920-03 2.033-03 1.874-03 1.704-03
      1.566-03 1.512-03 1.459-03 1.408-03 1.349-03
      1.259-03 1.188-03 1.081-03 9.973-04 9.967-04
      9.677-04 8.889-04 9.173-04 9.538-04 1.065-03
      1.198-03 3.088-04 3.905-04 4.130-04 4.180-04
      5.663-04 6.626-04 6.703-04 9.582-04 1.346-03
      1.361-03 1.646-03 2.523-03 2.564-03 2.656-03
      4.027-03 4.089-03 4.151-03 6.593-03 7.119-03
      7.256-03 1.892-02 2.595-02 2.631-02 9.472-02
      1.836-01 1.868-01 1.653-01 9.107-02 9.259-02
      9.046-02 7.991-04 8.150-04 0
c ****
c * material specification cards   *
c ****

```

Fig. A-4 Continued (2/3).

```

c      ----- iron (fe) -----
c      --- air
m1    7014.37c 3.8810-5      8016.37c 1.0400-5
c      --- sus316
m2    24000.37c 1.6787-2      25055.37c 1.3420-3
                26000.37c 6.0507-2      28000.37c 7.3429-3
c      --- al
m3    13027.37c 3.6244-3
c      --- n
m4    7014.37c 3.4756-2
c      drxs
c      ****
c      * tally specification cards
c      ****
fc5  --//fluxes at 5 pt dts(th=0.0, 12.2, 24.9, 41.8, 66.8 deg)
f5:n   0.0      0    703.0000      1
        148.7973     0    688.2148      1
        298.0163     0    642.0212      1
        477.4981     0    534.0526      1
        676.2307     0    289.8328      1
dd    0.5      100
e0    4.6308-02
      5.2474-02  5.9461-02  6.7378-02  7.6349-02  8.6515-02
      9.8035-02  1.1109-01  1.2588-01  1.4264-01  1.6163-01
      1.8315-01  2.0754-01  2.3517-01  2.6649-01  3.0197-01
      3.4217-01  3.8774-01  4.3936-01  4.9786-01  5.6415-01
      6.3927-01  7.2438-01  8.2084-01  9.3013-01  1.0540+00
      1.1943+00  1.3533+00  1.5335+00  1.7377+00  1.8498+00
      1.9691+00  2.0961+00  2.2313+00  2.3752+00  2.5284+00
      2.6914+00  2.8650+00  3.0498+00  3.2465+00  3.4559+00
      3.6787+00  3.9160+00  4.1686+00  4.4374+00  4.7236+00
      5.0282+00  5.3525+00  5.6978+00  6.0652+00  6.4564+00
      6.8728+00  7.3161+00  7.7879+00  8.2902+00  8.8249+00
      9.3940+00  9.9999+00  1.0157+01  1.0317+01  1.0480+01
      1.0645+01  1.0812+01  1.0983+01  1.1156+01  1.1331+01
      1.1510+01  1.1691+01  1.1875+01  1.2062+01  1.2252+01
      1.2445+01  1.2641+01  1.2840+01  1.3042+01  1.3248+01
      1.3456+01  1.3668+01  1.3883+01  1.4102+01  1.4324+01
      1.4550+01  1.4779+01  1.5012+01  1.5248+01  1.5488+01
      1.5732+01  1.5980+01  1.6231+01  1.6487+01
fq0    e      f
c      ****
c      * problem cutoff cards
c      ****
cut:n   0      4.0000-02  -10    -0.01
nps    2000000
ctme   180
c      ****
c      * peripheral crads
c      ****
prdmmp 1000000  1000000
lost    10      10
print

```

Fig. A-4 Continued (3/3).

```

fns-tof/ lo2 slab-tof                               JENDL-3.2          '94-08-18
c   ****
c   *           cell carad                         *
c   ****
c   **** external void ****
1    0      -13 : +13 -2 +14 : +34 : +2 -34 +29 +30 +31 +32 +33
2    0      -21 -2 -19
c   **** source vacuum region ****
3    1 4.9210-5      -14 +13 -1 : -27 +1 -20
c   **** material region ****
c   ----sus316
4    2 8.5979-2      +1 -3 -14 +20 : +4 -2 -14 +19 : +3 -4 -14 +15
5    2 8.5979-2      +27 -28 -20 : +21 -22 -19
6    2 8.5979-2      +9 -11 -17 +20 : +12 -10 -17 +20 : +11 -12 -17 +18
7    2 8.5979-2      +25 -26 -20 : +23 -24 -20
c   ---- vacuum
8    0      +3 -5 -15 +20 : +6 -4 -15 +19 : +5 -6 -15 +16
9    0      +28 -5 -20 : +22 +6 -19
10   0      +7 -9 -17 +20 : +10 -8 -17 +20
11   0      +26 +7 -20 : +24 -8 -20
c   ---- al
12   3 3.6244-3      +5 -7 -16 : +8 -6 -16 : +7 -8 -16 +17
c   ---- o
13   4 4.2947-2      +11 -12 -18 : -25 -11 -20 : -23 +12 -20
c   **** detector vacuum region ****
14   0      +2 -34 -29 : +2 -34 -30 : +2 -34 -31 : +2 -34 -32 : +2 -34
      -33
c   ----- the following is a blank delimiter
c   ****
c   * surface card                                *
c   ****
1    pz      -28.0
2    pz      0.0
3    pz      -27.5
4    pz      -0.5
5    pz      -25.90
6    pz      -2.10
7    pz      -25.20
8    pz      -2.80
9    pz      -24.80
10   pz      -3.20
11   pz      -24.0
12   pz      -4.0
13   pz      -70.0
c   -----
14   cz      35.0
15   cz      34.7
16   cz      30.8
17   cz      30.0
18   cz      29.8
19   cz      23.25
20   cz      15.0
c   ----- test
21   sz      134.146 136.146
22   sz      134.096 136.146
23   sz      -105.7227 102.8227
24   sz      -105.6727 102.8227
25   sz      77.7227 102.8227
26   sz      77.6727 102.8227
27   sz      -129.7227 102.8227
28   sz      -129.6727 102.8227
c   21      pz      -0.05
c   22      pz      -0.10
c   23      sz      -105.7227 102.8227
c   24      sz      -105.6727 102.8227
c   25      pz      -24.05
c   26      pz      -24.10
c   27      sz      -129.7227 102.8227
c   28      sz      -129.6727 102.8227
c   -----
29   cz      4.977
30   1 cz    4.985
31   2 cz    5.012

```

Fig. A-5      A typical example of input data of MCNP for the analysis of the FNS/TOF experiment on liquid oxygen.

```

32      3 cz      5.074
33      4 cz      5.212
34      so      1000.0
c      ----- the following is a blank delimiter
c      ****
c      * mode card - neutron only *
c      ****
mode n
c      ****
c      * transformation cards
c      * rotation about the y axis by theta*
c      ****
*tr1  0 0 0    12.2 90 102.2 90 0 90
    77.8 90 12.2 +1
*tr2  0 0 0    24.9 90 114.9 90 0 90
    65.1 90 24.9 +1
*tr3  0 0 0    41.8 90 131.8 90 0 90
    48.2 90 41.8 +1
*tr4  0 0 0    66.8 90 156.8 90 0 90
    23.2 90 66.8 +1
c      ****
c      * cell parameter cards
c      ****
imp:n  0 1 1 1 1 1 1
    1 1 1 1 1 1 1
c      ****
c      * source specification cards
c      * src1=point isotropic option
c      * sdir dirc. biasing - height reduction considered*
c      * si(eng.) and sp(prob.) taken from betof source *
c      * expt. data
c      ****
sdef erg=d1 pos=0 0 -44.0 vec=0 0 1 dir=d2 wgt=1.0
sb2 -31 4.0
sil  4.0867-02 4.6308-02
    5.2474-02 5.9461-02 6.7378-02 7.6349-02 8.6515-02
    9.8035-02 1.1109-01 1.2588-01 1.4264-01 1.6163-01
    1.8315-01 2.0754-01 2.3517-01 2.6649-01 3.0197-01
    3.4217-01 3.8774-01 4.3936-01 4.9786-01 5.6415-01
    6.3927-01 7.2438-01 8.2084-01 9.3013-01 1.0540+00
    1.1943+00 1.3533+00 1.5335+00 1.7377+00 1.8498+00
    1.9691+00 2.0961+00 2.2313+00 2.3752+00 2.5284+00
    2.6914+00 2.8650+00 3.0498+00 3.2465+00 3.4559+00
    3.6787+00 3.9160+00 4.1686+00 4.4374+00 4.7236+00
    5.0282+00 5.3525+00 5.6978+00 6.0652+00 6.4564+00
    6.8728+00 7.3161+00 7.7879+00 8.2902+00 8.8249+00
    9.3940+00 9.9999+00 1.0157+01 1.0317+01 1.0480+01
    1.0645+01 1.0812+01 1.0983+01 1.1156+01 1.1331+01
    1.1510+01 1.1691+01 1.1875+01 1.2062+01 1.2252+01
    1.2445+01 1.2641+01 1.2840+01 1.3042+01 1.3248+01
    1.3456+01 1.3668+01 1.3883+01 1.4102+01 1.4324+01
    1.4550+01 1.4779+01 1.5012+01 1.5248+01 1.5488+01
    1.5732+01 1.5980+01 1.6231+01 1.6487+01
sp1   0 1.4214-04 2.3162-04 2.1327-04 2.7087-04 2.6032-04
    3.1949-04 3.7848-04 4.3099-04 4.4082-04 5.6289-04
    6.0267-04 7.5334-04 8.3566-04 1.0281-03 1.1620-03
    1.3881-03 1.5339-03 1.8001-03 2.0387-03 2.3534-03
    2.6401-03 2.9843-03 3.2787-03 3.4783-03 3.7189-03
    3.8514-03 4.0062-03 4.1197-03 1.9596-03 2.0343-03
    2.0484-03 2.0263-03 1.9854-03 2.0112-03 2.0467-03
    2.1441-03 2.2558-03 2.4800-03 2.0399-03 1.7933-03
    1.6234-03 1.5383-03 1.4642-03 1.4261-03 1.3083-03
    1.3177-03 1.1970-03 1.1469-03 1.0180-03 1.0084-03
    1.0841-03 9.6395-04 9.2930-04 9.1702-04 1.1141-03
    1.1989-03 3.0970-04 3.1532-04 3.2121-04 3.2516-04
    3.9020-04 4.3484-04 4.3993-04 4.9814-04 5.7884-04
    5.8531-04 7.1724-04 1.1255-03 1.1435-03 1.2050-03
    2.3468-03 2.3827-03 2.4186-03 5.2339-03 5.8254-03
    5.9374-03 2.4164-02 3.5089-02 3.5570-02 9.9593-02
    1.8264-01 1.8583-01 1.6377-01 8.7669-02 8.9130-02
    8.7095-02 1.0017-03 1.0217-03 0
c      ****
c      * material specification cards
c      ****

```

Fig. A-5 Continued (2/3).

```

c      ----- iron (fe) -----
c      --- air
m1    7014.37c 3.8810-5      8016.37c 1.0400-5
c      --- sus316
m2    24000.37c 1.6787-2      25055.37c 1.3420-3
      26000.37c 6.0507-2      28000.37c 7.3429-3
c      --- al
m3    13027.37c 3.6244-3
c      --- o
m4    8016.37c 4.2947-2
c      drxs
c      ****
c      * tally specification cards
c      ****
fc5  --//fluxes at 5 pt dts(th=0.0, 12.2, 24.9, 41.8, 66.8 deg)
f5:n   0.0      0    703.0000      1
      148.7973     0    688.2148      1
      298.0163     0    642.0212      1
      477.4981     0    534.0526      1
      676.2307     0    289.8328      1
dd    0.5      100
e0    4.0867-02  4.6308-02
      5.2474-02  5.9461-02  6.7378-02  7.6349-02  8.6515-02
      9.8035-02  1.1109-01  1.2588-01  1.4264-01  1.6163-01
      1.8315-01  2.0754-01  2.3517-01  2.6649-01  3.0197-01
      3.4217-01  3.8774-01  4.3936-01  4.9786-01  5.6415-01
      6.3927-01  7.2438-01  8.2084-01  9.3013-01  1.0540+00
      1.1943+00  1.3533+00  1.5335+00  1.7377+00  1.8498+00
      1.9691+00  2.0961+00  2.2313+00  2.3752+00  2.5284+00
      2.6914+00  2.8650+00  3.0498+00  3.2465+00  3.4559+00
      3.6787+00  3.9160+00  4.1686+00  4.4374+00  4.7236+00
      5.0282+00  5.3525+00  5.6978+00  6.0652+00  6.4564+00
      6.8728+00  7.3161+00  7.7879+00  8.2902+00  8.8249+00
      9.3940+00  9.9999+00  1.0157+01  1.0317+01  1.0480+01
      1.0645+01  1.0812+01  1.0983+01  1.1156+01  1.1331+01
      1.1510+01  1.1691+01  1.1875+01  1.2062+01  1.2252+01
      1.2445+01  1.2641+01  1.2840+01  1.3042+01  1.3248+01
      1.3456+01  1.3668+01  1.3883+01  1.4102+01  1.4324+01
      1.4550+01  1.4779+01  1.5012+01  1.5248+01  1.5488+01
      1.5732+01  1.5980+01  1.6231+01  1.6487+01
fq0  e      f
c      ****
c      * problem cutoff cards
c      ****
cut:n   0      4.0000-02  -10      -0.01
nps    2000000
ctme   180
c      ****
c      * peripheral crads
c      ****
prdmp  1000000  1000000
lost   10      10
print

```

Fig. A-5 Continued (3/3).

```

fns-tof/31.4 cm(r)*5.06 cm(z)-fe cyl./J-3.2(MCNP4) re-cal 94.11.11
c **** cell card ****
c **** external void ****
1   0      -4 : +4 -2 +3 : +10 : +2 -10 +5 +6 +7 +8 +9
c ***** source vacuum region ****
2   0      -3 +4 -1
c ***** material region ****
3   1     8.391-2 -3 +1 -2
c ***** detector vacuum region ****
4   0 +2 -10 -5 : +2 -10 -6 : +2 -10 -7 : +2 -10 -8 : +2 -10 -9
c ----- the following is a blank delimiter

c **** surface card ****
c ****
1      pz      -5.06
2      pz      0
3      cz      31.4
4      pz      -50
5      cz      5.228
6      1 cz    5.235
7      2 cz    5.242
8      3 cz    5.270
9      4 cz    5.332
10     so     1000
c ----- the following is a blank delimiter

c **** mode card - neutron only ****
c ****
mode n
c **** transformation cards ****
c * rotation about the y axis by theta*
c ****
*tr1  0 0 0      12.2 90 102.2 90 0 90
      77.8 90 12.2 +1
*tr2  0 0 0      24.9 90 114.9 90 0 90
      65.1 90 24.9 +1
*tr3  0 0 0      41.8 90 131.8 90 0 90
      48.2 90 41.8 +1
*tr4  0 0 0      66.8 90 156.8 90 0 90
      23.2 90 66.8 +1
c **** cell parameter cards ****
c ****
imp:n 0 1 1 1
c ****
c * source miss fe05.mcn -> source ok fe5n.mcn *
c * source specification cards *
c * src1=point isotropic option *
c * sdir dirc. biasing - height reduction considered*
c * si(eng.) and sp(prob.) taken from betof source *
c * expt. data *
c ****
sdef erg=d1 pos=0 0 -25.06 vec=0 0 1 dir=d2 wgt=1.0
sb2 -31 4.0
sil 4.6308-02
5.2474-02 5.9461-02 6.7378-02 7.6349-02 8.6515-02
9.8035-02 1.1109-01 1.2588-01 1.4264-01 1.6163-01
1.8315-01 2.0754-01 2.3517-01 2.6649-01 3.0197-01
3.4217-01 3.8774-01 4.3936-01 4.9786-01 5.6415-01
6.3927-01 7.2438-01 8.2084-01 9.3013-01 1.0540+00
1.1943+00 1.3533+00 1.5335+00 1.7377+00 1.8498+00
1.9691+00 2.0961+00 2.2313+00 2.3752+00 2.5284+00
2.6914+00 2.8650+00 3.0498+00 3.2465+00 3.4559+00
3.6787+00 3.9160+00 4.1686+00 4.4374+00 4.7236+00
5.0282+00 5.3525+00 5.6978+00 6.0652+00 6.4564+00
6.8728+00 7.3161+00 7.7879+00 8.2902+00 8.8249+00
9.3940+00 9.9999+00 1.0157+01 1.0317+01 1.0480+01
1.0645+01 1.0812+01 1.0983+01 1.1156+01 1.1331+01
1.1510+01 1.1691+01 1.1875+01 1.2062+01 1.2252+01
1.2445+01 1.2641+01 1.2840+01 1.3042+01 1.3248+01

```

**Fig. A-6** A typical example of input data of MCNP for the analysis of the FNS/TOF experiment on iron.

```

1.3456+01 1.3668+01 1.3883+01 1.4102+01 1.4324+01
1.4550+01 1.4779+01 1.5012+01 1.5248+01 1.5488+01
1.5732+01 1.5980+01 1.6231+01 1.6487+01
spl 0
0      0      0      2.672-05 3.767-05
9.514-05 1.678-04 1.993-04 2.518-04 2.852-05
3.690-04 4.198-04 5.345-04 5.945-04 7.769-04
8.991-04 1.156-03 1.328-03 1.535-03 1.828-03
2.088-03 2.322-03 2.639-03 2.993-03 3.203-03
3.468-03 3.648-03 3.690-03 3.809-03 2.043-03
1.989-03 1.975-03 2.005-03 2.033-03 1.963-03
1.941-03 1.903-03 1.920-03 2.033-03 1.874-03
1.704-03 1.566-03 1.512-03 1.459-03 1.408-03
1.349-03 1.259-03 1.188-03 1.081-03 9.973-04
9.967-04 9.677-04 8.889-04 9.173-04 9.538-04
1.065-03 1.198-03 3.088-04 3.905-04 4.130-04
4.180-04 5.663-04 6.626-04 6.703-04 9.582-04
1.346-03 1.361-03 1.646-03 2.523-03 2.564-03
2.656-03 4.027-03 4.089-03 4.151-03 6.593-03
7.119-03 7.256-03 1.892-02 2.595-02 2.631-02
9.472-02 1.836-01 1.868-01 1.653-01 9.107-02
9.259-02 9.046-02 7.991-04 8.150-04
*****
c   * material specification cards *
c ****
c   ---- iron (fe) -----
m1 26000.37c 8.391-2
c   drxs
c ****
c   * tally specification cards *
c ****
fc5 --- fluxes at 5 pt dts(th=0.0, 12.2, 24.9, 41.8, 66.8 deg)
f5:n    0.0      0    738.0000      1
        156.16903     0    722.31035      1
        311.5665     0    671.21257      1
        495.90016     0    554.63414      1
        692.10891     0    296.63826      1
dd 0.5 100
e0 4.6308-02
5.2474-02 5.9461-02 6.7378-02 7.6349-02 8.6515-02
9.8035-02 1.1109-01 1.2588-01 1.4264-01 1.6163-01
1.8315-01 2.0754-01 2.3517-01 2.6649-01 3.0197-01
3.4217-01 3.8774-01 4.3936-01 4.9786-01 5.6415-01
6.3927-01 7.2438-01 8.2084-01 9.3013-01 1.0540+00
1.1943+00 1.3533+00 1.5335+00 1.7377+00 1.8498+00
1.9691+00 2.0961+00 2.2313+00 2.3752+00 2.5284+00
2.6914+00 2.8650+00 3.0498+00 3.2465+00 3.4559+00
3.6787+00 3.9160+00 4.1686+00 4.4374+00 4.7236+00
5.0282+00 5.3525+00 5.6978+00 6.0652+00 6.4564+00
6.8728+00 7.3161+00 7.7879+00 8.2902+00 8.8249+00
9.3940+00 9.9999+00 1.0157+01 1.0317+01 1.0480+01
1.0645+01 1.0812+01 1.0983+01 1.1156+01 1.1331+01
1.1510+01 1.1691+01 1.1875+01 1.2062+01 1.2252+01
1.2445+01 1.2641+01 1.2840+01 1.3042+01 1.3248+01
1.3456+01 1.3668+01 1.3883+01 1.4102+01 1.4324+01
1.4550+01 1.4779+01 1.5012+01 1.5248+01 1.5488+01
1.5732+01 1.5980+01 1.6231+01 1.6487+01
fq0 e f
*****
c   * problem cutoff cards *
c ****
c   cut:n      0      4.6308-02    -10    -0.01
nps 3000000
ctme 180
c ****
c   * peripheral crads *
c ****
prdmp 1000000 1000000
lost 10      10
print

```

Fig. A-6 Continued (2/2).

```

fns-tof pb - heiban t=5.06 (JENDL-3.2) '94-08-18
c **** cell card ****
c **** external void ****
1 0 -4 : +4 -2 +3 : +10 : +2 -10 +5 +6 +7 +8 +9
c ***** source vacuum region ****
2 0 -3 +4 -1
c ***** material region ****
c pb
3 1 3.2874-2 -3 +1 -2
c ***** detector vacuum region ****
4 0 +2 -10 -5 : +2 -10 -6 : +2 -10 -7 : +2 -10 -8 : +2 -10 -9
c ----- the following is a blank delimiter

c ****
c * surface card *
c ****
1 pz -5.06
2 pz 0
3 cz 31.5
4 pz -50
5 cz 5.228
6 1 cz 5.232
7 2 cz 5.244
8 3 cz 5.271
9 4 cz 5.329
10 so 1000
c ----- the following is a blank delimiter

c ****
c * mode card - neutron only *
c ****
mode n
c ****
c * transformation cards *
c * rotation about the y axis by theta*
c ****
*tr1 0 0 0 12.2 90 102.2 90 0 90
77.8 90 12.2 +1
-*tr2 0 0 0 24.9 90 114.9 90 0 90
65.1 90 24.9 +1
*tr3 0 0 0 41.8 90 131.8 90 0 90
48.2 90 41.8 +1
*tr4 0 0 0 66.8 90 156.8 90 0 90
23.2 90 66.8 +1
c ****
c * cell parameter cards *
c ****
imp:n 0 1 1 1
c ****
c * source specification cards *
c * srcl=point isotropic option *
c * sdir dirc. biasing - height reduction considered*
c * si(eng.) and sp(prob.) taken from betof source *
c * expt. data *
c ****
sdef erg=d1 pos=0 0 -25.06 vec=0 0 1 dir=d2 wgt=1.0
sb2 -31 4.0
si1 4.0867-02 4.6308-02
5.2474-02 5.9461-02 6.7378-02 7.6349-02 8.6515-02
9.8035-02 1.1109-01 1.2588-01 1.4264-01 1.6163-01
1.8315-01 2.0754-01 2.3517-01 2.6649-01 3.0197-01
3.4217-01 3.8774-01 4.3936-01 4.9786-01 5.6415-01
6.3927-01 7.2438-01 8.2084-01 9.3013-01 1.0540+00
1.1943+00 1.3533+00 1.5335+00 1.7377+00 1.8498+00
1.9691+00 2.0961+00 2.2313+00 2.3752+00 2.5284+00
2.6914+00 2.8650+00 3.0498+00 3.2465+00 3.4559+00
3.6787+00 3.9160+00 4.1686+00 4.4374+00 4.7236+00
5.0282+00 5.3525+00 5.6978+00 6.0652+00 6.4564+00
6.8728+00 7.3161+00 7.7879+00 8.2902+00 8.8249+00
9.3940+00 9.9999+00 1.0157+01 1.0317+01 1.0480+01
1.0645+01 1.0812+01 1.0983+01 1.1156+01 1.1331+01
1.1510+01 1.1691+01 1.1875+01 1.2062+01 1.2252+01

```

Fig. A-7 A typical example of input data of MCNP for the analysis of the FNS/TOF experiment on lead.

```

1.2445+01 1.2641+01 1.2840+01 1.3042+01 1.3248+01
1.3456+01 1.3668+01 1.3883+01 1.4102+01 1.4324+01
1.4550+01 1.4779+01 1.5012+01 1.5248+01 1.5488+01
1.5732+01 1.5980+01 1.6231+01 1.6487+01
sp1
0          0
0.12545e-03 0.12824e-03 0.17476e-03
0.15533e-03 0.16647e-03 0.22098e-03 0.19441e-03 0.25487e-03
0.32874e-03 0.34722e-03 0.43729e-03 0.52822e-03 0.62988e-03
0.77945e-03 0.90888e-03 0.11025e-02 0.12959e-02 0.14750e-02
0.17160e-02 0.19990e-02 0.22375e-02 0.25970e-02 0.29042e-02
0.32106e-02 0.33986e-02 0.36610e-02 0.38327e-02 0.38521e-02
0.39666e-02 0.21563e-02 0.20631e-02 0.20489e-02 0.20504e-02
0.20508e-02 0.20330e-02 0.21307e-02 0.23797e-02 0.30775e-02
0.37184e-02 0.20360e-02 0.18285e-02 0.17251e-02 0.15436e-02
0.15299e-02 0.14233e-02 0.13622e-02 0.12804e-02 0.12295e-02
0.11662e-02 0.11104e-02 0.10529e-02 0.10269e-02 0.95528e-03
0.91505e-03 0.91256e-03 0.10529e-02 0.11497e-02 0.29940e-03
0.32323e-03 0.33292e-03 0.33701e-03 0.38399e-03 0.41797e-03
0.42286e-03 0.48083e-03 0.56109e-03 0.56736e-03 0.65211e-03
0.90718e-03 0.92173e-03 0.95059e-03 0.13349e-02 0.13554e-02
0.13758e-02 0.26752e-02 0.29497e-02 0.30065e-02 0.19579e-01
0.29488e-01 0.29892e-01 0.10442e+00 0.20120e+00 0.20471e+00
0.17728e+00 0.83258e-01 0.84646e-01 0.82922e-01 0.63437e-02
0.64700e-02
c
c **** material specification cards ****
c * material specification cards *
c ****
c ----- Lead (pb) -----
m1 82000.37c 3.2874-2
c drxs
c ****
c * tally specification cards *
c ****
fc5 --- fluxes at 5 pt dts(th=0.0, 12.2, 24.9, 41.8, 66.8 deg)
f5:n
0.0      0    738.0000      1
156.0660   0    721.8340      1
311.6519   0    671.3965      1
495.9477   0    554.6874      1
691.7129   0    296.4685      1
dd 0.5 100
e0 4.0867-02 4.6308-02
5.2474-02 5.9461-02 6.7378-02 7.6349-02 8.6515-02
9.8035-02 1.1109-01 1.2588-01 1.4264-01 1.6163-01
1.8315-01 2.0754-01 2.3517-01 2.6649-01 3.0197-01
3.4217-01 3.8774-01 4.3936-01 4.9786-01 5.6415-01
6.3927-01 7.2438-01 8.2084-01 9.3013-01 1.0540+00
1.1943+00 1.3533+00 1.5335+00 1.7377+00 1.8498+00
1.9691+00 2.0961+00 2.2313+00 2.3752+00 2.5284+00
2.6914+00 2.8650+00 3.0498+00 3.2465+00 3.4559+00
3.6787+00 3.9160+00 4.1686+00 4.4374+00 4.7236+00
5.0282+00 5.3525+00 5.6978+00 6.0652+00 6.4564+00
6.8728+00 7.3161+00 7.7879+00 8.2902+00 8.8249+00
9.3940+00 9.9999+00 1.0157+01 1.0317+01 1.0480+01
1.0645+01 1.0812+01 1.0983+01 1.1156+01 1.1331+01
1.1510+01 1.1691+01 1.1875+01 1.2062+01 1.2252+01
1.2445+01 1.2641+01 1.2840+01 1.3042+01 1.3248+01
1.3456+01 1.3668+01 1.3883+01 1.4102+01 1.4324+01
1.4550+01 1.4779+01 1.5012+01 1.5248+01 1.5488+01
1.5732+01 1.5980+01 1.6231+01 1.6487+01
fq0
e f
c ****
c * problem cutoff cards *
c ****
cut:n      0    4.6308-02 -10   -0.01
nps 2000000
ctme 180
c ****
c * peripheral crads *
c ****
prdmp 1000000 1000000
lost 10      10
print

```

Fig. A-7 Continued (2/2).

```
>>> Analysis of Li2O Slab Experiment August 1994 <<
c ***** front air region *****
 1 4 4.921-5 +1 -2 -32 $ -1.00 - 20.00 cm
c ***** Li2O region *****
 2 1 8.623-2 +2 -3 -30 $ 20.00 - 21.60 cm
 3 2 3.278-2 +2 -3 +30 -31 $ 20.00 - 21.60 cm
 4 3 8.646-2 +2 -3 +31 -32 $ 20.00 - 21.60 cm
 5 1 8.623-2 +3 -4 -30 $ 21.60 - 22.40 cm
 6 2 3.278-2 +3 -4 +30 -31 $ 21.60 - 22.40 cm
 7 3 8.646-2 +3 -4 +31 -32 $ 21.60 - 22.40 cm
 8 1 8.623-2 +4 -5 -30 $ 22.40 - 23.90 cm
 9 2 3.278-2 +4 -5 +30 -31 $ 22.40 - 23.90 cm
10 3 8.646-2 +4 -5 +31 -32 $ 22.40 - 23.90 cm
11 1 8.623-2 +5 -6 -30 $ 23.90 - 24.90 cm
12 2 3.278-2 +5 -6 +30 -31 $ 23.90 - 24.90 cm
13 3 8.646-2 +5 -6 +31 -32 $ 23.90 - 24.90 cm
14 1 8.623-2 +6 -7 -30 $ 24.90 - 26.40 cm
15 2 3.278-2 +6 -7 +30 -31 $ 24.90 - 26.40 cm
16 3 8.646-2 +6 -7 +31 -32 $ 24.90 - 26.40 cm
17 1 8.623-2 +7 -8 -30 $ 26.40 - 27.50 cm
18 2 3.278-2 +7 -8 +30 -31 $ 26.40 - 27.50 cm
19 3 8.646-2 +7 -8 +31 -32 $ 26.40 - 27.50 cm
20 1 8.623-2 +8 -9 -30 $ 27.50 - 30.00 cm
21 2 3.278-2 +8 -9 +30 -31 $ 27.50 - 30.00 cm
22 3 8.646-2 +8 -9 +31 -32 $ 27.50 - 30.00 cm
23 1 8.623-2 +9 -10 -30 $ 30.00 - 31.50 cm
24 2 3.278-2 +9 -10 +30 -31 $ 30.00 - 31.50 cm
25 3 8.646-2 +9 -10 +31 -32 $ 30.00 - 31.50 cm
26 1 8.623-2 +10 -11 -30 $ 31.50 - 35.10 cm
27 2 3.278-2 +10 -11 +30 -31 $ 31.50 - 35.10 cm
28 3 8.646-2 +10 -11 +31 -32 $ 31.50 - 35.10 cm
29 1 8.623-2 +11 -12 -30 $ 35.10 - 36.60 cm
30 2 3.278-2 +11 -12 +30 -31 $ 35.10 - 36.60 cm
31 3 8.646-2 +11 -12 +31 -32 $ 35.10 - 36.60 cm
32 1 8.623-2 +12 -13 -30 $ 36.60 - 40.20 cm
33 2 3.278-2 +12 -13 +30 -31 $ 36.60 - 40.20 cm
34 3 8.646-2 +12 -13 +31 -32 $ 36.60 - 40.20 cm
35 1 8.623-2 +13 -14 -30 $ 40.20 - 41.60 cm
36 2 3.278-2 +13 -14 +30 -31 $ 40.20 - 41.60 cm
37 3 8.646-2 +13 -14 +31 -32 $ 40.20 - 41.60 cm
38 1 8.623-2 +14 -15 -30 $ 41.60 - 45.30 cm
39 2 3.278-2 +14 -15 +30 -31 $ 41.60 - 45.30 cm
40 3 8.646-2 +14 -15 +31 -32 $ 41.60 - 45.30 cm
41 1 8.623-2 +15 -16 -30 $ 45.30 - 46.70 cm
42 2 3.278-2 +15 -16 +30 -31 $ 45.30 - 46.70 cm
43 3 8.646-2 +15 -16 +31 -32 $ 45.30 - 46.70 cm
44 1 8.623-2 +16 -17 -30 $ 46.70 - 50.30 cm
45 2 3.278-2 +16 -17 +30 -31 $ 46.70 - 50.30 cm
46 3 8.646-2 +16 -17 +31 -32 $ 46.70 - 50.30 cm
47 1 8.623-2 +17 -18 -30 $ 50.30 - 51.70 cm
48 2 3.278-2 +17 -18 +30 -31 $ 50.30 - 51.70 cm
49 3 8.646-2 +17 -18 +31 -32 $ 50.30 - 51.70 cm
50 1 8.623-2 +18 -19 -30 $ 51.70 - 55.40 cm
51 2 3.278-2 +18 -19 +30 -31 $ 51.70 - 55.40 cm
52 3 8.646-2 +18 -19 +31 -32 $ 51.70 - 55.40 cm
53 1 8.623-2 +19 -20 -30 $ 55.40 - 56.90 cm
54 2 3.278-2 +19 -20 +30 -31 $ 55.40 - 56.90 cm
55 3 8.646-2 +19 -20 +31 -32 $ 55.40 - 56.90 cm
56 1 8.623-2 +20 -21 -30 $ 56.90 - 60.50 cm
57 2 3.278-2 +20 -21 +30 -31 $ 56.90 - 60.50 cm
58 3 8.646-2 +20 -21 +31 -32 $ 56.90 - 60.50 cm
59 1 8.623-2 +21 -22 -30 $ 60.50 - 61.80 cm
60 2 3.278-2 +21 -22 +30 -31 $ 60.50 - 61.80 cm
61 3 8.646-2 +21 -22 +31 -32 $ 60.50 - 61.80 cm
62 1 8.623-2 +22 -23 -30 $ 61.80 - 65.60 cm
63 2 3.278-2 +22 -23 +30 -31 $ 61.80 - 65.60 cm
64 3 8.646-2 +22 -23 +31 -32 $ 61.80 - 65.60 cm
65 1 8.623-2 +23 -24 -30 $ 65.60 - 67.10 cm
66 2 3.278-2 +23 -24 +30 -31 $ 65.60 - 67.10 cm
67 3 8.646-2 +23 -24 +31 -32 $ 65.60 - 67.10 cm
68 1 8.623-2 +24 -25 -30 $ 67.10 - 70.70 cm
69 2 3.278-2 +24 -25 +30 -31 $ 67.10 - 70.70 cm
70 3 8.646-2 +24 -25 +31 -32 $ 67.10 - 70.70 cm
71 1 8.623-2 +25 -26 -30 $ 70.70 - 72.00 cm
72 2 3.278-2 +25 -26 +30 -31 $ 70.70 - 72.00 cm
```

Fig. A-8 A typical example of input data of MCNP for the analysis of the FNS/clean benchmark experiment on lithium oxide.

```

73   3 8.646-2 +25 -26 +31 -32 $ 70.70 - 72.00 cm
74   1 8.623-2 +26 -27 -30 $ 72.00 - 75.70 cm
75   2 3.278-2 +26 -27 +30 -31 $ 72.00 - 75.70 cm
76   3 8.646-2 +26 -27 +31 -32 $ 72.00 - 75.70 cm
77   1 8.623-2 +27 -28 -30 $ 75.70 - 77.20 cm
78   2 3.278-2 +27 -28 +30 -31 $ 75.70 - 77.20 cm
79   3 8.646-2 +27 -28 +31 -32 $ 75.70 - 77.20 cm
80   1 8.623-2 +28 -29 -30 $ 77.20 - 81.00 cm
81   2 3.278-2 +28 -29 +30 -31 $ 77.20 - 81.00 cm
82   3 8.646-2 +28 -29 +31 -32 $ 77.20 - 81.00 cm
c ***** external void *****
83   0           -1 : +29 : +32 $

1          pz      -1.00 $ Source
2          pz      20.00 $ TPR & react rate & g-heat
3          pz      21.60 $ TPR & n-spec
4          pz      22.40 $ TPR & react rate
5          pz      23.90 $ fission
6          pz      24.90 $ TPR & react rate
7          pz      26.40 $ fission
8          pz      27.50 $ TPR & react rate
9          pz      30.00 $ TPR&fission&react rate&g-heat
10         pz      31.50 $ TPR & fission & n-spec
11         pz      35.10 $ TPR & react rate
12         pz      36.60 $ fission
13         pz      40.20 $ TPR & react rate & g-heat
14         pz      41.60 $ TPR & fission & n-spec
15         pz      45.30 $ TPR & react-rate
16         pz      46.70 $ fission
17         pz      50.30 $ TPR & react rate
18         pz      51.70 $ TPR & fission n-spec
19         pz      55.40 $ TPR & react rate
20         pz      56.90 $ fission
21         pz      60.50 $ TPR & react rate
22         pz      61.90 $ TPR & fission & n-spec
23         pz      65.60 $ TPR & react rate
24         pz      67.10 $ fission
25         pz      70.70 $ TPR & react rate
26         pz      72.00 $ TPR & fission & n-spec
27         pz      75.70 $ TPR & react rate
28         pz      77.20 $ fission
29         pz      81.00 $ TPR & n-spec
c
30         cz      2.719
31         cz      2.866
32         cz      31.50

imp:n 1 1 1 1 1 1 1 1 1 1 1 1
1 1 1 1 1 1 1 1 1 1 1 1
1 1 1 1 1 1 1 1 1 1 1 2
2 2 2 2 2 2 2 2 2 2 2 2
2 2 2 2 2 2 2 2 2 2 2 4
4 4 4 4 4 4 4 4 4 4 4 4
4 4 4 4 4 4 4 4 4 4 4 0
imp:p 1 1 1 1 1 1 1 1 1 1 1 1
1 1 1 1 1 1 1 1 1 1 1 1
1 1 1 1 1 1 1 1 1 1 2 2
2 2 2 2 2 2 2 2 2 2 2 2
2 2 2 2 2 2 2 2 2 2 2 4
4 4 4 4 4 4 4 4 4 4 4 4
4 4 4 4 4 4 4 4 4 4 4 0
c ****
c * source specification cards *
c ****
sdef erg=d1 pos=0 0 0 vec=0 0 1 dir=d2 wgt=1.1767
sb2 -31 4.0
sil 5.8293-04
9.6110-04 1.2341-03 1.5846-03 2.0346-03 2.6125-03
3.3546-03 4.3073-03 5.5307-03 7.1016-03 9.1186-03
1.1709-02 1.5034-02 1.9304-02 2.1874-02 2.4787-02
2.8087-02 3.1827-02 3.6065-02 4.0867-02 4.6308-02
5.2474-02 5.9461-02 6.7378-02 7.6349-02 8.6515-02
9.8035-02 1.1109-01 1.2588-01 1.4264-01 1.6163-01
1.8315-01 2.0754-01 2.3517-01 2.6649-01 3.0197-01
3.4217-01 3.8774-01 4.3936-01 4.9786-01 5.6415-01
6.3927-01 7.2438-01 8.2084-01 9.3013-01 1.0540+00
1.1943+00 1.3533+00 1.5335+00 1.7377+00 1.8498+00

```

Fig. A-8 Continued (2/4).

```

1.9691+00 2.0961+00 2.2313+00 2.3752+00 2.5284+00
2.6914+00 2.8650+00 3.0498+00 3.2465+00 3.4559+00
3.6787+00 3.9160+00 4.1686+00 4.4374+00 4.7236+00
5.0282+00 5.3525+00 5.6978+00 6.0652+00 6.4564+00
6.8728+00 7.3161+00 7.7879+00 8.2902+00 8.8249+00
9.3940+00 9.9999+00 1.0157+01 1.0317+01 1.0480+01
1.0645+01 1.0812+01 1.0983+01 1.1156+01 1.1331+01
1.1510+01 1.1691+01 1.1875+01 1.2062+01 1.2252+01
1.2445+01 1.2641+01 1.2840+01 1.3042+01 1.3248+01
1.3456+01 1.3668+01 1.3883+01 1.4102+01 1.4324+01
1.4550+01 1.4779+01 1.5012+01 1.5248+01 1.5488+01
1.5732+01 1.5980+01
sp1 0.0
4.3479-05 5.5907-05 6.3421-05 7.2417-05 8.3682-05
9.7598-05 1.1447-04 1.3521-04 1.6038-04 1.9164-04
2.1369-04 2.4812-04 3.0516-04 1.7891-04 2.0045-04
2.2407-04 2.5200-04 2.8444-04 3.2144-04 3.6436-04
4.1340-04 4.7077-04 5.3606-04 6.1088-04 6.9762-04
7.9663-04 9.1106-04 1.2219-03 1.4051-03 1.6141-03
1.8527-03 2.1040-03 2.4317-03 2.8136-03 3.2890-03
3.8479-03 4.9397-03 5.9791-03 6.8688-03 7.7929-03
8.6681-03 9.3421-03 9.7540-03 9.9713-03 9.7275-03
9.6236-03 9.7640-03 9.9677-03 1.0130-02 5.3179-03
5.3194-03 5.3383-03 5.3299-03 5.2928-03 5.0664-03
4.7354-03 4.3795-03 3.7938-03 3.4485-03 3.3610-03
3.6099-03 4.2412-03 4.3379-03 3.9704-03 3.5164-03
2.9628-03 2.5194-03 2.5754-03 2.7193-03 2.3830-03
2.1203-03 2.3331-03 2.4699-03 2.0821-03 1.9259-03
2.1711-03 2.3220-03 5.9892-04 5.9851-04 5.8562-04
6.0839-04 5.4544-04 5.2166-04 4.7551-04 3.3951-04
3.3956-04 3.5410-04 4.3340-04 4.9328-04 6.6341-04
9.1815-04 1.0510-03 1.3058-03 1.5353-03 2.0627-03
3.0739-03 4.0824-03 3.6889-03 4.7824-03 1.9619-02
8.8741-02 1.9088-01 2.8044-01 2.3566-01 7.1310-02
1.7363-02 2.7828-03
c ****
c * material specification cards *
c ****
c --- Li2O inner
m1 3006.37c 4.221-3 3007.37c 5.277-2
     8016.37c 2.850-2 24000.37c 1.433-4
    25055.37c 7.245-6 26000.37c 5.205-4
   28000.37c 6.296-5
c --- SS304
m2 24000.37c 6.398-3 25055.37c 3.295-4
  26000.37c 2.324-2 28000.37c 2.812-3
c --- Li2O outer
m3 3006.37c 4.191-3 3007.37c 5.240-2
     8016.37c 2.830-2 24000.37c 3.068-4
    25055.37c 1.880-5 26000.37c 1.112-3
   28000.37c 1.352-4
c --- air
m4 7014.37c 3.8810-5 8016.37c 1.0400-5
c --- materials for reaction rate
m5 3006.03y 1.0 $ Li-6(n,t)He-4
m6 3007.03y 1.0 $ Li-7(n,t)
m7 13027.03y 1.0 $ Al-27(n,alpha)
m8 28058.03y 1.0 $ Ni-58(n,2n)
m9 49115.03y 1.0 $ In-115(n,n') & In-115(n,g)
m10 90232.03y 1.0 $ Th-232(n,fission)
m11 92235.03y 1.0 $ U-235(n,fission)
m12 92238.03y 1.0 $ U-238(n,fission)
m13 93237.03y 1.0 $ Np-237(n,fission)
c ****
c * tally specification cards *
c ****
fc02 ---- neutron energy spectrum surface
f02:n 3 10 14 18 22 26 29
fq02 s m e f
fs02 -30
e2 1.0010-11 3.2241-07
     5.3156-07 8.7640-07 1.4449-06 2.3823-06 3.9278-06
     6.4758-06 1.0677-05 1.7603-05 2.9023-05 4.7850-05
     7.8891-05 1.3007-04 2.1445-04 3.5357-04 5.8293-04
     9.6110-04 1.2341-03 1.5846-03 2.0346-03 2.6125-03
     3.3546-03 4.3073-03 5.5307-03 7.1016-03 9.1186-03

```

Fig. A-8 Continued (3/4).

```

1.1709-02 1.5034-02 1.9304-02 2.1874-02 2.4787-02
2.8087-02 3.1827-02 3.6065-02 4.0867-02 4.6308-02
5.2474-02 5.9461-02 6.7378-02 7.6349-02 8.6515-02
9.8035-02 1.1109-01 1.2588-01 1.4264-01 1.6163-01
1.8315-01 2.0754-01 2.3517-01 2.6649-01 3.0197-01
3.4217-01 3.8774-01 4.3936-01 4.9786-01 5.6415-01
6.3927-01 7.2438-01 8.2084-01 9.3013-01 1.0540+00
1.1943+00 1.3533+00 1.5335+00 1.7377+00 1.8498+00
1.9691+00 2.0961+00 2.2313+00 2.3752+00 2.5284+00
2.6914+00 2.8650+00 3.0498+00 3.2465+00 3.4559+00
3.6787+00 3.9160+00 4.1686+00 4.4374+00 4.7236+00
5.0282+00 5.3525+00 5.6978+00 6.0652+00 6.4564+00
6.8728+00 7.3161+00 7.7879+00 8.2902+00 8.8249+00
9.3940+00 9.9999+00 1.0157+01 1.0317+01 1.0480+01
1.0645+01 1.0812+01 1.0983+01 1.1156+01 1.1331+01
1.1510+01 1.1691+01 1.1875+01 1.2062+01 1.2252+01
1.2445+01 1.2641+01 1.2840+01 1.3042+01 1.3248+01
1.3456+01 1.3668+01 1.3883+01 1.4102+01 1.4324+01
1.4550+01 1.4779+01 1.5012+01 1.5248+01 1.5488+01
1.5732+01 1.5980+01

fc12 ---- tritium production rate(TPR) surface r=2.719cm
f12:n 2 3 4 6 8 9 10 11 13 14 15 17
      18 19 21 22 23 25 26 27 29
fs12 -30
fq12 s e f m
fml2 (1) (1 5 105) (1 6 205)
fc22 ---- fission rate (U-235,U-238,Np-237,Th-232) surface
f22:n 5 7 9 10 12 14 16 18 20 22 24 26
fs22 -30
fq22 s e f m
fm22 (1) (1 10 18) (1 11 18) (1 12 18) (1 13 18)
fc32 ---- reaction rate (Al-27,Ni-58,In(n,n'),In(n,gamma)) surface
f32:n 2 4 6 8 9 11 13 15 17 19 21 23
      25 27
fs32 -30
fq32 s e f m
fm32 (1) (1 7 107) (1 8 16) (1 9 51) (1 9 102)
fc102 ---- gamma-ray heat rate surface r=2.719cm
f102:p 2 9 13 17 21
fs102 -30
fq102 s m e f
c -----
c **** problem cutoff cards ****
c **** peripheral cards ****
c -----
phys:n 16.0 0.0
phys:p 30.0 1 0
phys:e 30.0 1 1 1 1 1 1 1
mode n p
cut:n 0 1.0e-10 -0.5 -0.25 0
cut:p 0 0.0099 -0.5 -0.25 0
cut:e 0 0.3 -0.5 -0.25 0
nps 2000000
ctme 2000
c **** peripheral cards ****
c **** print cards ****
prdmp 200000 200000 1 1
lost 10 10
print

```

Fig. A-8 Continued (4/4).

```

>>> Analysis of Beryllium Slab Experiment August 1994 <<
c **** front air region ****
 1 2 4.921-5 +1 -2 -27 $ -1.00 - 20.00 cm
c **** Beryllium region ****
 2 1 1.2215-1 +2 -3 -26 $ 20.00 - 21.40 cm
 3 1 1.2215-1 +2 -3 +26 -27 $ 20.00 - 21.40 cm
 4 1 1.2215-1 +3 -4 -26 $ 21.40 - 24.12 cm
 5 1 1.2215-1 +3 -4 +26 -27 $ 21.40 - 24.12 cm
 6 1 1.2215-1 +4 -5 -26 $ 24.12 - 25.17 cm
 7 1 1.2215-1 +4 -5 +26 -27 $ 24.12 - 25.17 cm
 8 1 1.2215-1 +5 -6 -26 $ 25.17 - 26.60 cm
 9 1 1.2215-1 +5 -6 +26 -27 $ 25.17 - 26.60 cm
10 1 1.2215-1 +6 -7 -26 $ 26.60 - 29.20 cm
11 1 1.2215-1 +6 -7 +26 -27 $ 26.60 - 29.20 cm
12 1 1.2215-1 +7 -8 -26 $ 29.20 - 30.23 cm
13 1 1.2215-1 +7 -8 +26 -27 $ 29.20 - 30.23 cm
14 1 1.2215-1 +8 -9 -26 $ 30.23 - 31.70 cm
15 1 1.2215-1 +8 -9 +26 -27 $ 30.23 - 31.70 cm
16 1 1.2215-1 +9 -10 -26 $ 31.70 - 32.70 cm
17 1 1.2215-1 +9 -10 +26 -27 $ 31.70 - 32.70 cm
18 1 1.2215-1 +10 -11 -26 $ 32.70 - 34.28 cm
19 1 1.2215-1 +10 -11 +26 -27 $ 32.70 - 34.28 cm
20 1 1.2215-1 +11 -12 -26 $ 34.28 - 34.92 cm
21 1 1.2215-1 +11 -12 +26 -27 $ 34.28 - 34.92 cm
22 1 1.2215-1 +12 -13 -26 $ 34.92 - 40.35 cm
23 1 1.2215-1 +12 -13 +26 -27 $ 34.92 - 40.35 cm
24 1 1.2215-1 +13 -14 -26 $ 40.35 - 41.80 cm
25 1 1.2215-1 +13 -14 +26 -27 $ 40.35 - 41.80 cm
26 1 1.2215-1 +14 -15 -26 $ 41.80 - 45.06 cm
27 1 1.2215-1 +14 -15 +26 -27 $ 41.80 - 45.06 cm
28 1 1.2215-1 +15 -16 -26 $ 45.06 - 46.98 cm
29 1 1.2215-1 +15 -16 +26 -27 $ 45.06 - 46.98 cm
30 1 1.2215-1 +16 -17 -26 $ 46.98 - 47.90 cm
31 1 1.2215-1 +16 -17 +26 -27 $ 46.98 - 47.90 cm
32 1 1.2215-1 +17 -18 -26 $ 47.90 - 50.47 cm
33 1 1.2215-1 +17 -18 +26 -27 $ 47.90 - 50.47 cm
34 1 1.2215-1 +18 -19 -26 $ 50.47 - 52.00 cm
35 1 1.2215-1 +18 -19 +26 -27 $ 50.47 - 52.00 cm
36 1 1.2215-1 +19 -20 -26 $ 52.00 - 55.20 cm
37 1 1.2215-1 +19 -20 +26 -27 $ 52.00 - 55.20 cm
38 1 1.2215-1 +20 -21 -26 $ 55.20 - 57.14 cm
39 1 1.2215-1 +20 -21 +26 -27 $ 55.20 - 57.14 cm
40 1 1.2215-1 +21 -22 -26 $ 57.14 - 60.59 cm
41 1 1.2215-1 +21 -22 +26 -27 $ 57.14 - 60.59 cm
42 1 1.2215-1 +22 -23 -26 $ 60.59 - 62.10 cm
43 1 1.2215-1 +22 -23 +26 -27 $ 60.59 - 62.10 cm
44 1 1.2215-1 +23 -24 -26 $ 62.10 - 63.12 cm
45 1 1.2215-1 +23 -24 +26 -27 $ 62.10 - 63.12 cm
46 1 1.2215-1 +24 -25 -26 $ 63.12 - 65.54 cm
47 1 1.2215-1 +24 -25 +26 -27 $ 63.12 - 65.54 cm
c ***** external void *****
48 0 -1 : +25 : +27 $
 1      pz      -1.00 $ Source
 2      pz      20.00 $ TPR & react rate
 3      pz      21.40 $ n-spec
 4      pz      24.12 $ fission
 5      pz      25.00 $ TPR & react rate
 6      pz      26.60 $ fission & n-spec
 7      pz      29.20 $ fission
 8      pz      30.23 $ TPR
 9      pz      31.70 $ fission & n-spec
10     pz      32.70 $ TPR & n-spec
11     pz      34.28 $ fission
12     pz      34.92 $ react rate
13     pz      40.35 $ TPR
14     pz      41.80 $ fission & n-spec
15     pz      45.06 $ react rate
16     pz      46.98 $ fission
17     pz      47.90 $ TPR & n-spec
18     pz      50.47 $ TPR
19     pz      52.00 $ fission & n-spec
20     pz      55.20 $ react rate
21     pz      57.14 $ fission
22     pz      60.59 $ TPR

```

Fig. A-9 A typical example of input data of MCNP for the analysis of the FNS/clean benchmark experiment on beryllium.

```

23      pz      62.10 $ fission & n-spec
24      pz      63.12 $ TPR
25      pz      65.54 $ react rate
c
26      cz      3.00
27      cz      31.50

imp:n 1 1 1 1 1 1 1 1 1 1 1 1
      1 1 1 1 1 1 1 1 1 1 1 2
      2 2 2 2 2 2 2 2 2 2 2 2
      2 2 2 2 2 4 4 4 4 4 4 0

c ****
c * source specification cards *
c ****
sdef erg=d1 pos=0 0 0 vec=0 0 1 dir=d2 wgt=1.1261
sb2 -31 4.0
sil 1.0010-11 3.2241-07
      5.3156-07 8.7640-07 1.4449-06 2.3826-06 3.9278-06
      6.4758-06 1.0677-05 1.7603-05 2.9023-05 4.7850-05
      7.8891-05 1.3007-04 2.1455-04 3.5357-04 5.8293-04
      9.6110-04 1.2341-03 1.5846-03 2.0346-03 2.6125-03
      3.3546-03 4.3073-03 5.5307-03 7.1016-03 9.1186-03
      1.1709-02 1.5034-02 1.9304-02 2.1874-02 2.4787-02
      2.8087-02 3.1827-02 3.6065-02 4.0867-02 4.6308-02
      5.2474-02 5.9461-02 6.7378-02 7.6349-02 8.6515-02
      9.8035-02 1.1109-01 1.2588-01 1.4264-01 1.6163-01
      1.8315-01 2.0754-01 2.3517-01 2.6649-01 3.0197-01
      3.4217-01 3.8774-01 4.3936-01 4.9786-01 5.6415-01
      6.3927-01 7.2438-01 8.2084-01 9.3013-01 1.0540+00
      1.1943+00 1.3533+00 1.5335+00 1.7377+00 1.8498+00
      1.9691+00 2.0961+00 2.2313+00 2.3752+00 2.5284+00
      2.6914+00 2.8650+00 3.0498+00 3.2465+00 3.4559+00
      3.6787+00 3.9160+00 4.1686+00 4.4374+00 4.7236+00
      5.0282+00 5.3525+00 5.6978+00 6.0652+00 6.4564+00
      6.8728+00 7.3161+00 7.7879+00 8.2902+00 8.8249+00
      9.3940+00 9.9999+00 1.0157+01 1.0317+01 1.0480+01
      1.0645+01 1.0812+01 1.0983+01 1.1156+01 1.1331+01
      1.1510+01 1.1691+01 1.1875+01 1.2062+01 1.2252+01
      1.2445+01 1.2641+01 1.2840+01 1.3042+01 1.3248+01
      1.3456+01 1.3668+01 1.3883+01 1.4102+01 1.4324+01
      1.4550+01 1.4779+01 1.5012+01 1.5248+01 1.5488+01
sp1 0.0 1.5142-07
      2.2732-09 4.2225-09 7.4848-09 1.4264-08 8.3975-08
      1.8398-07 2.2450-07 1.3922-07 1.6817-07 2.9754-07
      3.8068-06 3.0541-06 2.2612-06 6.9372-06 7.2049-06
      8.7622-06 7.8013-06 1.4320-05 1.1820-05 1.6544-05
      1.4791-05 1.7624-05 2.8404-05 2.4899-05 3.7633-05
      4.4237-05 4.6320-05 6.1572-05 3.7185-05 5.3362-05
      4.4831-05 5.0292-05 5.7202-05 6.9230-05 8.0602-05
      8.3190-05 9.7450-05 1.0531-04 1.2632-04 1.4874-04
      1.7906-04 3.7225-04 4.9933-04 5.3824-04 6.0762-04
      7.0593-04 8.0965-04 9.5392-04 1.0785-03 1.2232-03
      1.3867-03 1.5803-03 1.6473-03 1.8238-03 2.0605-03
      2.2042-03 2.3040-03 2.5211-03 2.5709-03 2.5872-03
      2.5765-03 2.7699-03 2.8528-03 2.5945-03 1.3898-03
      1.4298-03 1.3270-03 1.3489-03 1.3820-03 1.4312-03
      1.3760-03 1.4329-03 1.4558-03 1.3518-03 1.4053-03
      1.2861-03 1.2741-03 1.1711-03 1.1937-03 1.0563-03
      1.0018-03 8.8451-04 7.9827-04 7.9293-04 7.5872-04
      6.9228-04 6.2956-04 5.1710-04 5.0750-04 5.1007-04
      4.1280-04 3.5649-04 9.0768-05 8.2287-05 9.2862-05
      9.1407-05 9.3708-05 7.9567-05 8.8737-05 8.7841-05
      1.1227-04 1.6798-04 1.5985-04 1.6563-04 2.1025-04
      4.1363-04 7.4899-04 7.8183-04 5.1771-04 4.5938-04
      4.6458-04 9.1020-04 2.6083-03 9.5007-04 5.1474-03
      3.0897-02 2.3565-01 4.0901-01 2.2296-01 1.4419-01

c ****
c * material specification cards *
c ****
c --- Beryllium
m1 4009.37c 1.2152-1 6012.37c 7.7109-5
      8016.37c 4.9813-4 13027.37c 2.9013-4
      26000.37c 2.4678-5
c --- air
m2 7014.37c 3.8810-5 8016.37c 1.0400-5
c --- materials for reaction rate
m3 3006.03y 1.0 $ Li-6(n,t)He-4

```

Fig. A-9 Continued (2/3).

```

m4    13027.03y   1.0 $ Al-27(n,alpha)
m5    22000.03y   1.0 $ Ti-47(n,x)Sc-47
m6    26056.03y   1.0 $ Fe-56(n,p)Mn-56
m7    28058.03y   1.0 $ Ni-58(n,2n) & Ni-58(n,p)
m8    40090.03y   1.0 $ Zr-90(n,2n)
m9    41093.03y   1.0 $ Nb-93(n,2n)Nb-92m
m10   49115.03y   1.0 $ In-115(n,n')In-115m
m11   79197.03y   1.0 $ Au-197(n,gamma)
m12   92235.03y   1.0 $ U-235(n,fission)
c ****
c * tally specification cards *
c ****
fc02 ---- neutron energy spectrum surface r=3cm
f02:n 3 6 9 10 14 17 19 23
fq02 s m e f
fs02 -26
e2 1.0010-11 3.2241-07
    5.3156-07 8.7640-07 1.4449-06 2.3823-06 3.9278-06
    6.4758-06 1.0677-05 1.7603-05 2.9023-05 4.7850-05
    7.8891-05 1.3007-04 2.1445-04 3.5357-04 5.8293-04
    9.6110-04 1.2341-03 1.5846-03 2.0346-03 2.6125-03
    3.3546-03 4.3073-03 5.5307-03 7.1016-03 9.1186-03
    1.1709-02 1.5034-02 1.9304-02 2.1874-02 2.4787-02
    2.8087-02 3.1827-02 3.6065-02 4.0867-02 4.6308-02
    5.2474-02 5.9461-02 6.7378-02 7.6349-02 8.6515-02
    9.8035-02 1.1109-01 1.2588-01 1.4264-01 1.6163-01
    1.8315-01 2.0754-01 2.3517-01 2.6649-01 3.0197-01
    3.4217-01 3.8774-01 4.3936-01 4.9786-01 5.6415-01
    6.3927-01 7.2438-01 8.2084-01 9.3013-01 1.0540+00
    1.1943+00 1.3533+00 1.5335+00 1.7377+00 1.8498+00
    1.9691+00 2.0961+00 2.2313+00 2.3752+00 2.5284+00
    2.6914+00 2.8650+00 3.0498+00 3.2465+00 3.4559+00
    3.6787+00 3.9160+00 4.1686+00 4.4374+00 4.7236+00
    5.0282+00 5.3525+00 5.6978+00 6.0652+00 6.4564+00
    6.8728+00 7.3161+00 7.7879+00 8.2902+00 8.8249+00
    9.3940+00 9.9999+00 1.0157+01 1.0317+01 1.0480+01
    1.0645+01 1.0812+01 1.0983+01 1.1156+01 1.1331+01
    1.1510+01 1.1691+01 1.1875+01 1.2062+01 1.2252+01
    1.2445+01 1.2641+01 1.2840+01 1.3042+01 1.3248+01
    1.3456+01 1.3668+01 1.3883+01 1.4102+01 1.4324+01
    1.4550+01 1.4779+01 1.5012+01 1.5248+01 1.5488+01
fc12 ---- Tritium production rate(TPR) Li-6(n,t) surface r=3cm
f12:n 2 5 8 10 13 17 18 22 24
fs12 -26
fq12 s e f m
fml2 (1) (1 3 105)
fc22 ---- fission rate (U-235) surface r=3cm
f22:n 4 6 7 9 11 14 16 19 21 23
fs22 -26
fc22 s e f m
fm22 (1) (1 12 18)
fc32 ---- reaction rate (Al27,Ti47,48,Fe56,Ni58,Zr90,Nb93,In115,Au197)
surface
f32:n 2 5 12 15 20 25
fs32 -26
fq32 s e f m
fm32 (1) (1 4 107) (1 5 211) (1 5 212) (1 6 103)
    (1 7 16) (1 7 103) (1 8 16) (1 9 16) (1 10 51)
    (1 11 102)
c -----
c ****
c * problem cutoff cards *
c ****
phys:n 16.0 0.0
mode n
cut:n 0 1.0e-10 -0.5 -0.25 0
nps 20000000
ctme 2000
c ****
c * peripheral cards *
c ****
prdmpr 200000 200000 1 1
lost 10 10
print

```

Fig. A-9 Continued (3/3).

```

>>> Analysis of Graphite Slab Experiment July 1994 <<<
c ***** front air region *****
1 2 4.921-5 +1 -2 -27 $ -1.00 - 20.00 cm
c ***** graphite region *****
2 1 8.2322-2 +2 -3 -26 $ 20.00 - 24.10 cm
3 1 8.2322-2 +2 -3 +26 -27 $ 20.00 - 24.10 cm
4 1 8.2322-2 +3 -4 -26 $ 24.10 - 26.60 cm
5 1 8.2322-2 +3 -4 +26 -27 $ 24.10 - 26.60 cm
6 1 8.2322-2 +4 -5 -26 $ 26.60 - 27.62 cm
7 1 8.2322-2 +4 -5 +26 -27 $ 26.60 - 27.62 cm
8 1 8.2322-2 +5 -6 -26 $ 27.62 - 30.00 cm
9 1 8.2322-2 +5 -6 +26 -27 $ 27.62 - 30.00 cm
10 1 8.2322-2 +6 -7 -26 $ 30.00 - 31.70 cm
11 1 8.2322-2 +6 -7 +26 -27 $ 30.00 - 31.70 cm
12 1 8.2322-2 +7 -8 -26 $ 31.70 - 36.80 cm
13 1 8.2322-2 +7 -8 +26 -27 $ 31.70 - 36.80 cm
14 1 8.2322-2 +8 -9 -26 $ 36.80 - 37.78 cm
15 1 8.2322-2 +8 -9 +26 -27 $ 36.80 - 37.78 cm
16 1 8.2322-2 +9 -10 -26 $ 37.78 - 40.20 cm
17 1 8.2322-2 +9 -10 +26 -27 $ 37.78 - 40.20 cm
18 1 8.2322-2 +10 -11 -26 $ 40.20 - 41.80 cm
19 1 8.2322-2 +10 -11 +26 -27 $ 40.20 - 41.80 cm
20 1 8.2322-2 +11 -12 -26 $ 41.80 - 46.90 cm
21 1 8.2322-2 +11 -12 +26 -27 $ 41.80 - 46.90 cm
22 1 8.2322-2 +12 -13 -26 $ 46.90 - 47.94 cm
23 1 8.2322-2 +12 -13 +26 -27 $ 46.90 - 47.94 cm
24 1 8.2322-2 +13 -14 -26 $ 47.94 - 50.40 cm
25 1 8.2322-2 +13 -14 +26 -27 $ 47.94 - 50.40 cm
26 1 8.2322-2 +14 -15 -26 $ 50.40 - 51.90 cm
27 1 8.2322-2 +14 -15 +26 -27 $ 50.40 - 51.90 cm
28 1 8.2322-2 +15 -16 -26 $ 51.90 - 57.00 cm
29 1 8.2322-2 +15 -16 +26 -27 $ 51.90 - 57.00 cm
30 1 8.2322-2 +16 -17 -26 $ 57.00 - 60.50 cm
31 1 8.2322-2 +16 -17 +26 -27 $ 57.00 - 60.50 cm
32 1 8.2322-2 +17 -18 -26 $ 60.50 - 62.10 cm
33 1 8.2322-2 +17 -18 +26 -27 $ 60.50 - 62.10 cm
34 1 8.2322-2 +18 -19 -26 $ 62.10 - 63.18 cm
35 1 8.2322-2 +18 -19 +26 -27 $ 62.10 - 63.18 cm
36 1 8.2322-2 +19 -20 -26 $ 63.18 - 67.10 cm
37 1 8.2322-2 +19 -20 +26 -27 $ 63.18 - 67.10 cm
38 1 8.2322-2 +20 -21 -26 $ 67.10 - 70.70 cm
39 1 8.2322-2 +20 -21 +26 -27 $ 67.10 - 70.70 cm
40 1 8.2322-2 +21 -22 -26 $ 70.70 - 72.20 cm
41 1 8.2322-2 +21 -22 +26 -27 $ 70.70 - 72.20 cm
42 1 8.2322-2 +22 -23 -26 $ 72.20 - 73.34 cm
43 1 8.2322-2 +22 -23 +26 -27 $ 72.20 - 73.34 cm
44 1 8.2322-2 +23 -24 -26 $ 73.34 - 77.20 cm
45 1 8.2322-2 +23 -24 +26 -27 $ 73.34 - 77.20 cm
46 1 8.2322-2 +24 -25 -26 $ 77.20 - 80.96 cm
47 1 8.2322-2 +24 -25 +26 -27 $ 77.20 - 80.96 cm
c ***** external void *****
48 0 -1 : +25 : +27 $

1      pz      -1.00 $ Source
2      pz      20.00 $ reaction rate
3      pz      24.10 $ fission & n-spec
4      pz      26.60 $ fission & n-spec
5      pz      27.62 $ g-spec
6      pz      30.00 $ reaction rate & g-heat
7      pz      31.70 $ fission & n-spec
8      pz      36.80 $ fission
9      pz      37.78 $ g-spec
10     pz      40.20 $ reaction rate & g-heat
11     pz      41.80 $ fission & n-spec
12     pz      46.90 $ fission
13     pz      47.94 $ g-spec
14     pz      50.40 $ reaction rate & g-heat
15     pz      51.90 $ fission & n-spec
16     pz      57.00 $ fission
17     pz      60.50 $ reaction rate & g-heat
18     pz      62.10 $ fission & n-spec
19     pz      63.18 $ g-spec
20     pz      67.10 $ fission
21     pz      70.70 $ reaction rate & g-heat
22     pz      72.20 $ fission & n-spec

```

Fig. A-10 A typical example of input data of MCNP for the analysis of the FNS/clean benchmark experiment on graphite.

```

23      pz      73.34 $ g-spec
24      pz      77.20 $ fission & n-spec
25      pz      80.96 $ reaction rate & g-heat
c
26      cz      3.00
27      cz      31.40

imp:n 1 1 1 1 1 1 1 1 1 1 1
1 1 1 1 1 2 2 2 2 2 2
2 2 2 2 2 2 2 4 4 4 4
4 4 4 4 4 4 4 4 4 4 0
imp:p 1 1 1 1 1 1 1 1 1 1 1
1 1 1 1 1 2 2 2 2 2 2
2 2 2 2 2 2 2 4 4 4 4
4 4 4 4 4 4 4 4 4 4 0
*****
c   * source specification cards *
c ****
sdef erg=d1 pos=0 0 0 vec=0 0 1 dir=d2 wgt=1.1767
sb2 -31 4.0
sil 5.8293-04
9.6110-04 1.2341-03 1.5846-03 2.0346-03 2.6125-03
3.3546-03 4.3073-03 5.5307-03 7.1016-03 9.1186-03
1.1709-02 1.5034-02 1.9304-02 2.1874-02 2.4787-02
2.8087-02 3.1827-02 3.6065-02 4.0867-02 4.6308-02
5.2474-02 5.9461-02 6.7378-02 7.6349-02 8.6515-02
9.8035-02 1.1109-01 1.2588-01 1.4264-01 1.6163-01
1.8315-01 2.0754-01 2.3517-01 2.6649-01 3.0197-01
3.4217-01 3.8774-01 4.3936-01 4.9786-01 5.6415-01
6.3927-01 7.2438-01 8.2084-01 9.3013-01 1.0540+00
1.1943+00 1.3533+00 1.5335+00 1.7377+00 1.8498+00
1.9691+00 2.0961+00 2.2313+00 2.3752+00 2.5284+00
2.6914+00 2.8650+00 3.0498+00 3.2465+00 3.4559+00
3.6787+00 3.9160+00 4.1686+00 4.4374+00 4.7236+00
5.0282+00 5.3525+00 5.6978+00 6.0652+00 6.4564+00
6.8728+00 7.3161+00 7.7879+00 8.2902+00 8.8249+00
9.3940+00 9.9999+00 1.0157+01 1.0317+01 1.0480+01
1.0645+01 1.0812+01 1.0983+01 1.1156+01 1.1331+01
1.1510+01 1.1691+01 1.1875+01 1.2062+01 1.2252+01
1.2445+01 1.2641+01 1.2840+01 1.3042+01 1.3248+01
1.3456+01 1.3668+01 1.3883+01 1.4102+01 1.4324+01
1.4550+01 1.4779+01 1.5012+01 1.5248+01 1.5488+01
1.5732+01 1.5980+01
sp1 0.0
4.3479-05 5.5907-05 6.3421-05 7.2417-05 8.3682-05
9.7598-05 1.1447-04 1.3521-04 1.6038-04 1.9164-04
2.1369-04 2.4812-04 3.0516-04 1.7891-04 2.0045-04
2.2407-04 2.5200-04 2.8444-04 3.2144-04 3.6436-04
4.1340-04 4.7077-04 5.3606-04 6.1088-04 6.9762-04
7.9663-04 9.1106-04 1.2219-03 1.4051-03 1.6141-03
1.8527-03 2.1040-03 2.4317-03 2.8136-03 3.2890-03
3.8479-03 4.9397-03 5.9791-03 6.8688-03 7.7929-03
8.6681-03 9.3421-03 9.7540-03 9.9713-03 9.7275-03
9.6236-03 9.7640-03 9.9677-03 1.0130-02 5.3179-03
5.3194-03 5.3383-03 5.3299-03 5.2928-03 5.0664-03
4.7354-03 4.3795-03 3.7938-03 3.4485-03 3.3610-03
3.6099-03 4.2412-03 4.3379-03 3.9704-03 3.5164-03
2.9628-03 2.5194-03 2.5754-03 2.7193-03 2.3830-03
2.1203-03 2.3331-03 2.4699-03 2.0821-03 1.9259-03
2.1711-03 2.3220-03 5.9892-04 5.9851-04 5.8562-04
6.0839-04 5.4544-04 5.2166-04 4.7551-04 3.3951-04
3.3956-04 3.5410-04 4.3340-04 4.9328-04 6.6341-04
9.1815-04 1.0510-03 1.3058-03 1.5353-03 2.0627-03
3.0739-03 4.0824-03 3.6889-03 4.7824-03 1.9619-02
8.8741-02 1.9088-01 2.8044-01 2.3566-01 7.1310-02
1.7363-02 2.7828-03
*****
c   * material specification cards *
c ****
c   --- graphite
m1 6012.37c 8.2322-2
c   --- air
m2 7014.37c 3.8810-5 8016.37c 1.0400-5
c   --- materials for reaction rate
m3 13027.03y 1.0 $ Al-27(n, alpha)
m4 28058.03y 1.0 $ Ni-58(n,2n) & Ni-58(n,p)
m5 40090.03y 1.0 $ Zr-90(n,2n)

```

Fig. A-10 Continued (2/4).

```

m6    41093.03y   1.0 $ Nb-93(n,2n)Nb-92m
m7    49115.03y   1.0 $ In-115(n,n')In-115m
m8    79197.03y   1.0 $ Au-197(n,gamma)
m9    90232.03y   1.0 $ Th-232(n,fission)
m10   92235.03y   1.0 $ U-235(n,fission)
m11   92238.03y   1.0 $ U-238(n,fission)
m12   93237.03y   1.0 $ Np-237(n,fission)
c ****
c * tally specification cards *
c ****
fc02 ---- neutron energy spectrum surface
f02:n 3 4 7 11 15 18 22 24
fq02 s m e f
fs02 -26
e2 1.0010-11 3.2241-07
      5.3156-07 8.7640-07 1.4449-06 2.3823-06 3.9278-06
      6.4758-06 1.0677-05 1.7603-05 2.9023-05 4.7850-05
      7.8891-05 1.3007-04 2.1445-04 3.5357-04 5.8293-04
      9.6110-04 1.2341-03 1.5846-03 2.0346-03 2.6125-03
      3.3546-03 4.3073-03 5.5307-03 7.1016-03 9.1186-03
      1.1709-02 1.5034-02 1.9304-02 2.1874-02 2.4787-02
      2.8087-02 3.1827-02 3.6065-02 4.0867-02 4.6308-02
      5.2474-02 5.9461-02 6.7378-02 7.6349-02 8.6515-02
      9.8035-02 1.1109-01 1.2588-01 1.4264-01 1.6163-01
      1.8315-01 2.0754-01 2.3517-01 2.6649-01 3.0197-01
      3.4217-01 3.8774-01 4.3936-01 4.9786-01 5.6415-01
      6.3927-01 7.2438-01 8.2084-01 9.3013-01 1.0540+00
      1.1943+00 1.3533+00 1.5335+00 1.7377+00 1.8498+00
      1.9691+00 2.0961+00 2.2313+00 2.3752+00 2.5284+00
      2.6914+00 2.8650+00 3.0498+00 3.2465+00 3.4559+00
      3.6787+00 3.9160+00 4.1686+00 4.4374+00 4.7236+00
      5.0282+00 5.3525+00 5.6978+00 6.0652+00 6.4564+00
      6.8728+00 7.3161+00 7.7879+00 8.2902+00 8.8249+00
      9.3940+00 9.9999+00 1.0157+01 1.0317+01 1.0480+01
      1.0645+01 1.0812+01 1.0983+01 1.1156+01 1.1331+01
      1.1510+01 1.1691+01 1.1875+01 1.2062+01 1.2252+01
      1.2445+01 1.2641+01 1.2840+01 1.3042+01 1.3248+01
      1.3456+01 1.3668+01 1.3883+01 1.4102+01 1.4324+01
      1.4550+01 1.4779+01 1.5012+01 1.5248+01 1.5488+01
      1.5732+01 1.5980+01
fc12 ---- fission rate (U-235,U-238,Np-237,Th-232) surface r=3cm
f12:n 3 4 7 8 11 12 15 16 18 20 22 24
fs12 -26
fq12 s e f m
fm12 (1) (1 9 18) (1 10 18) (1 11 18) (1 12 18)
fc22 ---- reaction rate (Al-27,Ni-58,Zn-64,Nb-93,In-115,Au-197) surface
f22:n 2 6 10 14 17 21 25
fs22 -26
fq22 s e f m
fm22 (1) (1 3 107) (1 4 16) (1 4 103) (1 5 16)
(1 6 16) (1 7 51) (1 8 102)
fc102 ---- gamma-ray energy spectrum & heat surface r=3cm
f102:p 5 6 9 10 13 14 17 19 21 23 25
fs102 -26
fq102 s m e f
e102 1.0000-02 2.0000-02 3.0000-02 4.5000-02 6.0000-02
      8.0000-02 1.0000-01 1.5000-01 2.0000-01 3.0000-01
      4.0000-01 5.0000-01 5.2000-01 6.0000-01 7.0000-01
      8.0000-01 9.0000-01 1.0000+00 1.1300+00 1.2500+00
      1.3800+00 1.5000+00 1.7500+00 2.0000+00 2.2500+00
      2.5000+00 3.0000+00 3.5000+00 4.0000+00 4.5000+00
      5.0000+00 5.5000+00 6.0000+00 6.5000+00 7.0000+00
      7.5000+00 8.0000+00 9.0000+00 1.0000+01 1.2000+01
      1.4000+01
c ****
c * problem cutoff cards *
c ****
phys:n 16.0 0.0
phys:p 30.0 1 0
phys:e 30.0 1 1 1 1 1 1 1 1
mode n p
cut:n 0 1.0e-10 -0.5 -0.25 0
cut:p 0 0.0099 -0.5 -0.25 0
cut:e 0 0.3 -0.5 -0.25 0
nps 20000000
ctme 2000

```

Fig. A-10 Continued (3/4).

```

c *****
c * peripheral cards *
c *****
prdmp 200000 200000 1 1
lost   10    10
print

```

Fig. A-10 Continued (4/4).

```

>>> Analysis for Clean Benchmark Experiment on Iron <<<
c *****
c * cell carad for Iron Assembly *
c *****
c ***** air region *****
1 2 4.9210-5 (+1 -2 -42) : (+2 -3 +41 -42)      $ source
void
3 2 4.9210-5 +2 -3 -41      $ cell detecter
c ***** test region *****
4 1 8.5182-2 +3 -4 -42      $ 0.0 - 1.5 cm
5 1 8.5182-2 +4 -5 -42      $ 1.5 - 2.5 cm
6 1 8.5182-2 +5 -6 -42      $ 2.5 - 4.0 cm
7 1 8.5182-2 +6 -7 -42      $ 4.0 - 5.0 cm
8 1 8.5182-2 +7 -8 -42      $ 5.0 - 6.5 cm
9 1 8.5182-2 +8 -9 -42      $ 6.5 - 10.0 cm
10 1 8.5182-2 +9 -10 -42     $ 10.0 - 11.0 cm
11 1 8.5182-2 +10 -11 -42     $ 11.0 - 11.5 cm
12 1 8.5182-2 +11 -12 -42     $ 11.5 - 20.0 cm
13 1 8.5182-2 +12 -13 -42     $ 20.0 - 21.0 cm
14 1 8.5182-2 +13 -14 -42     $ 21.0 - 21.5 cm
15 1 8.5182-2 +14 -15 -42     $ 21.5 - 30.0 cm
16 1 8.5182-2 +15 -16 -42     $ 30.0 - 31.0 cm
17 1 8.5182-2 +16 -17 -42     $ 31.0 - 31.5 cm
18 1 8.5182-2 +17 -18 -42     $ 31.5 - 40.0 cm
19 1 8.5182-2 +18 -19 -42     $ 40.0 - 41.0 cm
20 1 8.5182-2 +19 -20 -42     $ 41.0 - 41.5 cm
21 1 8.5182-2 +20 -21 -42     $ 41.5 - 50.0 cm
22 1 8.5182-2 +21 -22 -42     $ 50.0 - 51.5 cm
23 1 8.5182-2 +22 -23 -42     $ 51.5 - 60.0 cm
24 1 8.5182-2 +23 -24 -42     $ 60.0 - 61.0 cm
25 1 8.5182-2 +24 -25 -42     $ 61.0 - 70.0 cm
26 1 8.5182-2 +25 -26 -42     $ 70.0 - 71.5 cm
27 1 8.5182-2 +26 -27 -42     $ 71.5 - 80.0 cm
28 1 8.5182-2 +27 -28 -42     $ 80.0 - 81.0 cm
29 1 8.5182-2 +28 -29 -42     $ 81.0 - 90.0 cm
30 1 8.5182-2 +29 -30 -42     $ 90.0 - 91.5 cm
31 1 8.5182-2 +30 -31 -42     $ 91.5 - 95.0 cm
c ***** rear air region *****
32 2 4.9210-5 +31 -32 -41      $ cell detecter
33 2 4.9210-5 +31 -32 +41 -42      $
c ***** external void *****
34 0           -1 : +32 : +42      $
c ----- blank delimiter

c *****
c * surface card *
c *****
1      pz          -21.0 $ Source
2      pz          -2.0  $ keV

```

Fig. A-11 A typical example of input data of MCNP for the analysis of the FNS/clean benchmark experiment on iron.

```

3      pz      0.0 $ foil, TLD
4      pz      1.5 $ MeV, NE-g
5      pz      2.5 $ foil, TLD
6      pz      4.0 $ MeV
7      pz      5.0 $ foil
8      pz      6.5 $ MeV, NE-g
9      pz      10.0 $ foil, TLD, g-spec
10     pz      11.0 $ keV, eV
11     pz      11.5 $ MeV, NE-g
12     pz      20.0 $ foil, TLD
13     pz      21.0 $ keV, eV
14     pz      21.5 $ MeV, NE-g
15     pz      30.0 $ foil, TLD, g-spec
16     pz      31.0 $ keV, eV
17     pz      31.5 $ MeV, NE-g
18     pz      40.0 $ foil, TLD
19     pz      41.0 $ keV, eV
20     pz      41.5 $ MeV, NE-g
21     pz      50.0 $ foil, TLD, g-spec
22     pz      51.5 $ MeV
23     pz      60.0 $ TLD
24     pz      61.0 $ keV, eV
25     pz      70.0 $ foil, TLD, g-spec
26     pz      71.5 $ MeV, NE-g
27     pz      80.0 $ TLD
28     pz      81.0 $ keV, eV
29     pz      90.0 $ TLD
30     pz      91.5 $ NE-g
31     pz      95.0 $ TLD
32     pz      97.0 $ keV
c
41     cz      4.0
42     cz      50.0
43     cz      10.0
c ----- blank delimiter
c ****
c * mode card *
c ****
mode n p
c ****
c * weight window cards *
c ****
ext:n  0      0      0.1z  0.1z  0.1z  0.1z  0.1z  0.1z  0.1z  0.1z  0.1z
       0.1z  0.1z  0.1z  0.1z  0.1z  0.1z  0.1z  0.1z  0.1z  0.1z  0.1z
       0.1z  0.1z  0.1z  0.1z  0.1z  0.1z  0.1z  0.1z  0.1z  0.1z  0.1z
       0      0
wwe:n  1.0e-3 1.0  5.0  10.0  16.0
wwp:n  5      3      5      0      0
wwn1:n $ for eV neutrons
       1.0e-1  1.0e-1  1.0e-1  1.0e-1
       5.0e-2  2.0e-2  1.0e-2  0.7e-2  0.5e-2
       0.3e-2  0.2e-2  1.0e-3  1.0e-3  1.0e-3
       1.0e-3  1.0e-3  1.0e-3  1.0e-3  1.0e-3
       1.0e-3  1.0e-3  1.0e-3  7.0e-4  5.0e-4
       3.0e-4  2.0e-4  1.0e-4  1.0e-4  1.0e-4
       1.0e-4  1.0e-4  1.0e-4  -1
wwn2:n $ for keV neutrons
       1.0e-1  1.0e-1  1.0e-1  1.0e-1
       5.0e-2  3.0e-2  2.0e-2  1.4e-2  1.0e-2
       1.0e-2  1.0e-2  1.0e-2  1.0e-2  1.0e-2
       1.0e-2  1.0e-2  1.0e-2  1.0e-2  1.0e-2
       1.0e-2  1.0e-2  1.0e-2  7.0e-3  5.0e-3
       3.0e-3  2.0e-3  1.0e-3  1.0e-3  1.0e-3
       1.0e-3  1.0e-3  1.0e-3  -1
wwn3:n $ for 1-5MeV neutrons
       1.0e-1  1.0e-1  1.0e-1  1.0e-1
       5.0e-2  5.0e-2  5.0e-2  2.0e-2  2.0e-2
       2.0e-2  1.0e-2  5.0e-3  5.0e-3  3.0e-3
       2.0e-3  2.0e-3  1.0e-3  5.0e-4  5.0e-4
       2.0e-4  1.0e-4  5.0e-5  2.0e-5  1.0e-5
       5.0e-6  2.0e-6  1.0e-6  1.0e-6  1.0e-6
       1.0e-6  1.0e-6  1.0e-6  -1
wwn4:n $ for 5-13 MeV Neutrons
       1.0e-1  1.0e-1  1.0e-1  1.0e-1
       5.0e-2  5.0e-2  5.0e-2  1.5e-2  1.5e-2
       1.5e-2  5.0e-3  1.5e-3  1.5e-3  6.4e-4

```

Fig. A-11 Continued (2/4).

```

3.2e-4 3.2e-4 1.6e-4 8.0e-5 8.0e-5
4.0e-5 2.0e-5 1.0e-5 5.0e-6 2.5e-6
1.2e-6 6.0e-7 3.0e-7 3.0e-7 3.0e-7
3.0e-7 3.0e-7 3.0e-7 -1
wwn5:n $ for 14 MeV Neutrons
1.0e-1 1.0e-1 1.0e-1 8.5e-2
7.0e-2 5.0e-2 4.0e-2 3.0e-2 2.0e-2
1.0e-2 5.0e-3 1.5e-3 1.5e-3 5.0e-4
1.5e-4 1.5e-4 5.0e-5 1.5e-5 1.5e-5
6.4e-6 3.2e-6 1.6e-6 8.0e-7 4.0e-7
2.0e-7 1.0e-7 5.0e-8 5.0e-8 5.0e-8
5.0e-8 5.0e-8 5.0e-8 -1
wwe:p 100.0
wwp:p 5 3 5 0 0
wwnl:p $ for gamma-rays
1.0e-1 1.0e-1 1.0e-1 1.0e-1
5.0e-2 5.0e-2 5.0e-2 2.0e-2 2.0e-2
2.0e-2 1.0e-2 7.0e-3 7.0e-3 5.0e-3
3.0e-3 3.0e-3 2.0e-3 1.4e-3 1.4e-3
1.0e-3 7.0e-4 5.0e-4 3.0e-4 2.0e-4
1.0e-4 7.0e-5 5.0e-5 5.0e-5 5.0e-5
5.0e-5 5.0e-5 5.0e-5 -1
*****
c * source specification cards *
c * a user supplied source subroutine is used. *
c * material specification cards *
c ****
c --- Iron
m1 26000.37c 0.083490      6012.37c 0.000727
    14000.37c 0.000249      25055.37c 0.000716
c --- air
m2 7014.37c 3.8810-5      8016.37c 1.0400-5
c --- materials for reaction rate
m3 5010.03y 1.0 $ B-10(n,alpha)
m4 13027.03y 1.0 $ Al-27(n,alpha)
m5 22000.03y 1.0 $ Ti-nat(n,x)Sc-48
m6 25055.34c 1.0 $ Mn-55(n,gamma)
m7 26056.03y 1.0 $ Fe-56(n,p)
m8 28058.03y 1.0 $ Ni-58(n,2n) & Ni-58(n,p)
m9 30064.03y 1.0 $ Zn-64(n,p)
m10 40090.03y 1.0 $ Zr-90(n,2n)
m11 41093.03y 1.0 $ Nb-93(n,2n)Nb-92m
m12 49115.03y 1.0 $ In-115(n,n')In-115m
m13 79197.03y 1.0 $ Au-197(n,gamma)
m14 92235.03y 1.0 $ U-235(n,fission)
c ****
c * tally specification cards *
c ****
fc02 ---- neutron reaction rate      surface r=4cm
f02:n 3 4 5 6 7 8 9 10 11 12
      13 14 15 16 17 18 19 20 21 22
      23 24 25 26 27 28 29 30 31
fs02 -41
fg02 s e f m
e02 16.0
fm02 (1)      (1 1 1) (1 1 2) (1 1 102)
      (1 3 107) (1 3 207) (1 4 107) (1 5 212) (1 6 102)
      (1 7 103) (1 8 16) (1 8 103) (1 9 103) (1 10 16)
      (1 11 16) (1 12 51) (1 13 102) (1 14 18)
fc12 ---- neutron energy spectrum (decade)      surface r=4cm
f12:n 3 4 5 6 7 8 9 10 11 12
      13 14 15 16 17 18 19 20 21 22
      23 24 25 26 27 28 29 30 31
fq12 s f e
fs12 -41
e12 1e-7 1e-6 1e-5 1e-4 1e-3 1e-2 1e-1 1e+0 1e+1 2e+1
fc24 ---- neutron energy spectrum (decade)      cell
f24:n 3 32
e24 1e-7 1e-6 1e-5 1e-4 1e-3 1e-2 1e-1 1e+0 1e+1 2e+1
fc32 ---- neutron energy spectrum      surface r=4cm
f32:n 3 4 5 6 7 8 9 10 11 12
      13 14 15 16 17 18 19 20 21 22
      23 24 25 26 27 28 29 30 31
fs32 -41
fc44 ---- neutron energy spectrum      cell
f44:n 3 32

```

Fig. A-11 Continued (3/4).

```

fc102 ---- gamma-ray energy spectrum      surface r=4cm
f102:p 3 4 5 6 7 8 9 10 11 12
       13 14 15 16 17 18 19 20 21 22
       23 24 25 26 27 28 29 30 31
fs102 -41
e102  1.0000-02  2.0000-02  3.0000-02  4.5000-02  6.0000-02
      8.0000-02  1.0000-01  1.5000-01  2.0000-01  3.0000-01
      4.0000-01  5.0000-01  5.2000-01  6.0000-01  7.0000-01
      8.0000-01  9.0000-01  1.0000+00  1.1300+00  1.2500+00
      1.3800+00  1.5000+00  1.7500+00  2.0000+00  2.2500+00
      2.5000+00  3.0000+00  3.5000+00  4.0000+00  4.5000+00
      5.0000+00  5.5000+00  6.0000+00  6.5000+00  7.0000+00
      7.5000+00  8.0000+00  9.0000+00  1.0000+01  1.2000+01
      1.4000+01

c
fq0  s m e f
e0  1.0010-11  3.2241-07
      5.3156-07  8.7640-07  1.4449-06  2.3823-06  3.9278-06
      6.4758-06  1.0677-05  1.7603-05  2.9023-05  4.7850-05
      7.8891-05  1.3007-04  2.1445-04  3.5357-04  5.8293-04
      9.6110-04  1.2341-03  1.5846-03  2.0346-03  2.6125-03
      3.3546-03  4.3073-03  5.5307-03  7.1016-03  9.1186-03
      1.1709-02  1.5034-02  1.9304-02  2.1874-02  2.4787-02
      2.8087-02  3.1827-02  3.6065-02  4.0867-02  4.6308-02
      5.2474-02  5.9461-02  6.7378-02  7.6349-02  8.6515-02
      9.8035-02  1.1109-01  1.2588-01  1.4264-01  1.6163-01
      1.8315-01  2.0754-01  2.3517-01  2.6649-01  3.0197-01
      3.4217-01  3.8774-01  4.3936-01  4.9786-01  5.6415-01
      6.3927-01  7.2438-01  8.2084-01  9.3013-01  1.0540+00
      1.1943+00  1.3533+00  1.5335+00  1.7377+00  1.8498+00
      1.9691+00  2.0961+00  2.2313+00  2.3752+00  2.5284+00
      2.6914+00  2.8650+00  3.0498+00  3.2465+00  3.4559+00
      3.6787+00  3.9160+00  4.1686+00  4.4374+00  4.7236+00
      5.0282+00  5.3525+00  5.6978+00  6.0652+00  6.4564+00
      6.8728+00  7.3161+00  7.7879+00  8.2902+00  8.8249+00
      9.3940+00  9.9999+00  1.0157+01  1.0317+01  1.0480+01
      1.0645+01  1.0812+01  1.0983+01  1.1156+01  1.1331+01
      1.1510+01  1.1691+01  1.1875+01  1.2062+01  1.2252+01
      1.2445+01  1.2641+01  1.2840+01  1.3042+01  1.3248+01
      1.3456+01  1.3668+01  1.3883+01  1.4102+01  1.4324+01
      1.4550+01  1.4779+01  1.5012+01  1.5248+01  1.5488+01

c ****
c   * problem cutoff cards *
c ****
phys:n  16.0  0.0
phys:p  30.0  1  0
phys:e  30.0  1  1  1  1  1  1  1  1
cut:n  0  1.0e-11  -0.5  -0.25  0
cut:p  0  0.0099  -0.5  -0.25  0
nps  1000000
ctme  1000000
c ****
c   * user data arrays *
c ****
idum  1
rdum  0.0  0.0  -20.0
c ****
c   * peripheral crads *
c ****
prdmp  100000  100000  1  1
lost   10          10
print

```

Fig. A-11 Continued (4/4).

```

Analysis of the FNS Bulk Shielding Experiment #2 JENDL-3.2 Oct. 1994
c ****
c * cell card *
c ****
1   4  4.9210-5  (1 -2 -30) : (2 -3 -34) #34      $ source region
34  4  4.9215-5  19   -3   -31                      $ cell for track
length
2   1  8.5792-2   3   -4   -33                      $ SS316
3   1  8.5792-2   4   -5   -33                      $ SS316
4   1  8.5792-2   5   -6   -33                      $ SS316
5   1  8.5792-2   6   -7   -33                      $ SS316
6   1  8.5792-2   7   -8   -33                      $ SS316
7   1  8.5792-2   8   -9   -33                      $ SS316
8   1  8.5792-2   9   -10  -33                      $ SS316
9   1  8.5792-2  10  -11  -33                      $ SS316
10  1  8.5792-2  11  -12  -33                      $ SS316
11  1  8.5792-2  12  -13  -33                      $ SS316
12  1  8.5792-2  13  -14  -33                      $ SS316
13  1  8.5792-2  14  -15  -33                      $ SS316
14  1  8.5792-2  15  -16  -33                      $ SS316
15  1  8.5792-2  16  -17  -33                      $ SS316
16  1  8.5792-2  17  -18  -33                      $ SS316
17  1  8.5792-2   3   -4   33  -35                  $ SS316
18  1  8.5792-2   4   -5   33  -35                  $ SS316
19  1  8.5792-2   5   -6   33  -35                  $ SS316
20  1  8.5792-2   6   -7   33  -35                  $ SS316
21  1  8.5792-2   7   -8   33  -35                  $ SS316
22  1  8.5792-2   8   -9   33  -35                  $ SS316
23  1  8.5792-2   9   -10  33  -35                  $ SS316
24  1  8.5792-2  10  -11  33  -35                  $ SS316
25  1  8.5792-2  11  -12  33  -35                  $ SS316
26  1  8.5792-2  12  -13  33  -35                  $ SS316
27  1  8.5792-2  13  -14  33  -35                  $ SS316
28  1  8.5792-2  14  -15  33  -35                  $ SS316
29  1  8.5792-2  15  -16  33  -35                  $ SS316
30  1  8.5792-2  16  -17  33  -35                  $ SS316
31  1  8.5792-2  17  -18  33  -35                  $ SS316
32  3  8.5699-2  (1 -2 30 -35) : (2 -3 34 -35) $ source reflector
33  0           -1 : 18 : 35                         $ void

.c ****
c * surface card *
c ****
1    pz   -51.28
2    pz   -30.96
3    pz   30.00
4    pz   38.00
5    pz   40.16
6    pz   50.00
7    pz   52.86
8    pz   62.00
9    pz   65.56
10   pz   74.00
11   pz   83.34
12   pz   86.00
13   pz   96.00
14   pz   101.12
15   pz   106.00
16   pz   116.00
17   pz   121.44
18   pz   141.80
19   pz   28.00
30   cz   6.83
31   cz   4.00
33   cz   20.00
34   cz   40.00
35   cz   60.00

c ****
c * mode card - neutron & photon *
c ****
mode n p
c ****
c * weight window card *
c ****

```

Fig. A-12 A typical example of input data of MCNP for the analysis of the FNS/clean benchmark experiment on SS-316.

```

ext:n   0      0      0.1z  0.1z  0.1z  0.1z  0.1z  0.1z  0.1z  0.1z  0.1z
        0.1z  0.1z  0.1z  0.1z  0.1z  0.1z  0.1z  0.1z  0.1z  0.1z  0.1z
        0.1z  0.1z  0.1z  0.1z  0.1z  0.1z  0.1z  0.1z  0.1z  0.1z  0.1z
        0.1z  0.1z  0      0
wwe:n   1.0e-5  1.0    5.0   13.0  100.0
wwp:n   5      3      5      0      0
wwn1:n $ for thermal neutrons
        0.4      0.4      $ source void
        0.1      0.03     0.02     0.015    0.01
        0.006    0.004    0.0025   0.0015   0.001
        6.0e-4   4.0e-4   2.5e-4   1.5e-4   1.0e-4
        0.4      0.12     0.08     0.06     0.04
        0.024    0.016    0.01     0.006    0.004
        0.0024   0.0016   0.001    6.0e-4   4.0e-4
        0.4      -1      $ source reflector, external void
wwn2:n $ for eV, keV neutrons
        0.4      0.4      $ source void
        0.4      0.4      0.4      0.4      0.25
        0.15     0.1      0.06     0.04     0.025
        0.015     0.01     0.006    0.004    0.0025
        0.8      0.8      0.8      0.8      0.8
        0.6      0.4      0.24     0.16     0.1
        0.06     0.04     0.024    0.016    0.01
        0.4      -1      $ source reflector, external void
wwn3:n $ for 1-5MeV neutrons
        0.4      0.4      $ source void
        0.1      0.06     0.04     0.02     0.01
        0.004    0.002    0.001    3.0e-4   1.0e-4
        3.0e-5   1.0e-5   3.0e-6   1.0e-6   3.0e-7
        0.4      0.24     0.16     0.08     0.04
        0.016    0.008    0.004    0.0012   4.0e-4
        1.2e-4   4.0e-5   1.2e-5   4.0e-6   1.2e-6
        0.4      -1      $ source reflector, external void
wwn4:n $ for 5-13MeV neutrons
        0.4      0.4      $ source void
        0.1      0.025    0.0064   0.0016   8.0e-4
        2.0e-4   1.0e-4   2.5e-5   1.2e-5   3.2e-6
        8.0e-7   4.0e-7   2.0e-7   1.0e-7   5.0e-8
        0.4      0.1      0.025    0.0064   0.0032
        8.0e-4   4.0e-4   1.0e-4   4.8e-5   1.2e-5
        3.2e-6   1.6e-6   8.0e-7   4.0e-7   2.0e-7
        0.4      -1      $ source reflector, external void
wwn5:n $ for 14MeV neutrons
        0.4      0.4      $ source void
        0.1      0.025    0.0064   0.0016   4.0e-4
        1.0e-4   4.8e-5   1.2e-5   6.0e-6   1.5e-6
        4.0e-7   1.9e-7   4.8e-8   1.2e-8   6.4e-9
        0.4      0.1      0.025    0.0064   0.0016
        4.0e-4   1.9e-4   4.8e-5   2.4e-5   6.0e-6
        1.6e-6   7.6e-7   1.9e-7   4.8e-8   2.5e-8
        0.4      -1      $ source reflector, external void
wwe:p   100.0
wwp:p   5      3      5      0      0
wwn1:p $ for gamma-rays
        0.4      0.4      $ source void
        0.1      0.03     0.015    0.01     0.007
        0.005    0.0035   0.0025   0.0018   0.0013
        9.0e-4   6.3e-4   4.5e-4   3.2e-4   2.2e-4
        0.4      0.12     0.06     0.04     0.028
        0.02     0.014    0.01     0.0072   0.00
        0.0036   0.00252  0.0018    0.00128  8.8e-4
        0.4      -1      $ source reflector, external void
c ****
c * source specification cards *
c ****
c an user supplied source subroutine is used.
c ****
c * material specification cards *
c ****
c ----- materials for the assembly -----
m1   14000.37c  9.8440-4  24000.37c  1.5476-2  $ SS316 in test
region
25055.37c  9.7963-4  26000.37c  5.7589-2
28000.37c  9.7128-3  42000.37c  1.0503-3
m3   14000.37c  8.1608-4  24000.37c  1.5025-2  $ SS316 in source
reflector
25055.37c  1.3561-3  26000.37c  5.8331-2

```

Fig. A-12 Continued (2/4).

```

28000.37c 9.1456-3 42000.37c 1.0254-3
m4      7014.37c 3.8810-5 8016.37c 1.0400-5   $ air
c ----- materials for dosimetry reactions -----
m5      2003.37c 1.0  $ He-3 (n,p)
m6      5010.03y 1.0  $ B-10 (n,a)  a-prod.
m7      7014.37c 1.0  $ N-14 (n,p)
m8      13027.03y 1.0  $ Al-27(n,a)
m9      22000.03y 1.0  $ Ti-0 (n,x) Sc-46, Sc-47, Sc-48
m10     25055.03y 1.0  $ Mn-55(n,g)
m11     26054.03y 1.0  $ Fe-54(n,p)
m12     26056.03y 1.0  $ Fe-56(n,p)
m13     27059.37c 1.0  $ Co-59(n,2n), (n,g), (n,a), (n,p)
m14     28058.03y 1.0  $ Ni-58(n,2n), (n,p)
m15     29063.03y 1.0  $ Cu-63(n,2n), (n,g), (n,a)
m16     29065.37c 1.0  $ Cu-65(n,2n), (n,g)
m17     30064.03y 1.0  $ Zn-64(n,p)
m18     40090.03y 1.0  $ Zr-90(n,2n)
m19     41093.03y 1.0  $ Nb-93(n,2n)Nb-92m
m20     49115.03y 1.0  $ In-115(n,n')In-115m
m21     74186.03y 1.0  $ W-186(n,g)
m22     79197.03y 1.0  $ Au-197(n,g)
m23     92235.03y 1.0  $ U-235(n,f)
m24     92238.03y 1.0  $ U-238(n,f)
c ----- materials for (n,g) reactions of the assembly itself -----
m31     1001.37c 1.0  $ Hydrogen
m32     8016.37c 1.0  $ Oxygen
m33     14000.37c 1.0  $ Silicon
m34     24000.37c 1.0  $ Chromium
m38     25055.37c 1.0  $ Manganese
m35     26000.37c 1.0  $ Iron
m36     28000.37c 1.0  $ Nickel
m37     42000.37c 1.0  $ Molybdenum
c ****
c * tally specification cards *
c ****
fc12 >>> neutron reaction rate surface (r=4cm) <<<<
f12:n 3 4 5 6 7 8 9 10 11 12
      13 14 15 16 17 18
fm12 (1) (1 1 1) (1 1 2) (1 1 102)
      (1 5 103) (1 6 107) (1 6 207) (1 7 103) (1 8 107)
      (1 9 210) (1 9 211) (1 9 212) (1 10 102) (1 11 103)
      (1 12 103) (1 13 16) (1 13 102) (1 13 103) (1 13 107)
      (1 14 16) (1 14 103) (1 15 16) (1 15 102) (1 15 107)
      (1 16 16) (1 16 102) (1 17 103) (1 18 16) (1 19 16)
      (1 20 51) (1 21 102) (1 22 102) (1 23 18) (1 24 18)
      (1 33 102) (1 34 102) (1 35 102) (1 36 102) (1 37 102)
      (1 38 102)
fs12 -31
fq12 s e f m
e12 15.488
fc22 >>> neutron energy-dependent reaction rate surface (r=4cm)
<<<<
f22:n 3 4 5 6 7 8 9 10 11 12
      13 14 15 16 17 18
fm22 (1) (1 1 1) (1 1 2) (1 1 102)
      (1 5 103) (1 6 107) (1 6 207) (1 7 103) (1 8 107)
      (1 9 210) (1 9 211) (1 9 212) (1 10 102) (1 11 103)
      (1 12 103) (1 13 16) (1 13 102) (1 13 103) (1 13 107)
      (1 14 16) (1 14 103) (1 15 16) (1 15 102) (1 15 107)
      (1 16 16) (1 16 102) (1 17 103) (1 18 16) (1 19 16)
      (1 20 51) (1 21 102) (1 22 102) (1 23 18) (1 24 18)
      (1 33 102) (1 34 102) (1 35 102) (1 36 102) (1 37 102)
      (1 38 102)
fs22 -31
fq22 s m e f
e22 1e-7 1e-6 1e-5 1e-4 1e-3 1e-2 1e-1 2e-1 5e-1 1e+0
      2e+0 5e+0 1e+1 15.488
fc42 >>> neutron spectrum surface (r=4cm) <<<<
f42:n 3 5 7 9 11 14 17
fs42 -31
fc52 >>> neutron spectrum-decade surface (r=4cm) <<<<
f52:n 3 4 5 6 7 8 9 10 11 12
      13 14 15 16 17 18
fs52 -31
e52 1e-7 1e-6 1e-5 1e-4 1e-3 1e-2 1e-1 1 2 10 15.488
fc64 >>> neutron spectrum cell (r=4cm) <<<<

```

Fig. A-12 Continued (3/4).

```

f64:n 34
fc74 >>>> neutron spectrum-decade cell (r=4cm) <<<<
f74:n 34
e74 1e-7 1e-6 1e-5 1e-4 1e-3 1e-2 1e-1 1 2 10 15.488
fc102 >>>> photon spectrum surface (r=4cm) <<<<
f102:p 3 4 5 6 7 8 9 10 11 12
13 14 15 16 17 18
e102 1.0000-02 2.0000-02 3.0000-02 4.5000-02 6.0000-02
8.0000-02 1.0000-01 1.5000-01 2.0000-01 3.0000-01
4.0000-01 5.0000-01 5.2000-01 6.0000-01 7.0000-01
8.0000-01 9.0000-01 1.0000+00 1.1300+00 1.2500+00
1.3800+00 1.5000+00 1.7500+00 2.0000+00 2.2500+00
2.5000+00 3.0000+00 3.5000+00 4.0000+00 4.5000+00
5.0000+00 5.5000+00 6.0000+00 6.5000+00 7.0000+00
7.5000+00 8.0000+00 9.0000+00 1.0000+01 1.2000+01
1.4000+01
fs102 -31
c -----
fq0 s m e f
e0 1.0010-11 3.2241-07
5.3156-07 8.7640-07 1.4449-06 2.3823-06 3.9278-06
6.4758-06 1.0677-05 1.7603-05 2.9023-05 4.7850-05
7.8891-05 1.3007-04 2.1445-04 3.5357-04 5.8293-04
9.6110-04 1.2341-03 1.5846-03 2.0346-03 2.6125-03
3.3546-03 4.3073-03 5.5307-03 7.1016-03 9.1186-03
1.1709-02 1.5034-02 1.9304-02 2.1874-02 2.4787-02
2.8087-02 3.1827-02 3.6065-02 4.0867-02 4.6308-02
5.2474-02 5.9461-02 6.7378-02 7.6349-02 8.6515-02
9.8035-02 1.1109-01 1.2588-01 1.4264-01 1.6163-01
1.8315-01 2.0754-01 2.3517-01 2.6649-01 3.0197-01
3.4217-01 3.8774-01 4.3936-01 4.9786-01 5.6415-01
6.3927-01 7.2438-01 8.2084-01 9.3013-01 1.0540+00
1.1943+00 1.3533+00 1.5335+00 1.7377+00 1.8498+00
1.9691+00 2.0961+00 2.2313+00 2.3752+00 2.5284+00
2.6914+00 2.8650+00 3.0498+00 3.2465+00 3.4559+00
3.6787+00 3.9160+00 4.1686+00 4.4374+00 4.7236+00
5.0282+00 5.3525+00 5.6978+00 6.0652+00 6.4564+00
6.8728+00 7.3161+00 7.7879+00 8.2902+00 8.8249+00
9.3940+00 9.9999+00 1.0157+01 1.0317+01 1.0480+01
1.0645+01 1.0812+01 1.0983+01 1.1156+01 1.1331+01
1.1510+01 1.1691+01 1.1875+01 1.2062+01 1.2252+01
1.2445+01 1.2641+01 1.2840+01 1.3042+01 1.3248+01
1.3456+01 1.3668+01 1.3883+01 1.4102+01 1.4324+01
1.4550+01 1.4779+01 1.5012+01 1.5248+01 1.5488+01
c ****
c * problem cutoff cards *
c ****
phys:n 16.0 0.0
phys:p 30.0 0 0
phys:e 30.0 1 1 1 1 1 1 1
cut:n 0 0.0 -0.5 -0.25 0
cut:p 0 0.0099 -0.5 -0.25 0
nps 4000000
ctme 1000000
c ****
c * user data arrays *
c ****
idum 1
rdum 0.0 0.0 0.0
c ****
c * peripheral cards *
c ****
prdmp 1000000 1000000 1 1
lost 10 10
print

```

Fig. A-12 Continued (4/4).

```

Analysis of copper cclean benchmark experiment with JENDL-3.2
C ****
C * cell card *
C ****
1 2 4.9210-5 1 -2 -22
2 2 4.9210-5 2 -3 -22
3 1 8.4627-2 3 -4 -22
4 1 8.4627-2 4 -5 -22
5 1 8.4627-2 5 -6 -22
6 1 8.4627-2 6 -7 -22
7 1 8.4627-2 7 -8 -22
8 1 8.4627-2 8 -9 -22
9 1 8.4627-2 9 -10 -22
10 1 8.4627-2 10 -11 -22
11 1 8.4627-2 11 -12 -22
12 1 8.4627-2 12 -13 -22
13 1 8.4627-2 13 -14 -22
14 1 8.4627-2 14 -15 -22
15 1 8.4627-2 15 -16 -22
16 1 8.4627-2 16 -17 -22
17 1 8.4627-2 17 -18 -22
18 1 8.4627-2 18 -19 -22
19 2 4.9210-5 19 -20 -22
20 0 -1 : 20 : 22

C ****
C * surface card *
C ****
C -----< surfaces normal to z-axis >-
1 pz -21.00
2 pz -1.00 $ n & gamma spectrum
3 pz 0.00 $ foil & tld
4 pz 5.77 $ tld
5 pz 7.605 $ n & gamma spectrum
6 pz 10.11 $ foil
7 pz 15.00 $ change cell importance
8 pz 20.37 $ foil
9 pz 20.98 $ tld
10 pz 22.815 $ n & gamma spectrum
11 pz 30.00 $ change cell importance
12 pz 35.61 $ foil
13 pz 36.19 $ tld
14 pz 38.025 $ n & gamma spectrum
15 pz 45.00 $ change cell importance
16 pz 50.85 $ foil
17 pz 51.40 $ tld
18 pz 53.235 $ n & gamma spectrum
19 pz 60.84 $ foil & tld
20 pz 61.84 $ n & gamma spectrum
C -----< cylinders centered on z-axis >-
21 cz 3.00
22 cz 31.50
C ***** blank delimiter *****

C ****
C * mode card - neutron & photon *
C ****
mode n
wwe:n 5e-6 1e-4 1e-2 1 5 13 16
wwp:n 5 3 5 0 0
wwe:p 100
wwp:p 5 3 5 0 0
ext:n 0 0 0.1z 0.1z 0.1z 0.1z 0.1z 0.1z
      0.1z 0.1z 0.1z 0.1z 0.1z 0.1z 0.1z 0.1z
      0.1z 0.1z 0 0
wwn1:n 1.0e-4 1.0e-4 1.0e-4 1.0e-4 3.0e-5 1.0e-5 1.0e-5 1.0e-5
      1.0e-5 1.0e-5 1.0e-5 7.0e-6 7.0e-6 5.0e-6 2.0e-6 2.0e-6
      1.0e-6 1.0e-6 1.0e-6 -1
wwn2:n 1.0e-3 1.0e-3 1.0e-3 1.0e-3 3.0e-4 1.0e-4 1.0e-4 1.0e-4
      1.0e-4 1.0e-4 1.0e-4 7.0e-5 7.0e-5 5.0e-5 2.0e-5 2.0e-5
      1.0e-5 1.0e-5 1.0e-5 -1
wwn3:n 1.0e-2 1.0e-2 1.0e-2 1.0e-2 3.0e-3 1.0e-3 1.0e-3 1.0e-3
      1.0e-3 1.0e-3 1.0e-3 7.0e-4 7.0e-4 5.0e-4 2.0e-4 2.0e-4
      1.0e-4 1.0e-4 1.0e-4 -1
wwn4:n 1.0e-1 1.0e-1 3.0e-2 2.0e-2 1.0e-2 1.0e-2 1.0e-2 1.0e-2

```

Fig. A-13 A typical example of input data of MCNP for the analysis of the FNS/clean benchmark experiment on copper.

```

    1.0e-2 1.0e-2 1.0e-2 7.0e-3 5.0e-3 2.0e-3 1.0e-3 1.0e-3
    5.0e-4 5.0e-4 5.0e-4 -1
wwn5:n 1.0e-1 1.0e-1 4.0e-2 2.0e-2 2.0e-2 1.0e-2 5.0e-3 5.0e-3
        4.0e-3 2.0e-3 1.0e-3 7.0e-4 5.0e-4 2.0e-4 1.0e-4 1.0e-4
        5.0e-5 5.0e-5 5.0e-5 -1
wwn6:n 1.0e-1 1.0e-1 4.0e-2 2.0e-2 2.0e-2 1.0e-2 5.0e-3 5.0e-3
        2.0e-3 5.0e-4 2.0e-4 2.0e-4 1.0e-4 5.0e-5 2.0e-5 2.0e-5
        1.0e-5 1.0e-5 -1
wwn7:n 1.0e-1 1.0e-1 4.0e-2 2.0e-2 1.0e-2 3.0e-3 1.0e-3 1.0e-3
        7.0e-4 2.0e-4 5.0e-5 4.0e-5 2.0e-5 5.0e-6 2.0e-6 2.0e-6
        1.0e-6 1.0e-6 1.0e-6 -1
wwn1:p 1.0e-1 1.0e-1 4.0e-2 2.0e-2 2.0e-2 1.0e-2 5.0e-3 5.0e-3
        4.0e-3 2.0e-3 1.0e-3 1.0e-3 7.0e-4 5.0e-4 5.0e-4
        3.0e-4 3.0e-4 3.0e-4 -1
c ****
c * source specification cards *
c ****
c * material specification cards *
c ****
c -----< copper >-
m1 29000.37c 1
c -----< air >-
m2 7014.37c 3.8810-5 8016.37c 1.0400-5
c -----< materials for reaction rate>-
m3 5010.03y 1.0 $ B-10 (n,a)
m4 13027.03y 1.0 $ Al-27 (n,a)
m5 22000.03y 1.0 $ Ti-0 (n,x)Sc-46 (n,x)Sc-47 (n,x)Sc-48
m6 25055.03y 1.0 $ Mn-55 (n,g)
m7 26054.03y 1.0 $ Fe-54 (n,p)
m8 26056.03y 1.0 $ Fe-56 (n,p)
m9 27059.37c 1.0 $ Co-59 (n,2n) (n,g) (n,a) (n,p)
m10 28058.03y 1.0 $ Ni-58 (n,2n) (n,p)
m11 29063.37c 1.0 $ Cu-63 (n,2n) (n,g) (n,a)
m12 29065.37c 1.0 $ Cu-65 (n,2n) (n,g)
m13 30064.03y 1.0 $ Zn-64 (n,p)
m14 40090.03y 1.0 $ Zr-90 (n,2n)
m15 41093.03y 1.0 $ Nb-93 (n,2n)Nb-92m
m16 49115.03y 1.0 $ In-115 (n,n')In-115m
m17 79197.03y 1.0 $ Au-197 (n,g)
m18 92235.03y 1.0 $ U-235 (n,f)
c ****
c * tally specification cards *
c ****
fc2 -- neutron spectrum surface -----
f2:n 2 3 4 5 6 7 8 9 10 11
     12 13 14 15 16 17 18 19 20
fs2 -21
fc12 -- neutron reaction rate surface -----
f12:n 2 3 4 5 6 7 8 9 10 11
     12 13 14 15 16 17 18 19 20
fml2 (1 1 102) (1 3 107) (1 4 107) (1 5 210) (1 5 211)
      (1 5 212) (1 6 102) (1 7 103) (1 8 103) (1 9 16)
      (1 9 102) (1 9 103) (1 9 107) (1 10 16) (1 10 103)
      (1 11 16) (1 11 102) (1 11 107) (1 12 16) (1 12 102)
      (1 13 103) (1 14 16) (1 15 16) (1 16 51) (1 17 102)
      (1 18 18)
fs12 -21
e12 20
fq12 s e f m
fc22 -- neutron decade spectrum surface -----
f22:n 2 3 4 5 6 7 8 9 10 11
     12 13 14 15 16 17 18 19 20
fs22 -21
e22 1e-7 1e-6 1e-5 1e-4 1e-3 1e-2 1e-1 1e+0 1e+1 1e+2
fc32 -- gamma-ray spectrum surface -----
f32:p 2 3 4 5 6 7 8 9 10 11
     12 13 14 15 16 17 18 19 20
fs32 -21
e32 1.0000-02 2.0000-02 3.0000-02 4.5000-02 6.0000-02
      8.0000-02 1.0000-01 1.5000-01 2.0000-01 3.0000-01
      4.0000-01 5.0000-01 5.2000-01 6.0000-01 7.0000-01
      8.0000-01 9.0000-01 1.0000+00 1.1300+00 1.2500+00
      1.3800+00 1.5000+00 1.7500+00 2.0000+00 2.2500+00
      2.5000+00 3.0000+00 3.5000+00 4.0000+00 4.5000+00
      5.0000+00 5.5000+00 6.0000+00 6.5000+00 7.0000+00
      7.5000+00 8.0000+00 9.0000+00 1.0000+01 1.2000+01

```

Fig. A-13 Continued (2/3).

```

c          1.4000+01
c
e0-----+
fg0      s m e   f
1.0010-11 3.2241-07
5.3156-07 8.7640-07 1.4449-06 2.3823-06 3.9278-06
6.4758-06 1.0677-05 1.7603-05 2.9023-05 4.7850-05
7.8891-05 1.3007-04 2.1445-04 3.5357-04 5.8293-04
9.6110-04 1.2341-03 1.5846-03 2.0346-03 2.6125-03
3.3546-03 4.3073-03 5.5307-03 7.1016-03 9.1186-03
1.1709-02 1.5034-02 1.9304-02 2.1874-02 2.4787-02
2.8087-02 3.1827-02 3.6065-02 4.0867-02 4.6308-02
5.2474-02 5.9461-02 6.7378-02 7.6349-02 8.6515-02
9.8035-02 1.1109-01 1.2588-01 1.4264-01 1.6163-01
1.8315-01 2.0754-01 2.3517-01 2.6649-01 3.0197-01
3.4217-01 3.8774-01 4.3936-01 4.9786-01 5.6415-01
6.3927-01 7.2438-01 8.2084-01 9.3013-01 1.0540+00
1.1943+00 1.3533+00 1.5335+00 1.7377+00 1.8498+00
1.9691+00 2.0961+00 2.2313+00 2.3752+00 2.5284+00
2.6914+00 2.8650+00 3.0498+00 3.2465+00 3.4559+00
3.6787+00 3.9160+00 4.1686+00 4.4374+00 4.7236+00
5.0282+00 5.3525+00 5.6978+00 6.0652+00 6.4564+00
6.8728+00 7.3161+00 7.7879+00 8.2902+00 8.8249+00
9.3940+00 9.9999+00 1.0157+01 1.0317+01 1.0480+01
1.0645+01 1.0812+01 1.0983+01 1.1156+01 1.1331+01
1.1510+01 1.1691+01 1.1875+01 1.2062+01 1.2252+01
1.2445+01 1.2641+01 1.2840+01 1.3042+01 1.3248+01
1.3456+01 1.3668+01 1.3883+01 1.4102+01 1.4324+01
1.4550+01 1.4779+01 1.5012+01 1.5248+01 1.5488+01
c ****
c * problem cutoff cards *
c ****
phys:n 20 0
phys:p 20 1 0
phys:e 20 1 1 1 1 1 1 1 1
cut:n 0 0.0 -0.5 -0.25 0
cut:p 0 0.999-02 -0.5 -0.25 0
nps 500000
ctme 1000000
c ****
c * peripheral cards *
c ****
idum 1
rdum 0 0 -20
prdmp 1000000 100000 1 1
lost 10 10
print
c ***** blank terminator *****

```

Fig. A-13 Continued (3/3).

```

>>> Analysis of Tungsten Slab Experiment JENDL-3.2 <<<
c ***** front air region *****
1 2 4.921-5 (+1 -2 -22) : (+2 -3 +21 -22)      $ source
void
2 2 4.921-5 +2 -3 -21      $ cell detecter
c ***** test region *****
3 1 6.423-2 +3 -4 -21      $ 0.00 - 5.07 cm
4 1 6.544-2 +3 -4 +21 -22      $ 5.07 - 7.605cm
5 1 6.423-2 +4 -5 -21      $ 7.605- 10.14 cm
6 1 6.544-2 +4 -5 +21 -22      $ 10.14 - 20.28 cm
7 1 6.423-2 +5 -6 -21      $ 20.28 - 22.815cm
8 1 6.544-2 +5 -6 +21 -22      $ 22.815- 25.35 cm
9 1 6.423-2 +6 -7 -21      $ 25.35 - 35.49 cm
10 1 6.544-2 +6 -7 +21 -22      $ 35.49 - 38.025cm
11 1 6.423-2 +7 -8 -21      $ 38.025- 40.56 cm
12 1 6.544-2 +7 -8 +21 -22      $ 40.56 - 50.70 cm
13 1 6.423-2 +8 -9 -21      $ 40.56 - 50.70 cm
14 1 6.544-2 +8 -9 +21 -22      $ 50.70 $ n-spec
15 1 6.423-2 +9 -10 -21      $ 52.70 $ n-spec
16 1 6.544-2 +9 -10 +21 -22      $ 52.70 $ n-spec
17 1 6.423-2 +10 -11 -21      $ 52.70 $ n-spec
18 1 6.544-2 +10 -11 +21 -22      $ 52.70 $ n-spec
19 1 6.423-2 +11 -12 -21      $ 52.70 $ n-spec
20 1 6.544-2 +11 -12 +21 -22      $ 52.70 $ n-spec
21 1 6.423-2 +12 -13 -21      $ 52.70 $ n-spec
22 1 6.544-2 +12 -13 +21 -22      $ 52.70 $ n-spec
c ***** rear air region *****
23 2 4.921-5 +13 -14 -21      $ cell detector
24 2 4.921-5 +13 -14 +21 -22      $ cell detector
c ***** external void *****
25 0 -1 : +14 : +22      $ cell detector

1      pz      -21.00 $ Source
2      pz      -2.00 $ n-spec
3      pz      0.00 $ Front Surface
4      pz      5.07 $ #1-1
5      pz      7.605 $ Drawer #1
6      pz      10.14 $ #1-2
7      pz      20.28 $ #2-1
8      pz      22.815 $ Drawer #2
9      pz      25.35 $ #2-2
10     pz      35.49 $ #3-1
11     pz      38.025 $ Drawer #3
12     pz      40.56 $ #3-2
13     pz      50.70 $ Rear Surface
14     pz      52.70 $ n-spec
c
21     cz      2.86
22     cz      23.76

ext:n 0 0 0.1z 0.1z 0.1z 0.1z 0.1z 0.1z 0.1z 0.1z 0.1z 0.1z
       0.1z 0.1z 0.1z 0.1z 0.1z 0.1z 0.1z 0.1z 0.1z 0.1z 0.1z
       0.1z 0.1z 0 0 0
wwe:n 1.0e-3 1.0e-2 1.0 10.0 16.0
wwp:n 5 3 5 0 0
wwnl:n $ for eV Neutrons
       0.08 1r 0.02 1r 0.005 1r 0.00128 1r
       0.00032 1r 0.00008 1r 0.00002 1r 0.000005 1r
       0.0000025 7r -1
wwn2:n $ for 1-10keV Neutrons
       0.08 1r 0.03 1r 0.008 3r 0.003 1r
       0.0008 3r 0.0003 1r 0.00008 7r -1
wwn3:n $ for 0.01-1MeV Neutrons
       0.08 1r 0.08 1r 0.08 3r 0.04 1r
       0.02 3r 0.01 1r 0.005 7r -1
wwn4:n $ for 1-13 MeV Neutrons
       0.08 1r 0.02 1r 0.005 3r 0.00128 1r
       0.00032 3r 0.00008 1r 0.00002 7r -1
wwn5:n $ for 14 MeV Neutrons
       0.08 1r 0.02 1r 0.005 3r 0.00128 1r
       0.00032 3r 0.00008 1r 0.00002 7r -1
wwe:p 100.0
wwp:p 5 3 5 0 0
wwnl:p $ for Gamma-Rays
       0.4 1r 0.15 1r 0.04 3r 0.015 1r

```

Fig. A-14 A typical example of input data of MCNP for the analysis of the FNS/clean benchmark experiment on tungsten.

```

      0.004 3r      0.0015 lr      0.0004 7r      -1
wwe:e 100.0
wwp:e 5 3 5 0 0
wwn1:e $ for Electrons
      0.4    1r     0.15   lr     0.04   3r     0.015   1r
      0.004 3r     0.0015 lr     0.0004 7r     -1
c ****
c * source specification cards *
c * a user supplied source subroutine is used. *
c ****
c * material specification cards *
c ****
c --- Tungsten
m1 74000.37c 0.05600 28000.37c 0.00580
29000.37c 0.00364
c --- air
m2 7014.37c 3.8810-5 8016.37c 1.0400-5
c --- materials for reaction rate
m3 5010.03y 1.0 $ B-10(n,alpha)
m4 13027.03y 1.0 $ Al-27(n,alpha)
m5 22000.03y 1.0 $ Ti-nat((n,x)Sc-48
m6 25055.03y 1.0 $ Mn-55(n,gamma)
m7 26056.03y 1.0 $ Fe-56(n,p)
m8 28058.03y 1.0 $ Ni-58(n,2n) & Ni-58(n,p)
m9 28060.03y 1.0 $ Ni-60(n,p)
m10 29063.03y 1.0 $ Cu-63(n,2n) & Cu-63(n,g) & Cu-63(n,a)
m11 29065.03y 1.0 $ Cu-65(n,2n)
m12 30064.03y 1.0 $ Zn-64(n,p)
m13 40090.03y 1.0 $ Zr-90(n,2n)
m14 41093.03y 1.0 $ Nb-93(n,2n)Nb-92m
m15 49115.03y 1.0 $ In-115(n,n')In-115m
m16 74186.03y 1.0 $ W-186(n,gamma)
m17 79197.03y 1.0 $ Au-197(n,gamma)
m18 92235.03y 1.0 $ U-235(n,fission)
c
m21 28000.37c 1.0 $ Ni(n,gamma)
m22 29000.37c 1.0 $ Cu(n,gamma)
m23 74000.37c 1.0 $ W(n,gamma)
c ****
c * tally specification cards *
c ****
fc02 ---- neutron energy spectrum (decade) surface
f02:n 3 4 5 6 7 8 9 10 11 12 13
fq02 s f e
fs02 -21
e02 1e-7 1e-6 1e-5 1e-4 1e-3 1e-2 1e-1 1e+0 1e+1 2e+1
fc14 ---- neutron energy spectrum (decade) cell
f14:n 2 5 7 11 13 17 19 23
fq14 s f e
e14 1e-7 1e-6 1e-5 1e-4 1e-3 1e-2 1e-1 1e+0 1e+1 2e+1
fc22 ---- neutron reaction rate surface
f22:n 3 4 5 6 7 8 9 10 11 12 13
fs22 -21
fq22 s e f m
e22 16.0
fm22 (1)      (1 3 107) (1 3 207) (1 4 107) (1 5 212)
(1 6 102) (1 7 103) (1 8 16) (1 8 103) (1 9 103)
(1 10 16) (1 10 102) (1 10 107) (1 11 16) (1 12 103)
(1 13 16) (1 14 16) (1 15 51) (1 16 102) (1 17 102)
(1 18 18) (1 21 102) (1 22 102) (1 23 102)
fc34 ---- neutron reaction rate cell
f34:n 2 5 7 11 13 17 19 23
fq34 s e f m
e34 16.0
fm34 (1)      (1 3 107) (1 3 207) (1 4 107) (1 5 212)
(1 6 102) (1 7 103) (1 8 16) (1 8 103) (1 9 103)
(1 10 16) (1 10 102) (1 10 107) (1 11 16) (1 12 103)
(1 13 16) (1 14 16) (1 15 51) (1 16 102) (1 17 102)
(1 18 18) (1 21 102) (1 22 102) (1 23 102)
fc42 ---- neutron energy spectrum surface
f42:n 3 4 5 6 7 8 9 10 11 12 13
fs42 -21
fc54 ---- neutron energy spectrum cell
f54:n 2 5 7 11 13 17 19 23
fc62 ---- neutron energy reaction rate (decade) surface
f62:n 3 4 5 6 7 8 9 10 11 12 13
fq62 s m e f

```

Fig. A-14 Continued (2/3).

```

fs62 -21
e62  1e-7 1e-6 1e-5 1e-4 1e-3 1e-2 1e-1 1e+0 1e+1 2e+1
fm62 (1)      (1 3 107) (1 3 207) (1 4 107) (1 6 102)
      (1 10 102) (1 12 103) (1 14 16) (1 15 51) (1 16 102)
      (1 17 102) (1 18 18) (1 21 102) (1 22 102) (1 23 102)
fc102 ---- gamma-ray energy spectrum   surface r=4cm
f102:p 3 4 5 6 7 8 9 10 11 12 13
fs102 -21
e102  1.0000-02 2.0000-02 3.0000-02 4.5000-02 6.0000-02
      8.0000-02 1.0000-01 1.5000-01 2.0000-01 3.0000-01
      4.0000-01 5.0000-01 5.2000-01 6.0000-01 7.0000-01
      8.0000-01 9.0000-01 1.0000+00 1.1300+00 1.2500+00
      1.3800+00 1.5000+00 1.7500+00 2.0000+00 2.2500+00
      2.5000+00 3.0000+00 3.5000+00 4.0000+00 4.5000+00
      5.0000+00 5.5000+00 6.0000+00 6.5000+00 7.0000+00
      7.5000+00 8.0000+00 9.0000+00 1.0000+01 1.2000+01
      1.4000+01
c -----
fq0  s m e f
e0  1.0010-11 3.2241-07
      5.3156-07 8.7640-07 1.4449-06 2.3823-06 3.9278-06
      6.4758-06 1.0677-05 1.7603-05 2.9023-05 4.7850-05
      7.8891-05 1.3007-04 2.1445-04 3.5357-04 5.8293-04
      9.6110-04 1.2341-03 1.5846-03 2.0346-03 2.6125-03
      3.3546-03 4.3073-03 5.5307-03 7.1016-03 9.1186-03
      1.1709-02 1.5034-02 1.9304-02 2.1874-02 2.4787-02
      2.8087-02 3.1827-02 3.6065-02 4.0867-02 4.6308-02
      5.2474-02 5.9461-02 6.7378-02 7.6349-02 8.6515-02
      9.8035-02 1.1109-01 1.2588-01 1.4264-01 1.6163-01
      1.8315-01 2.0754-01 2.3517-01 2.6649-01 3.0197-01
      3.4217-01 3.8774-01 4.3936-01 4.9786-01 5.6415-01
      6.3927-01 7.2438-01 8.2084-01 9.3013-01 1.0540+00
      1.1943+00 1.3533+00 1.5335+00 1.7377+00 1.8498+00
      1.9691+00 2.0961+00 2.2313+00 2.3752+00 2.5284+00
      2.6914+00 2.8650+00 3.0498+00 3.2465+00 3.4559+00
      3.6787+00 3.9160+00 4.1686+00 4.4374+00 4.7236+00
      5.0282+00 5.3525+00 5.6978+00 6.0652+00 6.4564+00
      6.8728+00 7.3161+00 7.7879+00 8.2902+00 8.8249+00
      9.3940+00 9.9999+00 1.0157+01 1.0317+01 1.0480+01
      1.0645+01 1.0812+01 1.0983+01 1.1156+01 1.1331+01
      1.1510+01 1.1691+01 1.1875+01 1.2062+01 1.2252+01
      1.2445+01 1.2641+01 1.2840+01 1.3042+01 1.3248+01
      1.3456+01 1.3668+01 1.3883+01 1.4102+01 1.4324+01
      1.4550+01 1.4779+01 1.5012+01 1.5248+01 1.5488+01
c ****
c * problem cutoff cards *
c ****
phys:n 16.0 0.0
phys:p 30.0 0 0
phys:e 30.0 0 0 0 1 1 1 1
mode n p e
cut:n 0 1.0e-10 -0.5 -0.25 0
cut:p 0 0.0099 -0.5 -0.25 0
cut:e 0 0.3 -0.5 -0.25 0
nps 2000000
ctme 2000000
c ****
c * peripheral crads *
c ****
idum 1
rdum 0 0 -20
prdmp 100000 100000 1 1
lost 10 10
print

```

Fig. A-14 Continued (3/3).

```

LEAKAGE FROM COPPER(60CM DIA) BMCCS
C      ***** CELL CARDS *****
1      0          3 -1 -6                                imp:n=1 $ void
2      2      -7.87    (1 -2   4 -5):(4 -3 -1)      imp:n=1 $ Iron shell
3      1      -6.01    (2 -5   4):(-5 -4)        imp:n=1 $ Copper sample
4      2      -7.87    (-6 5   4 1):(-6 5 -4)     imp:n=1 $ Iron shell
5      0          6 -7                                imp:n=0 $ Outer world

C      ***** SURFACE CARDS *****
1      CX      2.5
2      CX      2.8
3      PX      -2.5
4      PX      -2.8
5      SO      30.0
6      SO      30.5
7      SO      100.0

C      ***** DATA CARDS *****
MODE N
SDEF pos=0 0 0 cel=1 wgt=1 erg=d1
C      *** ENERGY BIN FOR SOURCE NEUTRON ***
SI1   1.000E-01 1.120E-01 1.260E-01 1.410E-01 1.590E-01
      1.780E-01 2.000E-01 2.240E-01 2.520E-01 2.830E-01
      3.170E-01 3.560E-01 4.000E-01 4.490E-01 5.040E-01
      5.660E-01 6.350E-01 7.130E-01 8.000E-01 8.780E-01
      9.640E-01 1.058E+00 1.162E+00 1.275E+00 1.400E+00
      1.542E+00 1.698E+00 1.871E+00 2.061E+00 2.270E+00
      2.500E+00 2.704E+00 2.924E+00 3.162E+00 3.419E+00
      3.699E+00 4.000E+00 4.165E+00 4.337E+00 4.516E+00
      4.703E+00 4.897E+00 5.099E+00 5.310E+00 5.529E+00
      5.757E+00 5.995E+00 6.242E+00 6.500E+00 6.765E+00
      7.041E+00 7.327E+00 7.627E+00 7.938E+00 8.261E+00
      8.598E+00 8.949E+00 9.314E+00 9.693E+00 1.009E+01
      1.050E+01 1.082E+01 1.114E+01 1.148E+01 1.183E+01
      1.218E+01 1.255E+01 1.277E+01 1.300E+01 1.324E+01
      1.348E+01 1.372E+01 1.397E+01 1.422E+01 1.447E+01
      1.474E+01 1.500E+01 1.527E+01 1.554E+01 1.583E+01
      1.611E+01 1.640E+01

C      *** SOURCE DISTRIBUTION ***
SP1   0.000E-00 0.000E-00 0.000E-00 0.000E-00 2.425E-04
      1.251E-04 5.573E-04 3.466E-04 5.228E-04 7.037E-04
      7.558E-04 8.497E-04 1.052E-03 1.026E-03 1.554E-03
      1.703E-03 2.019E-03 2.127E-03 2.395E-03 2.104E-03
      2.273E-03 2.328E-03 2.626E-03 2.657E-03 2.742E-03
      3.011E-03 2.826E-03 2.959E-03 2.834E-03 3.016E-03
      2.767E-03 2.705E-03 2.884E-03 2.018E-03 2.115E-03
      2.048E-03 1.865E-03 1.038E-03 8.851E-04 8.555E-04
      8.894E-04 7.964E-04 7.842E-04 7.874E-04 6.657E-04
      7.509E-04 7.248E-04 6.520E-04 7.586E-04 6.969E-04
      6.792E-04 5.810E-04 6.129E-04 6.333E-04 6.168E-04
      6.705E-04 7.635E-04 8.469E-04 9.340E-04 9.920E-04
      1.152E-03 9.053E-04 1.046E-03 1.204E-03 1.473E-03
      1.771E-03 2.299E-03 1.784E-03 2.416E-03 2.553E-03
      3.342E-03 4.524E-03 7.935E-03 2.257E-02 9.582E-02
      2.261E-01 2.954E-01 1.847E-01 4.704E-02 1.275E-02
      3.679E-03 7.569E-04

```

Fig. A-15 A typical example of input data for MCNP for the analysis of the OKTAVIAN leakage neutron spectrum measurement.

```

C      ***** MATERIALARDS *****
M1    29063.41 -0.691 29065.41 -0.309
M2    26000.41 1
C      ***** TALLY CARDS *****
F1:n  1 2 3 4 5 6
FT1   INC
FU1   0 1 2 5 10 20 30 40 50 60 70 80 90 100 1000 10000 20000
C      ***** ENERGY BIN *****
E1:n  1.000E-03 1.290E-03 1.670E-03 2.150E-03
      2.780E-03 3.590E-03 4.640E-03 5.990E-03 7.740E-03
      1.000E-02 1.290E-02 1.670E-02 2.150E-02 2.780E-02
      3.590E-02 4.640E-02 5.990E-02 7.740E-02
      1.000E-01 1.120E-01
      1.260E-01 1.410E-01 1.590E-01 1.780E-01 2.000E-01
      2.240E-01 2.520E-01 2.830E-01 3.170E-01 3.560E-01
      4.000E-01 4.490E-01 5.040E-01 5.660E-01 6.350E-01
      7.130E-01 8.000E-01 8.780E-01 9.640E-01 1.058E+00
      1.162E+00 1.275E+00 1.400E+00 1.542E+00 1.698E+00
      1.871E+00 2.061E+00 2.270E+00 2.500E+00 2.704E+00
      2.924E+00 3.162E+00 3.419E+00 3.699E+00 4.000E+00
      4.165E+00 4.337E+00 4.516E+00 4.703E+00 4.897E+00
      5.099E+00 5.310E+00 5.529E+00 5.757E+00 5.995E+00
      6.242E+00 6.500E+00 6.765E+00 7.041E+00 7.327E+00
      7.627E+00 7.938E+00 8.261E+00 8.598E+00 8.949E+00
      9.314E+00 9.693E+00 1.009E+01 1.050E+01 1.082E+01
      1.114E+01 1.148E+01 1.183E+01 1.218E+01 1.255E+01
      1.277E+01 1.300E+01 1.324E+01 1.348E+01 1.372E+01
      1.397E+01 1.422E+01 1.447E+01 1.474E+01 1.500E+01
      1.527E+01 1.554E+01 1.583E+01 1.611E+01 1.640E+01
C      ***** CUT OFF CARD *****
CUT:N  1.0E16 1.0E-3 0.01
C      ***** NEUTRON HISTORY *****
NPS   10000000
PRINT

```

Fig. A-15 Continued. (2/2)

```

Analysis of OKTAVIAN Experiment for Secondary Gamma-Rays << Al-n >>
 1   0      -1
 2   2    -7.90     1  -2
 3   1    -1.22     2  -3
 4   2    -7.90     3  -4
 5   0          4  -5
 6   0          5

 1   so    10.00
 2   so    10.20
 3   so    19.75
 4   so    19.95
 5   so   580.00

mode n p e
imp:n 1 1 1 1 1 0
imp:p 1 1 1 1 1 0
imp:e 1 1 1 1 1 0
sdef erg=d1
s1  1.000e-1 1.120e-1 1.260e-1 1.410e-1 1.590e-1 1.780e-1 2.000e-1 2.240e-1
    2.520e-1 2.830e-1 3.170e-1 3.560e-1 4.000e-1 4.490e-1 5.040e-1 5.660e-1
    6.350e-1 7.130e-1 8.000e-1 8.780e-1 9.640e-1 1.058e+0 1.162e+0 1.275e+0
    1.400e+0 1.542e+0 1.698e+0 1.871e+0 2.061e+0 2.270e+0 2.500e+0 2.704e+0
    2.924e+0 3.162e+0 3.419e+0 3.699e+0 4.000e+0 4.165e+0 4.337e+0 4.516e+0
    4.703e+0 4.897e+0 5.099e+0 5.310e+0 5.529e+0 5.757e+0 5.995e+0 6.242e+0
    6.500e+0 6.765e+0 7.041e+0 7.327e+0 7.627e+0 7.938e+0 8.261e+0 8.598e+0
    8.949e+0 9.314e+0 9.693e+0 1.009e+1 1.050e+1 1.082e+1 1.114e+1 1.148e+1
    1.183e+1 1.218e+1 1.255e+1 1.277e+1 1.300e+1 1.324e+1 1.348e+1 1.372e+1
    1.397e+1 1.422e+1 1.447e+1 1.474e+1 1.500e+1 1.527e+1 1.554e+1 1.583e+1
    1.611e+1 1.640e+1
sp1  0.000e-4 0.000e-0 0.000e-0 1.270e-4 5.774e-5 2.536e-4 2.722e-4 2.076e-4
    4.366e-4 3.873e-4 4.756e-4 6.161e-4 6.727e-4 6.648e-4 8.581e-3 1.098e-3
    1.184e-3 1.412e-3 1.616e-3 1.546e-3 1.556e-3 1.631e-3 1.771e-3 1.804e-3
    1.823e-3 1.891e-3 1.935e-3 2.002e-3 2.052e-3 2.004e-3 2.068e-3 2.091e-3
    3.354e-3 1.492e-3 1.322e-3 1.451e-3 1.401e-3 7.112e-4 6.423e-4 6.514e-4
    6.195e-4 6.428e-4 6.209e-4 5.788e-4 5.227e-4 5.250e-4 5.456e-4 5.106e-4
    5.789e-4 5.391e-4 4.998e-4 4.813e-4 5.300e-4 5.756e-4 5.230e-4 5.394e-4
    6.256e-4 7.047e-4 7.729e-4 7.951e-4 8.659e-4 8.106e-4 8.923e-4 1.022e-3
    1.281e-3 1.687e-3 2.286e-3 1.825e-3 2.479e-3 3.794e-3 7.010e-3 1.565e-2
    3.634e-2 7.492e-2 1.279e-1 1.768e-1 1.916e-1 1.500e-1 8.676e-2 3.950e-2
    1.430e-2 4.269e-3

c
m1  13027.41c 1
m2  24000.41c -0.185  25055.41c -0.013  26000.41c -0.691
28000.41c -0.111
c
fc32 ----- photon spectrum -----
f32:p 5
fm32 4227327.1      $ 4*pi*580*580
fq32 e t
e32 0.3 56i 6.0 19i 10.0 24i 20.0
t32 8.8 1e6 t
c
phys:n 20.0 0
phys:p 20.0 0
phys:e 20.0 0 0 0 0 1 0 1 1
cut:n 1e6 0.0 -0.5 -0.25 0
cut:p 1e6 0.299 -0.5 -0.25 0
cut:e 1e6 0.3 -0.5 -0.25 0
nps 1000000
ctme 1000000
prdmp 10000000 10000000 1 1
lost 10 10
print

```

Fig. A-16 A typical example of input data for MCNP with the D-T neutron source for the analysis of the OKTAVIAN leakage gamma-ray spectrum measurement.

```

Analysis of OKTAVIAN Experiment for Secondary Gamma-Rays << Al-g >>
 1   0      -1
 2   2    -7.90    1 -2
 3   1    -1.22    2 -3
 4   2    -7.90    3 -4
 5   0      4 -5
 6   0      5

 1   so    10.00
 2   so    10.20
 3   so    19.75
 4   so    19.95
 5   so   580.00

mode p e
imp:p 1 1 1 1 1 0
imp:e 1 1 1 1 1 0
sdef erg=d1 wgt=0.0862
si1 0.6 93i 10.0
spl  0.000e+0 2.961e-3 4.793e-3 9.615e-3 4.543e-3 4.082e-3 5.335e-3 6.609e-3
     4.793e-3 3.476e-3 2.035e-3 1.733e-3 1.733e-3 1.557e-3 1.326e-3 1.257e-3
     1.191e-3 1.070e-3 1.014e-3 1.070e-3 1.129e-3 1.014e-3 8.638e-4 7.761e-4
     8.188e-4 8.638e-4 8.638e-4 8.188e-4 7.761e-4 7.356e-4 7.356e-4 7.356e-4
     6.973e-4 6.264e-4 5.628e-4 5.335e-4 5.335e-4 5.628e-4 5.938e-4 6.264e-4
     5.938e-4 5.057e-4 4.082e-4 3.476e-4 3.295e-4 3.476e-4 3.667e-4 4.082e-4
     4.082e-4 3.869e-4 3.667e-4 3.295e-4 2.960e-4 2.806e-4 2.806e-4 2.960e-4
     2.960e-4 2.960e-4 2.806e-4 2.659e-4 2.521e-4 2.389e-4 2.389e-4 2.521e-4
     2.521e-4 2.389e-4 1.929e-4 1.642e-4 1.476e-4 1.399e-4 1.326e-4 1.326e-4
     1.326e-4 1.326e-4 1.326e-4 1.326e-4 1.257e-4 1.070e-4 9.113e-5 8.188e-5
     6.973e-5 6.609e-5 6.264e-5 5.938e-5 5.938e-5 5.628e-5 5.628e-5 5.335e-5
     5.057e-5 4.306e-5 3.667e-5 2.960e-5 2.659e-5 2.659e-5 2.806e-5

c
m1  13027. 1
m2  24000. -0.185  25055. -0.013  26000. -0.691
     28000. -0.111

c
fc32 ----- photon spectrum -----
f32:p 5
fm32 4227327.1      $ 4*pi*580*580
fq32 e t
e32 0.3 56i 6.0 19i 10.0
t32 6.9 1e6 t
c
phys:p 20.0 0 0
phys:e 20.0 0 0 0 0 1 0 1 1
cut:p 1e6 0.299 -0.5 -0.25 0
cut:e 1e6 0.3 -0.5 -0.25 0
nps 1000000
ctme 1000000
prdmp 10000000 10000000 1 1
lost 10 10
print

```

**Fig. A-17** A typical example of input data for MCNP with the target gamma-ray source for the analysis of the OKTAVIAN leakage gamma-ray spectrum measurement.

# 国際単位系(SI)と換算表

表1 SI基本単位および補助単位

量	名称	記号
長さ	メートル	m
質量	キログラム	kg
時間	秒	s
電流	アンペア	A
熱力学温度	ケルビン	K
物質量	モル	mol
光度	カンデラ	cd
平面角	ラジアン	rad
立体角	ステラジアン	sr

表3 固有の名称をもつSI組立単位

量	名称	記号	他のSI単位による表現
周波数	ヘルツ	Hz	$s^{-1}$
力	ニュートン	N	$m \cdot kg/s^2$
圧力、応力	パスカル	Pa	$N/m^2$
エネルギー、仕事、熱量	ジュール	J	$N \cdot m$
功率、放射束	ワット	W	$J/s$
電気量、電荷	クーロン	C	$A \cdot s$
電位、電圧、起電力	ボルト	V	$W/A$
静電容量	フアラード	F	$C/V$
電気抵抗	オーム	$\Omega$	$V/A$
コンダクタンス	ジemens	S	$A/V$
磁束	ウェーバ	Wb	$V \cdot s$
磁束密度	テスラ	T	$Wb/m^2$
インダクタンス	ヘンリー	H	$Wb/A$
セルシウス温度	セルシウス度	°C	
光束度	ルーメン	lm	$cd \cdot sr$
照度	ルクス	lx	$lm/m^2$
放射能	ベクレル	Bq	$s^{-1}$
吸収線量	グレイ	Gy	$J/kg$
線量等量	シーベルト	Sv	$J/kg$

表2 SIと併用される単位

名称	記号
分、時、日	min, h, d
度、分、秒	°, ', "
リットル	l, L
トントン	t
電子ボルト	eV
原子質量単位	u

$$1 \text{ eV} = 1.60218 \times 10^{-19} \text{ J}$$

$$1 \text{ u} = 1.66054 \times 10^{-27} \text{ kg}$$

表5 SI接頭語

倍数	接頭語	記号
$10^{18}$	エクサ	E
$10^{15}$	ペタ	P
$10^{12}$	テラ	T
$10^9$	ギガ	G
$10^6$	メガ	M
$10^3$	キロ	k
$10^2$	ヘクト	h
$10^1$	デカ	da
$10^{-1}$	デシ	d
$10^{-2}$	センチ	c
$10^{-3}$	ミリ	m
$10^{-6}$	マイクロ	μ
$10^{-9}$	ナノ	n
$10^{-12}$	ピコ	p
$10^{-15}$	フェムト	f
$10^{-18}$	アト	a

(注)

- 表1~5は「国際単位系」第5版、国際度量衡局1985年刊行による。ただし、1eVおよび1uの値はCODATAの1986年推奨値によった。
- 表4には海里、ノット、アール、ヘクタールも含まれているが日常の単位なのでここでは省略した。
- barは、JISでは流体の圧力を表わす場合に限り表2のカテゴリーに分類されている。
- EC閣僚理事会指令ではbar、barnおよび「血圧の単位」mmHgを表2のカテゴリーに入れている。

## 換算表

力	N( $-10^5$ dyn)	kgf	lbf
1	0.101972	0.224809	
9.80665	1	2.20462	
4.44822	0.453592	1	

$$\text{粘度 } 1 \text{ Pa} \cdot \text{s} (\text{N} \cdot \text{s}/\text{m}^2) = 10 \text{ P} (\text{ボアズ})(\text{g}/(\text{cm} \cdot \text{s}))$$

$$\text{動粘度 } 1 \text{ m}^2/\text{s} = 10^3 \text{ St} (\text{ストークス})(\text{cm}^2/\text{s})$$

圧	MPa( $=10$ bar)	kgf/cm <sup>2</sup>	atm	mmHg(Torr)	lbf/in <sup>2</sup> (psi)
力	0.0980665	1	0.967841	735.559	14.2233
	0.101325	1.03323	1	760	14.6959
	$1.33322 \times 10^{-1}$	$1.35951 \times 10^{-3}$	$1.31579 \times 10^{-3}$	1	$1.93368 \times 10^{-2}$
	$6.89476 \times 10^{-3}$	$7.03070 \times 10^{-2}$	$6.80460 \times 10^{-2}$	51.7149	1

エネルギー・仕事・熱量	J( $=10^7$ erg)	kgf·m	kW·h	cal(計量法)	Btu	ft·lbf	eV
	1	0.101972	$2.77778 \times 10^{-7}$	0.238889	$9.47813 \times 10^{-1}$	0.737562	$6.24150 \times 10^{18}$
	9.80665	1	$2.72407 \times 10^{-6}$	2.34270	$9.29487 \times 10^{-3}$	7.23301	$6.12082 \times 10^{19}$
	$3.6 \times 10^6$	$3.67098 \times 10^5$	1	$8.59999 \times 10^5$	3412.13	$2.65522 \times 10^6$	$2.24694 \times 10^{25}$
	4.18605	0.426858	$1.16279 \times 10^{-6}$	1	$3.96759 \times 10^{-3}$	3.08747	$2.61272 \times 10^{19}$
	1055.06	107.586	$2.93072 \times 10^{-1}$	252.042	1	778.172	$6.58515 \times 10^{21}$
	1.35582	0.138255	$3.76616 \times 10^{-7}$	0.323890	$1.28506 \times 10^{-3}$	1	$8.46233 \times 10^{18}$
	$1.60218 \times 10^{19}$	$1.63377 \times 10^{20}$	$4.45050 \times 10^{26}$	$3.82743 \times 10^{-26}$	$1.51857 \times 10^{-22}$	$1.18171 \times 10^{-19}$	1

1 cal = 4.18605J (計量法)  
= 4.184J (熱化学)  
= 4.1855J (15°C)  
= 4.1868J (国際蒸気表)  
仕事率 1 PS(仮馬力)  
= 75 kgf·m/s  
= 735.499W

放射能	Bq	Ci	吸収線量	Gy	rad	照射線量	C/kg	R	線量率	Sv	rem
	1	$2.70270 \times 10^{-11}$	1	0.01	1	$2.58 \times 10^{-4}$	1	1	0.01	1	1

(86年12月26日現在)

**COMPILED BY THE INTERNATIONAL ATOMIC ENERGY AGENCY  
COMPILATION OF BENCHMARK RESULTS FOR FUSION RELATED NUCLEAR DATA**